Asphaltenes Conversion by Chemical Modification

by

Glaucia Helena Carvalho Do Prado

A thesis submitted in partial fulfillment of the requirements for the degree of

Doctor of Philosophy

In

Chemical Engineering

Department of Chemical and Materials Engineering
University of Alberta

Abstract

Canadian oilsands bitumen contains one of the highest amounts of asphaltenes (16-20 wt %) among all crude oils. Asphaltenes are the lowest value fraction of bitumen. It differs from the other fractions of bitumen because of its insolubility in paraffinic solvents. Asphaltenes are insoluble in paraffinic solvents because their molecules can aggregate and also because they have high molecular mass, high heteroatom content, and presence of large ring structures. Asphaltenes could be converted into more valuable products by modifying the properties responsible for insolubility in paraffinic solvents. The disaggregation of asphaltenes molecules by different chemical conversions was considered in this study. The objective was to explore new conversion strategies that were not already being applied by industry. The work focused on three conversion pathways: halogenation, Friedel-Crafts alkylation, and donor-acceptor reaction by acid treatment.

Halogenation reactions had the objective of weakening π-π stacking of aromatic sheets in asphaltenes. Even though ~5 wt % increase of lighter boiling fractions was observed, the products were harder (penetration hardness). The solubility of asphaltenes in various solvents decreased after halogenation reaction. These changes could benefit road paving applications, but not oil upgrading, althouth it was observed that halogenation could demetalate porphyrins in bitumen and maltenes. In order to gain a better fundamental understanding of the influence of halogenation, hardness and demetalation of porphyrins were investigated with model compounds. The results showed that hardness was caused mainly by increased hydrogen bonding. A 74 % decrease of the nickel content in model compounds was observed due to acid-base and metal-ligand equilibrium disruption by bromine. The work also suggested that chloride salts originally present in bitumen could potentially influence coke chemistry and coke yield

during bitumen upgrading. Friedel-Crafts alkylation had the objective of disrupting hydrogen bonding in asphaltenes by removal of alcohol groups or convertion of alcohol groups into ethers. The study employed $FeCl_3$ as catalyst and *o*-xylene and methanol as alkylating agents, targeting alkylation of alcohols and thiols specifically. Alkylation of asphaltenes with *o*-xylene resulted in 6 % conversion of asphaltenes to maltenes and an increase of 9 % in straight run distillate and vacuum gas oil. Alkylation of asphaltenes with methanol was not beneficial. Model compounds were used to understand the chemistry and observed results. Alkylation of 2-naphthol showed that the two dominant reactions were dimerization of 2-naphthol and coordination with iron. Alkylation with methanol resulted in chlorination of the product by the catalyst. Alkylation of dibenzyl ether showed that ether bonds were cleaved by $FeCl_3$ catalyst, which was followed by C-alkylation with *o*-xylene. The slight conversion of asphaltenes into maltenes is better explained by C-alkylation after ether cleavage than hydrogen bonding disruption. Disruption of metal-bridged structures in asphaltenes was also investigated. Divalent metals responsible for keeping smaller molecules together were removed with hydrochloric acid. The total of divalent metals removed from asphaltenes was about 2600 μg/g, iron was the metal most affected by acid washing. Around 8 % of asphaltenes could be converted into maltenes. The micro carbon residue of asphaltenes after demetalation decreased from 45 to 40 wt %. This investigation also highlighted the potential role of phenolic to phenoxide conversion in the formation of emulsions. The new conversion strategies investigated did not result in significant asphaltenes to maltenes conversion, but the investigation contributed to the fundamental understanding of asphaltenes conversion, and in particular, reactions involving halogens and acidic compounds.

Keywords: Asphaltenes, Halogenation, Friedel-Crafts Alkylation, Acid Demetalation.

Preface
(Mandatory due to collaborative work)

Chapter 3 of this thesis has been published as Glaucia H. C. Prado and Arno de Klerk, "Halogenation of Oilsands Bitumen, Maltenes, and Asphaltenes", *Energy & Fuels* **2014**, 28, 4458-4468. I was responsible for experimental design, data collection and analysis as well as the manuscript composition. Arno de Klerk was the supervisory author and was involved with concept formation, data analysis, and manuscript composition.

Chapter 4 of this thesis was submitted for publication as Glaucia H. C. Prado and Arno de Klerk, "Origin of halogenated bitumen and asphaltenes hardness", *Energy & Fuels*. I was responsible for concept formation, experimental design, data collection and analysis as well as the manuscript composition. Arno de Klerk was the supervisory author and was involved with concept formation, data analysis, and manuscript composition.

Chapter 5 of this thesis was accepted for publication as Glaucia H. C. Prado and Arno de Klerk, "Demetalation of Metallophthalocyanines by Mild Halogenation without Disrupting the Tetrapyrrole Macrocycle", *Fuel*. I was responsible for concept formation, experimental design, data collection and analysis as well as the manuscript composition. Arno de Klerk was the supervisory author and was involved with concept formation, data analysis, and manuscript composition.

Chapter 7 of this thesis was published as Glaucia H. C. Prado and Arno de Klerk, "Alkylation of asphaltenes using a $FeCl_3$ catalyst", *Energy & Fuels* 2015, DOI: 10.1021/acs.energyfuels.5b01292. I was responsible for experimental design, data collection and analysis as well as the manuscript composition. Arno de Klerk was the supervisory author and was involved with concept formation, data analysis, and manuscript composition.

Chapter 8 of this thesis was submitted for publication as Glaucia H. C. Prado and Arno de Klerk, "Metals Removal from Oilsands Bitumen and Subfractions by Acid Washing", *Energy & Fuels*. I was responsible for experimental design, data collection and analysis as well as the manuscript

composition. Arno de Klerk was the supervisory author and was involved with concept formation, data analysis, and manuscript composition.

Dedication

To Ivor Prado for all the love

To my parents and brothers for always supporting my decisions

Acknowledgments

I would like to thank my supervisor Dr. Arno de Klerk. The only thing I wanted when I decided to change from Food Engineering to Chemical Engineering was a supervisor with a good heart and that was a good human being. But God gave me a supervisor not only with all I wanted, but also a supervisor who provided all technical and support that I needed to conduct my research.

I would like to thank you Nexen Energy ULC for the financial support.

I would like to thank Shaofeng Yang for all the help with all the questions about the lab and Andree Koenig for let me using her TGA and also for her advices.

I would like to thank you Bharathi Devandran and Yong Ling Yap for the help with alkylation and donor-acceptor experiments.

I also would like to thank you my lab mates.

To my Brazilian friends, who live in Canada and made my life here much happier.

To Flavia Picolli that even living so far in Brazil was always worried about me.

I would like to thank you my parents (Lucia and Messias) and brothers (Gian and Giulio) for all the support and comfort words.

A special thanks to Ivor Martin do Prado who always believed in my potential for research, for the patience to handle my worries, and especially for all the love.

Table of contents

List of Tables

List of Figures or Illustrations

Chapter 1. Introduction to the Upgrading of Oilsands Bitumen Derived Asphaltenes to Liquid Products

1.1 Background

Canada has the largest oilsands reserves in the world. Oil sand is a type of sandstone which contains sand, clays, and bitumen. The initial established reserves of crude bitumen in Canada correspond to 176.7 billion barrels. The initial established reserves of crude bitumen estimate the amount of bitumen before the deduction of any production. It is necessary to point out that established reserves of crude bitumen correspond to the "reserves recoverable under current technology". At the end of 2008 the remaining established reserves was ~ 170.3 billion barrels, which indicates that ~ 3 % of the initial established reserves were produced since commercial production started in 1967 (Masliyah *et al.*, 2011). Considering the size of the reserves, the study of oil sand bitumen and the asphaltenes and maltenes subfractions of oil sand bitumen is justified.

Bitumen is a type of petroleum, but its processing is harder compared to conventional oil processing. The difficulty of bitumen processing is related to its high viscosity (>500 Pa.s), high density (970< kg/m^3 <1015), high content of metals and heavy molecules, and presence of complex sulfur and nitrogen compounds. The presence of these heavy molecules without an appreciable lighter boiling fraction is attributed to bacterial biodegradation which consumed the lighter components over millions of years (Masliyah *et al.*, 2011). Despite its challenging processing, the interest in bitumen has increased considerably in the last decades, due to the higher energy demand and higher depletion rates of conventional oils reserves (Sorrel *et al*., 2012).

Asphaltenes are the lowest value fraction of bitumen and are defined by its solubility (soluble in toluene/benzene and insoluble in paraffinic solvent). They differ from the other fractions of bitumen only because they are insoluble in paraffinic solvents. They are a very complex mixture and are the most polar fraction of bitumen. Asphaltenes have a high heteroatom content (sulfur, oxygen, and nitrogen) and metals content (nickel and vanadium). Most of the carbon present in

asphaltenes is in aromatic form, which results in a low hydrogen to carbon ratio (1.1 to 1.2). The most of the asphaltenes in bitumen are present in the vacuum residue fraction and represent 14-20 wt % of total Alberta oilsands bitumens. The difference of asphaltenes content in Alberta bitumens depends on type of reservoir and reservoir depth. As asphaltenes are coke precursors in bitumen upgrading, the coke deposits formed during conversion can accumulate in equipment and can also deactivate catalysts. Moreover, under certain conditions (change in pressure or temperature), raw asphaltenes form aggregates and precipitate, which can be a problem during bitumen processing, causing clogging and fouling of equipment. Depending of the method employed in bitumen processing, for example, froth treatment with paraffinic solvent, asphaltenes are rejected as waste materials (Masliyah *et al.*, 2011; Gray, 2010; Strausz and Lown, 2003).

Work with asphaltenes is a very difficult task because the exact molecular structure, molecular weight, aggregation mechanism as well as true melting point of asphaltenes are not known, and there is much debate in the literature regarding these characteristics. Two models are reported about molecular structure: continental and archipelago. Briefly, in the continental model asphaltenes are assumed to be composed of one big aromatic core with small paraffinic side chains (Mullins, 2008), while in archipelago model asphaltenes are assumed to be composed of small aromatic cores connected by paraffinic bridges (Strausz and Lown, 2003). There are also several models to describe the asphaltenes aggregation mechanism. Most recent studies have demonstrated that aggregation may be caused by different chemical interactions such as π-π stacking of aromatic molecules, hydrogen bonding of polar groups and/or acid-base interactions (Gray *et al*., 2011).

Current technologies deal with asphaltenes in different ways that include assimilation, conversion and separation: Ebulated Bed Hydrocracking, Delayed Coking, Fluid Coking, Gasification, and diluent addition to meet pipeline specifications. However, there are some drawbacks for each technology. For example, conversion of asphaltenes into hydrogen, steam, and synthetic gas through gasification requires high capital investment with lower internal rate of return (10%). For Delayed Coking technology, asphaltenes are converted to coke and some light gases. Although coke can be used in electrical power plants, transportation costs do not

compensate for the energy value and post-combustion treatment cost of using coke for this purpose. Thus, usually coke is disposed of as solid waste in a land-fill. Another important aspect related to these technologies is environmental performance. In the case of Delayed Coking, for example, it produces about 64% of coke, which is disposed of as solid waste. Although Gasification does not produce solid waste, it releases higher amounts of CO_2 (77% higher) to produce same amounts of hydrogen compared to natural gas. Therefore, it is concluded that at the moment asphaltenes are converted to low value products, are rejected as waste materials or have economic/environmental performance issues (Zerpa, 2012).

Facing this scenario, it is important to explore new conversion strategies, which can convert asphaltenes into more valuable products, such as liquid fuels. The extent of possible upgrading with traditional thermal and hydroprocessing approaches is known and optimization of existing industrial processes was not of interest. New approaches to asphaltenes conversion were needed. It was reasoned that substantial conversion into liquid products may be achieved by manipulating the molecular properties responsible for insolubility in paraffinic solvents, such as aggregation. However, it is also very challenging to propose non-traditional (i.e. not thermal or hydroprocessing) conversion chemistries to address such molecular properties, because some basic physical and chemical properties, as well as interactions like the aggregation mechanism, are not definitively known.

1.2 Objectives

The objective of this study was to investigate non-traditional methods (halogenation, Friedel-Crafts alkylation, and donor-acceptor reactions) for asphaltenes conversion. These methods have been selected because they have the potential to disrupt interactions that may cause aggregation, or lead to paraffin insolubility. The product obtained from asphaltenes conversion may be paraffinic soluble oil which can be further refined into more valuable products such as liquid fuels by using conventional upgrading and refining technologies. Specific objectives include:

(a) Study halogenation reaction for π-π stacking interaction disruption in asphaltenes. Working hypothesis: because halogens are big and bulky they could sterically force the aromatic sheets apart and consequently weakening π-π stacking of aromatic sheets.

(b) Study alkylation reaction for removal or conversion of polar groups in asphaltenes. Working hypothesis: polar groups may form hydrogen bonding and link different molecules of asphaltenes. Therefore, removal of polar groups may disaggregate the linked molecules and by making the molecules less polar, paraffinic solubility may increase.

(c) Study acid-base reaction for removal of divalent cations in asphaltenes. Working hypothesis: divalent cations can bind with carboxylic acid groups and consequently link different molecules of asphaltenes. Therefore, removal of divalent cations may disaggregate the linked molecules.

1.3 Scope of Experimental Work

(a) Chapter 3 presents halogenation reaction results of bitumen, maltenes, and asphaltenes.

(b) Chapter 4 presents a model compound study to investigate hardness of halogenated bitumen, maltenes, and asphaltenes. This study evolved from the observations made during the halogenation study in Chapter 3.

(c) Chapter 5 presents a model compound study to investigate selective demetalation of tetrapyrrolic macrocycles by halogenation reaction. As was the case with Chapter 4, this study followed on a lead provided by the work performed in Chapter 3.

(d) Chapter 6 presents a theoretical discussion of potential role of chloride salts in coke formation during bitumen upgrading. This work was initiated to assist with explaining the observations in Chapter 3, but also addresses a topic of more general value.

(e) Chapter 7 presents Friedel-Crafts alkylation results of bitumen, maltenes, and asphaltenes. The study includes alkylation strategies resulting in heteroatom containing links and carbon containing links respectively.

(f) Chapter 8 presents Donor-acceptor reaction by acid treatment of bitumen, maltenes, and asphaltenes.

The work in Chapters 7 and 8 also served to front-end load two parallel research projects to gain more insight into these topics.

Literature Cited

Gray, M. R. *Fundamentals of Oilsands Upgrading*. University of Alberta: Edmonton, AB, 2010.

Gray, M. R.; Tykwinski, R. R.; Stryker, J. M.; Tan, X. Supramolecular assembly model for aggregation of petroleum asphaltenes. *Energy Fuels* **2011**, *25*, 3125-3134.

Masliyah, J. H.; Czarnecki, J. A.; Xu, Z. *Handbook on theory and practice of bitumen recovery from Athabasca oilsands. Theoretical basis.* Kingsley Publishing Services: Canada, 2011; Volume I, pp. 1-49.

Mullins, O. C. Review of the molecular structure and aggregation of asphaltenes and petroleomics. *SPE Journal* **2008**, *13*, 48-57.

Sorrel, S.; Speirs, J.; Bentley, R.; Miller, R.; Thompson, E. Shaping the global oil peak: a review of the evidence on field sizes, reserve growth, decline rates and depletion rates. *Energy* **2012**, *37*, 709-724.

Strausz, O. P.; Lown, E. M. *The chemistry of Alberta oilsands, bitumens, and heavy oils*. Alberta Energy Research Institute: Calgary, AB, 2003; pp. 459-662.

Zerpa, N. Creating more value from asphaltenes – The innovation challenge. Nexen Energy ULC bulletin, 2012.

Chapter 2. Literature Review

2.1 Asphaltenes

Oilsands derived bitumen is a type of petroleum and large reserves are located in Canada. Bitumen is characterized to contain high content of heavy molecules and metals when compared to conventional oils (Masliyah et al., 2011). There is a fraction of bitumen that is insoluble in paraffinic solvents (e.g. pentane, hexane, heptane, etc) and soluble in benzene or toluene. This fraction of bitumen is called asphaltenes (Long, 1981; Strausz and Lown, 2003; Gray, 2010; Groenzin and Mullins, 2007; Masliyah et al., 2011). Asphaltenes are also described as "the most polar and the highest molecular weight species in petroleum" (Long, 1981). Another asphaltenes characteristic is that they are polydisperse monomers with a strong tendency to form aggregates (Strausz and Lown, 2003; Masliyah et al., 2011).

Asphaltenes are not specific species and asphaltenes are not a subfraction that is present just in bitumen, but asphaltenes are also present in all types of petroleum, coal liquids, shale oil, and coal tar. Nevertheless, bitumen contains the highest asphaltenes content (14-20 wt %) between all of these sources. Asphaltenes are defined as a solubility class; the chemical structure and physical properties can differ from each asphaltene source (Strausz and Lown, 2003). Representative molecular structures, molecular weights as well as some physical characteristics, such as the melting point of asphaltenes, are not known, and there is debate in the literature regarding these characteristics (Strausz and Lown, 2003; Gray, 2003; Mulins, 2008; Sabbah et al., 2011; Sheremata et al., 2004; Groenzin and Mullins, 2000). Furthermore, these properties are mixture properties unique to each asphaltene sample, even though some common characteristics and properties can be found.

Although a molecular structure of asphaltenes is undefined, its elemental composition is very established and it is shown in Table 2.1 for different Canadian deposits. It also contains metals, being Ni, V, Fe, and Mo the major components. Metal content in asphaltenes is present in trace amounts, typically in the order of 100-1000 parts per million (Strausz and Lown, 2003).

Table 2.1. Elemental composition of asphaltenes from different Canadian deposits (Strausz and Lown, 2003)[1]

wt %	Source					
	Athabasca	**Cold Lake**	**Peace River**	**Wabasca**	**Lloydminster**	**Carbonate Triangle**
Carbon	79.9	82.7	80.2	80.5	81.7	79.7
Hydrogen	8.3	7.6	8.2	8.2	8.2	7.9
Nitrogen	1.2	1.2	0.8	1.0	1.0	1.1
Oxygen	3.2	1.8	2.1	1.2	1.5	2.7
Sulfur	7.6	6.7	8.8	8.4	7.5	8.6

Approximately 40-50% of the total carbon is present in aromatic rings, which results in low hydrogen to carbon ratio (1.1-1.2) (Strausz and Lown, 2003). Sulfur is present in the form of thiophene and sulfide groups, nitrogen is present as pyrrolic nitrogen in aromatic rings, and oxygen is mainly present as carboxylic acid, ether, and esters (Strausz and Lown, 2003). Asphaltenes from different petroleum sources (Canada, Iran, Iraq, and Kuwait) presented similar nitrogen, carbon, and hydrogen content, while sulfur and oxygen varied significantly (Speight and Moschopedis, 1981). According to Speight and Moschopedis (1981), it is because asphaltenes can react with sulfur and oxygen when exposed to atmospheric air and elemental sulfur (e.g. minerals containing sulfur). Hydrocarbons present in asphaltenes are alkanes, naphthenes, and aromatics (Strausz and Lown, 2003).

2.1.1 Asphaltenes Characteristics

2.1.1.1 Molecular Weight

Molecular weight of asphaltenes is not exactly known. However, there is interest in molecular weight of asphaltenes, as it would help understand asphaltenes molecular structure. The knowledge of asphaltenes molecular weight would be beneficial for this study, as it would provide better understanding of molecular structure which would be more feasible to propose conversion chemistries for asphaltenes upgrading. In addition, more accurate reactions

[1] Data extracted from Strausz, O. P.; Lown, E. M. *The Chemistry of Alberta Oilsands, Bitumens, and Heavy Oils*. Alberta Energy Research Institute: Calgary, AB, 2003; pp. 459-662

stoichiometry between substrate, reactants, and catalysts would be achieved if the exact molecular weight was known.

Several techniques to measure molecular weight of asphaltenes have been reported. However, the results differ significantly. The difficult in measuring molecular weight is attributed to the ability of asphaltenes to form aggregates. The results found are in the range of 400 Da to 1500 Da for vapour pressure osmometry (VPO) technique, 3000 Da to 10000 Da for gel permeation chromatography (GPC) technique, 500 Da to 1200 Da for field ionization mass spectroscopy, and 500 to 1000 Da for time-resolved fluorescence depolarization technique (TRFD) (Masliyah et al., 2011; Mullins, 2008).

In VPO method, a solution is prepared with asphaltene and solvent. Then, molecular mass of the solute (in this case the solute is asphaltene) is calculated through the solute molar fraction obtained by the equilibrium vapor pressure and solution mass composition. As asphaltenes can agglomerate, the molecular mass obtained is related to this association instead of the monomer. Thus, in order to avoid asphaltenes aggregation, a higher dilution should be used, however, the equilibrium vapor pressure measurements obtained in this case would be close to the pure solvent. Therefore, the determination of molecular weight of asphaltenes is performed at different dilutions and the result is extrapolated leading to errors (Masliyah et al., 2011). On the other hand, according to Strausz and Lown (2003), asphaltenes precipitated from bitumen may also contain resins. Resins are defined by their adsorption properties, that is, they are the "portion of maltenes that is adsorbed on a clay" or "a portion of the maltenes that is eluted from silica gel by polar eluents". Thus, the low molecular weight obtained at high dilution might be due to the release of the resins instead of dissociation of aggregates (Strausz and Lown 2003).

In GPC method, molecular weight is determined according to the molecular size obtained by the time that the particles take to pass through a porous gel with known porous size. Big particles pass fast, while small particles go inside the porous taking more time to leave the column. As was the case with VPO, the errors related to this technique are also due to the agglomeration of asphaltenes, as the agglomerates are larger than the monomers, agglomerates can lead to misinterpretation of the results (Masliyah et al., 2011).

For a compound to be identified and its molecular weight obtained by mass spectroscopy, it should be ionized, because only ionized material is detected. The main difficulty with this method to measure molecular weight of asphaltenes is because asphaltenes are difficult to vaporize, ionize and to not decompose the asphaltenes during the analysis (Masliyah et al., 2011).

In TRFD technique the fluorescence decay lifetime is measured after polarization of the sample and the molecular size is obtained as it correlates with time measured of rotational diffusion of the molecule. The advantage of TRFD method to measure molecular weight of asphaltenes is that it works with highly diluted asphaltenes solutions, which avoids the aggregates (Mullins, 2008). Yet, even by dilution it cannot be guaranteed that aggregates already present will be dispersed. This technique is presented in more detail in Section 2.1.1.4.

2.1.1.2 Solubility of Asphaltenes

The onset of precipitation of asphaltenes from bitumen is dependent of several properties such as composition of the bulk oil, molecular composition, structure, size, conformation, and colloidal structure (Strausz and Lown, 2003).

Asphaltenes precipitation can occur during bitumen processing and cause fouling of pipelines and equipment. One example of where asphaltenes can precipitate is during bitumen transport in pipelines (where a solvent is blended with bitumen in order to reduce its viscosity). Therefore it is important to know the onset of precipitation for each blend and each process condition in order to avoid this problem (Gray, 2010).

There are some factors that are responsible for asphaltenes insolubility in paraffinic solvents and they are presented as follows.

One of the factors responsible for asphaltenes insolubility in paraffinic solvents is the asphaltenes tendency to aggregate. Even though the exact aggregation mechanism is not fully

understood (more details about this topic is found in Section 2.1.1.4), it is agreed that they can aggregate. Aggregation may be caused by different interactions such as hydrogen bonding, donor-acceptor interactions, π-π stacking of aromatic sheets, metal coordination, etc. (Mullins, 2008; Gray *et al*. 2011). According to Wiehe (2008), hydrogen bonding between asphaltenes molecules is one of the reasons that make asphaltenes insoluble in paraffinic solvents.

Another factor responsible for asphaltenes insolubility in paraffinic solvents is their high molecular weight. This is because the free energy of Gibbs ($\Delta G_m = \Delta H_m - T\Delta S_m$) should be negative for a solid to dissolve in a non-polar solvent. As large molecules such as asphaltenes do not have many possible arrangements, they will have lower entropy of mixing than small molecules. Large molecules also have greater enthalpy of mixing than small molecules because they have high interaction energy due to greater surface of interaction. Thus, it will result in higher ΔG_m, which will cause asphaltenes insolubility (Wiehe 2008).

High dispersion energy of asphaltenes molecules is another factor responsible for asphaltenes insolubility in paraffinic solvent. It is explained that the stacking of polycyclic aromatics in asphaltenes causes the high dispersion interaction energy between asphaltenes molecules that results in low solubility (Wiehe 2008).

Stability of asphaltenes in a solvent or a blend is verified by the solubility parameter. Solubility parameter is defined as the cohesive energy density ($\delta = [(\Delta H_v - RT)/V]^{1/2}$) or internal pressure ($\delta = \gamma V^{-1/3}$) of non-polar solvents. Solubility parameter indicates the solvency behavior of a solvent. The limitation of solubility parameter calculated through the equations above is that it works only for non-polar solvents as their primary intermolecular forces are London dispersion forces. The amount of precipitated asphaltenes correlates linearly with the solubility parameter of the solvent. Asphaltenes remain soluble when the solubility parameter of the solvent is higher than 17.1 $MPa^{1/2}$ and precipitation increases by decreasing solubility parameter. This statement explains the solubility of asphaltenes in toluene, once its solubility parameter is equal to 18.2 $MPa^{1/2}$ (Strausz and Lown, 2003).

The amount of precipitated asphaltenes in paraffinic solvent depends of several parameters including type of the paraffinic solvent, volume ratio of precipitant to bitumen, contact time, temperature, pressure and exposure to oxygen and light (Strausz and Lown, 2003).

The amount of precipitated asphaltenes increases with the decrease of carbon number in the paraffinic solvent. However, solvents with higher carbon number such as decane provide more inorganic material and higher ash content compared to the lower *n*-alkanes. These inorganic materials are called pre-asphaltenes and they are defined as the soluble material obtained after washing the asphaltenes with fresh paraffinic solvent. The type of paraffinic solvent also dictates the amount of solvent required to precipitate the asphaltenes. In general, *n*-heptane requires more volume of solvent than *n*-pentane. In addition, if an aromatic solvent such as benzene or toluene is present, an excess of paraffinic solvent is required in order to precipitate the asphaltenes (Strausz and Lown, 2003).

The contact time between the solvent and bitumen also influences the quantity of precipitated asphaltenes. In general, asphaltenes yield is constant after 12 hours of contact (Strausz and Lown, 2003).

Decrease of temperature leads to higher content of asphaltenes precipitation. It is explained that aggregates dissociate at high temperatures which causes dissolution. In addition, temperature changes the solubility parameter of asphaltenes and the solvent (Strausz and Lown, 2003).

As well as for temperature, the amount of precipitated asphaltenes increases with the decrease of pressure. This is because from Le Chatelier's principle, the increase of pressure will shifts the equilibrium to the side with lower volume. In bitumen, the aggregate asphaltenes are more closely packed, whereas in solution they will swell. Thus, asphaltenes volume is smaller in bitumen then in solution, which leads to increase in solubility with the increase of pressure. (Strausz and Lown, 2003).

When bitumen is exposed to air, the resins can oxidize and convert to asphaltenes. Because temperature and light accelerate oxidation reaction, asphaltenes content and asphaltenes molecular weight increases with high temperature and light exposure (Strausz and Lown, 2003).

2.1.1.3 Molecular Structure of Asphaltenes

The molecular structure of asphaltenes is not defined by a single structure; after all, the asphaltenes is a solubility class. Nevertheless, two representations (models) of the general configuration of asphaltenes molecules are reported in the literature based on different techniques such as TRFD, VPO, GPC, ruthenium-ion-oxidation (RICO), thermal degradation of asphaltenes, etc (Strausz and Lown, 2003; Strauz et al., 1992; Groenzin and Mullins, 2000). The models proposed are discussed below.

2.1.1.3.1 Archipelago Model

The archipelago model was proposed based on the results from RICO, thermal degradation of asphaltenes, GPC, VPO, reductive degradation, and spectroscopy methods. The suggested molecular structure contains small aromatic ring systems connected by bridges. An illustration of archipelago model is shown in Figure 2.1. These bridges might be alkanes, ethers, esters, sulfides and naphthenic carbons. These functional groups can also be present as side chains. The aromatic cores can also have heteroatoms such as sulfur and nitrogen, where some nitrogen may be present as porphyrins containing metals. The occurrence of bridges was proposed based on the results of RICO, because alkane chains connecting two aromatic rings will result in dicarboxylic acids, while alkane chains presented as side chains will result in carboxylic acid. Sulfides groups were also determined by RICO analysis, as saturated sulfides are oxidized to saturated sulphones. The number of sulfide bridges was determined by nickel boride (NiB) reduction reaction of asphaltenes. Naphthalene radical anion (NRA) reduction provided the number of aromatic rings in an aromatic ring system (up to four rings) (Strausz and Lown, 2003). RICO analysis did not provide only the presence of bridges between the aromatic cores, but also their quantification (Strausz et al., 1992; Strausz and Lown, 2003). It was shown that alkyl side chains might contain up to 32 carbons (being the most of the chains containing one carbon),

while alkyl bridges might contain up to 24 carbons (being the most of the bridges containing three carbons) (Strausz et al., 1992). In addition, each structural unit can have just one or two covalent bonds (Strausz and Lown, 2003).

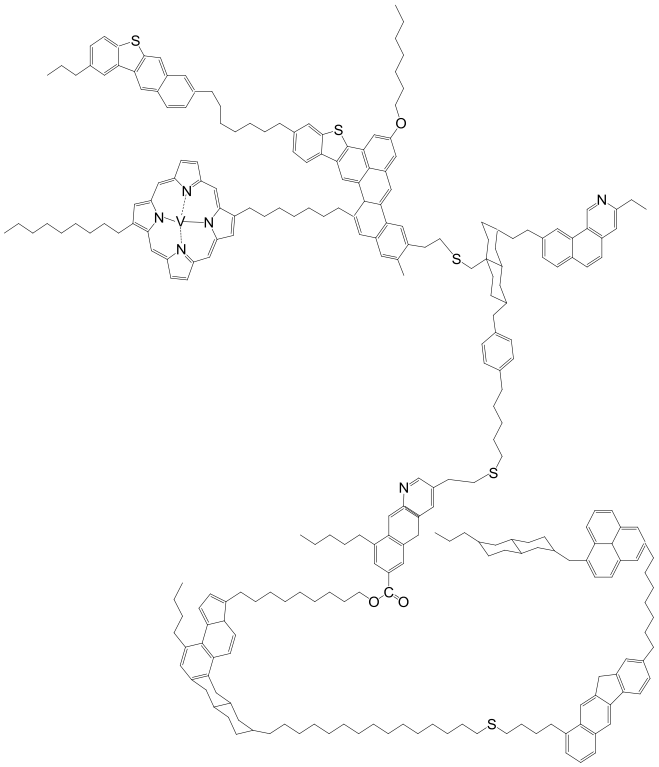

Figure 2.1. Illustration of archipelago model adapted from Strausz *et al*. (1992)[2]

In this model it is expected that the bridges are very flexible, thus, the aromatic ring systems would be randomly rotated in the crude oil. However, in the precipitated asphaltenes, the large aromatic rings systems stack, while the small aromatic ring systems still rotate randomly. However, if the stain of the bridges is too high, the larger molecules cannot achieve the planar alignment (Strausz et al., 1992).

Gray (2003) presents some evidences for archipelago model based on pyrolysis and coke behavior of asphaltenes. He states that only the archipelago model can provide the mass yield of volatiles obtained as well as a wide range of product sizes. Moreover, the continental model

[2] Adapted from Fuel, 71(12), Strausz, O. P., Mojelsky, T. W., Lown, E. M. The molecular structure of asphaltenes: an unfolding story, 1355-1363, Copyright 1992, with permission from Elsevier

(presented in Section 2.1.1.3.2) during pyrolysis would present mainly light ends due to the scission of side chains bonds followed by dehydrogenation and cracking of naphthenic rings. In addition, the cracking of asphaltenes obtained by supercritical fluid presented gas oil as the largest fraction, while naphtha presented minor amounts (naphtha is the only light liquid product expected from the continental model). Figure 2.2 shows the liquid products obtained during pyrolysis of asphaltenes for both molecular models to illustrate the statement made by Gray (2003).

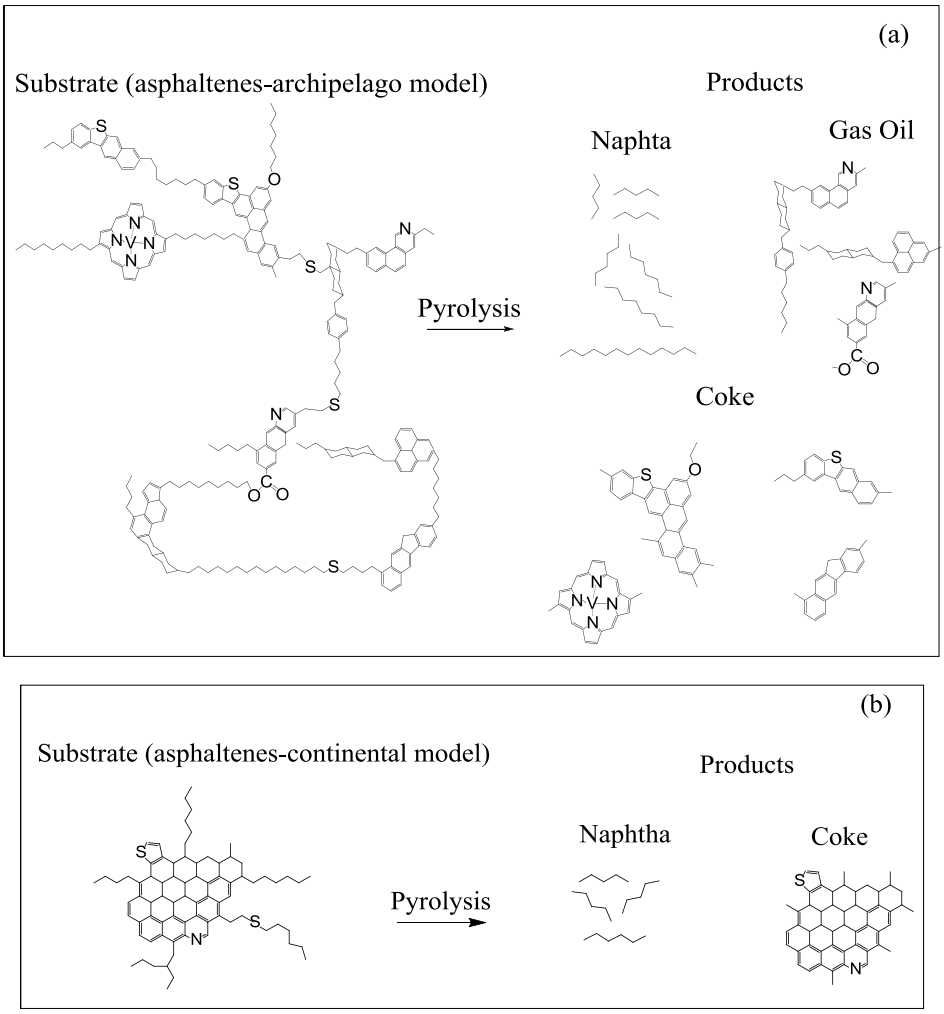

Figure 2.2. (a) Pyrolysis of asphaltene for archipelago model (b) Pyrolysis of asphaltene for continental model

2.1.1.3.2 Continental Model

The continental model proposes that asphaltenes consists of a fused ring system in the core of the molecule with alkane side chains with four or five carbons. This model (Figure 2.3) is also known as the "like-your-hand" model, as the core is like the palm and the alkane side chains represent the fingers (Mullins, 2011).

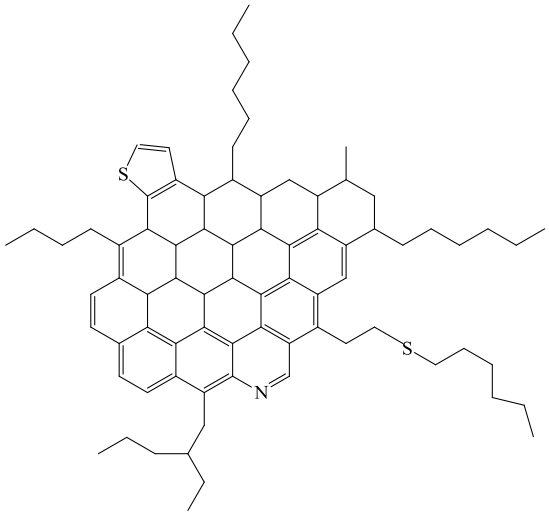

Figure 2.3. Illustration of continental model adapted from Mullins (2011)[3]

This model was proposed based on the results obtained from using the TRFD technique. In this technique, polycyclic aromatic hydrocarbons (PAH) in the asphaltenes molecules are polarized and the fluorescence decay lifetime is measured. The rotational correlation time measured when the molecule is submitted to rotational diffusion is directly related to its molecular size. It was found that the asphaltenes molecules were small with a molecular weight ranging from 500 to 1000 Da. It was also found by the emission wavelength that the molecule contains one or two chromophores with 7 fused ring systems on average (Groenzin and Mullins, 2000). However, some criticism regarding the use of this technique is reported. One of the main arguments is that the instrument used for the measurements is not appropriate, because it cannot detect decay times less than 300 ps (because the exciting flash time duration was 2 ns). Another argument is that the relation between correlation time and molecular size is demonstrated for pure solutions with

[3] Adapted from Annual Review of Analytical Chemistry, 4, Mullins, O. The asphaltenes, 393-418, Copyright 2011, with permission from Annual Reviews

known molecular geometry and a single chromophore. As asphaltenes is a complex mixture, this technique would not be applicable for asphaltenes, as the decay time is different for each component of the complex mixture (Strausz et al., 2008).

Apart the critique leveled against the continental model, a recent review was published about other analyses that support this model (Mullins, 2011). An example is the work performed by Sabbah *et al*. (2011). The authors used laser desorption laser ionization to obtain mass spectra of 23 model compounds and 2 petroleum asphaltenes samples. They observed that the two petroleum asphaltenes did not present fragmentation. The same behavior was observed for the models consisting of one aromatic core, while the models having more than one aromatic core showed easy fragmentation in the same range of laser pulse energy. They also found that the upper limit of molecular weight is 1500 Da. Therefore, they suggest that the architecture of asphaltenes is best represented by a continental model.

Physical characteristics of asphaltenes have also been reported to support the continental model. One characteristic is the color. It is explained that because it was found by TRFD technique that asphaltenes contain seven aromatics rings on average, they are fused in a single core in the continental model, while in the archipelago model these seven aromatic rings would be distributed in 2 or 3 fused ring systems. According to the authors, the isolated ring systems do not have color, and because asphaltenes are colored, this observation suggests that asphaltenes structure is better represented by a continental model. The other characteristic is adherence. They affirm that small aromatic ring systems are not sticky, while large aromatic ring systems are very sticky. Because asphaltenes is very sticky, they concluded that the continental model is the correct model for asphaltenes structure (Groenzin and Mullins, 2007).

This type of molecular structure of asphaltenes led to the development of the asphaltenes nano-aggregation concept, also known as Yen-Mullins model or modified Yen model (Sharma and Mullins, 2007). This type of aggregation is discussed in the Section 2.1.1.4.

2.1.1.3.3 Implications of the Molecular Structure for this Study

The strategies needed to convert asphaltenes into liquid products are clearly different for molecules that are predominantly of the archipelago structure (smaller linked aromatic cores) than for molecules of the continental structure (large fused aromatic cores). For all reactions carried out in this study (halogenation, Friedel-Crafts alkylation, and donor-acceptor by acid treatment), the model which is expected to be more difficult to accomplish the objective of producing liquid products is the continental model. This is because the insertion of a new element such as halogens to bonds common to two aromatic rings is expected to be more difficult to be achieved. Thus, for continental model there are few reactive centers. However, although there are more reactive centers in archipelago model, the bridges "show progressively increasing reactivity, as the aromatic rings are now forced towards coplanarity by the bridging side chain" which decreases the reactivity of PAHs (De La Mare and Ridd, 1959). The presence of substituents also influences the occurrence of each reaction. For example, electron withdrawing groups such as CO_2R and COR present in the archipelago model decrease the reactivity of the ring for halogenation reactions. Even though Friedel-Crafts alkylation reaction used in this study was focused in the conversion or removal of alcohol groups; ether, esters, and thioethers, as reported by the archipelago model to be present in asphaltenes, can also be affected by the reaction (Wang *et al*., 2008). Moreover, the purpose of treat asphaltenes with acid is to remove metals from asphaltenes structure. Nevertheless, the method can also break ester bonds reported to be present in the archipelago model (Van Bodegom et al., 1984). Details for each reaction utilized in this study are present in their correspondent section along this chapter.

2.1.1.4 Asphaltenes Association

It is known that asphaltenes can associate and form colloidal-sized aggregates in crude oil. However, the mechanisms of association and limiting factor of its growth is not known (Strausz and Lown, 2003; Masliyah et al., 2011; Friberg, 2007).

As reported by Strausz and Lown (2003), Masliyah et al. (2011), and Friberg (2007), it was initially believed that asphaltenes were present like surfactants as inverse micelles in organic

medium. However, some points do not support a micelle model. According to the Masliyah et al. (2011) and Friberg (2007), surfactants in an aqueous system form micelles after critical micelle concentration (CMC) is achieved (indicated by the sharp transition between micellar and monomer molecules). In micelle state, the polar heads are facing the aqueous phase, while the non-polar tails are oriented inside the micelle. The limiting factor of growth in this case is the repulsion between the polar groups. When the surfactant is introduced in an organic media there is the formation of inverse micelles. That is, the polar heads are located in the interior of the micelle, while the tails are oriented facing the organic phase. Inverse micelles in organic media are stabilized by intermolecular forces. However, unlike micelle formation in an aqueous system, there is no CMC in inverted micelles in organic media. This is because inverted micelles contain few monomer molecules in organic media, while micelles in an aqueous system contain around 50 to 100 molecules. The size of the micelles in water is due to the repulsive interactions between the polar heads and geometrical factors, while the size of reverse micelles in organic media is due to the attraction of polar heads mediated through the presence of water. Asphaltenes contain around two to six monomers in their aggregations, therefore, it is concluded that CMC is not presented in organic media and cannot explain the aggregation formation in asphaltenes, although there are reports in the literature about CMC values of asphaltenes (Masliyah et al., 2011). The association of asphaltenes cannot be explained by inverse micelles in organic media, because "there is no mechanism that would give a reduction of the intermolecular forces with increased number of molecules added to as stacked association structure" (Friberg, 2007). In addition, the colloidal model of asphaltenes association states that the micelles are stabilized by the resins adsorbed on the surface of colloidal particles (asphaltenes) (Pfeiffer and Saal, 1940). However, Masliyah et al. (2011) refuted this claim of the model description by saying that a published work presents a colloidal-sized aggregate of asphaltenes in toluene in the absence of resins.

An asphaltenes aggregation model is proposed by the Yen-Mullins model or modified Yen model. This model was proposed based on work performed with high-resolution transmission electron microscopy. In this model, the molecular structure of asphaltenes is that of the continental type. The fused rings in the core of the structure stack by van der Waals interaction of π electrons by decreasing solubility of asphaltenes. However, alkane side chains attached to

PAH causes steric repulsion which increases solubility and limit the size of aggregates (Sharma and Mullins, 2007). Van Bodegom et al. (1984) also observed that the solubility of Morwell coal containing alkyl side chains was higher than the simple coal fragments. The number of layers in asphaltenes per stack is 2-3 and the layer spacing is around 3.7 Å. In addition, the aromatic ring system measures 1 nm in diameter. An illustration of this aggregation model is shown in Figure 2.4. These aggregates are formed at low concentrations with few molecules of asphaltenes and are called nano-aggregates. When the concentration is increased, nano-aggregates will associate and form clusters (Sharma and Mullins, 2007). The authors point out that the nano-aggregates are formed when the critical nano-aggregation concentration (CNAC) is achieved and the literature also report CNAC values for the initial asphaltene nano-aggregation (Sharma and Mullins, 2007; Mullins, 2011). CNAC is similar to CMC in surfactants, that is, below CNAC there is monomer state and above CNAC there is a nano-aggregate state (Mullins, 2008). However, Masliyah et al. (2011) contested this point by saying that CNAC and CMC do not occur at low aggregation number. In this case, "small aggregation number necessarily implies a diffuse transition from a monomer to an aggregate state".

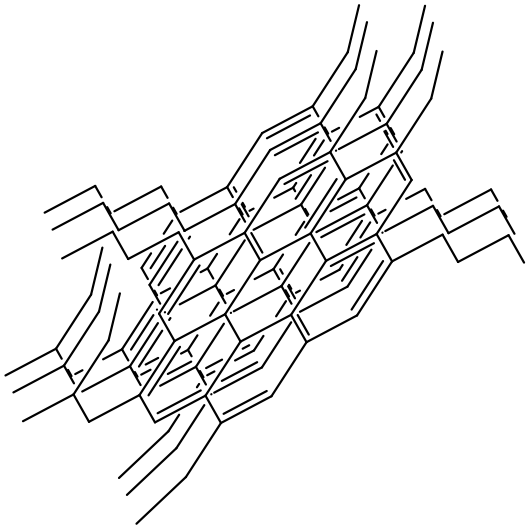

Figure 2.4. Illustration of Yen-Mullins model or modified Yen model as described by Sharma and Mullins (2007)

There is another association model for asphaltenes reported in the literature. This model describes association like polymerization and considers that the asphaltenes structure is

described by the archipelago model. Because there are different groups in the molecule (acids, ketones, pyridines, thiophenes, aromatic rings, etc), the molecule can link in several manners. Thus, free asphaltenes are considered propagators (because of their multiple active sites) and they can form aggregates. In addition, resins molecules are treated as terminators of the propagating polymerization reaction, because they can have just one active site and consequently link with just one molecule. The participation of resins in this model are different from the colloidal model, because in this case they are part of asphaltene/resin oligomers, while in the colloidal model they are adsorbed on the asphaltene colloid surfaces (Agrawala and Yarranton, 2001). Figure 2.5 shows an illustration of this aggregation model.

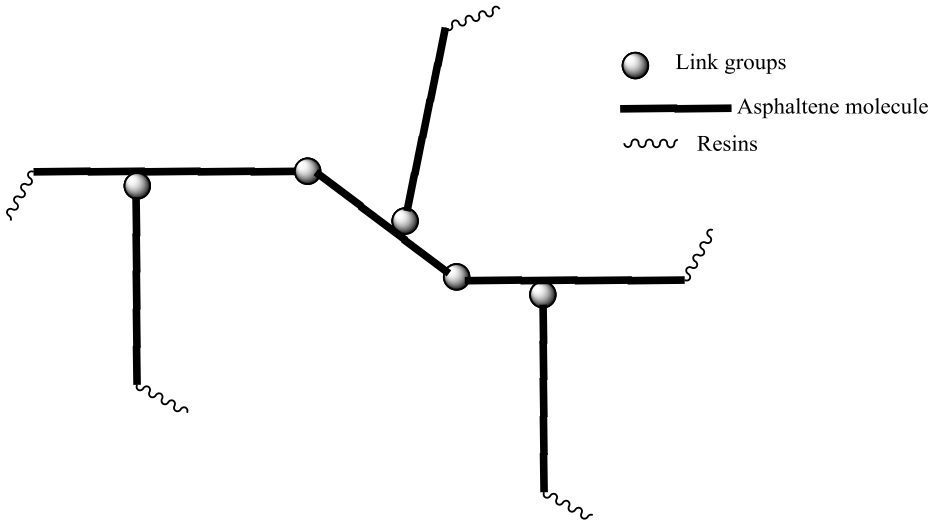

Figure 2.5. Illustration of polymerization aggregation model adapted from Agrawala and Yarranton (2001)[4]

A porous structure model of asphaltenes aggregation was suggested by Zielinski *et al*. (2010). This model was developed by using NMR relaxation and diffusion experiments. In this model, maltenes molecules rapidly migrate "between these porous asphaltene aggregates and regions free of asphaltene".

The most recent model was proposed by Gray *et al*. (2011) based on observations reported for asphaltenes. This aggregation model consists of supramolecular assembly (non-covalent

[4] Adapted with permission from Agrawala, M. and Yarranton, H. W. An asphaltenes association model analogous to linear polymerization, *Ind. Eng. Chem. Res*. 40, 4664-4672. Copyright 2001, American Chemical Society.

interactions) of molecules in an archipelago model resulting in host-guest interactions in a three dimensional porous network. The interactions include acid-base interactions between carboxylic acids and bases (pyridines), hydrogen bonding between carboxylic acid and hydroxyl groups and with weak nitrogen bases, metal coordination of nickel and vanadium, hydrophobic pockets driven by van der Waals interactions, and π-π stacking between parallel aromatic rings. This model is illustrated in Figure 2.6.

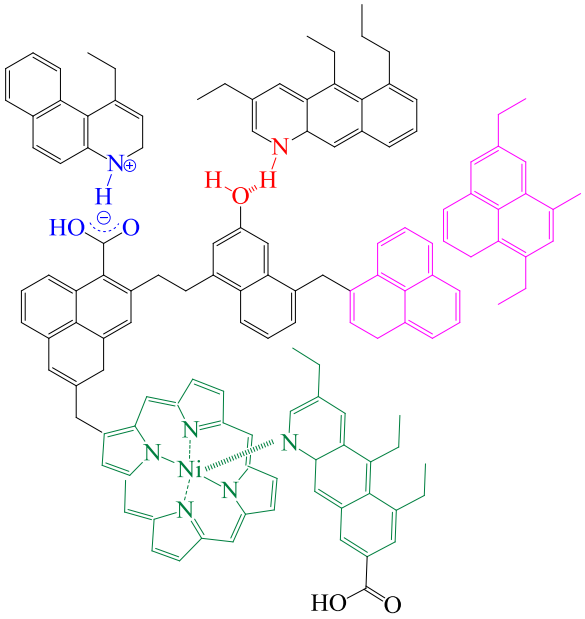

Figure 2.6. Illustration of supramolecular assembly model: acid-base interaction (blue), hydrogen bonding (red), metal coordination complex (green), π-π stacking (pink), adapted from Gray *et al.* (2011).[5]

2.1.1.4.1 Implications of the Nature of Asphaltene Association for this Study

Just like solubility in bitumen cannot be described purely in terms of molecular solubility, it is not possible to discuss precipitation of asphaltenes purely in terms of molecular insolubility. The strategies required to convert asphaltenes into liquid products must take cognizance of the nature of the association that lead to asphaltenes precipitation. Disrupting inverse micelles, π-π-

[5] Adapted with permission from Gray, M. R., Tykwinsk, R. R., Stryker, J. M., Tan, X. Supramolecular assembly model for aggregation of petroleum asphaltenes. *Energy Fuels,* 25, 3125-3134. Copyright 2011, American Chemical Society

stacking in nano-aggregates, polymer-type, and supramolecular assembly (host-guest interactions in a porous structure) associations all require different approaches.

Inverse micelles are stabilized by the attraction of polar compounds due to the presence of water. Thus, the strategy for conversion of asphaltenes into maltenes would involve a procedure to overcome the attraction of the polar compounds if the inverse micelles model is true.

Disruption of polymer-type model involves the cleavage of the bounded link groups which connect one asphaltene molecule to another. Strategies for this model would be those to break the type of bonds involved in connecting the link groups together such as hydrogen bonding. In this study, Friedel-Crafts alkylation was used for disruption of hydrogen bonds in asphaltenes and acid treatment was used to remove multivalent cations that may link different asphaltenes molecules through carboxylic bridges.

Both nano-aggregates and supramolecular assembly model present π-π stacking. Thus, tactics to disrupt this type of interaction should be used during conversion of asphaltenes studies. In this study, one strategy was used for disruption of π-π stacking (halogenation reaction). The reasons why this reaction can disrupt this interaction are presented separately in Section 2.2. Comparing the two models containing π-π stacking, it is believed that the reagents may have more difficulty to access the aromatic rings presented in the middle layer of nano-aggregates model, as the middle layer is less exposed. On the other hand, the porous structure presented in the supramolecular assembly facilitates diffusion of reagents leading to easier access to the components present in the interior of the structure.

2.1.2 Summary

Based on the literature dealing with asphaltenes, it was possible to highlight the following implications for this study:

a) If the molecular structure of asphaltenes is best represented by the archipelago model, the reactions (halogenation, Friedel-Crafts alkylation, and donor-acceptor by acid treatment)

would have more chance to succeed due to the higher presence of reactive centers. However, the non-planarity occasioned by the bridges would be a problem for halogenation reaction, as PAH containing bridges are less reactive for electrophilic aromatic substitution (De La Mare and Ridd, 1959).

b) If the molecular structure of asphaltenes is best represented by the continental model, it would be expected that reactions will be less effective. This is because the rings present in the middle of the structure are less exposed and consequently less reactive. In order to convert asphaltenes of a continental type, more aggressive conversion chemistries should be considered, such as oxidative ring-opening of aromatics. This type of chemistry was not investigated in the present study.

c) If the aggregation model of asphaltenes is best represented by nano-aggregates, it would be expected that π-π-stacking can be disrupted by halogenation. However, halogenation of nano-aggregates would take place with lower efficiency compared to supramolecular assembly model, due to the difficult in access the rings presented in the middle layer.

d) If the aggregation model of asphaltenes is best represented by the supramolecular assembly model in a porous structure, faster and/or more efficient conversion would be expected due to higher accessibility of the reagents to the reactive centers, occasioned by diffusion of the solvent into the porous structure. However, because several interactions are anticipated in this model, lower conversion of asphaltenes to maltenes could be achieved by a single conversion strategy as other functional groups and interactions can remain unaffected or can be caused by the reactions.

2.2 Halogenation

Halogenation is a reaction that inserts a halogen, fluorine (F), chlorine (Cl), bromine (Br), or iodine (I), into a compound (March, 1992). Halogens contain seven valence electrons which make them electron-deficient. However, they are found in nature as salts of the halide ions and not in their elemental form. Halogens also have the property to form diatomic molecules (F_2,

Cl_2, Br_2, and I_2). These diatomic molecules are weaker electrophiles and special conditions such as use of catalyst allow increase the electrophile nature of molecular halogens to react with aromatic systems in electrophilic aromatic substitution (Hepworth et al., 2002).

Aromatics (the main organic functional group present in asphaltenes) are conjugated cyclic systems. Benzene has high electron density moving through π-bonds which is evenly distributed in the ring, while other arenes have a slightly different charge on each carbon due to resonance and other substituents effects. Thus, because aromatics are electron rich, they can react with the halogens. Halogens are electronegative, therefore, when they are introduced to aromatics they can decrease the electron density of aromatic core (Hepworth et al., 2002). Fluorine has the highest electron-withdrawing inductive effect, followed by chlorine, bromine and iodine. Thus, halogens "make the aromatic nucleus deficient in electrons, as is shown by the dipole moments of the halogenobenzenes" (De La Mare and Ridd, 1959).

Halogenation of aromatics (Figure 2.7) occurs by electrophilic substitution reaction which consists of two steps. In the first step, the halogen attacks the ring by forming an arenium ion (a resonance hybrid) (March, 1992). The attacked carbon in the ring changes from sp^2 to sp^3 and the aromaticity is momentarily destroyed (Hepworth et al., 2002). Then, the second step consists of the release of a proton (hydrogen), reversion to sp^2 and restoration of the aromatic ring (March, 1992, Hepworth et al., 2002). Because the first step is slower than the second, it is rate-determining (March, 1992).

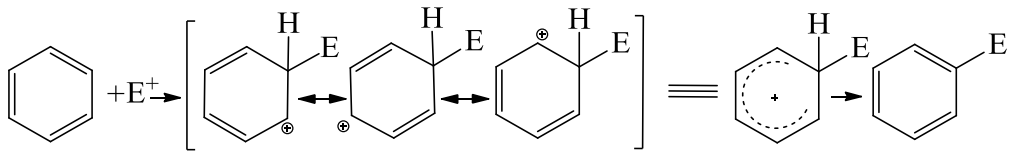

Figure 2.7. Schematic of electrophilic aromatic substitution of aromatics adapted from Smith (2013)[6]

[6] Reprinted from March's Advanced Organic Chemistry, Reactions, Mechanisms and Structures 7th ed, Michael B. Smith, John Wiley and Sons. Copyright 2013 John Wiley and Sons

Halogenation of aromatics can also occur by free-radical mechanism, however it is less common to occur. In this case, the bond of molecular halogen is broken due to the application of energy such as heat or light, and then the radicals containing an unpaired electron are formed and will attack the aromatic ring. However, halogenation by using this mechanism is harder to control and only bromination and chlorination of the aromatic ring are common. Fluorination is violent, making it difficult to control the reaction and the carbon-iodine bond is very weak, making iodination thermodynamically unfavorable (Parsons, 2000). Free-radical reaction of benzene with chlorine can result in addition product (Hepworth et al., 2002). Nevertheless, in aromatics containing side-chains, halogenation by free-radical reaction will occur in the side chains as their carbon-hydrogen bonds are weaker than in the aromatic ring (Parsons, 2000). Therefore, as pointed out later, the most aromatic ring halogenations with molecular halogens occurs in special conditions, such as in the presence of a Lewis acid catalyst (De La Mare and Ridd, 1959).

The main methods to perform halogenation are presented below:

The first consist in the use of only halogen molecules (De La Mare and Ridd, 1959). However, benzene and PAH do not react with halogen molecules, unless the molecules can be dissociated into their corresponding free radicals. For unsubstituted aromatics, halogen substitution reactions with PAH are faster than for benzene (March, 1992). Free-radical reaction with halogen molecules is more often used when the purpose is to halogenate side chains of the aromatics containing substituents (Krishna Mohan and Narender, 2012).

The second method also uses halogen molecules, but in the presence of a catalyst (Lewis acid) in order to increase the electrophile nature of the halogen to react with aromatic ring (De La Mare and Ridd, 1959). In this case, one of the halogen atoms present in the molecule donates a pair of electrons to the catalyst and becomes electron deficient. Then, a complex is formed between the halogen molecule and the catalyst and this complex is the electrophile (Hepworth et al., 2002). At the end of the reaction, the catalyst is regenerated and a hydrogen halide is formed (Krishna Mohan and Narender, 2012). The main drawback of Lewis acid catalyzed halogenation is that the process must make provision for catalyst recovery after synthesis, because of many of the Lewis acid catalysts are corrosive and/or toxic.

The third and newer method consists of using halide salts and oxidants. The mechanism involves oxidation of the halide salts into their positive halogens or hypohalous acids (Firouzabard et al., 2009). Positive halogens are the most effective reagents in aromatic substitution because they are more electrophilic reactive species (De La Mare and Ridd, 1959; Hepworth et al., 2002). Recent studies have reported the use of oxone as oxidant agent, due to its lower toxicity and higher efficiency compared to other oxidants (Krishna Mohan and Narender, 2012; Kumar et al., 2010; Firouzabadi et al., 2009; Lee et al., 2002; Narender et al., 2002a; Narender et al., 2002b; Tamhankar et al., 2001; Narender et al., 2002c). Figure 2.8 illustrates the reactions involved in halogenation with oxone reagent. In all studies, substitution occurred in the ring, even for compounds presenting side chains. The main advantage of this methodology is to achieve the same results than Lewis acid catalyzed halogenation with a simpler procedure and non-expensive reagents. Nevertheless, the effectiveness and regioselectivity is higher by using higher polar solvents such as water and methanol, although for some systems acetonitrile solvent presented higher efficiency. Oxidation of molecular iodine with other oxidants such as hydrogen peroxide is also reported, as molecular iodine is less reactive and does not react with aromatics (Hepworth et al., 2002). However, oxone/iodine salts have shown higher halogenation than hydrogen peroxide/iodine (Krishna Mohan and Narender, 2012; Firouzabadi et al., 2009; Narender et al., 2002a).

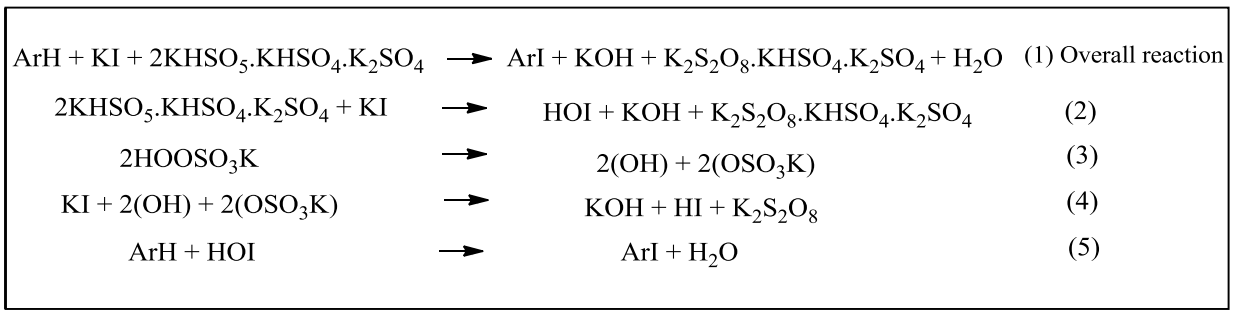

Figure 2.8. Mechanism of halogenation of aromatics with oxone (Narender et al., 2002a)[7]

[7] Reprinted from Synthetic Communications, 32(15), Narender, N., Srinivasu, P., Kulkarni, S. J., Raghavan, K. V. Regioselectivy oxyiodination of aromatic compounds using potassium iodide and oxone®, 2319-2324, Copyright 2002, with permission from Taylor & Francis

The presence of side chains and heteroatoms in the aromatic ring influences halogenation efficiency in the ring by changing the reactivity of the molecule and controlling orientation of attack (Hepworth et al., 2002; De La Mare and Ridd, 1959). The influence during halogenation of each group present in asphaltenes is discussed below.

A group presented as side chain might be an electron-donation group such as alkyls, alcohols, and amino or electron-withdrawing group such as halogens, NO_2, CO_2R, COR, CN, and SO_3R (Newkome and Paudler, 1982; Hepworth et al., 2002). Electron-donor groups increase electron density of the ring, while electron-withdrawing groups decrease electron density of the ring. Therefore, electron-donor groups increase electrophilic attack and electron-withdrawing groups decrease electrophilic attack.

In the continental model of asphaltenes the most of side chains are alkyls, some of which contain sulfur atoms as sulfides (Mullins, 2008). As alkyls are electron-donor groups, they increase the reactivity of the ring for electrophilic attack (Hepworth et al., 2002). On the other hand, in the archipelago model, groups such as CO_2R and COR can also be attached in the aromatic ring, which would decrease electrophilic attack as they are electron-withdrawing groups (Strausz and Lown, 2003; Hepworth et al., 2002). However, it is important to note that if halogenation is performed at high temperature, in the presence of UV light, and/or the absence of a suitable catalyst, the halogenation will occur at the side chains instead of the ring (Krishna Mohan and Narender, 2012).

Heteroaromatics are also found in petroleum asphaltenes and is described by both molecular models. The main heteroaromatics present in asphaltenes are present as heterocyclic pyridine, pyrrole, and thiophene rings that form part of the larger structure (Strausz and Lown, 2003; Mullins, 2008). Electrophilic substitution of pyridine is very difficult and is possible just under severe conditions (March, 1992). This is because the electron-density is drawn by the nitrogen due to its higher electronegativity (Newkome and Paudler, 1982). On the other hand, pyrrole and thiophene are substituted faster than benzene (March, 1992). It is explained that for these groups, the six π-electrons are distributed over four carbons instead of six. Moreover, differently to benzene, electron-withdrawing substituents help promote monosubstitution of pyrrole, while

carboxylic acids substituents in pyrrole are substituted by bromine and iodine (Newkome and Paudler, 1982).

Aromatic rings in asphaltenes are present as polycyclic aromatic hydrocarbons (fused aromatic systems) in both proposed molecular models (Strausz and Lown, 2003; Mullins, 2008). These PAH differ in some aspects during halogenation compared to benzene on its own (De La Mare and Ridd, 1959; March, 1992). PAH are substituted faster than benzene because there are more delocalization of charges in arenium ions (March, 1992). In addition, substitution tends to occur at the rings centrally located instead of the outermost rings (De La Mare and Ridd, 1959). Nevertheless, if one of the rings contains a substituent, halogenation tends to occur in the substituted ring. Addition reactions tend to accompany substitution reactions in PAH with no substituents. However, substitution predominates if light is excluded. Halogenation of phenanthrene is shown on Figure 2.9 to illustrate this statement. According to the authors, both reactions involved the common intermediate and addition reaction was reversible and independent of substitution (March, 1992).

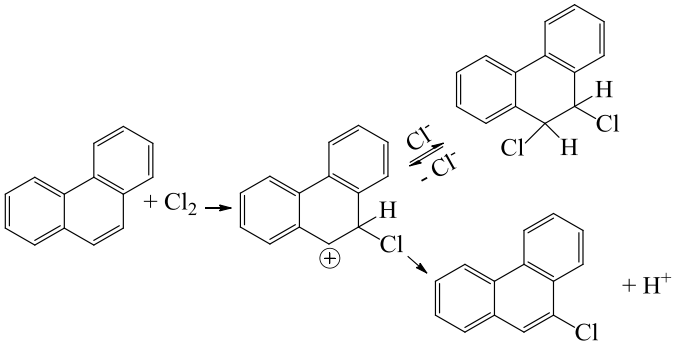

Figure 2.9. Addition and substitution halogenation in phenanthrene (De La Mare and Ridd, 1959)[8]

Another characteristic of PAH in electrophilic aromatic substitution is that aromatics containing bridges (as in archipelago model) are less reactive because "the rings are forced towards coplanarity by the bridging side chains". For example, diphenyl that is bridged is 290 times less reactive than fluorene that is planar (De La Mare and Ridd, 1959).

[8] Adapted from De La Mare, P. B. D. and Ridd, J. H. *Aromatic substitution: nitration and halogenation*. Butterworths Scientific Publications: London, 1959; pp. 5-25, 105-209.

2.2.1 Reports on Halogenation of Asphaltenes

There are few reports in the literature regarding halogenation of asphaltenes by using different methods and they are presented below.

The first report is iodination of petroleum asphaltenes and resistivity measurement of iodine-asphaltenes complexes. Iodination methodology is not very clear and it seems that iodine was introduced to asphaltenes by mixing two different stock solutions (benzene + iodine and benzene + asphaltenes) at different concentrations followed by lyophilization to obtain powered solids for resistivity measurement. Iodine uptake ranged from 15.7 to 17.2%. The authors concluded that iodine formed a donor-acceptor complex (Figure 2.10) with the aromatic portion due to an observed absorption at 1080 cm^{-1} in the infra-red spectra, while C-I frequencies was not observed. In the X-ray diffraction analysis they observed a new band, which led to the conclusion that iodine molecules intercalated between the layers of the aromatic systems of asphaltenes. They also observed an iodine:asphaltene ratio equal to 1.5:1 and suggested that the size of aromatic disks can accommodate more than one molecule of iodine (Sill and Yen, 1969).

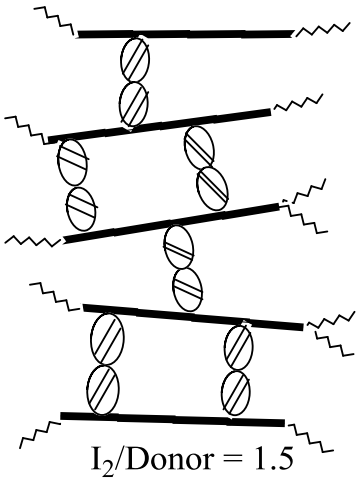

Figure 2.10. Proposed model of asphaltene-iodine complex adapted from Sill and Yen (1969)[9]

[9] Adapted from Sill, G. A.; Yen, T. F. Semiconduction of iodine complexes of asphaltenes. *Fuel* 1969, *48*, 61-74.

Halogenation of Athabasca asphaltenes with elemental halogen in the absence of catalyst was carried out by Moschopedis and Speight (1971a). They achieved ~35 wt % chlorine incorporation during chlorination, ~37 wt % bromine incorporation during bromination, and ~11 wt % iodine incorporation during iodination, all expressed on a product mass basis. Nevertheless, because the reactions were conducted without catalyst, most of chlorine was substituted in the alkyl and naphthenic moieties (~85 % of Cl incorporated), while the remainder was added to the aromatic portion. All bromine and iodine were substituted in the alkyls and naphthenic moieties. However, iodinated asphaltenes were further extracted with ethanol or ether and iodine was removed during extraction as hydrogen iodide. The authors suggested that the reaction resulted in σ-bonding of halogens to the asphaltenes instead of the formation of a charge-transfer complex. They came up with this hypothesis because only up to 20% of the halogen was removed during reflux with aqueous sodium hydroxide and at the same time the O/C ratio was increased. Figure 2.11 shows a representation of the chemistry of an alkylbenzene with halogenated alkyl substituent and sodium hydroxide to help understand the results obtained when halogenated asphaltenes were refluxed with sodium hydroxide. The introduction of –OH groups in asphaltenes obtained by hydrolysis of the chloro-asphaltenes did not improve water-solubilization of asphaltenes (Moschopedis and Speight, 1971b). Physical properties of the halogenated asphaltenes also changed. They were black, shiny and sparingly soluble in benzene and carbon tetrachloride (Moschopedis and Speight, 1971a).

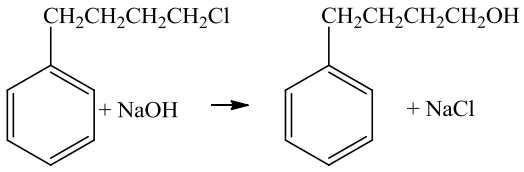

Figure 2.11. Illustration of the reaction between benzene with halogenated alkyl substituent and sodium hydroxide

Speight (1971) also performed chlorination of asphaltenes using metal chlorides. The physical characteristics of halogenated asphaltenes were the same compared to the halogenation with elemental halogen. Although chlorine was successfully bound to asphaltenes, the reaction was accompanied by dehydrogenation. The author proposed a dehydrogenation condensation instead of elimination with olefin formation, because IR spectroscopy did not present bands

corresponding to C=C bonds (Speight, 1971). An illustration of dehydrogenation by condensation and olefin formation reactions are shown in Figure 2.12.

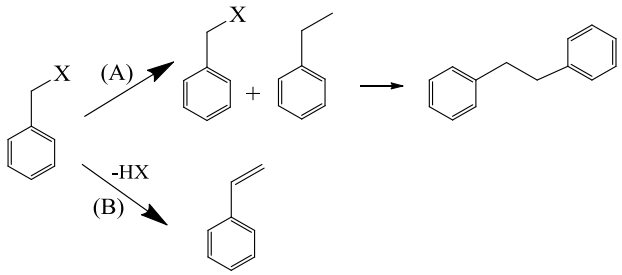

Figure 2.12. Illustration of dehydrogenation reactions: (A) condensation (B) olefin formation

Chlorination of asphaltenes from Saudi Arabian crude oil is also reported. The procedure consisted of using sulfuryl chloride as chlorinating agent with an initiator (azoisobutylnitrile). The reaction starts with radical formation from sulfuryl chloride and abstraction of a hydrogen atom. Infra-red analysis showed that chlorination occurred in aliphatic carbons as well as aromatic carbons (Siddiqui, 2009).

Athabasca asphaltenes were also halogenated by the Gomberg reaction. The halogenating agent was *p*-halophenyl and the product was (*p*-halophenyl)asphaltene. Unfortunately, the procedure and results were not reported in detail by Moschopedis and Speight (1970).

Fluorination of petroleum asphaltenes was not successful. The authors suggested that the failure was caused by molecular association of asphaltenes (Kowanko et al., 1978).

2.2.2 Implications for this Study

One of the possible interactions responsible for asphaltenes aggregation is π-π stacking of aromatic sheets. Based on the chemistry of halogenation reaction it could be possible to provide a steric disruption of π-π stacking of aromatic sheets with halogenation. Large halogens such as Br and I could decrease the electron density of the condensed aromatic structures by bringing the aromatic sheets apart. The chemistry challenges are alkyl halogenation, addition reactions, and hydrogen bonding.

2.3 Friedel-Crafts Alkylation

Friedel-Crafts alkylation reaction was discovered in May 1877 by Charles Friedel and James Mason Crafts (Olah *et al*., 1991). The first experiments were conducted by using alkyl halides as alkylating agents and electron-rich arenes in the presence of strong Lewis acid catalysts, specially $AlCl_3$ (Roberts and Khalaf, 1984). However, since its discovery, many other alkylating agents and catalysts have been reported. The mechanism of the reaction and products depend of the alkylating agents and catalysts employed. The alkylating agents usually used in Friedel-Crafts alkylation are ethers, esters, alcohols, alkanes, alkynes, alkanes, ketones, aldehydes, mercaptans, and thyocianates, while the catalysts are acid halides, metal alkyls and alkoxides, acidic oxides, sulfides, modified zeolites, acidic cation- exchange resins, proton acids (Brønsted acids), superacids, Lewis superacids, Brønsted-Lewis superacids, and solid superacids (Olah *et al*., 1991). The choice of alkylating agent and catalyst used in Friedel-Crafts alkylation reaction depends on the functional group that is desired to convert and what type of product is expected to obtain with the reaction.

The reason why Lewis acids are used as catalysts is because they can accept electrons, as they are electron deficient. The mechanism regarding Lewis acid catalysts is that they react with the functional group that has a "donor atom with nonbonded pair of electrons". Then, a carbocationic species is formed which attacks the π-donor substrate. However, some strong Lewis acid catalysts, as $AlCl_3$ used in the early experiments, are very sensitive to moisture and oxygen. Because it is very difficult to keep a completely water free environment some impurities, also called cocatalysts, are also found in the reaction medium. These cocatalysts can be trace amounts of acids that originated from hydrolysis of the metal halides, or oxygen and organic halides (Olah *et al*., 1991).

$FeCl_3$ is a Lewis acid catalyst and the more recent works have reported its use in catalytic Friedel-Crafts alkylation reaction. The use of $FeCl_3$ has increased because the exclusion of air and moisture is not necessary. In addition, it is a cheap catalyst and has been shown to be the

most active and selective catalyst when compared to other catalysts such as $ZnCl_2$, $MnCl_2$, $CuBr_2$, etc (Iovel *et al*., 2005; Wang *et al*., 2008; Li *et al*., 2008).

One interesting fact about Friedel-Crafts alkylation is that once an alkyl group is introduced to the aromatic ring, other alkyl groups can also be attached resulting in di-, tri-, and higher alkylated benzenes. In addition, transfer of alkyl groups from one aromatic ring to another can takes place during alkylation due to the effect of the catalyst. Moreover, after alkyl side chain attachment, isomerization of the side chain can also occur (Roberts and Khalaf, 1984).

2.3.1 Friedel-Crafts C-Alkylation Reaction

Friedel-Crafts *C*-alkylation reaction results in a C-C bond formation. For example, some functional groups such as alcohol groups can be removed from a molecule by using an aromatic as the alkylating agent. Some studies are reported in the literature regarding removal of alcohol groups by using $FeCl_3$ as catalyst and aromatics as alkylating agent and some of them are presented below.

One study is the work conducted by Iovel *et al*. (2005) which showed that some functional groups attached to aromatic rings such as -H, -OMe, -F, and -Cl can be removed from the ring by reacting the molecules with *o*-xylene in the presence of $FeCl_3$ catalyst. Figure 2.13 illustrates this reaction.

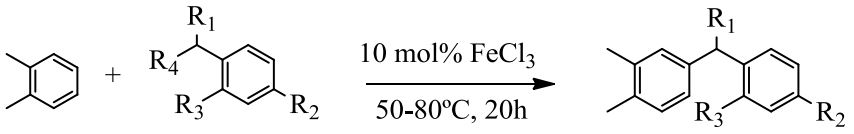

R_1 = H, Me, Ph, CH_2CO_2Et, CN
R_2 = H, OMe, Cl, F
R_3 = H, Cl, F
R_4 = OH, OAc, OCO_2Me, Cl

Figure 2.13. Reaction of *o*-xylene with different benzylating agents (Iovel *et al*., 2005)[10]

[10] Reprinted from An efficient and general iron-catalyzed arylation of benzyl alcohols and benzyl carboxylates, Iovel, I.; Mertins, K.; Kischel, J.; Zapf, A.; Beller, M., *Angew. Chem. Int*. 44. Copyright 2005 WILEY-VCH Verlag GmbH & Co. KGaA, Weinheim

Wang *et al*. (2008) also studied the reaction between several benzyl methyl ethers and different arenes such as substituted aromatics and thiophenes. The reaction was also catalyzed by $FeCl_3$ and the objective was formation of C-C bonds and removal of the –OMe functional group through sp^3 C-O activation of benzyl methyl ether. Figure 2.14 shows some of the reactions conducted in that work. They observed that both electronic effects and steric effects were responsible for the selectivity of the reaction. For instance, aromatics containing side chains such as mesitylene, 1,2,4,5-tetramethylbenzene, and pentamethylbenzene presented lower yields, even when higher temperature was used. They attributed this result to steric hindrance of methyl groups. On the other hand, thiophene and 2,5-dimethylthiophene presented high yields and high selectivity. Because both asphaltenes molecular structure models present aromatics containing side chains, the steric effect can decrease the efficiency of the reaction catalyzed by $FeCl_3$ for formation of C-C bonds.

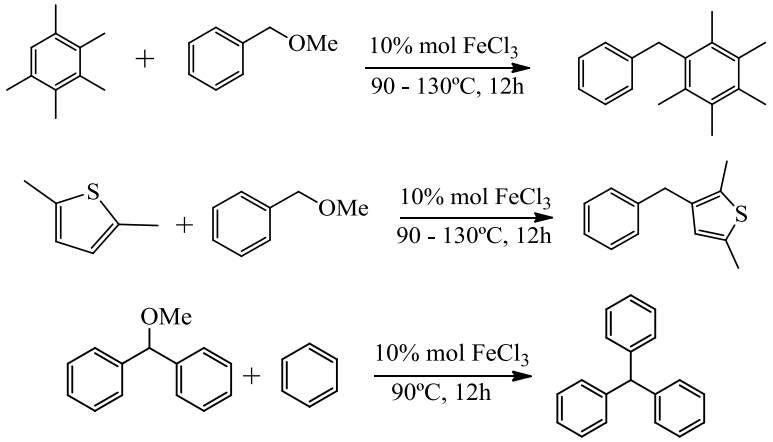

Figure 2.14. Friedel-Crafts alkylation between benzyl methyl ethers and arenes (Wang *et al*., 2008)[11]

Friedel-Crafts alkylation between aromatic aldehydes and arenes catalyzed by $FeCl_3$ is also reported and is shown in Figure 2.15. Unlike the benzyl methyl ether substrate, substitution and functional groups in the substrate did not affect the yield. However, for the reaction to occur, the

---

[11] Reprinted from Tetrahedron Letters, 49, Wang, B-Q.; Xiang, S-K.; Sun, Z-P.; Guan, B-T.; Hu, P.; Zhao, K-Q.; Shi, Z-J. Benzylation of arenes through $FeCl_3$ catalyzed Friedel-Crafts reaction via C-O activation of benzyl ether, 4310-4312, Copyright 2008, with permission from Elsevier

addition of acetic anhydride is essential. The authors explained that acetic anhydride forms more reactive germinal diacetate, which reacts more easily with arenes (Li *et al*., 2008).

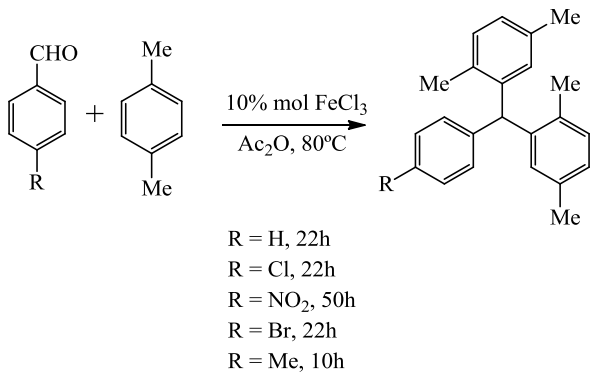

Figure 2.15. Friedel-Crafts alkylation between aromatic aldehydes and arenes (Li *et al*., 2008)[12]

Rare earth metal triflates supported on MCM-41 mesoporous silica was also used as catalyst in the Friedel-Crafts *C*-alkylation between aromatics and benzyl alcohols. The authors observed that an enhancement of the reaction is obtained when there is electron donating -CH_3 groups attached to the rings. It is explained that it is due to the stabilization of the transition state of the electron donating groups in both benzene and benzene alcohol (Mantri *et al*., 2005).

It was already described that the reaction mechanism depends of the alkylating agent and the catalyst used. However, the alkylation of arenes in general can be interpreted by "carbocationic electrophilic aromatic substitution". That is, first there is the formation of an alkyl cation or related polarized complex formation between the alkylating agent and the catalyst. Then, the formed complex reacts with the aromatic ring via a Wheland-intermediate (Figure 2.16). However, when the reaction is performed between an arene and alcohol, ethers, esters, or lactones, there is the occurrence of side-reactions ("isomerization, fragmentation and dealkylation, together with side-chain and positional rearrangements") (Olah *et al*., 1991).

[12] Reprinted from Tetrahedron, 133, Li, Z.; Duan, Z.; Kang, J.; Wang, H.; Yu, L.; Wu, Y. A simple access to triarylmethane derivatives from aromatic aldehydes and electron-rich arenes catalyzed by $FeCl_3$, 1924-1930, Copyright 2007, with permission from Elsevier

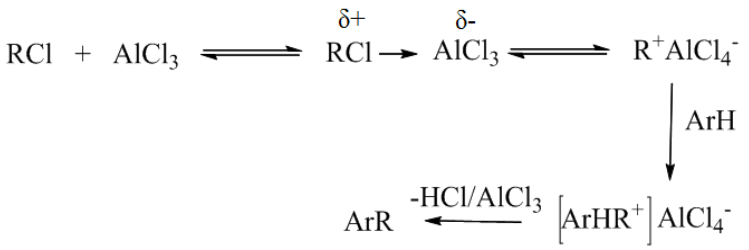

Figure 2.16. Illustration of Wheland intermediate (Olah *et al*., 1991)[13]

Based on the aforementioned discussion, it should be clear that any Brønsted acid catalyst in combination with an organic substrate that can be protonated to yield a carbocationic intermediate will also be capable of performing Friedel-Crafts alkylation. In the petrochemical industry most of the large volume chemical production requiring Friedel-Crafts alkylation is performed with heterogeneous Brønsted acid catalysts (Perego and Ingallina, 2002).

2.3.2 Friedel-Crafts O-Alkylation Reaction

Friedel-Crafts *O*-alkylation consists in the formation of C-O bond. For example, alcohols or phenols are converted into ethers when they are alkylated by another alcohol. Alkylation reactions using alcohols as alkylating agents have been studied since 1897. The main catalysts utilized when alcohols are used as alkylating agent are halides, proton-donating acids, and oxides. Within the group of halides catalysts, the most used are aluminum chloride and boron fluoride. Few studies are reported in using $FeCl_3$ catalyst. For the $FeCl_3$ catalyst, reactions conditions such as time and temperature will depend of the type of alcohol (e.g. primary or secondary alcohol, iso-alcohols, etc) that is been used to alkylate the compound (Schriesheim, 1964).

Cazorla *et al*. (2011) investigated the formation of ethers from 2-naphthol by using different types of Lewis and Brønsted acid catalysts, including $FeCl_3$. Even though the $FeCl_3$ catalyst provided complete conversion, the major product formed was 1,1'-bi-2-naphthol (binol), the dimerisation product of 2-naphthol.

[13] Reprinted from Elsevier, 3, Olah, G. A.; Krishnamurti, R.; Surya Prakash, G. K. Friedel Crafts Alkylation. In *Compreensive Organic Synthesis*; Trost,B. M., Krishnamurti, R., Surya Prakash, G. K., Eds.; 293-339, Copyright 1991, with permission from Elsevier

2.3.3 Alkylation of Coal

Although the present study does not involve coal conversion, coal is also a macromolecular mixture that has some properties in common with petroleum derived asphaltenes. The alkylation of coal may therefore be pertinent to the present investigation.

Alkylation of coal is amply studied and many works are reported in the literature for both reductive and non-reductive alkylation of coal. Both reductive and non-reductive alkylation of coal improved solubility and liquefaction (Baldwin *et al*. 1991).

Selective O-alkylation and reductive alkylation were used as pre-treatment for liquefaction of high oxygen coals. The results showed that the conversion of coal to liquids was higher for selective O-alkylation compared to reductive alkylation. It was explained that the removal or minimization of oxygen in coal can avoid polymerization and then improve the conversion during liquefaction (Baldwin *et al*., 1991, Sasaki *et al*., 2000).

Illinois No. 6 coal was also submitted to both reductive alkylation and O-alkylation. The analysis of the alkylated products showed that the disruption of hydrogen bonds was higher for reductive alkylation than O-alkylation. In addition, subsequent liquefaction of the products and parent coal showed that the oil yield increased from 37 to 60 wt % for the coal submitted to reductive alkylation pretreatment compared to raw coal, while for the O-alkylated coal it was increased to 50 wt % (Sasaki *et al*., 2000). These two works about alkylation of coals show that the results depend of the type of alkylation (reductive and non-reductive) and the nature of the substrate.

The mechanism of reductive alkylation is different to standard Friedel-Crafts alkylation, because it does not proceed through a cationic intermediate. In coals reductive alkylation involves four basic steps: i) formation of hydrocarbons anions through the addition of electrons to the aromatic hydrocarbons structures of coal ii) formation of phenolate anions due to the break of ether bonds iii) “C-alkylation of the aromatic hydrocarbon anions” iv) “O-alkylation of the phenolate

anions". However, it is stated that free radical and elimination reactions can also occur during reductive alkylation. In addition, it is not known if the increase in solubility is attributed to C-alkylation or ether bonds cleavage (Sternberg, 1976).

2.3.4 Alkylation of Asphaltenes

Both asphaltenes molecular structure models propose that there are alkyl side chains attached to the aromatic rings. Apparently, as reported by Mantri *et al*. (2005), these electron donating groups would facilitate the Friedel-Crafts alkylation reaction. If Friedel-Crafts alkylation is performed between asphaltenes and an arene, or an alcohol, it is expected to achieve higher conversion into liquid products through C-C bond formation if the molecule contains –OH, -CO_2R, and –COR functional groups, that could be removed from the molecule. In addition, the conversion of asphaltenes into liquids would be higher through this reaction for the aggregation models that have polar interactions in the aggregation mechanism. Therefore, this chemical conversion would result in higher asphaltenes conversion if asphaltenes structures are actually based on a supramolecular assemblies, or polymerization aggregation.

Two works report classical Friedel-Crafts alkylation of asphaltenes by using a strong Lewis acid catalyst ($AlCl_3$).

The first work was conducted by Ignasiak *et al*. (1981). The objective in performing Friedel-Crafts alkylation was to decrease the average molecular weight of the aggregated asphaltenes and understand the chemical changes in the asphaltenes structure. A strong acid catalyst ($AlCl_3$) and a weak Lewis acid catalyst ($ZnCl_2$) were used with different solvents, different temperatures, and different pressures. The results showed that all the parameters influenced the solubility. $AlCl_3$ obtained higher solubility at lower temperatures (below 100ºC), while $ZnCl_2$ obtained better results at high temperatures (above 250ºC). Benzene was the solvent which promoted higher solubility when $AlCl_3$ was used as catalyst. It was explained that when asphaltenes react with $AlCl_3$ catalyst, it forms carbonium ions that may suffer electrophilic substitution. The asphaltenes molecules may then react with each other and form a bigger molecule due to the electrophilic substitution. However, when the reaction is performed in the presence of benzene,

intra-molecular interactions will be prevented, as the intermediate carbocations will react with benzene. It is also reported that due to the high complexity of asphaltenes molecule many side reactions can also occur (Ignasiak *et al.*, 1981).

The other work, using $AlCl_3$ as catalyst, was conducted by Sidiqqui (2003) to alkylate Arabian asphaltenes. The alkylating agent used was 1-chlorobutane. The success of the reaction was verified by Fourier Transform Infra-Red (FTIR) and Nuclear Magnetic Resonance (NMR) analysis. ^{13}C NMR analysis showed that the aliphatic/aromatic ratio increased after reaction compared to the parent asphaltene. Thermal Gravimetric analysis (TGA) showed that the loss of material in the parent asphaltenes started to occur at 360 ºC, while in the alkylated products it started to occur below 360 ºC. This result was attributed to the cleavage of more fragile structures obtained during alkylation reaction. The cleavage of more fragile structures is probably because if butyl groups were added to aromatics during alkylation, the alkyl chains would be susceptible to thermal cracking because the formation of benzylic radicals requires less bond dissociation energy.

Non-reductive alkylation of Athabasca oilsands asphaltenes in liquid ammonia is also reported. However, addition of ethyl groups was not accomplished with this method, "regardless of the nature of the amide used". Heteroatom content was also not decreased with this treatment. The molecular weight of alkylated asphaltenes was slightly lower than the parent asphaltenes, which were attributed to the elimination of intermolecular interactions between hydroxyl groups (Wachowska *et al*., 1986).

Reductive alkylation of French petroleum asphaltenes was studied by Cagniant et al. (2001). The alkylation was realized in the absence of electron transfer reagent. They concluded that the aromatic portion of asphaltenes acted as electron transfer agents. Moreover, C-O and C-S linkages were cleaved during the reaction which resulted in an increase of solubility. According to the authors, the increase in solubility is due to the reduction of polar compounds.

2.3.5 Implications for this Study

Friedel-Crafts C- and O-alkylation reaction is one of the conversion chemistries studied in this work for conversion of asphaltenes into liquid fuels. The hypothesis is that –OH groups present in asphaltenes and which are responsible for hydrogen bonding can be removed from the molecule. As hydrogen bonding is one of the interactions occurring in asphaltenes molecules that are responsible for aggregation, it was expected that solubility and conversion to liquid products would increase by decreasing aggregation. A C-alkylation reaction was performed with *o*-xylene as alkylating agent while O-alkylation was performed with methanol as alkylating agent. Alcohol groups are totally removed in C-alkylation while alcohols are converted into ethers in O-alkylation. Although oxygen is still present after O-alkylation reaction, ethers are less polar than alcohols and do not participate in hydrogen bonding. The catalyst chosen for both alkylation reactions was $FeCl_3$. The choice of this catalyst was justified based on its lower propensity for side-reactions. Side-reactions will likely occur if strong catalysts such as $AlCl_3$ are used in a complex medium such as asphaltenes, as was indeed reported by Ignasiak et al. (1981). In addition, $FeCl_3$ can operate in the presence of water and air.

2.4 Donor-Acceptor Interaction

Donor-acceptor interaction takes place when a component is a Lewis acid (electron acceptor) and the other component is a Lewis base (electron donor) (McGlynn, 1959). Carboxylic groups present in asphaltenes can participate in donor-acceptor interactions. One example is the formation of bridged carboxylate groups between two asphaltenes molecules and a multivalent metal cation as shown in Figure 2.17.

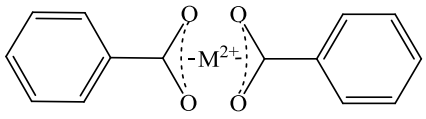

Figure 2.17. Bridged carboxylate groups

The multivalent metal cation can be removed from the molecule by different techniques as described below.

Ion exchangers are insoluble solid materials used for removal of ions, usually by exchange with H^+ or OH^-. This technique is the often used by industry, mostly for water treatment. The ion exchangers carry exchangeable cations or anions and when they are in contact with an electrolyte solution these ions can be exchanged. The exchange is done with ions of the same sign. Thus, if the objective is to exchange cations, a cation exchanger is used while an anion exchanger is used for the exchange of anions. Figure 2.18 illustrates a cation exchange reaction. Ion exchange is a diffusion, reversible, and selective process. Different type of materials can be used as ion exchangers such as natural minerals, synthetic zeolites, resins, membranes, and coals. Although the definition of ion exchangers is that they are solid materials, some liquids can also be ion exchangers. In this case, the two liquids should be immiscible. One application of ion exchanger is water softening by removal of dissolved $CaCl_2$ (Helfferich, 1962).

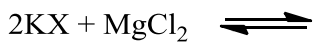

Figure 2.18. Typical cation exchange reaction (Helfferich, 1962)[14]

Another technique that can be used to remove metal cations is acid washing. The acids employed are typically diluted hydrochloric acid, sulphuric acid, and nitric acid. The reaction between a metal divalent cation and diluted hydrochloric acid is schematized in Figure 2.19. The efficiency of the process is related to acid and cation concentrations, and also to the feed-acid contact. In general, calcium is the metal most often removed through this technique.

Figure 2.19. Reaction between divalent metals and hydrochloric acid

One drawback of hydrochloric acid is that the reaction introduces chloride compounds in the mixture, which must be removed, because chlorides may cause corrosion in high temperature processes if they are not efficiently removed after the reaction (Marsden and House, 2006).

[14] Adapted from Helfferic, F. *Ion exchange*. McGraw-Hill Book Company, Inc.: New York, 1962, pp. 5-9.

The removal of multivalent metals cations would be more likely to succeed in converting asphaltenes to maltenes if supramolecular assembly model is a good descriptor of interactions in asphaltenes, as it is the only model that suggests this type of interaction. However, as this model suggests a "porous" structure, the residual chloride compounds can be difficult to remove if they are trapped inside the macromolecular assembly.

2.4.1 Donor-Acceptor Interaction of Coal and Asphaltenes

The removal of exchangeable cations from coal in order to disrupt carboxylic bridges is amply reported in the literature and they are presented below. However, similar studies were not found for asphaltenes. Nevertheless, reports of asphaltenes washed with hydrochloric acid solutions to remove inorganic salts can be found in the literature (Becker, 1997).

Acid washing of coal is performed as pretreatment before liquefaction. Van Bodegom *et al*. (1984) performed acid washing of brown coals. They observed that the pretreatment with 1 N HCl increased dissolution of different kinds of coal in different solvents such as pyridine and ethylene-diamine. They attributed this result to two reasons. The first reason is disruption of carboxylic bridges as shown in Figure 2.17 through the removal of divalent cations by acid washing. The disruption will enhance solubility. The second reason is that HCl may hydrolyze ester groups.

Shams *et al*. (1992) also used HCl as pretreatment of Wyodak coal to remove exchangeable cations before liquefaction. However, they used not only HCl, but also HCl with other organic solvents such as methanol, acetone, and hexane. Liquefaction was performed at 350 ºC and 7 MPa using hydrogen gas and tetrahydrofuran solvent. The results showed that methanol/HCl pretreatment presented the highest conversion to liquid products (31.5%) compared to untreated coal and other pretreatments. They also attribute the results due to removal of calcium (90%) and consequent disruption of carboxylic bridges. The explanation offered of why enhancement of reactivity was higher when methanol was used in combination with HCl is because it was claimed that the organic solvent provided better contact between coal and acid by improving wettability of the coal surface. Even though it was not pointed out by the authors, the higher

liquefaction achieved with methanol/HCl could also be because of some alkylation may have occurred. HCl can act as a proton-donating acid catalyst while methanol can act as alkylating agent in Friedel-Crafts O-alkylation. Friedel-Crafts O-alkylation could convert alcohol groups in coal into ethers. As alcohol groups participate in hydrogen bonding and ether groups does not, the removal of such groups would decrease inter-molecular interactions that lead to some disaggregation of coal molecules.

Pretreatment with HCl was also used before liquefaction of Turkish coals using supercritical toluene. The results showed that pretreatment with HCl also increased the conversion to liquids for this type of liquefaction. The increase in conversion is also related to the removal of cations such as calcium and magnesium as their removal reduces cross-linking which results in better contact between coal and solvent. Even though sodium and potassium cations do not participate in cross-linking, they were also removed with HCl washing (Şimşek *et al*., 2002).

Joseph and Forrai (1992) studied the effect of different cations on low rank coal liquefaction through ion-exchange technique. In order to evaluate the effect of each cation (Na^+, K^+, and Ca^{2+}) separately, they first removed all exchangeable cations using ammonium acetate solution. Then, they introduced the desired cation (calcium, sodium, or potassium) through metal ion exchange technique and compared the results with the coal pretreated with ammonium acetate (as it does not have any exchangeable cation). The results showed that sodium does not affect conversion to liquid oil, while calcium was the cation that provided the highest conversion to liquid oil. The order of effect on liquefaction was $Na^+ < K^+ << Ca^{2+}$. As well as for the studies presented above, the explanation is that calcium-exchanged coal promoted crosslinking between carboxylic groups of different molecules and reduced liquefaction.

2.4.2 Implications for this Study

By analogy with coal, carboxylic acid groups in asphaltenes could form bridges by interaction with multivalent cations. The bridges can cause aggregation of asphaltenes molecules. The hypothesis is that removal of multivalent cations can disrupt such bridges and reduce aggregation. A plausible approach would be to treat asphaltenes with hydrochloric acid in order

to remove multivalent cations and consequently decrease aggregation. However, the risk of doing this is that the acid may also catalyze side-reactions, such as Friedel-Crafts alkylation between asphaltene molecules.

Literature Cited

Agrawala, M. and Yarranton, H. W. An asphaltene association model analogous to linear polymerization. *Ind. Eng. Chem. Res*. **2001**, *40*, 4664-4672.

Baldwin, R. M.; Kennar, D. R.; Nguanprasert, O.; Miller, R. L. Liquefaction reactivity enhancement of coal by mild alkylation and solvent swelling techniques. *Fuel* **1991**, *70*, 429-433.

Becker, J. R. *Crude oil. Waxes, emulsions, and asphaltenes.* PennWell: Tulsa, Okla, 1997.

Cagniant, D.; Nosyrev, I.; Cebolla, V.; Vela, J.; Membrado, L.; Gruber, R. Structural modifications of petroleum asphaltenes by reductive alkylation investigated by TLC-FID. *Fuel* **2001**, *80*, 107-115.

Cazorla, C.; Pfordt, É.; Duclos, M-C.; Métay, E.; Lemaire, M. O-Alkylation of phenol derivatives *via* a nucleophilic substitution. *Green Chem*. **2011**, *13*, 2482

De La Mare; P. B. D.; Ridd, J. H. *Aromatic substitution: nitration and halogenation*. Butterworths Scientific Publications: London, 1959; pp. 5-25, 105-209.

Firouzabadi, H.; Iranpoor, N.; Kazemi, S. Direct halogenation of organic compounds with halides using oxone in water – a green protocol. *Can. J. Chem*. **2009**, *87*, 1675-1681.

Friberg, S. E. Micellization. In *Asphaltenes, heavy oils, and petroleomics*, Mullins, O. C.; Sheu, E. Y.; Hammami, A.; Marshall, A. G., Eds.; Springer: New York, 2007; pp. 189-203.

Gray, M. R. Consistency of asphaltenes chemical structures with pyrolysis and coking behavior. *Energy Fuels* **2003**, *17*, 1566-1569.

Gray, M. R. *Fundamentals of Oilsands Upgrading.* University of Alberta: Edmonton, AB, 2010.

Gray, M. R.; Tykwinski, R. R.; Stryker, J. M.; Tan, X. Supramolecular assembly model for aggregation of petroleum asphaltenes. *Energy Fuels* **2011**, *25*, 3125-3134.

Groenzin, H. and Mullins, O. C. Molecular size and structure of asphaltenes from various sources. *Energy Fuels* **2000**, *14*, 677-684.

Groenzin, H. and Mullins, O. C. Asphaltene molecular size and weight by time-resolved fluorescence depolarization. In *Asphaltenes, heavy oils, and petroleomics*, Mullins, O. C.; Sheu, E. Y.; Hammami, A.; Marshall, A. G., Eds.; Springer: New York, 2007; pp. 17-62.

Helfferic, F. *Ion exchange*. McGraw-Hill Book Company, Inc.: New York, 1962.

Hepworth, J. D.; Waring, D. R.; Waring, M. J. *Aromatic chemistry*. The Royal Society of Chemistry: Cambridge, 2002.

Ignasiak, T.; Bimer, J.; Samman, N.; Montgomery, D. S.; Strausz, O. P. Lewis acids assisted degradation of athabasca asphaltene. In: *Chemistry of asphaltenes*, Bunger, J., Norman, C. L., Eds. Advances in Chemistry; American Chemical Society: Washington, DC, 1981, pp. 183-201.

Iovel, I.; Mertins, K.; Kischel, J.; Zapf, A.; Beller, M. An efficient and general iron-catalyzed arylation of benzyl alcohols and benzyl carboxylates. *Angew. Chem. Int.* **2005**, *44*, 3913-3917.

Joseph, J. T. and Forrai, T. R. Effect of exchangeable cations on liquefaction of low rank coals. *Fuel* **1992**, *71*, 75-80.

Kowanko, N.; Branthaver, J. F.; Sugihara, J. M. Direct liquid-phase fluorination of petroleum. *Fuel* **1978**, *57*, 769-775.

Krishna Mohan, K. V. V. and Narender, N. Ecofriendly oxidative nuclear halogenation of aromatic compounds using potassium and ammonium halides. *Synthesis* **2012**, *44*, 15-26.

Kumar, M. A.; Rohitha, C. N.; Kulkarni, S. J.; Narender, N. Bromination of aromatic compounds using ammonium bromide and oxone®. *Synthesis* **2010**, *10*, 1629-1632.

Lee, K-J.; Cho, H. K.; Song, C-E. Bromination of activated arenes by oxone® and sodium bromide. *Bull. Korean Chem. Soc.* **2002,** *23* (5), 773-775.

Li, Z.; Duan, Z.; Kang, J.; Wang, H.; Yu, L.; Wu, Y. A simple access to triarylmethane derivatives from aromatic aldehydes and electron-rich arenes catalyzed by $FeCl_3$. *Tetrahedron* **2008**, *64*, 1924-1930.

Long, R. B. The concept of asphaltenes. In *Chemistry of asphaltenes*; Bunger, J. W. and Li, N. C., Eds.; ACS Advances in Chemistry Series 195; American Chemical Society: Washington, DC, 1981; pp.17-27.

Mantri, K.; Komura, K.; Kubota, Y.; Sugi, Y. Friedel-Crafts alkylation of aromatics with benzyl alcohols catalyzed by rare earth metal triflates supported on MCM-41 mesoporous silica. *Journal of Molecular Catalysis A: Chemical* **2005**, *236*, 168-175.

March, J. *Advanced organic chemistry: reactions, mechanisms, and structure*. John Wiley & Sons: New York, 1992; pp. 501-568.

Marsden, J. O. and House, C. I. *The chemistry of gold extraction. society for mining, metallurgy, and exploration*, Inc.: Littleton, US-CO, 2006.

Masliyah, J. H.; Czarnecki, J. A.; Xu, Z. *Handbook on theory and practice of bitumen recovery from athabasca oilsands. theoretical basis*. Kingsley Publishing Services: Canada, 2011; Volume I, pp. 1-49; 361-372.

McGlynn, S. P. In *Donor-acceptor interaction*. Radiation Research, Supplement 1, 1959 - Proceedings of the International Congress of Radiation Research; Smith, D. E., Ed.; Academic Press: New York, 1959, p. 302.

Moschopedis, S. E. and Speight, J. G. Introduction of halogen into asphaltenes via the gomberg reaction. *Fuel* **1970**, *49*, 335.

Moschopedis, S. E. and Speight, J. G. The halogenation of Athabasca asphaltenes with elemental halogen. *Fuel* **1971a**, *50*, 58-64.

Moschopedis, S. E. and Speight, J. G. Water-soluble derivatives of Athabasca asphaltenes. *Fuel* **1971b**, *50*, 34-40.

Mullins, O. C. Review of the molecular structure and aggregation of asphaltenes and petroleomics. *SPE Journal* **2008**, *13*, 48-57.

Mullins, O. C. The asphaltenes. *Annu. Rev. Anal. Chem*. **2011**, 4, 393-418.

Narender, N.; Srinivasu, P.; Kulkarni, S. J.; Raghavan, K. V. Regioselective oxyiodination of aromatic compounds using potassium iodide and oxone®. *Synthetic Communications* **2002a**, *32* (15), 2319-2324.

Narender, N.; Srinivasu, P.; Prasad, M. R.; Kulkarni, S. J.; Raghavan, K. V. An efficient and regioselective oxybromination of aromatic compounds using potassium bromide and oxone®. *Synthetic Communications* **2002b**, *32* (15), 2313-2318.

Narender, N.; Srinivasu, P.; Prasad, M. R.; Kulkarni, S. J.; Raghavan, K. V. Highly efficient, para-selective oxychlorination of aromatic compounds using potassium chloride and oxone®. *Synthetic Communications* **2002c**, *32* (2), 279-286.

Newkome, G. R. and Paudler, W. W. *Contemporary heterocyclic chemistry: syntheses, reactions, and applications*. John Wiley & Sons: New York, 1982.

Olah, G. A.; Krishnamurti, R.; Surya Prakash, G. K. Friedel-Crafts alkylations. In *Comprehensive Organic Synthesis*, Trost, B. M., Krishnamurti, R., Surya Prakash, G. K., Eds. Elsevier: 1991, 293-339.

Parsons, A. F. *An introduction to free radical chemistry*. Blackwell Science: Oxford, 2000.

Perego, C. and Ingallina, P. Recent advances in the industrial alkylation of aromatics: new catalysts and new processes. *Cataysis Today* **2002**, *73*, 3-22

Pfeiffer, J. P. H. and Saal, R. N. J. Asphaltic bitumen as colloid system. *The Journal of Physical Chemistry* **1940**, *44* (2), 139-149.

Roberts, R. M. and Khalaf, A. A. *Friedel-Crafts alkylation chemistry*. Marcel Dekker, Inc.: New York, 1984.

Sabbah, H.; Morrow, A. L.; Pomerants, A. E.; Zare, R. N. Evidence for island structures as the dominant architecture of asphaltenes. *Energy Fuels* **2011**, *25*, 1597-1604.

Sasaki, M.; Kotanigawa, T.; Yoshida, T. Liquefaction reactivity of methylated Illinois no. 6 coal. *Energy & Fuels* **2000**, *14*, 76-82.

Schriesheim, A. Alkylation of aromatics with alcohols and ethers. In *Friedel-Crafts and Related Reactions. Part I*; Olah, G. A., Ed.; Jhon Wiley & Sons: New York, 1964, pp. 486-533.

Shams, K.; Miller, R. L.; Baldwin, R. M. In *Enhanced low severity coal liquefaction using selective calcium removal*. Symposium on Reaction Pathways and Mechanisms in Fuel Processings 1992, 37(2), pp. 1017-1024.

Sharma, A. and Mullins, O. C. Insights into molecular and aggregate structures of asphaltenes using HRTEM. In *Asphaltenes, heavy oils, and petroleomics*, Mullins, O. C.; Sheu, E. Y.; Hammami, A.; Marshall, A. G., Eds.; Springer: New York, 2007; pp. 205-257.

Sheremata, J. M; Gray, M. R.; Dettman, H. D.; McCaffrey, W. C. Quantitative molecular representation and sequential optimization of athabasca asphaltenes. *Energy Fuels* **2004**, *18*, 1377-1384.

Siddiqui, M. N. Alkylation and oxidation reactions of Arabian asphaltenes. *Fuel* **2003**, *82*, 1323-1329.

Siddiqui, M. N. Exploring the chemical reactivity of asphaltenes. *Prepr. Pap.-Am. Chem. Soc., Div. Fuel Chem.* **2009**, *54*(1), 14-15.

Sill, G. A. and Yen, T. F. Semiconduction of iodine complexes of asphaltenes. *Fuel* **1969**, *48*, 61-74.

Şimşek, E. H.; Karaduman, A.; Çalışkan, S.; Togrul, T. The effect of preswelling and/or pretreatment of some Turkish coals on the supercritical fluid extract yield. *Fuel* **2002**, *81*, 503-506.

Speight, J. G. Reactions of Athabasca asphaltenes and heavy oil with metal chlorides. *Fuel* **1971**, *50*, 175-186.

Speight, J. G. and Moschopedis, S. E. On the molecular nature of petroleum asphaltenes. In *Chemistry of asphaltenes*; Bunger, J. W., Li, N. C., Eds.; ACS Advances in Chemistry Series 195; American Chemical Society: Washington, DC, 1981; pp.17-27.

Sternberg, H. W. Second look at the reductive alkylation of coal and at the nature of asphaltenes. *Am Chem Soc Div Chem Prepr* **1976**, *21*(7), 1-10.

Strausz, O. P., Mojelsky, T. W., Lown, E. M. The molecular structure of asphaltene: an unfolding story. *Fuel* **1992**, *71* (12), 1355-1363.

Strausz, O. P.; Lown, E. M. *The chemistry of Alberta oilsands, bitumens, and heavy oils*. Alberta Energy Research Institute: Calgary, AB, 2003.

Strausz, O. P.; Safaraki, I.; Lown, E. M.; Morales-Izquierdo; A. A critique of asphaltene fluorescence decay and depolarization-based claims about molecular weight and molecular architecture. *Energy Fuels* **2008**, *22*, 1156-1166.

Tamhankar, B. V.; Desai, U. V.; Mane, R. B.; Wadgaonkar, P. P.; Bedekar, A. V. A simple and pratical halogenation of activated arenes using potassium halide and oxone® in water-acetonitrile medium. *Synthetic Communications* **2001**, *31* (13), 2021-2027.

Van Bodegom, B.; Van Veen, J. A. R.; Van Kessel, G. M. M.; Sinnige-Nijssen, M. W.; Stuiver, H. C. M. Action of solvents on coal at low temperatures. 1. low-rank coals. *Fuel* **1984**, *63*, 346-354.

Wachowska, H.; Ignasiak, T.; Strausz, O. P.; Carson, D.; Ignasiaki, B. Application of non-reductive alkylation in liquid ammonia to studies on macromolecular structure of coals and bitumen-derived asphaltene. *Fuel* **1986**, *65*, 1081-1084

Wang, B-Q.; Xiang, S-K.; Sun, Z-P.; Guan, B-T.; Hu, P.; Zhao, K-Q.; Shi, Z-J. Benzylation of arenes through $fecl_3$ catalyzed friedel-crafts reaction via c-o activation of benzyl ether. *Tetrahedron Letters* **2008**, *49*, 4310-4312.

Wiehe, I. A. *Process chemistry of petroleum macromolecules*. Boca Raton, CRC Press: 2008.

Zielinski, L.; Saha, I.; Freed, D. E.; Hürlimann, M. D. Probing asphaltene aggregation in native crude oils with low-field NMR. *Langmuir* **2010**, *26* (7), 5014-5021.

Chapter 3. Halogenation of Oilsands Bitumen, Maltenes, and Asphaltenes[15]

Abstract

Bromination of oilsands derived materials was investigated as part of a search to find conversion pathways other than traditional hydroprocessing and thermal processing for the upgrading of asphaltenes. The working hypothesis was that the insertion of a bulky halogen substituent on an aromatic carbon of a multinuclear aromatic might sterically disrupt π-π ring stacking. Mild bromination (1-3 wt % Br incorporation) caused observable changes in the physical appearance of bitumen, maltenes and asphaltenes. The hardness was increased and the asphaltenes gained solvent resistance, suggesting potential application as pretreatment for road paving asphalt. UV-vis spectrometry indicated that metalloporphyrin structures were disrupted, suggesting possible demetalation. There was also an increased association of oxygenate-rich asphaltenes with iron pyrite particulates already present in this fraction. Bromination was deleterious in its effect on bitumen and the maltenes, resulting in a decrease in straight run gas vacuum oil yield and increase in micro carbon residue. Conversely, bromination of asphaltenes resulted in an increase in straight run vacuum gas oil yield from 2.0 ± 0.3 wt % to 7.5 ± 1.8 wt %, without affecting the micro carbon residue. It was not possible to unequivocally attribute the observed changes in the asphaltenes to the disruption of π-π ring stacking.

Keywords: Bromination, Multinuclear Aromatics, Oilsands Asphaltenes

[15] Reprinted with permission from Prado, G. H. C. and De Klerk, A. Halogenation of oilsands bitumen, maltenes, and asphaltenes, *Energy & Fuels* 2014, 28, 4458-4468. Copyrigth 2014 American Chemical Society. http://pubs.acs.org/doi/abs/10.1021/ef500712r

3.1 Introduction

The upgrading of heavy petroleum fractions is normally associated with process chemistry that results in the cleavage of chemical bonds to produce lighter products. The cleavage of chemical bonds is indeed very important in the upgrading or refining of heavy materials to transport fuels, but in the case of oilsands derived bitumen, there are additional aspects to consider. Oilsands bitumen has poor fluidity, it is prone to aggregating behavior and it has a high asphaltenes content (Masliyah et al., 2011; De Klerk et al., 2014). For many bitumen producers the first challenge is to convert the bitumen into a transportable product. Upgrading the bitumen under severe operating conditions to produce a lighter and more refined product is one strategy. This approach is associated with some form of carbon rejection, either directly, by co-producing coke or asphaltenes, or indirectly, by producing hydrogen. Although the resulting product is of a higher quality, the conversion is associated with product loss.

Finding an alternative conversion chemistry that can improve bitumen fluidity by reducing aggregation, or that can convert some of the asphaltenes into maltenes, is desirable. It is for this purpose that halogenation was considered.

If at least some of the asphaltenes in bitumen has a structure with an aromatic core, as suggested by the continental-model for asphaltenes structure (Mullins et al., 2007; Ancheyta et al., 2009), then there will be π-π ring stacking interactions. It is recognized that there are many interactions contributing to aggregation (Gray et al., 2011), and π-π ring stacking is just one of them. In the context of this paper π-π ring stacking refers to the planar graphene-like stacking of multinuclear rings in asphaltenes that have been extensively studied by X-ray diffraction (Mullins et al., 2007; Andersen et al., 2005).

The exact nature of the π-π ring stacking interaction and how it leads to asphaltenes aggregation is nebulous, but it is often enough observed. The working hypothesis was that substitution by bulky strong electrophiles, either on the aromatic core, or close to the aromatic core, might sterically disrupt the ability of asphaltenes to aggregate by π-π ring stacking (Figure 3.1). This type of steric disruption of π-π ring stacking was reported as the explanation for increased

solubilization of bituminous coal after base catalyzed aromatic C-alkylation with bulky iodoalkanes (Miyake and Stock, 1988). Our interest was in the direct use of bulky halogens, such as bromine and iodine, which might have enough steric bulk to weaken stacking. In extreme cases the aromaticity can be destroyed by the halogens (Parsons, 2000), but that was not a specific objective.

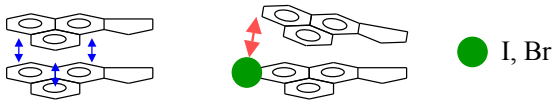

Figure 3.1. Proposed strategy to disrupt π-π ring stacking in asphaltenes

In this study the bromination of oilsands derived bitumen and asphaltenes was investigated to determine whether the halogenation reaction could convert some asphaltenes into maltenes. As a secondary objective, this study evaluated the upgradeability of the brominated products. The approach taken in this investigation was different from previous studies (Moschopedis and Speight, 1970; Moschopedis and Speight, 1971; Moschopedis and Speight, 1976; Patwardhan, 1979; Siddiqui, 2009; Kowanko, 1978; Sill, 1969). A lower level of halogenation was employed, halogenation was performed by a method that was reported to result in nuclear substitution for compounds containing fused rings with alkyl side chains (Lee, 2002), and, in addition to product characterization, the upgradeability of the product was investigated.

3.2 Past Work on Halogenation of Oil and Asphaltenes

Halogenation is a process chemistry that is seldom investigated for the upgrading of heavy oils, residua and bitumens. There are only a few studies in the literature evaluating halogenation of crude oils and asphaltenes. Most of these were conducted in order to investigate the physico-chemical implications of halogenation and to understand the molecular structure and behavior of asphaltenes.

Moschopedis and Speight investigated the chlorination, bromination and iodination of Athabasca asphaltenes (Moschopedis and Speight, 1970; Moschopedis and Speight, 1971; Moschopedis and

Speight, 1976). High levels of halogenation were achieved during halogenation of asphaltenes (precipitated with *n*-pentane) with Cl_2, Br_2 and I_2 (Moschopedis and Speight, 1971). The halogenated asphaltenes contained ~35 wt % Cl during chlorination, ~37 wt % Br during bromination, and ~11 wt % I during iodination. It was observed that most of the chlorine was incorporated on the alkyl groups and cycloalkanes, with little chlorination of aromatic rings. Chlorination of the aromatic rings required elevated temperature or a catalyst, such as $FeCl_3$. Iodination was reportedly also on alkyl groups and cycloalkanes. Presumably the same occurred during bromination, but no specific mention was made of this. In all cases there was a marked change in appearance and in the physical properties of the products.

Halogenation of asphaltic bitumen was investigated as an alternative method for preparing hardened bitumen (Pfeiffer, 1950). Most of the reported work focused on chlorination as an alternative to oxidative hardening; mention only was made of bromination.

Patwardhan (1979) chlorinated different petroleum bitumens to produce materials containing around 20 wt % Cl. The location of chlorination in the bitumens was not investigated. The physical properties of the product were changed and some reference was made to the use of chlorination for bitumen hardening to produce road-paving asphalt.

Chlorination of asphaltenes from Saudi Arabian crude oil showed that chlorine uptake occurred in both aliphatic and aromatic carbons (Sidiqqui, 2009). The chlorination was carried out using sulfuryl chloride. No comment was made about the physical appearance of the chlorinated product.

Fluorination of asphaltenes from Boscan crude oil showed that asphaltenes have less capacity to absorb fluorine compared to maltenes and the crude oil. The explanation that was forwarded was that the aggregation of the asphaltenes limited the transport of fluorine and therefore its reaction with the asphaltenes (Kowanko, 1978).

Iodination of asphaltenes from Boscan and Baxterville crude oils was performed to investigate if iodine insertion in the molecules present in asphaltenes would increase their conductivity. The

results showed that addition of iodine decreased resistivity about a million-fold. In addition, the authors explored structural changes obtained after reaction. Based on the absence of C–I stretching in the infrared spectra, they suggested that iodine formed a charge-transfer complex with the asphaltenes, where the asphaltenes would be the aromatic donor and the iodine would be the acceptor. Moreover, it was suggested that iodine was intercalated between the aromatic layers of asphaltenes, which resulted in an expansion of the aromatic sheets (Sill and Yen, 1969).

3.3 Experimental

3.3.1 Materials

Oilsands derived bitumen from the Athabasca region was acquired from Syncrude Canada Ltd. The asphaltenes fraction was precipitated from the bitumen using *n*-pentane solvent deasphalting. In a typical solvent deasphalting experiment, 10 g of bitumen was mixed with 400 mL of *n*-pentane in a 500 mL flask. Then, it was placed in the fume hood at ambient conditions for 1 hour while continuously stirring the mixture with a stirrer bar on a magnetic stirrer. At the end of this period the mixture was left for 24 hours in the dark, before the mixture was filtered with a 0.22 μm Millipore Nitrocellulose membrane filter under vacuum and rinsed with fresh *n*-pentane. Finally, the membrane filter was transferred to an aluminium cup and dried in the fume hood for 48 hours. The membrane filter and aluminium cup were previously weighed in order to calculate asphaltenes content in bitumen. The maltenes, or deasphalted oil (DAO), was obtained by evaporating *n*-pentane in a rotary evaporator at 50 ºC. The bitumen and its prepared fractions, asphaltenes and maltenes, were characterized (Table 3.1). It is worthwhile pointing out two deviations in the material balance over the fractions. The carbon content in the maltenes and asphaltenes are 2 % (relative) too low compared to the bitumen analysis. The sulfur content of the maltenes and asphaltenes are about 8 % (relative) less than anticipated from the bitumen analysis. As a result, the cumulative difference indicated that the oxygen content of the asphaltenes in particular was higher than anticipated (typically ~2.5 wt %). It was also observed that the density of the maltenes was about 20 kg/m^3 lower than anticipated.

Table 3.1. Characterization of Athabasca bitumen and bitumen fractions.[a]

Description	Bitumen		Maltenes [b]		Asphaltenes [b]	
	x	s	x	s	x	s
Fraction of bitumen (wt %)	100	-	81.55	0.96	18.45	0.95
Elemental analysis (wt %)						
Carbon	83.54	0.08	83.08	0.05	77.62	0.18
Hydrogen	10.11	0.02	10.71	0.02	7.61	0.01
Nitrogen	0.47	0.01	0.31	0.02	1.18	0.04
Sulfur	5.16	0.05	3.98	0.01	8.07	0.02
Oxygen (by difference)	0.71	0.05	1.90	0.05	5.52	0.14
Mineral matter content (wt %)	1.03	0.10	0 [c]	0 [c]	4.01	0.10
Liquid density at 25 °C (kg/m^3)	1012.2	1.1	961.8	3.1	- [d]	- [d]
Refractive index [e]	1.5835	0.0004	1.5409	0.0011	- [d]	- [d]

[a] Average (x) and sample standard deviation (s) of three experiments are reported.
[b] Separation of asphaltenes and maltenes by precipitation with *n*-pentane.
[c] None detected.
[d] Solid material.
[e] Refractive index relative to air using the sodium D-line, 589 nm, measured at 25 °C.

The chemicals and cylinder gases employed during this study were commercially obtained and used without further purification (Table 3.2).

Table 3.2. Chemicals and cylinder gases employed in this study

Compound	Formula	CASRN [a]	Mass fraction purity [b]	Supplier
Chemicals				
chloroform	$CHCl_3$	67-66-3	0.99	Sigma-Aldrich
oxone®	$KHSO_5 \cdot 0.5KHSO_4 \cdot 0.5K_2SO_4$	70693-62-8	-	Sigma-Aldrich
n-pentane	C_5H_{12}	109-66-0	0.98	Fisher Scientific
sodium bromide [c]	NaBr	7647-15-6	0.99	Sigma-Aldrich
0.05M sodium thiosulfate	$Na_2S_2O_3$	7772-98-7	-	Sigma-Aldrich
sodium sulfate	Na_2SO_4	7757-82-6	0.99	Sigma-Aldrich
tetrahydrofuran	C_4H_8O	109-99-9	0.95	Fisher Scientific
toluene	C_7H_8	108-88-3	0.995	Fisher Scientific
Cylinder gases				
nitrogen	N_2	7727-37-9	0.99999 [d]	Praxair
air	O_2/N_2 mix	132259-10-0	-	Praxair
Calibration substances				
indium	In	7440-74-6	0.99999	Impag AG
potassium iodate	KIO_3	7758-05-6	0.995	Sigma-Aldrich
sodium chloride	NaCl	7647-14-5	0.995	Sigma-Aldrich
zinc	Zn	7440-66-6	0.99999	Impag AG

[a] CASRN = Chemical Abstracts Services Registry Number.
[b] This is the purity of the material guaranteed by the supplier; material was not further purified.
[c] Also used as a calibration substance.
[d] Mole fraction purity.

3.3.2 Equipment and Procedure

Bromination of the starting materials was performed using the methodology described by Lee *et al*. (2002). Some modifications were made to apply this to oilsands derived material and the complete procedure is given. First, 5 g of the starting material (bitumen, asphaltenes or maltenes) and 30 mL of chloroform were mixed and stirred. Then, 5 mmol of sodium bromide (0.51g) was added. Afterwards, 10 mL of an aqueous solution of Oxone® (5 mmol in 20 mL of water) was added dropwise. Oxone® oxidizes the halide salt into their corresponding halogens or hypohalous acids. The solution was stirred under reflux for 24 hours. After completion of the reaction, 30 mL of 0.05M sodium thiosulfate solution was added to quench the reaction. The reaction mixture was extracted with chloroform (30 mL) to separate the organic and aqueous

phases. The organic layer was separated and dried over anhydrous sodium sulphate. After drying, the solvent was evaporated under vacuum to obtain the product. The dried products were left in the fume hood to evaporate the remaining solvent until constant weight was obtained. The products were then characterized. The reactions and characterization were performed in triplicate.

A control experiment was also performed in triplicate, which followed the same bromination procedure, but during which only NaBr and no Oxone® was added. Under these conditions bromination failed to occur. This was also evident from the physical appearance of the bitumen.

The thermal conversion of raw and brominated bitumen, asphaltenes and maltenes was performed by thermogravimetric analysis based on the method outlined by Juyal *et al*. (2013). The objective was to determine the change in distillation yields and product yields that could be obtained during thermal conversion of the brominated materials in comparison to the raw starting materials. All experiments were performed in triplicate.

3.3.3 Analyses

Elemental analyses were performed by the Analytical Services of the Chemistry Department at University of Alberta using a Carlo Erba Elemental Analysis EA1108 Analyzer. During a typical analysis a small amount of sample is oxidatively pyrolized at 1700-1800 °C in order to produce N_2, CO_2, H_2O, and SO_2. The product gases pass through a reactive column with helium as the carrier. The first section of the column contains tungsten trioxide (WO_3) on alumina (Al_2O_3) which is used to ensure that complete oxidation occurs. The second section of the column contains a layer of reduced copper where excess oxygen is removed. The products are then separated on a chromatographic column at 70 °C and are detected by a thermal conductivity detector. A calibration curve based on the concentration of known standards is used to quantify the gases.

The mineral matter content of the bitumen, maltenes, and asphaltenes were determined by thermogravimetric analysis (TGA) using a Mettler Toledo TGA/DSC1 equipped with LF 1100

furnace, sample robot, and MX5 internal microbalance. In a typical analysis approximately 5 mg of sample was weighed in an aluminium oxide crucible. The sample was then heated from 25 to 900 ºC at 10 °C/min in an oxidizing atmosphere to remove the organic matter by combustion. The air flow rate was controlled at 100 mL/min with Mettler GC 10 gas controller.

Liquid density measurement of the bitumen and the maltenes was performed using a density meter from Anton Paar, model DMA 4500M. Densities were recorded at a controlled temperature of 25 °C.

The refractive indexes of bitumen and maltenes were determined relative to that of air using the sodium D-line (589 nm). The measurements were performed at a controlled temperature of 25 °C.

Fourier transform infrared (FTIR) spectrometry was performed to identify compound class functional groups. The instrument used was ABB MB3000 FTIR spectrometer equipped with a Pike MIRacle^{TM} Reflection Attenuated Total Reflectance diamond crystal plate and a pressure clamp. The spectral region covered was 4000-500 cm^{-1}. Each spectrum was the average of 120 scans collected at a resolution of 4 cm^{-1}.

X-Ray fluorescence (XRF) spectrometry was performed in order to quantify halogens (chlorine, bromine, and iodine) in the feed and the products. The XRF instrument was a Bruker S2 Ranger that employed a Peltier cooled silicon drift detector and Pd-target as primary X-ray source. Analyses were performed at 50 kV. Quantification was performed using an external calibration curve. The calibration standards employed were NaCl, NaBr and KIO_3, which were diluted in tetrahydrofuran at different concentrations (0.2, 0.04, 0.008, 0.0016 wt %).

Ultraviolet-visible (UV-Vis) spectrometry was performed using a Shimadzu UV2700 UV-Vis spectrometer. Spectra were collected in the wavelength region 185-800 nm. Samples were placed in quartz cuvettes with 1 cm path length. The samples were diluted in toluene to a concentration equal to 40 mg/L.

Carbon-13 nuclear magnetic resonance (^{13}C NMR) spectrometry was performed by the Analytical Services of the Chemistry Department at University of Alberta using a 400 MHz Varian Unity Inova spectrometer. The samples were diluted in $CDCl_3$ solvent in a ratio equal to 1:1 (wt/wt) by the NMR technician and spectra were collected at 27 ºC and 100.577 MHz.

Optical microscopy was performed using a Carl Zeiss Discovery V.20 stereomicroscope.

The hardness of liquid products was determined using an electric penetrometer, Humboldt model ML 1200. It was not possible to follow the standard test method, which requires a larger sample size than was available. The hardness values were obtained for approximately 3 g of sample at ambient conditions with an applied load of 100 g for 0.01s, instead of 5 s.

Scanning Electron Microscopy (SEM) analysis of asphaltenes feed and halogenated asphaltenes was performed at Earth Sciences Department at University of Alberta. A Zeiss EVO MA 15 LaB_6 filament scanning electron microscope was used for this analysis. The instrument provided a resolution of approximately 5 nm. Backscattered images were taken using a Si diode detector. The instrument was equipped with an energy dispersive X-ray fluorescence spectrometer (Bruker, model Quantax 200) with a Peltier-cooled 10 mm^2 silicon drift detector with 123 eV resolution. Secondary electron images were obtained using an Everhart-Thornley detector. Prior to analysis the samples were coated with carbon using a Leica EM SCD005 evaporative carbon coater.

The thermal behavior of the feed and the halogenated products was evaluated with a heat flux differential scanning calorimeter (DSC). The instrument, Mettler Toledo DSC 1, was equipped with FRS-5 sensor employing 56 thermocouples, Haake intracooler and 400 W power amplifier. All measurements were conducted at atmospheric pressure and under a nitrogen atmosphere. Nitrogen flow rate was 100 mL/min and it was controlled through a Mettler Toledo GC 10 gas controller. Nitrogen gas was also used as purge gas at 100 mL/min and it was controlled by a gas flow meter, Cole Palmer PMR1-010750. In a typical analysis approximately 10 mg of sample was placed in an aluminium crucible with pin (40 µL). The lid was pierced with a needle on a clean rubber surface and the crucible was sealed with a Mettler crucible sealing press. The

temperature programme was to cool down the sample from 25 to –60 °C at –10 °C/min, followed by an isothermal period of 10 minutes at –60 °C, where after the sample was heated from –60 to 260 °C at 10 °C/min. The temperature and heat flow calibration of the DSC was performed with In and Zn standards.

Product yield during thermal conversion was determined by TGA following the procedure reported by Juyal *et al*. (2013) with some modifications as indicated. A Netzsch TGA was employed, which was capable of analysis under vacuum. In a typical analysis approximately 10 mg of sample was placed in an aluminum oxide crucible. The sample was then heated from 25 to 350 ºC at 10 ºC/min under vacuum. During this period, material present in the sample that is boiling in the naphtha, distillate and vacuum gas oil ranges was evaporated, with little or no thermal cracking taking place. This step simulates atmospheric and vacuum distillation. The mass of product that remains at the end of this step is equivalent to the vacuum residue fraction present in the material. The remainder of the analysis was performed under nitrogen flow of 50 mL/min, which involved heating from 350 to 500 ºC at 10 ºC/min followed by an isothermal period of 30 minutes at 500 °C. These two steps allow thermal cracking of the remaining sample to take place and they simulated a delayed coking process. The final isotherm at 500 ºC was employed to evaluate the micro carbon residue (MCR) content.

Weighing for the preparation of calibration standards and samples was performed using a Mettler XS105 Dual Range Analytical Balance with 0.01 mg readability at maximum capacity of 41 g and 0.1 mg readability at 120 g.

3.4 Results and Discussion

3.4.1 Halogen Content of Raw Materials and Brominated Products

The halogen content of the raw materials and the products after bromination was determined by XRF spectrometry (Table 3.3). The raw materials did not contain any bromine and incorporation of bromine was easily confirmed. After bromination the Br content of the bitumen, maltenes and asphaltenes were 1.6, 0.8 and 2.7 wt % respectively. As intended, the level of bromination was an order of magnitude lower than in the bromination work by Moschopedis and Speight (1971).

Table 3.3. Halogen content of raw materials and brominated products by quantitative XRF analysis.[a]

Description	Halogen content (μg/g)			
	Raw material		Brominated product	
	x	s	x	s
Bitumen				
Cl	57	5	240	6
Br	-[b]	-[b]	15913	1337
I	33	15	111	100
Maltenes				
Cl	42	5	48	3
Br	-[b]	-[b]	7824	58
I	-[b]	-[b]	-[b]	-[b]
Asphaltenes				
Cl	108	3	323	59
Br	-[b]	-[b]	26620	717
I	167	7	152	82

[a] Average (x) and sample standard deviation (s) of analyses in triplicate are reported.
[b] Below detection limit, or present at ≤ 1 μg/g.

Since the maltenes and asphaltenes were prepared from the bitumen, it was possible to perform a material balance using the information in Tables 3.1 and 3.3. The material balance closure on Cl and I was 94 % (i.e. 6 % difference), which was within the sample standard deviation of the XRF analysis of the bitumen reported in Table 3.3. There was no Br in any of the raw materials.

Trace element analysis of Athabasca bitumen using neutron activation reported low levels of Cl, but no Br or I (Strausz and Lown, 2003). The reported Cl contents of two different samples of Athabasca bitumen were 23.3 ± 3.1 and 13.8 ± 2.9 μg/g respectively. The first of these samples was also demineralized by centrifugation and the mineral-free Athabasca bitumen had a Cl content of 19.4 ± 3.2 μg/g. This implied that most of the Cl was associated with the organic matter. The reported Cl values are of the same order of magnitude as the Cl content of the Athabasca bitumen in this study, which was 57 ± 5 μg/g (Table 3.3). No mention was made of bromine associated with oilsands in the review by Vainikka and Hupa on bromine in solid fuels (Vainikka and Jupa, 2012).

Two additional observations were made based on the halogen content of the brominated samples (Table 3.3). First, under similar bromination conditions, more Br was incorporated into the asphaltenes fraction than in the maltenes fraction. Second, the NaBr employed for bromination (Table 3.2) contained some halogenated impurities, which caused a measurable increase in the Cl content of the brominated products.

3.4.2 Nature of the Brominated Carbon

Elemental analysis (Table 3.3) demonstrated that Br was successfully incorporated in the materials during bromination. It also indicated that the asphaltenes fraction was more readily brominated than the maltenes fraction. Based on this observation, one could infer that bromination favored aromatic carbon over aliphatic carbon.

In order to provide direct evidence of aromatic bromination, as was intended by the bromination methodology, the raw materials and the brominated products were analyzed by infrared spectrometry. There were two regions of interest, namely, 680-515 cm^{-1} where there is absorption by aliphatic C–Br bonds and 1300-1000 cm^{-1} where the strong CH_2 wag of Br–CH_2 at 1230 cm^{-1} can be found, as well as the aromatic ring vibrations that are influenced by C–Br bonds (Colthup et al., 1990).

The asphaltenes was the raw material most likely to show the effect of bromination (Table 3.3). The 680-515 cm^{-1} spectral region of the asphaltenes was convoluted and although that of the brominated asphaltenes was less convoluted, there was no indication of aliphatic C–Br bonds that could be discerned (Figure A1 in the Appendix A). The 562 cm^{-1} absorption of the C–Br was reported for a 3 % brominated asphalt (Boucher et al., 1990), but it was generally noted that the C–Br absorption in this spectral region is difficult to observe (Zabicky, and Ehrlich-Rogozinski, 1973). The 1300-1000 cm^{-1} spectral region provided more information (Figure 3.2). The strong CH_2 wag at 1230 cm^{-1} was present both in the raw and brominated asphaltenes and could not be a useful indicator of aliphatic bromination. The main differences that were observed in the infrared spectrum of the brominated asphaltenes compared to the raw asphaltenes were the absorptions at 1188, 1079 and 1056 cm^{-1} (Figure 3.2). The absorption at 1188 cm^{-1} can

possibly be due to Br–CH, which absorbs about 50 cm^{-1} lower than the Br–CH_2 wag (Colthup et al., 1990). The absorptions at 1079 and 1056 cm^{-1} straddle the 1073-1065 cm^{-1} region where the aromatic ring vibrations for *para*- and *meta*-brominated benzenes are found (Colthup et al., 1990). The information on the nature of the C–Br bonds from the infrared spectra was inconclusive, but suggested that both aliphatic and aromatic bromination occurred.

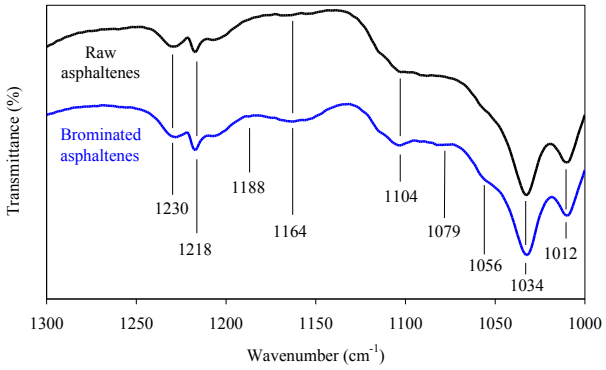

Figure 3.2. Infrared spectra of raw asphaltenes and brominated asphaltenes in the region 1300-1000 cm^{-1}

In a previous asphaltene halogenation study, it was reported that no absorption bands in the infrared spectrum could be unequivocally assigned to carbon-halogen bonds, despite considerably higher halogen content than in the present study (Moschopedis and Speight, 1971). It reflected the same inconclusiveness about the assignment of spectral differences as was found in our study. Yet, to be clear, the spectral data that was presented by Moschopedis and Speight (1971) showed clear differences between the IR spectra of raw and brominated asphaltenes.

The infrared spectra of the raw and brominated bitumen, maltenes and asphaltenes can be found in the Appendix A (Figures A2-A4). The spectra of the brominated bitumen and maltenes suggested that at least some aliphatic carbons were brominated.

The raw and brominated materials were also studied by ^{13}C NMR in the hope of determining the extent of bromination of aromatic compared to aliphatic carbon (Table 3.4). The brominated asphaltenes could not be analyzed, because we were incapable of dissolving the material in any of the standard laboratory solvents that were tried: toluene, chloroform, acetone, methyl chloride, and carbon disulphide. Although the analyses provided information on the aromatic versus

aliphatic content of the materials, it was not possible to discern the impact of bromination on the ^{13}C NMR spectra of the brominated bitumen or brominated maltenes. Nevertheless, some general observations could be made based on the ^{13}C NMR data:

(a) Bromination did not measurably affect the ratio of aromatic to aliphatic carbon.
(b) The asphaltenes were more aromatic in nature than the other materials. Of its carbon mass 48 % was aromatic, compared to 28-30 % in the bitumen and maltenes.
(c) The material balance closure on aromatic carbon closed to within 6 % relative error. The aromatic carbon content in bitumen was either under reported, or the aromatic carbon content in the maltenes and asphaltenes was over reported.
(d) The identification of carbon as either aromatic or aliphatic depended on the chemical shift in the ^{13}C NMR spectrum and the assignments are valid only when little or no alkenes are present. The materials were not thermally processed and little (if any) alkenes were anticipated (Strausz and Lown, 2003).

Table 3.4. Identification of the nature of the carbon in the raw materials and brominated products by ^{13}C NMR analysis

Material	Nature of carbon (wt %) [a]	
	aromatic	aliphatic
raw bitumen	30	70
brominated bitumen	31	69
raw maltenes	28	72
brominated maltenes	28	72
raw asphaltenes	48	52
brominated asphaltenes	- [b]	- [b]

[a] Brominated carbon of either type could not be discerned
[b] Could not dissolve material for analysis

3.4.3 Physical Changes Caused by Bromination

It was clear from visual inspection of the brominated products that halogenation had a significant impact on the properties of the raw materials (Figure 3.3). Compared to the raw bitumen, the brominated bitumen was harder and appeared more viscous. The maltenes after bromination was darker and harder compared to the raw maltenes and the brominated maltenes appeared very similar to raw bitumen. Pentrometer tests confirmed that hardening of the bitumen and maltenes

took place (Table 3.5). The change in the appearance of the asphaltenes after bromination was considerable. The brown powdery asphaltenes turned into a darker, harder and shiny substance after bromination. The formation of some crystalline structures was observed after bromination. Furthermore, the brominated asphaltenes were insoluble in toluene, chloroform, acetone, methyl chloride and carbon disulfide.

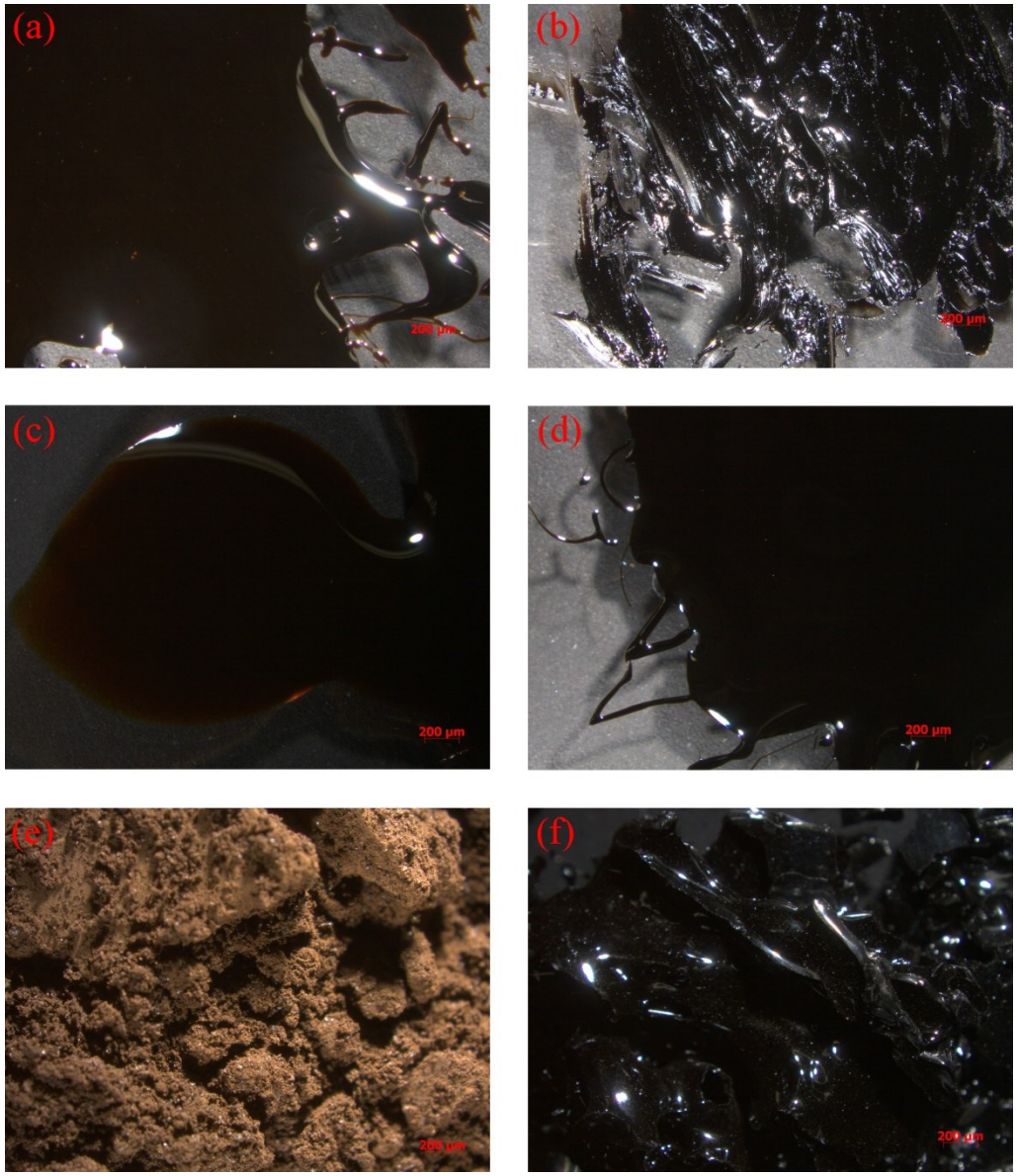

Figure 3.3. Images of the materials: (a) raw bitumen, (b) brominated bitumen, (c) raw maltenes, (d) brominated maltenes, (e) raw asphaltenes, and (f) brominated asphaltenes

Table 3.5. Pentrometry of raw and brominated bitumen and maltenes

Material	Penetration (mm) [a,b]	
	x	s
raw bitumen	1.0	0.1
brominated bitumen	0.3	0.1
raw maltenes	3.6	0.2
brominated maltenes	1.8	0.4

[a] Applied load of 100 g for 0.01 s.
[b] Average (x) and sample standard deviation (s) of analyses in triplicate are reported.

Our observations were in line with that from previous reports in literature. It was reported that halogenated asphaltenes were black and shiny and insoluble in solvents such as benzene, nitrobenzene, and carbon tetrachloride (Moschopedis and Speight, 1976). Chlorination of bitumen with elemental chlorine also provided hard and brittle products (Patwardhan, 1979). Fluorination was different from other types of halogenation. It reacted in a more controlled fashion, which suggested that "fluorine is acting essentially as an opportunistic reagent" and fluorinated asphaltenes were only partially insoluble in benzene and 1-chloronaphthalene (Kowanko et al., 1978).

There are two aspects related to the observations that may be worthwhile to investigate further.

First is the application of mild halogenation as pretreatment for the preparation of asphalt for road paving. Halogenation causes hardening (Table 3.5) and is a possible alternative to oxidative hardening (Petersen, 1993; Vassiliev et al., 2001) that is commonly used for road asphalt preparation. The potential advantage that halogenation may have over oxidation is the observed insolubility of the product, which may make it more resistant to degradation during environmental exposure. However, halogenation is a more expensive conversion than autoxidation (Pfeiffer, 1950), and it is not clear that it would be an economically viable alternative to oxidative hardening.

Second is the potential role of halogens in affecting the chemistry during bitumen upgrading. As shown in Table 3.3, bitumen already contains some halogens. Metal chlorides that are Lewis acids may act as catalysts. When asphaltenes were heated in the presence of $AlCl_3$ and $ZnCl_2$,

Friedel-Crafts alkylation of the asphaltenes took place, which in some instances resulted in a significant decrease in benzene solubility (Ignasiak et al., 1981). For example, heating Athabasca asphaltenes to 200 °C in the presence of $ZnCl_2$ resulted in 55 % of the asphaltenes becoming insoluble in benzene. Furthermore, according to Gray (2010), residual chlorine in bitumen may be present as crystalline chloride salts. These crystalline salts are hydrophobic and are coated with asphaltenes in the diluted bitumen. Because asphaltenes are potential coke precursors and coke is insoluble in toluene, residual halogens present in bitumen may also have some physical influence during coke formation.

3.4.4 Chemical Changes Detected by Thermal Analysis

It was possible that the physical changes that were caused by bromination would also cause a change in the low temperature behavior of the materials. Differential scanning calorimetry was employed to determine the thermal behavior in the temperature range 25 to –60 °C (Appendix A Figures A5-A7). All of the raw and brominated materials exhibited a measurable and distinct change in heat flow, which was indicative of a second-order phase transition (Table 3.6). Bromination did not affect the temperature of this transition in bitumen, but it caused opposite effects in the maltenes and asphaltenes. The brominated maltenes had a lower transition temperature, whereas the brominated asphaltenes had a higher transition temperature than the corresponding raw materials.

The second-order phase transitions of the bitumen and maltenes (Table 3.6) are likely related to the glass transition of these materials. Glass transition temperatures in the range –17 to –33 °C were reported for different bitumens and maltenes (Jiménez-Mateos et al., 1996). However, Masson et al. (2002;2005) pointed out that the glass transition in bitumen and its sub-fractions is complex and consists of multiple events over a wider temperature range, typically –50 to 100 °C, and that it is affected by the time allowed for restructuring to occur.

The glass transition of asphaltenes generally occur at higher temperatures, typically >0 °C (Masson et al., 2005; Kopsh, 1994; zhang et al., 2004; Masson et al., 2007). Yet, in our work a

clear second-order transition was also observed at –29 °C, which increased in temperature to –25 °C on bromination.

Table 3.6. Low temperature transitions in raw and brominated materials measured by DSC

Material	Transition temperature (°C) [a]
raw bitumen	-23
brominated bitumen	-23
raw maltenes	-23
brominated maltenes	-25
raw asphaltenes	-29
brominated asphaltenes	-25

[a] Onset temperature on cooling, with an uncertainty of ~1 °C.

3.4.5 Chemical Changes Detected by Ultraviolet-Visible Spectrometry

It was reported that chlorination is an effective methodology for demetalation of metalloporphyrin compounds (Sugihara et al., 1975). Fluorination was less effective for demetalation (Kowanko et al., 1978). In general demetalation of metalloporphyrins rely on strong oxidants (Yin, 2009). Demetalation was not a specific objective of this work, but coordinative interactions contribute to asphaltenes aggregation (Gray et al., 2011), and the high-level objective was to convert asphaltenes into maltenes.

The materials were analyzed by UV-vis spectrometry before and after bromination (Figure 3.4). The brominated asphaltenes could not be analyzed, because it was insoluble. The Soret bands of nickel (~395 nm) and vanadyl (~410 nm) porphyrins are intense and can be used to detect these compounds at low concentration (Van Berkel, G. J.; Filby, 1987; Dechaine and Gray, 2010). The exact absorption maxima depend on the chemical nature of the porphyrins and their solvent environment. The intensity of the Soret bands of the metalloporhyrins decreased, suggesting that bromination is capable of some demetalation. It was reported by Chorgade et al. (1996) that exposing metalloporhyrins to bromination for longer periods of time at room temperature led to decomposition of the porphyrin, but they did not offer an explanation of why this was the case.

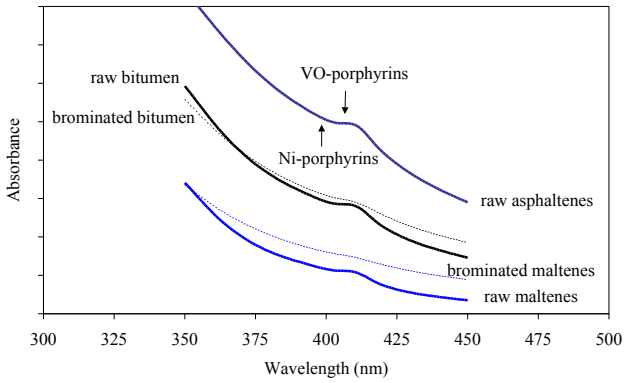

Figure 3.4. Soret bands of the nickel and vanadyl porphyrins in raw bitumen, maltenes and asphaltenes, as well as the brominated bitumen and maltenes

3.4.6 Chemical Changes Detected by SEM with X-Ray Microanalysis

Following up on the observations by UV-vis spectrometry, the asphaltenes and halogenated asphaltenes were studied by scanning electron microscopy with microanalysis by energy dispersive X-ray fluorescence spectrometry (SEM-EDX). The backscattered electron image (Appendix A Figure A8) indicated particulates of 1-2 μm diameter in the asphaltenes that contained heavier elements than the organic bulk. A semi-quantitative analysis was performed on the asphaltenes sample to represent an average composition, as well as microanalysis of a particle containing heavier elements and microanalysis of the organic matrix devoid of particulates (Appendix A Table A1). These values provide a reasonable estimate of the relative atomic concentrations. In order to obtain better absolute concentration values for the SEM-EDX analyses, the value for the sulfur content in the bulk asphaltenes analysis was corrected using the elemental analysis presented in Table 3.1. The same correction factor was applied to all of the values and the results are presented in Table 3.7. Despite this calibration, the numerical values should not be over-interpreted. The standard deviations that are reported are for the repeatability of the analyses and they do not reflect the true uncertainty of quantification. X-ray fluorescence is matrix sensitive and performing microanalysis on the particulates, the matrix of particulate microanalysis is inherently dissimilar to that of the bulk asphaltenes sample. Nevertheless, the following general observations could be made:

a) The particulates in the raw asphaltenes are likely iron pyrite (FeS_2), because the calculated atomic ratio of Fe:S is 1:2.2.

b) There was no qualifiable difference in the amount of O, Al, or Si associated with the particulates compared to that of the organic matrix.

c) The Ni and V present in the asphaltenes were not associated with the particulates.

d) The Ni and V content of the organic matrix was below the detection limit, yet, it was not during the bulk analysis. This suggests that Ni and V are not evenly distributed in the matrix.

Table 3.7. Semi-quantitative SEM-EDX analyses of raw asphaltenes

Element	Composition (wt %) [a,b]					
	Bulk		Particulate		Organic matrix	
	x	s	x	s	x	s
O	6.67	1.23	6.65	1.82	5.32	1.08
Al	0.46	0.06	0.76	0.09	0.60	0.06
Si	0.82	0.06	0.79	0.09	0.76	0.06
S	8.07	0.32	12.96	0.74	8.30	0.33
V	0.14	0.04	- [c]	- [c]	- [c]	- [c]
Fe	0.27	0.05	10.43	0.47	0.42	0.05
Ni	0.03	0.04	- [c]	- [c]	- [c]	- [c]

[a] Average (x) and sample standard deviation (s) to indicate repeatability of analyses.
[b] Values corrected from Table A1 (Appendix A) based on S-content of asphaltenes.
[c] Concentration below the quantification limit of the instrument.

The brominated asphaltenes was analyzed in an analogous way (Appendix A Figure A9). The 1-2 μm diameter particulates that contained heavier elements were likewise observed in the brominated asphaltenes. In addition to the particulates there were regions that contained a higher concentration of heavier elements than the bulk organic matrix. These regions were diffuse in nature, rather than being particulates and it seemed like organic aggregates or domains within the organic matrix. As with the raw asphaltenes, a semi-quantitative analysis was performed on the brominated asphaltenes sample to obtain an average composition, which was followed by microanalysis on the particulates, aggregate regions of intermediate heaviness and the organic matrix (Appendix A Table A2). A correction value was applied based on the sulfur

concentration of the bulk analysis (Table 3.8). The uncertainty associated with the quantification is high as indicated by difference in the value for the Br content compared to the value obtained by XRF analysis (Table 3.3). Some general observations are nevertheless possible:

a) After bromination, the iron pyrite particles present in the asphaltenes are associated with sulfur-containing compounds from the asphaltenes. The atomic ration of Fe:S increased from 1:2.2 in raw asphaltenes to 1:5.3 in brominated asphaltenes. The total sulfur content of the particulates approximated that of the bulk asphaltenes.

b) The iron pyrite particles seemed to collect oxygenate rich material in particular. Although the quantification of oxygen is associated with large uncertainty, the oxygen content of the particulates were 23 ± 4 wt % compared to the bulk that was 10 ± 2 wt %.

c) There was no qualifiable difference in the amount of Al, Si or Br associated with the particulates or aggregates compared to that of the organic matrix.

d) The aggregate material contained elevated levels of P, K, Ca and Fe compared to the bulk organic matrix. The concentration of Ca was particularly high, 1.2 ± 0.1 wt %, considering that it was below quantification limit in the bulk of the sample. The oxygen content was also slightly elevated, but this may not be significant considering the large uncertainty in oxygen analysis.

e) Similar observations about Ni and V were made for brominated asphaltenes as for raw asphaltenes; the Ni and V were not associated with the particulates and were not evenly distributed in the matrix.

One potential benefit of bromination is the association of oxygen-rich material in the asphaltenes with the small iron pyrite particles. The oxygen-rich material is multi-functional and also contains sulfur, as was reported in characterization studies (Purcell et al., 2007). In the liquid or molten state it may be possible to employ magnetic separation to selectively remove such aggregates, as was previously suggested for the cleaning of high sulfur coals by magnetic

separation of pyrites (Oder, 1985). The impact of such a separation is potentially beneficial, although neither the separation nor the benefit was demonstrated in the present study.

Table 3.8. Semi-quantitative SEM-EDX analyses of brominated asphaltenes

Element	Composition (wt %) [a,b]							
	Bulk		Particulate		Organic aggregate		Organic matrix	
	X	s	x	s	x	s	x	s
O	9.92	1.70	22.91	4.44	12.61	2.33	9.75	1.67
Al	0.43	0.06	0.36	0.06	0.34	0.06	0.16	0.04
Si	0.73	0.07	0.39	0.06	0.51	0.06	0.50	0.06
P	- [c]	- [c]	- [c]	- [c]	0.14	0.04	- [c]	- [c]
S	7.86	0.31	7.22	0.40	8.66	0.39	7.73	0.31
Cl	0.09	0.04	- [c]	- [c]	0.10	0.04	- [c]	- [c]
K	- [c]	- [c]	- [c]	- [c]	0.19	0.04	- [c]	- [c]
Ca	- [c]	- [c]	0.16	0.04	1.19	0.09	- [c]	- [c]
V	0.13	0.04	- [c]	- [c]	- [c]	- [c]	- [c]	- [c]
Fe	0.26	0.06	2.36	0.14	0.69	0.07	0.23	0.06
Ni	0.09	0.04	- [c]	- [c]	- [c]	- [c]	- [c]	- [c]
Br	4.39	0.27	5.15	0.39	5.25	0.34	4.83	0.29

[a] Average (x) and sample standard deviation (s) to indicate repeatability of analyses.
[b] Values corrected from Table A2 (Appendix A) based on S-content of asphaltenes.
[c] Concentration below the quantification limit of the instrument.

3.4.7 Changes in Pyrolysis Yield due to Bromination

The raw and brominated bitumen, asphaltenes and maltenes were analyzed by vacuum TGA to determine changes in the yield of lighter fractions and thermal cracking behavior. There were two stages in each analysis. In the first stage the samples were heated under vacuum to simulate distillation to an equivalent normal boiling point temperature of 525 °C, but without exceeding 350 °C and causing thermal cracking. This provided the yield of the straight run distillation fractions of the samples. The material that was not volatilized, was the vacuum residue (>525 °C boiling fraction). In the second stage the vacuum residue was pyrolyzed to a temperature of 500 °C over an extended period of time to obtain the cracking yields. The yield of pyrolysis gas / liquid represents all of the products that could be volatilized at 500 °C under nitrogen flow. The remaining solid material is the micro carbon residue (MCR), which represents the yield of coke.

It was found (Table 3.9) that bromination was deleterious in its effect on bitumen and the maltenes, but that bromination was somewhat beneficial for asphaltenes. The straight run naphtha and distillate yields were not affected in a statistically meaningful way. However, the straight run vacuum gas oil yield of the brominated bitumen and maltenes were lower, whereas the straight run vacuum gas oil yield of the asphaltenes increased from 2.0 ± 0.3 wt % to 7.5 ± 1.8 wt % due to bromination. The additional straight run vacuum gas oil in the brominated asphaltenes seem to have originated from material that would otherwise have produced lighter products on pyrolysis, because bromination decreased the pyrolysis gas/liquid yield, without affecting the coke yield. Hence, there was not net benefit in terms of liquid yield due to the bromination of the asphaltenes. The decrease in vacuum gas oil yield in the bitumen and the maltenes were reflected by a concomitant increase in MCR yield. Consequently there was a net decrease in liquid yield due to bromination of the bitumen and maltenes.

Bromination was capable of liberating material in the asphaltenes fraction that would otherwise only be liberated on pyrolysis. If the initial hypothesis (Figure 3.1) is true, then approximately 5 wt % of the asphaltenes were aggregated by π-π ring stacking and could be liquefied by bromination. However, bromination of bulk bitumen was deleterious, because it can also facilitate side-reactions. Based on the yield profile (Table 3.9), the material in bitumen that is prone to side-reactions that ultimately led to an increase in coke, is material that can be found mainly in the maltenes fraction of the bitumen. One aspect that was not addressed in this study was how sensitive each of these outcomes is to the degree of bromination. It may well be that very limited bromination can be beneficial and that the negative side-reactions are a result of over-bromination.

Table 3.9. Product yields of raw and brominated materials

Material	Distillation yield (wt %) [a,b]						Cracking yield (wt %) [a,c]			
	naphtha (<177 °C)		Distillate (177-343 °C)		vacuum gas oil (343-525 °C)		pyrolysis gas / liquid		micro carbon residue	
	x	s	x	s	x	s	x	s	x	s
raw bitumen	0.2	0.3	5.6	1.4	41.4	2.6	41.1	1.2	11.7	1.5
brominated bitumen	0.5	0.2	5.1	3.0	36.4	6.8	41.2	2.6	16.8	2.7
raw maltenes	0.6	0.2	10.4	0.7	49.4	0.3	33.0	1.3	6.6	1.3
brominated maltenes	0.4	0.2	9.9	1.3	43.1	0.6	35.4	1.2	11.2	0.6
raw asphaltenes	0.5	0.3	0.5	0.5	2.0	0.3	51.6	0.8	45.4	0.5
brominated asphaltenes	0.5	0.2	1.2	1.2	7.5	1.8	45.6	0.8	45.2	2.0

[a] Average (x) and sample standard deviation (s) of analyses in triplicate are reported.
[b] Yield on total sample by vacuum distillation in the TGA without thermal cracking.
[c] Yield on total sample by pyrolysis of the vacuum residue (>525 °C) fraction in the TGA.

3.4.8 Explaining the Effects of Halogenation

Bromination resulted in chemical, as well as physical changes in the nature of bitumen, maltenes and asphaltenes. Some of the most notable changes after mild (3 %) bromination were an increase in hardness, decrease in solubility, changes in metal-related interactions and changes in product yields on distillation and pyrolysis. Based on literature three possible explanations for the observations can be forwarded.

a) Increased π-π ring stacking by alternating halogenated and non-halogenated aromatic sheets, contrary to the working hypothesis outlined in the introduction. It was reported that π-π ring stacking between a halogenated aromatic sheet and a non-halogenated aromatic sheet may be stronger than either class individually (Li et al., 2012). It was explained in terms of the generation of a region of positive electrostatic potential that could be generated by a covalently bounded halogen on an aromatic ring. Thus, an electron-rich molecule, such as a non-halogenated aromatic sheet, will interact with the region of positive electrostatic potential and the strength of the stacking interactions is controlled by electrostatic terms. In addition, it was reported that the interaction between halogen bonds and π-π stacking resulted in crystal structures (Li et al., 2012). The formation of stronger π-π stacking of aromatic sheets would help explain the increase in hardness after bromination (Table 3.5), as well as the increase in crystallinity of the brominated asphaltenes (Figure 3.3).

b) Addition reactions caused by halogenation. Bromination did not occur exclusively on aromatic carbons, as could be seen from the infrared spectra (Figure 3.2). Addition reactions could have taken place through dehydrohalogenation with elimination of the bromine from aliphatic C–Br bonds, the formation of C=C double bonds and subsequent olefinic addition reactions (Boucher et al., 1990). The resulting products would be cross-linked and have lower solubility in any solvent medium. Although such carbon-carbon cross-linking is not completely analogous to vulcanization of rubber, the effect on the physical properties follows the same trend. In fact, on heating the liberation of HCl from chlorinated asphaltic bitumen was reported (Pfeiffer, 1950), supporting this pathway as explanation for the observed hardening. Additionally, demetalation as was suggested by Figure 3.4, may lead to the formation of metal halides. If the metal halides are Lewis acids, the metal halides could have resulted in Friedel-Crafts type coupling reactions, as was previously reported (Speight, 1971). Conversion in the presence of $CuCl_2$, $FeCl_3$ and $AlCl_3$ caused products to have significantly changed solubility behavior, as was indeed observed in this study. It is possible that analogous behavior may have resulted from Lewis acids with bromine instead of chlorine.

c) Increased hydrogen-bonding interactions. The factors that affected the strength of hydrogen bonding between the halogens in C–X bonds and hydrogen were discussed by Smith (1973). Of specific importance was that halogens attached to aromatic carbons formed weaker hydrogen bonding interactions and that intra- and intermolecular hydrogen bonding have opposite effects on the physical properties of materials. When intramolecular hydrogen bonding takes place, the boiling point of the substance may be decreased. This may explain the conversion of some asphaltenes to lighter boiling material after bromination (Table 3.9). Conversely, intermolecular hydrogen bonding will cause molecules to interact more strongly and increase boiling point.

3.5 Conclusions

The investigation into mild halogenation of asphaltenes was justified based on the hypothesis that the insertion of a bulky halogen substituent on an aromatic carbon in a multinuclear aromatic compound might sterically disrupt π-π ring stacking (Figure 3.1), thereby disaggregating the

material. It was appreciated that π-π ring stacking was just one of the possible aggregation forces present in asphaltenes. Unfortunately it was not possible to unequivocally demonstrate that π-π ring stacking was a significant force, or whether the ~5 wt % of asphaltenes that became lighter boiling products after bromination (Table 3.9) was liberated due to a disruption of π-π ring stacking. In fact, the hardening behavior may even indicate that the hypothesis forwarded in the introduction was invalid. Still, there were a number of potentially valuable observations that could be made from the experimental investigation:

a) Athabasca bitumen naturally contains low levels (10-100 μg/g range) of Cl and I, but no detectable Br. On asphaltene precipitation with *n*-pentane, the Cl partitions between the maltenes and asphaltenes fraction, but I is contained exclusively in the asphaltenes fraction.

b) The bromination method was selected to perform mild halogenation of carbon in aromatic rings. Analysis of the brominated materials by infrared and ^{13}C NMR spectrometry suggested that both aliphatic and aromatic bromination occurred.

c) It was found that 1-3 wt % Br was incorporated into the bitumen, maltenes and asphaltenes by mild bromination of the individual fractions.

d) Mild bromination caused observable changes in the physical appearance of bitumen, maltenes and asphaltenes. The hardness of all materials was increased and in the case of asphaltenes it became a hard, shiny and brittle black solid that was insoluble in toluene, chloroform, acetone, methyl chloride and carbon disulfide.

e) Clear second-order phase transitions were observed for bitumen, maltenes and asphaltenes in the temperature range –20 to –30 °C. Bromination caused a minor change in the temperature of this transition.

f) UV-vis spectrometry indicated that metalloporphyrin structures were disrupted by bromination.

g) The association behavior of organic matter in the asphaltenes with small iron pyrite particulates present in the asphaltenes changed after bromination, with a meaningful increase of oxygen-rich material being associated with the iron pyrite particulates. There were no meaningful differences in the Br content associated with particulate matter, aggregates or the bulk of the organic matrix in the brominated asphaltenes.

h) Bromination was deleterious in its effect on bitumen and the maltenes, resulting in a decrease in straight run vacuum gas oil yield and increase in micro carbon residue.

i) Bromination of asphaltenes resulted in an increase in straight run vacuum gas oil yield from 2.0 ± 0.3 wt % to 7.5 ± 1.8 wt %. This change was accompanied by a decrease in the yield of liquids and gases produced during pyrolysis, with the yield of micro carbon residue being unaffected by bromination.

In addition to the experimental observations, potential opportunities and leads for future investigation were identified:

j) Halogenation may be considered as pretreatment in the preparation of asphalt for road paving. Not only does halogenation cause an increase in hardness, but it renders the product resistant to organic solvents. The economic viability of this was not evaluated.

k) Even though the halogen content of raw bitumen and its fractions is low, halogens may be affecting the chemistry during bitumen upgrading. There were indications of Friedel-Crafts alkylation chemistry taking place. The presence of halogens may also influence coke formation and coke yield during bitumen upgrading.

l) Mild halogenation may be sufficient to disrupt metalloporhyrins, suggesting that halogenation may be considered for demetalation of bitumen.

m) The combination of halogenation with magnetic separation may have potential for the removal of oxygen-rich asphaltenes that become associated with iron pyrite particles already present in the asphaltenes fraction.

n) The extent of halogenation may affect the trade-off between benefits and deleterious impacts that were observed. Even 1-3 wt % Br incorporation may already be an over-halogenation of the materials. If this is indeed the case, the aforementioned potential benefits may be achieved with low levels of halogenation, which would make halogenation a more palatable industrial proposition than it is at present.

Literature Cited

Ancheyta, J.; Trejo, F.; Rana, M. S. *Asphaltenes. Chemical transformation during hydroprocessing of heavy oils*; CRC Press: Boca Raton, 2009.

Asphaltenes, heavy oils, and petroleomics; Mullins, O. C., Sheu, E. Y., Hammami, A., Marshall, A. G. Eds.; Springer: New York, 2007.

Boucher, J. L.; Wang, I.-H.; Martinez, D. F. Elimination chemistry in asphalt. *Prepr. Pap.-Am. Chem. Soc., Div. Petrol. Chem.* **1990**, *35* (3), 550-555.

Chorghade, M. S.; Dolphin, D.; Dupré, D.; Hill, D. R.; Lee, E. C.; Wijesekera, T. P. Improved protocols for the synthesis and halogenation of sterically hindered metalloporphyrins. *Synthesis* **1996**, *11*, 1320-1324.

Colthup, N. B.; Daly, L. H.; Wiberley, S. E. *Introduction to infrared and Raman spectroscopy*, 3ed; Academic Press: San Diego, CA, 1990.

De Klerk, A.; Gray, M. R.; Zerpa, N. Unconventional oil and gas: Oilsands. In *Future energy. Improved, sustainable and clean options for our planet*, 2ed; Letcher, T. M. Ed.; Elsevier: Amsterdam, 2014, pp. 95-116.

Dechaine, G. P.; Gray, M. R. Chemistry and association of vanadium compounds in heavy oil and bitumen, and implications for their selective removal. *Energy Fuels* **2010**, *24*, 2795-2808.

Gray, M. R. *Fundamentals of oilsands upgrading*; Notes, University of Alberta: Edmonton, AB, 2010.

Gray, M. R.; Tykwinski, R. R.; Stryker, J. M.; Tan, X. Supramolecular assembly model for aggregation of petroleum asphaltenes. *Energy Fuels* **2011**, *25*, 3125-3134.

Ignasiak, T.; Bimer, J.; Samman, N.; Montgomery, D.S.; Strausz, O.P. Lewis acids assisted degradation of Athabasca aspaltene. *Adv. Chem. Ser.* **1981**, *195*, 183-201.

Jiménez-Mateos, J. M.; Quintero, L. C.; Rial, C. Characterization of petroleum bitumens and their fractions by thermogravimetric analysis and differential scanning calorimetry. *Fuel* **1996**, *75*, 1691-1700.

Juyal, P.; McKenna, A. M.; Fan, T.; Cao, T.; Rueda-Velásquez, R. I.; Fitzsimmons, J. E.; Yen, A.; Rodgers, R. P.; Wang, J.; Buckley, J. S.; Gray, M. R.; Allenson, S. J.; Creek, J. A joint industrial case study for asphaltene deposition. *Energy Fuels* **2013**, *27*, 1899-1908.

Kopsh, H. On the thermal behaviour of petroleum asphaltenes. *Thermochimica Acta* **1994**, *235*, 271-275.

Kowanko, N.; Branthaver, J. F.; Sugihara, J. M. Direct liquid-phase fluorination of petroleum. *Fuel* **1978**, 57, 769-775.

Lee, K-J.; Cho, H. K.; Song, C-E. Bromination of activated arenes by Oxone® and sodium bromide. *Bull. Korean Chem. Soc.* **2002**, *23* (5), 773-775.

Li, H., Lu, Y., Liu, Y., Zhu, X., Liu, H., Zhu, W. Interplay between halogen bonds and π-π stacking interactions: CSD search and theoretical study. *Phys. Chem. Chem. Phys.* **2012**, *14*, 9948-9955.

Masliyah, J. H.; Czarnecki, J. A.; Xu, Z. *Handbook on Theory and Practice of Bitumen Recovery from Athabasca Oilsands. Theoretical basis*. Kingsley Publishing Services: Canada, 2011.

Masson, J-F.; Collins, P.; Polomark, G. Steric hardening and the ordering of asphaltenes in bitumen. *Energy Fuels* **2005**, *19*, 120-122.

Masson, J-F.; Leblond, V.; Margeson, J.; Bundalo-Perc, S. Low-temperature bitumen stiffness and viscous paraffinic nano- and micro-domains by cryogenic AFM and PDM. *J. Microscopy* **2007**, *227* (3), 191-202.

Masson, J-F.; Polomark, G.; Collins, P. Time-dependent microstructure of bitumen and its fractions by modulated differential scanning calorimetry. *Energy Fuels* **2002**, *16*, 470-476.

Miyake, M.; Stock, L. M. Coal solubilization. Factors governing successful solubilization through C-alkylation. *Energy Fuels* **1988**, *2*, 815-818.

Moschopedis, S. E.; Speight, J. G. Chemical modification of bitumen heavy ends and their nonfuel uses. *Adv. Chem. Ser.* **1976**, *151*, 144-152.

Moschopedis, S. E.; Speight, J. G. Introduction of halogen into asphaltenes via the Gomberg reaction. *Fuel* **1970**, *49*, 335.

Moschopedis, S. E.; Speight, J. G. The halogenation of Athabasca asphaltenes with elemental halogen. *Fuel* **1971**, *50*, 58-64.

Oder, R. R. Magnetic desulfurization of coal. In *Processing and utilization of high sulfur coals* (Coal Sci. Technol. 9); Attia, Y. A. Ed.; Elsevier: Amsterdam, 1985, pp. 195-214.

Parsons, A. F. *An introduction to free radical chemistry*; Blackwell Science: Oxford, 2000, pp. 124.

Patwardhan, S. R. Chlorination of petroleum bitumens. *Fuel* **1979**, *58*, 375-378.

Petersen, J. C. Asphalt oxidation - an overview including a new model for oxidation proposing that physicochemical factors dominate the oxidation kinetics. *Fuel Sci. Technol. Int.* **1993**, *11*, 57-87.

Purcell, J. M.; Juyal, P.; Kim, D-G.; Rodgers, R. P.; Hendrickson, C. L.; Marshall, A. G. Sulfur speciation in petroleum: Atmospheric pressure photoionization or chemical derivatization and electrospray ionization Fourier transform ion cyclotron resonance mass spectrometry. *Energy Fuels* **2007**, *21*, 2869-2874.

Siddiqui, M. N. Exploring the chemical reactivity of asphaltenes. *Prepr. Pap.-Am. Chem. Soc., Div. Fuel. Chem.* **2009**, *54* (1), 14-15.

Sill, G. A.; Yen, T. F. Semiconduction of iodine complexes of asphaltenes. *Fuel* **1969**, 48, 61-74.

Smith, J. W. Hydrogen-bonding and complex-forming properties. In *The chemistry of the carbon-halogen bond. Part 1*; Patai, S., Ed.; John Wiley and Sons: London, 1973, pp. 265-300.

Speight, J. G. Reactions of Athabasca asphaltenes and heavy oil with metal chlorides. *Fuel* **1971**, *50*, 175-186.

Strausz, O. P.; Lown, E. M. *The chemistry of Alberta oilsands, bitumens and heavy oils*; Alberta Energy Research Institute: Calgary, AB, 2003.

Sugihara, J.; Branthaver, J.; Willcox, K. Oxidative demetalation of oxovanadium(IV) porphyrins. In *The role of trace metals in petroleum*; Yen, T. F. Ed.; Ann Arbor Science Publishers: Ann Arbor, MI, 1975, pp. 183-193.

Van Berkel, G. J.; Filby, R. H. Generation of nickel and vanadyl porphyrins from kerogen during simulated catagenesis. *ACS Symp. Ser.* **1987**, *344*, 110-134.

Vassiliev, N. Y.; Davison, R. R.; Williamson, S. A.; Glover, C. J. Air blowing of supercritical asphalt fractions; *Ind. Eng. Chem. Res.* **2001**, *40*, 1773-1780.

Yin, C.-X.; Stryker, J. M.; Gray, M. R. Separation of petroporphyrins from asphaltenes by chemical modification and selective affinity chromatography. *Energy Fuels* **2009**, *23*, 2600-2605.

Zabicky, J.; Ehrlich-Rogozinski, S. Analysis of organic halogen compounds. In *The chemistry of the carbon-halogen bond. Part 1*; Patai, S., Ed.; John Wiley & Sons, Inc.: London, 1973, pp. 179.

Zhang, Y.; Takanohashi, T.; Sato, S.; Saito, I. Observation of glass transition in asphaltenes. *Energy Fuels* **2004**, *18*, 283-284.

Chapter 4. Origin of Halogenated Bitumen and Asphaltenes Hardness

Abstract

Halogenation of bitumen and asphaltenes as unconventional upgrading technology to convert some asphaltenes into maltenes resulted in products with increased hardness. Three hypotheses were forwarded to explain these observations: stronger stacking due to electrostatic differences, free radical addition reactions, and increased hydrogen bonding.

A model compound investigation was performed. No evidence was found that stacking strength increased due to electrostatic differences between halogenated and non-halogenated material. Addition reactions were found on heating halogenated materials, but not on mixing without heating. Evidence was presented of increased hydrogen bonding, although not necessarily stronger hydrogen bonding. Changes in the properties of mixtures of halogenated and non-halogenated materials were observed and in one instance the development of a new crystal configuration. Based on this work, the most plausible explanation for the increased hardness after halogenation bitumen and asphaltenes is an increase in hydrogen bonding.

Keywords: Hardness, Asphaltenes, Bromination, Stacking Strength, Free Radical Addition, Hydrogen Bonding.

4.1 Introduction

Halogenation of bitumen and asphaltenes was intensely investigated in the past, mainly in the 1970s (Moschopedis and Speight, 1970; Moschopedis and Speight, 1971; Moschopedis and Speight, 1976; Kowanko *et al*., 1978). The main purpose in study halogenation reaction of asphaltenes at that time was to understand its molecular structure and the physical-chemical changes prevenient from halogenation reaction. The main observations were that halogenated asphaltenes were harder and shiny compared to the parent asphaltenes. The solubility of halogenated asphaltenes also changed, as it was insoluble in solvents such as benzene and carbon tetrachloride.

Like asphaltenes, halogenation of bitumen also resulted in harder and shiny materials (Patwardhan, 1979), and an increase in asphaltenes content of chlorinated bitumen was observed (Pfeiffer, 1950). It was mentioned that harder materials from halogenation reaction may find application in the road paving industry as an alternative to oxidation, known as air-blowing. Even though it is not known if halogenation is viable from an economic perspective, the main advantage of using halogenation instead of oxidation for road paving is its high resistance to different types of solvents and oils, which makes it more resistant to degradation (Patwardhan, 1979; Pfeiffer, 1950; Prado and De Klerk, 2014).

A different proposed application of halogenation was to convert some of the asphaltenes in oilsands bitumen into maltenes (Prado and De Klerk, 2014). The initial hypothesis was that bulky halogens, such as bromine or iodine, could pry aromatic sheets apart and consequently weaken π-π ring stacking to cause some disaggregation of the asphaltenes. Mild bromination was investigated under conditions that would favor aromatic halogenation, but despite the mild treatment there was a considerable increase in hardness, just like was observed for more severe halogenation (Moschopedis and Speight, 1970; Moschopedis and Speight, 1971; Moschopedis and Speight, 1976; Kowanko *et al*., 1978).

A number of hypotheses can be forwarded in attempt to explain these observations.

The first hypothesis is that halogenation actually increases the strength of stacking of aromatic sheets, not decrease stacking as originally postulated. This is caused by the electron withdrawing properties of halogens. The halogens reduce the electron density of the aromatic ring to which they are bonded, which in turn creates an electrostatic difference between halogenated and non-halogenated aromatics. An electron-rich molecule such as a non-halogenated aromatic sheet will interact with the positive electrostatic potential of a halogenated aromatic sheet resulting in a stronger stacking interaction. It was also reported that crystalline structures are formed due to the interaction between halogen bonds and stacking structures (Li *et al*., 2012), as was observed in the halogenated products (Prado and De Klerk, 2014).

A second hypothesis is that intermolecular addition takes place as side-reaction during mild halogenation. Infrared spectra indicated that during aromatic selective halogenation, aliphatic halogenation also occurred (Prado and De Klerk, 2014). Aliphatic carbon-halogen bonds are susceptible to elimination of the halogen. Addition reactions can happens by elimination of aliphatic halogen substituents through two different ways. One way is dehydrogenation condensation, resulting in inter- and/or intra-molecular interactions, as suggested by Speight (1971). Another way is by C=C bond formation due to dehydrohalogenation. Olefins, once formed, can participate in addition reactions resulting in a cross-linked product with lower solubility, as noted by Petersen (1993).

The third hypothesis was an increase of hydrogen bonding interactions after halogenation. Smith (1973) outlined the attributes that caused hydrogen bonding to carbon-bonded halogen atoms. One factor that favours hydrogen bonding is acidity of the hydrogen to act as electron-acceptor. Hydrogen atoms attached to electronegative elements are more acidic. For example, the hydroxyl group in phenol is a very strong proton donor and it is capable of hydrogen bonding with halogens, as illustrated by Figure 4.1. As aromatics containing hydroxyl groups present in asphaltenes and bitumen would be susceptible to hydrogen bonding with halogen atoms, it might explain the formation of less soluble materials after halogenation reaction, even though this is a very weak hydrogen bonding. Another factor that favours bond formation is proximity of the donor and acceptor atoms. Asphaltenes are complex and inter- and intramolecular movement is already constrained by numerous interactions (Gray *et al*., 2011), which might make it more

difficult for new hydrogen bonds to be formed. Furthermore, the atoms involved in hydrogen bonding should ideally be collinear, although hydrogen bonds at an angle can occur. More electronegative halogens form stronger hydrogen bonds (Smith, 1973).

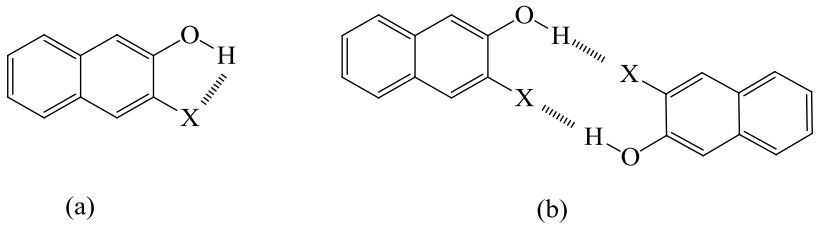

(a) (b)

Figure 4.1. Illustration of hydrogen bonding with a halogen (a) intramolecular hydrogen bonding (b) intermolecular hydrogen bonding (Smith, 1973).[16]

The fourth hypothesis was halogen bonding. According to the IUPAC definition, halogen bonding is the non-covalent bonding that occurs when an electrophilic region associated with a halogen atom interacts with a nucleophilic region of another molecule or within the same molecule. For example, the interaction with the lone pair electrons of nitrogen in a pyridine, or oxygen in a carbonyl group. A further requirement for halogen bonding, in addition to the need for an electrophilic region, is that the bonding angle must be close to 180° (Desijaru, 2013). This is a demanding requirement. Although pyridines and carbonyl groups are present in asphaltenes, halogen bonding would be difficult. There are many constraining interactions that are already present in the asphaltenes to restrict molecular movement (Gray *et al*., 2011), so that it would be difficult to meet the bonding angle requirement for halogen bonding, even though the bond between bromine and phenol oxygen lone pair is stronger than hydrogen bonding. It is therefore unlikely that halogen bonding contributes meaningfully to properties of halogenated asphaltenes because of the angle requirement.

The objective of this work was to explain the dramatic increase in hardness and decrease in aromatic solubility that was observed even with mild halogenation of asphaltenes. Due to the analytical challenges presented by asphaltenes characterization, this study employed model compounds as surrogates. The three most plausible hypotheses that were outlined were tested:

[16] Reprinted from Hydrogen-bonding and complex-forming properties. Smith, J. W. In *The chemistry of the carbon-halogen bond. Part 1*; Patai, S., Ed.; John Wiley and Sons: London, 1973, pp. 265-300. Copyright 1973 John Wiley and Sons Ltd.

stronger stacking due to electrostatic differences, free radical addition reactions, and increased hydrogen bonding.

4.2 Experimental

4.2.1 Materials

All the chemicals and cylinder gases used in this study are presented in Table 4.1 and were used without additional purification.

Table 4.1. Chemicals and cylinder gases employed in this study

Compound	Formula	CASRN [a]	Mass fraction purity [b]	Supplier
Chemicals				
phenanthrene	$C_{14}H_{10}$	85-01-8	0.98	Sigma-Aldrich
anthracene	$C_{14}H_{10}$	120-12-7	0.97	Sigma-Aldrich
dibenzothiophene	$C_{12}H_8S$	132-65-0	0.98	Sigma-Aldrich
chloroform	$CHCl_3$	67-66-3	0.99	Sigma-Aldrich
sodium bromide	NaBr	7647-15-6	0.99	Sigma-Aldrich
oxone®	$KHSO_5 \cdot 0.5KHSO_4 \cdot 0.5K_2SO_4$	70693-62-8	-	Sigma-Aldrich
1-methylnaphthalene	$C_{11}H_{10}$	90-12-0	0.95	Sigma-Aldrich
sodium sulfate	Na_2SO_4	7757-82-6	0.99	Sigma-Aldrich
hexane	C_6H_{14}	110-54-3	0.985	Fisher cientific
2-naphthol	$C_{10}H_8O$	135-19-3	0.99	Acros Organics
0.05M sodium thiosulfate solution	$Na_2S_2O_3$	7772-98-7	-	Sigma-Aldrich
acetonitrile	C_2H_3N	75-05-8	0.999	Sigma-Aldrich
2-ethylnaphthalene	$C_{12}H_{12}$	939-27-5	0.99	Sigma-Aldrich
d-chloroform	$CDCl_3$	865-49-6	0.9996 atom D	Sigma-Aldrich
Cylinder gases				
nitrogen	N_2	7727-37-9	0.99999[c]	Praxair
helium	H_2	7440-59-7	0.99999[c]	Praxair
Calibration materials				
indium	In	7440-74-6	0.99999	Impag AG
zinc	Zn	7440-66-6	0.99999	Impag AG

[a] CASRN = Chemical Abstracts Services Registry Number
[b] This is the purity of the material guaranteed by the supplier; material was not further purified
[c] Mole fraction purity

4.2.2 Equipment and Procedure

4.2.2 Stronger Stacking due to Electrostatic Differences

Three model compounds were selected to evaluate the hypothesis that halogenation would cause stronger stacking due to electrostatic differences between halogenated and non-halogenated compounds: phenanthrene, anthracene, and dibenzothiophene. These compounds were selected

because they are polycyclic aromatic hydrocarbons. Phenanthrene and anthracene have the same carbon number, however their structures are different. Dibenzothiophene contains a heteroatom compound (sulfur). All of these molecules were planar to enable stacking.

The first step was to perform halogenation of each model compound. The procedure was the same that employed previously for mild bromination of bitumen, asphaltenes, and maltenes (prado and De Klerk, 2014), and based on the aromatic selective halogenation protocol of Lee *et al*. (2002). The only difference was the amount of reactants used: 20 mmol of substrate in 120 mL of chloroform, 20 mmol of NaBr and 20 mmol of oxone solubilized in 40 mL demineralized water.

The halogenated products (0.5 g) were then mixed with the corresponding non-halogenated starting materials (0.5 g) and dissolved in 20 mL of chloroform. The mixtures were stirred for 1 hour on a magnetic stirrer plate at ambient conditions. Then, the flasks containing the diluted mixtures were covered with a parafilm. Small holes were made in the parafilm and the flasks were left in the fumehood to allow slow evaporation of the solvent. Evaporation was continued until constant weight of each sample was obtained. The purpose of mixing pure and halogenated materials was to enable the solidification of mixed halogenated and non-halogenated aromatic sheets, as suggested by the hypothesis.

The feed, halogenated products and mixtures were analysed by stereomicroscopy, FTIR spectrometry, and powder X-ray Diffraction (XRD).

4.2.3 Free Radical Addition Reactions

Two different pathways that could potentially lead to free radical addition reactions were evaluated: dehydrogenation condensation and olefin formation followed by addition reactions to the olefin.

Dehydrogenation condensation takes place by free radical hydrogen abstraction and free radical chain termination by radical on radical addition (Figure 4.2). The model compound used to evaluate this reaction was 1-methylnaphthalene. 1-Methylnaphthalene was chosen because the

aromatic carbon to which the methyl group is attached does not have a C–H bond. Bromination of the methyl group and subsequent debromination of the methyl group cannot yield an olefin. Furthermore, the formation of a free radical intermediate is favoured due to the resonance stabilization of the free radical on a benzylic carbon. Thus, in this case, addition reaction due to halogen elimination must be intermolecular.

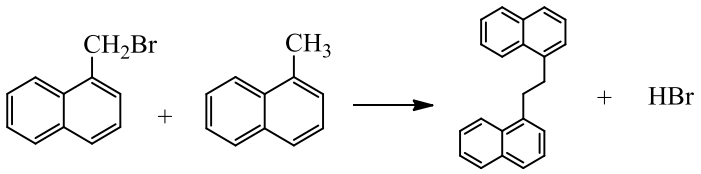

Figure 4.2 Schematic of condensation reaction following on elimination of HBr

Halogenation and the preparation of a 1:1 mixture of halogenated and non-halogenated material was performed in the same way as described for anthracene, phenanthrene, and dibenzothiophene. The work-up procedure was different. After stirring the mixture for 1 hour, the solution was washed with water in order to remove any residual bromine. The organic layer was separated and anhydrous sodium sulfate was added to remove any remaining water. The flask containing the organic mixture was left in the fumehood to allow slow evaporation of the solvent until constant weight of the sample was obtained.

All the samples (pure, halogenated, and mixture) were also thermally treated to evaluate possible C–Br bond dissociation, as well as to evaluate the hypothesis for materials exposed to higher temperature. The thermal treatment consisted of placing the samples (0.1-0.3 g) in a stainless 316 micro-reactor (Swagelok, 1 inch diameter) with a glass tube insert. The samples were thermally treated by placing the micro-reactors in a furnace (Carbolite, model CWF-1100) at 250 ºC for 2 hours. The only exception was 1-methylnaphthalene that was heated only to 200 °C to avoid exceeding its boiling point temperature. Thermal treatment was performed only once.

The analyses that were performed on all materials were FTIR, high pressure liquid chromatography (HPLC), gas chromatography coupled with mass spectrometry (GC-MS), ^{1}H NMR, and TGA.

Olefin formation followed by carbocation or free radical addition to the olefin (Figure 4.3 and Figure 4.4) was investigated by using 2-ethylnaphthalene as model compound. When the ethyl group in 2-ethylnaphthalene is brominated, the bromine can be eliminated with aliphatic hydrogen on the adjacent carbon to form HBr and an olefin. This elimination pathway was not available in the halogenated 1-methylnaphthalene. The halogenation, work-up procedure, thermal treatment and analyses were the same as for 1-methylnaphthalene.

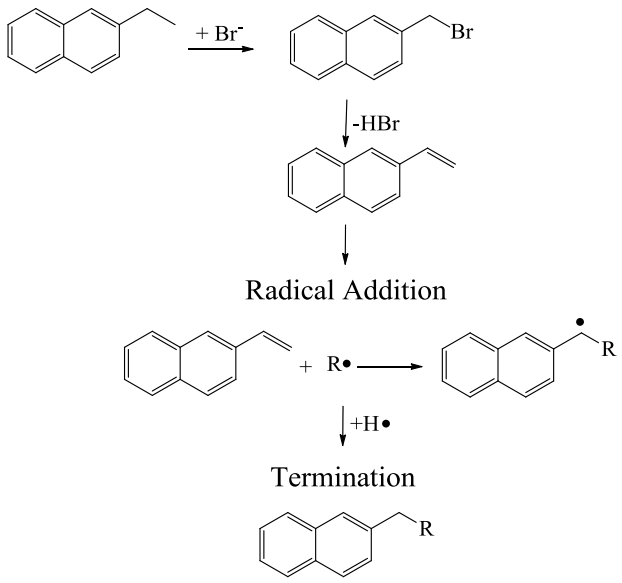

Figure 4.3 Olefin formation and free radical addition

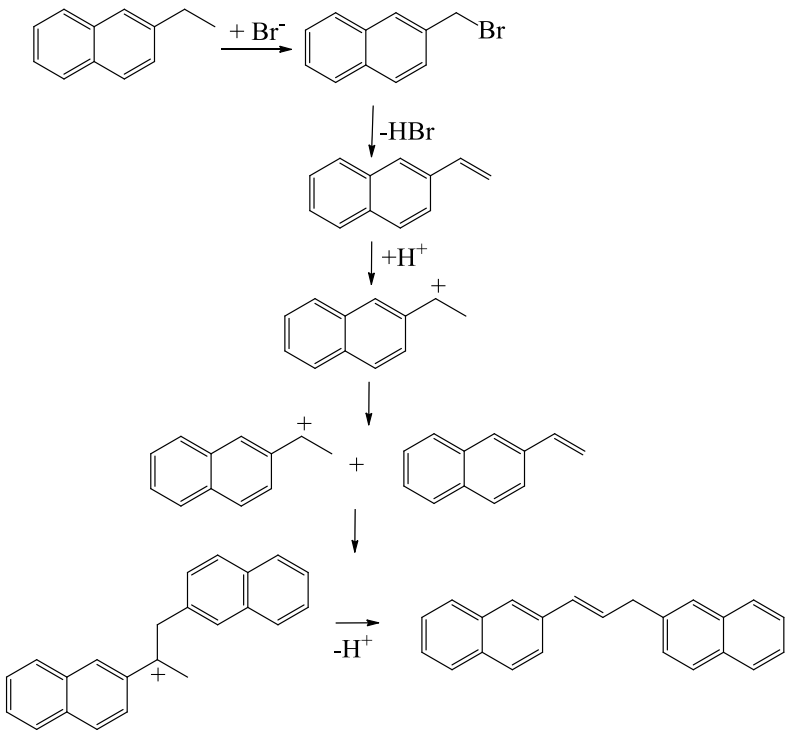

Figure 4.4 Olefin formation and olefin dimerization by a carbocation formation

4.2.4 Increased Hydrogen Bonding

Increased hydrogen bonding caused by halogenation due to the interaction with hydrogen attached to electronegative atoms, as illustrated in Figure 4.1, was evaluated using 2-naphthol as model compound. Using 2-naphthol, it would in principle be possible to generate increased intra- and intermolecular hydrogen bonding, depending on the position of halogenation.

The halogenation procedure, preparation of a 1:1 mixture of halogenated and non-halogenated material, and work-up were performed in the same way as described for anthracene, phenanthrene, and dibenzothiophene.

The samples were analysed by FTIR, DSC, UV-Vis spectroscopy, GC-MS, XRD, and stereomicroscopy.

4.2.5 Analyses

Stereomicroscopy was performed as in Chapter 3.

XRD analysis was performed at Earth Science Department at University of Alberta. The instrument used for the analysis was a Rigaku Geigerflex Powder Diffractometer equipped with a cobalt tube, graphite monochromator and scintillation detector. The samples were mounted on zero-background plates and scanned from 5 to 90 º.

FTIR analyses were performed as in Chapter 3.

A Mettler Toledo DSC 1 with Haake intracooler was employed for the DSC analyses. The DSC was calibrated with pure In and Zn standards. The onset temperature and enthalpy of melting for In were 156.5 ± 0.2 ºC and -27.7 ± 1.3 J/g respectively. Reference values for In are 156.6 °C and –28.6 J/g (Höhne *et al*., 2003). The onset temperature and enthalpy of melting for Zn were 419.4 ± 0.3 ºC and -101.3 ± 3.7 J/g, respectively. Reference values for Zn are 419.5 °C and –108.6 J/g (Höhne *et al*., 2003). All analyses and calibrations were performed under a constant nitrogen flow rate of 100 mL/min and constant heating or cooling rates of 10 °C/min. In a typical analysis ~10 mg of samples was analysed in a 40 µL aluminium crucible with a pierced lid. The temperature range covered by the analysis was heating from 25 to 250 °C, cooling from 250 to 25 °C, and heating from 25 to 250 °C.

HPLC analyses were performed with an Alliance e2695 model from Waters with two detectors: 410 refractive index and 2998 photo diode array. The instrument was equipped with a 5 mm precolumn and three columns in series (µ-Bondapack NH_2 3.9 x 300 mm with 125 Å of pore size and 10 µm of particle diameter). The samples were diluted in hexane to a concentration of 0.20 g/mL; 10 µL of the diluted sample was injected in the HPLC instrument for analysis. The liquid phase consisted of hexane and chloroform in different concentrations in a flow equal to 1 mL/L. At the first 30 minutes only hexane was used as the liquid phase, then at 30 minutes the liquid phase was changed to a mixture of equal concentrations of hexane and chloroform. At 40 minutes the liquid phase was changed back to 100% hexane. Moreover, at 25 minutes, the flow

of the liquid phase was reversed in order to remove contaminants in the column. The system was operated in a backflushing mode for 15 minutes. The temperature of the column was kept constant at 35 ºC.

GC-MS analyses were performed with an Agilent 7820A GCand Agilent 5977E mass selective detector. The samples were diluted in chloroform to 1 mg/mL. Helium was used as carrier gas at 20 mL/min. The column used for separation was a HP-5MS 30m × 250 μm × 0.25 μm from Agilent. The samples (1 μL) were injected in a split mode (1:10) at 280 ºC. The oven temperature program was 40 ºC for 0.5 min, then heating to 100 ºC at 40 ºC/min and hold for 0.5 min, heating to 120 ºC at 2 ºC/min followed by heating to 320 ºC at 20 ºC/min. The temperature was held constant at 320 ºC for 3 min. MS parameters were: 4 min solvent delay, quadrupole temperature of 150 ºC and source temperature of 230 ºC.

^{1}H NMR analyses were performed with a 60 MHz bench top NMR spectrometer from Nanalysis. The samples were diluted in d-chloroform to 0.1 g/mL and 0.7 mL of the solution was taken for analysis. The scan delay was 5 seconds while each sample was scanned 64 times.

UV-Vis spectrometry was performed as in Chapter 3. The samples were diluted in acetonitrile solvent in a concentration equal to 5 mg/100 mL.

TGA instrument was a Mettler Toledo TGA/DSC1 equipped with a LF 1100 furnace, sample robot, and MX5 internal microbalance. Approximately 20 mg of sample was placed in an oxide crucible and heated from 25 to 350 °C at 5 °C/min followed by an isothermal period of 30 minutes at 350 °C. The analysis was performed in a nitrogen atmosphere at a flow rate equal to 100 mL/min.

4.3 Results and Discussion

4.3.1 Stronger Stacking due to Electrostatic Differences (Hypothesis 1)

4.3.1.1 Stereomicroscopy

One of the most striking differences between halogenated and non-halogenated asphaltenes was their physical appearance. It was reported that halogenation turned the brown, powdery asphaltenes into shiny black and crystalline halogenated products (Prado and De Klerk, 2014).

Figure 4.5 shows the images of pure model compounds, halogenated model compounds and their mixtures. The purpose of this analysis was to visually identify the formation of crystal structures formed due to the postulated stronger stacking interaction resulting from the influence of halogen atoms bonded to some of the aromatics. All pure model compounds, anthracene (Figure 4.5a), phenanthrene (Figure 4.5d), and dibenzothiophene (Figure 4.5g), are already crystalline substances. Halogenated anthracene (Figure 4.5b), halogenated phenanthrene (Figure 4.5e), and halogenated dibenzothiophene (Figure 4.5h) are darker and the particles are closer packed, forming a more compacted structure.

It seems that halogenation of dibenzothiophene did not occur in the whole sample, because it is possible to see in Figure 4.5h that some non-halogenated particles are covering the surface of halogenated dibenzothiophene. This result is contrary to expectation, as thiophenes are substituted more readily than benzene during halogenation (March, 1992).

When the pure compound was mixed with the halogenated product it was possible to observe what appeared to be the formation of new crystal structures for anthracene (Figure 4.5c) and for phenanthrene (Figure 4.5f). The dibenzothiophene mixture (Figure 4.5i) did not show visual evidence that a new crystal structure formed. It is also possible to observe that some non-halogenated particles are covering the surface of halogenated dibenzothiophene.

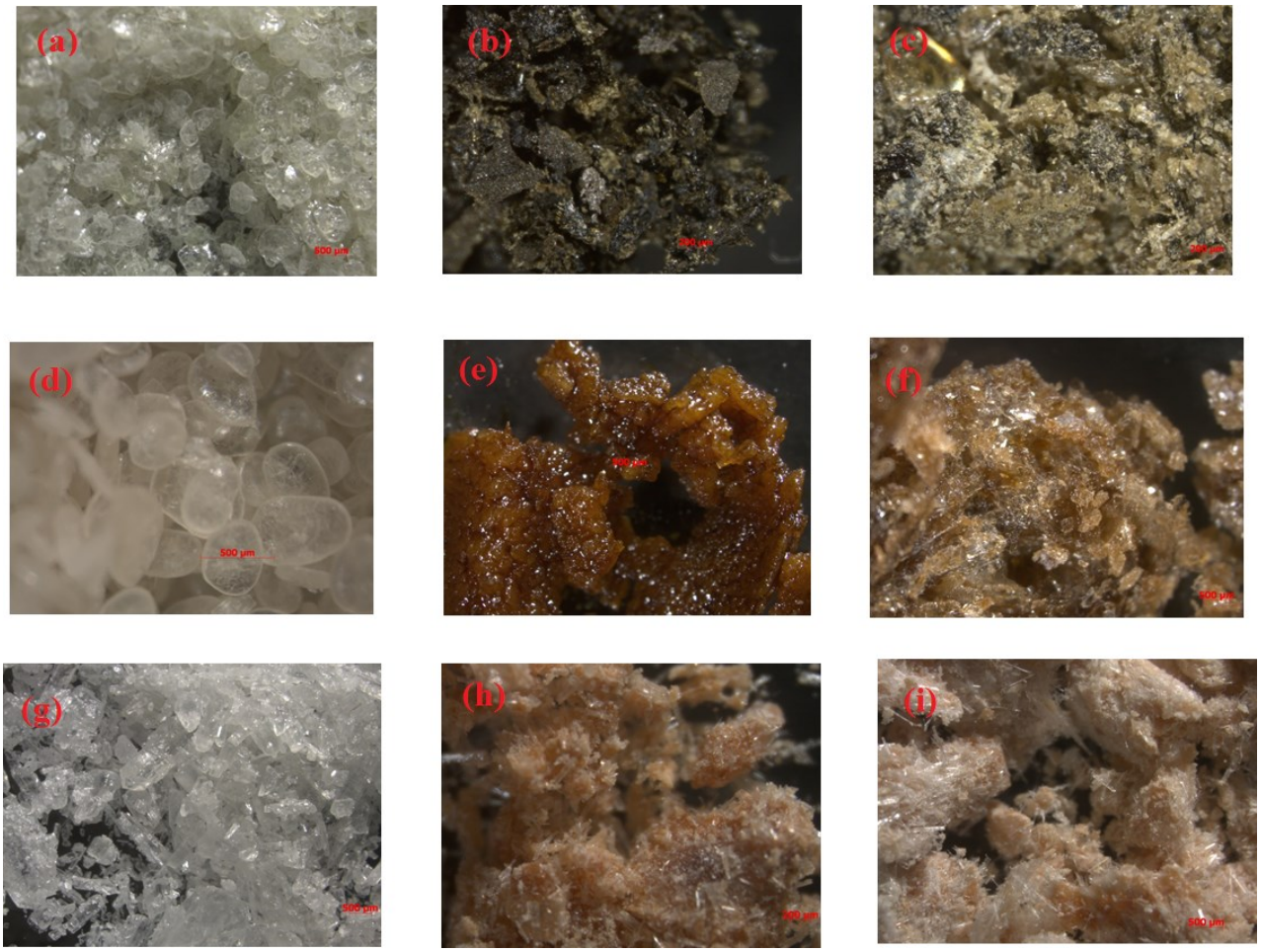

Figure 4.5 Zeiss microscopy analysis (a) pure anthracene (b) halogenated anthracene (c) mixture of halogenated and pure anthracene (d) pure phenanthrene (e) halogenated phenanthrene (f) mixture of halogenated phenanthrene and pure phenanthrene (g) pure dibenzothiophene (h) halogenated dibenzothiophene (i) mixture of halogenated dibenzothiophene and pure dibenzothiophene

Visual observations alone are not sufficient evidence of the presence or absence of stronger stacking or different crystal structures. The samples were therefore submitted for XRD analysis to determine the crystalline aspect of the samples and verify the visual observations.

4.3.1.2 X-Ray Diffraction

The XRD patterns of non-halogenated, halogenated and 1:1 mixtures of halogenated and non-halogenated anthracene (Figure B1), phenanthrene (Figure B2), and dibenzothiophene (Figure B3) were collected and can be found in the Appendix B.

Crystallinity, as a property of a solid, is represented by sharp and narrow peaks in the XRD pattern of the solid. The XRD patterns confirmed that the pure compounds were crystalline, as observed by stereomicroscopy. The halogenated anthracene was also crystalline. Even though the halogenated phenanthrene presented a few broad peaks, the majority of the peaks was sharp and narrow, indicating that the sample also contained crystals. It was not possible to observe crystals in the halogenated dibenzothiophene by microscopy (Figure 4.5h), but XRD analysis indicated that the halogenated dibenzothiophene was crystalline.

The mixtures of halogenated and non-halogenated materials for all the compounds were also found to be crystalline (Figures B1-B3). In the case of anthracene and dibenzothiophene the XRD pattern of the mixture resembled that of a mixture of the crystals of the pure and halogenated materials. The XRD pattern of the phenanthrene mixture was quite different, with three very distinct peaks at 11.0, 22.0 and 30.7 degrees. The XRD of the phenanthrene mixture indicates that a different crystal structure was formed, which was not just a mixture of the crystals of the halogenated and non-halogenated phenanthrene. This implied that at least some molecular structures are prone to form new spatial arrangements when halogenated and non-halogenated compounds are present in the mixture.

4.3.1.3 Infrared Spectroscopy

Figure 4.6 shows FTIR spectra of pure anthracene, halogenated anthracene and the mixture of halogenated anthracene and pure anthracene at two different regions. It can be observed from Figure 4.6a that three new absorption bands formed at 638, 621, and 578 cm^{-1} for the halogenated and mixture products. These infrared absorption bands are in the C–Br vibration region (650-560 cm^{-1}) (Zabicky and Ehrlich-Rogozinski, 1973), indicating that bromination was

successful. The appearance of three absorption bands indicated that C–H substitution with Br occurred on all carbon positions, because there are three unique positions for mono-bromination.

Figure 4.6b shows that there are also new absorption bands at 837, 808, 767, and 692 cm^{-1} occurring in the C–H out-of-plane bending region of polycyclic aromatic hydrocarbons (900-675 cm^{-1}) (Silverstein and Webster, 1997). This result indicates that substitution by bromine affected C-H out-of-plane bending. Apart from a difference in intensity, there was no indication that the brominated anthracene on its own and that in a mixture with anthracene were different. Infrared spectroscopy provided no evidence of an interaction between the halogenated and non-halogenated anthracene.

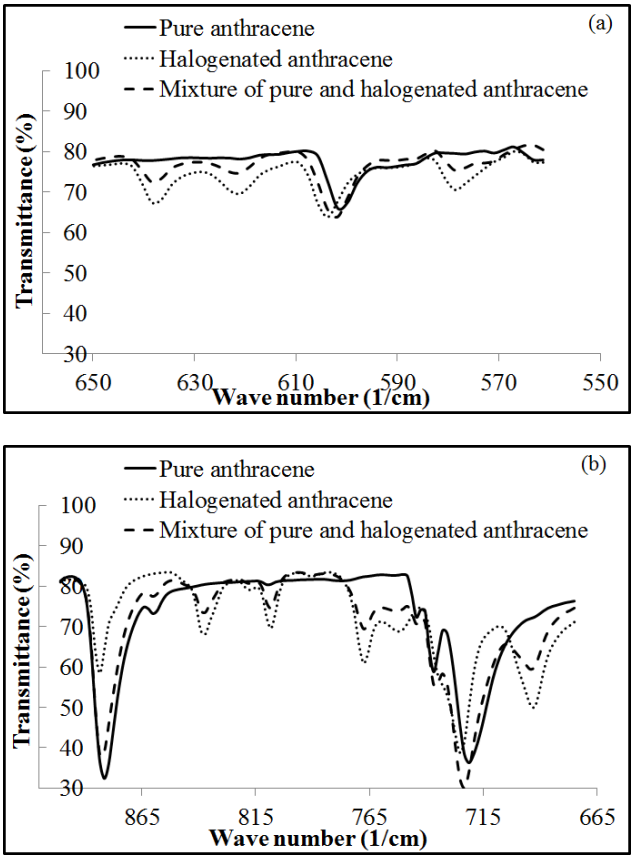

Figure 4.6. FTIR analysis of pure anthracene, halogenated anthracene, and anthracene mixture (a) 650-560 cm^{-1} region (b) 900-675 cm^{-1} region

Figure 4.7 shows FTIR spectrum of pure phenanthrene, halogenated phenanthrene and the mixture of halogenated phenanthrene and pure phenanthrene. It can be observed from Figure 4.7a that there was the formation of a new absorption band at 588 cm^{-1} in the halogenated product and in the mixture that was not present in the pure phenanthrene. This indicates that bromination was achieved, but the appearance of only a single absorption in C–Br absorption region indicated that bromination preferentially occurred on one position only. It is likely that C–H substitution by Br took place on the middle ring (9, 10-positions).

Figure 4.7b shows that there are new absorption bands at 1589, 1371, 1189, 1170, and 1157 cm^{-1} in the skeletal stretching vibrations of C=C and C–C of the aromatic ring region (1100-1641 cm^{-1}). The changes in the stretching vibrations of C=C and C–C could indicate the stacking of aromatic sheets (Xie *et al*., 2009). More precisely, benzene substituted with chlorine presents semicircle stretching of the carbon ring at 1350 cm^{-1} and in non-substituted benzene "this semicircle stretching vibration mixes strongly with C-H in plane bending" and absorbs at different frequencies (Colthup *et al*., 1975). This may be the reason why 1371 cm^{-1} is present in halogenated phenanthrene and its mixture, but not in the pure phenanthrene. The new band at 1589 cm^{-1} could be the quadrant stretching of the ring C⁼⁼C bonds of substituted aromatics (Colthup *et al*., 1975).

It is possible to observe in Figure 4.7c that the band at 815 cm^{-1} decreased for halogenated and the mixture products compared to the pure phenanthrene. This band is in the 900-675 cm^{-1} region of C–H out-of-plane bending of polycyclic aromatic hydrocarbons (Silverstein and Webster, 1997), indicating that some hydrogen were substituted by bromine. In addition, the intensity of this band is higher for the mixture than the halogenated phenanthrene, which was expected, as more C–H bonds are found in the mixture than the halogenated product.

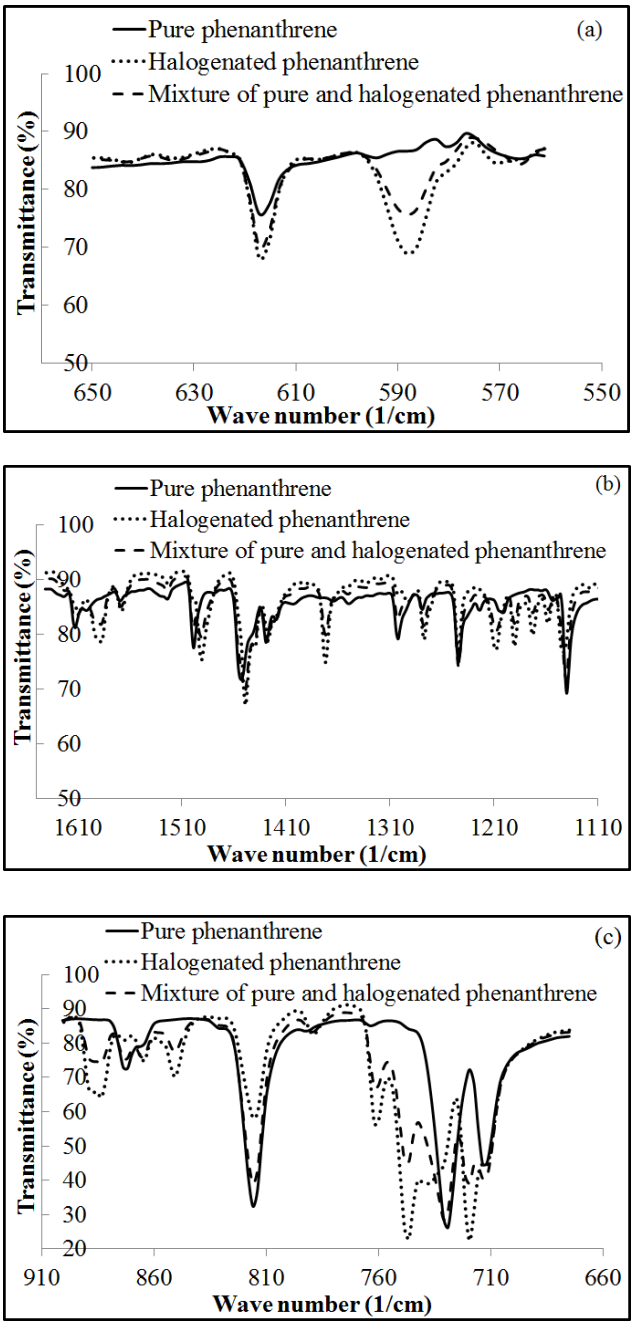

Figure 4.7. FTIR analysis of pure penanthrene, halogenated phenanthrene, and phenanthrene mixture (a) 650-560 cm^{-1} region (b) 1641-1100 cm^{-1} region (c) 900-675 cm^{-1} region

The FTIR spectra of dibenzothiophene, halogenated dibenzothiophene and the mixture of halogenated dibenzothiophene and pure dibenzothiophene are shown in Figure 4.8. Figure 4.8a shows a new band at 578 cm^{-1} for the halogenated and mixture products, which is in the C–Br region (Zabicky and Ehrlich-Rogozinski, 1973), indicating that bromination was achieved. The

detection of only a single C–Br absorption indicated that one specific position of bromination was favoured, likely the 2 or 8-positions, which are the furthest away from the sulfur (Colthup, 1975).

Ring stretching vibrations of heteroaromatics appear at 1600-1300 cm^{-1} region (Silverstein and Webster, 1997). It is observed from Figure 4.8b that the intensity of 1425 cm^{-1} band which is in this region is smaller for halogenated dibenzothiophene and higher for the pure compound. It is also stated that the intensities of these bands depend on the substitution pattern and nature of the substituent. Thus, the decrease of the intensity observed at this region may be due to contraction of the bonds resulting from substitution by bromine. It is also possible to observe that new bands were formed in the halogenated product and the mixture. However, it was not possible to interpret each of these bands individually.

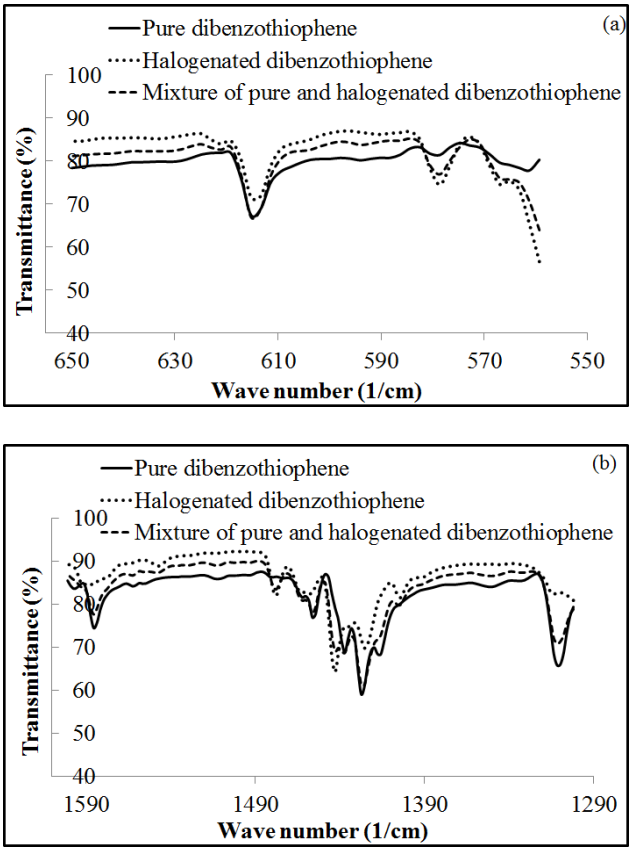

Figure 4.8. FTIR analysis of pure dibenzothiophene, halogenated dibenzothiophene, and dibenzothiophene mixture (a) 650-560 cm^{-1} region (b) 1600-1300 cm^{-1} region

4.3.1.4 Evaluation of Hypothesis

The hypothesis that stacking strength could be increased due to the electrostatic difference between the halogenated and non-halogenated material was investigated. No evidence could be presented that there were specific interactions unique to mixtures of halogenated and non-halogenated anthracene, or dibenzothiophene. However, in the case of phenanthrene XRD analysis of the mixture of halogenated and non-halogenated material revealed the formation of a new crystal configuration.

If stacking strength was increased through alternating halogenated and non-halogenated layers, this should have been apparent in all of the model compounds. Mixtures formed crystalline phases, but only in the case of phenanthrene did the mixture result in a different structure and not in a mixture of the individual crystals. In the case of phenanthrene it provided evidence of hydrogen or possibly halogen bonding. It is speculated that it was a consequence of selective bromination at the 9, 10-position, which facilitated in-plane halogen bonding with hydrogen at the 9, 10-position of non-halogenated phenanthrene to form a sheet-like crystal network. The crystal network satisfied the near 180 ° bonding angle requirement for halogen bonding (Figure 4.9), as well as hydrogen bonding that does not have this bonding angle requirement.

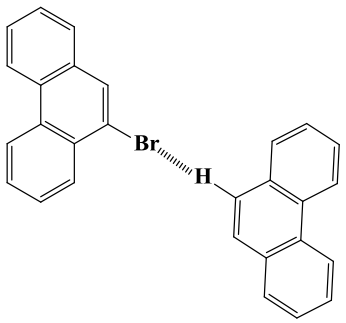

Figure 4.9. Illustration of interaction between bromine and hydrogen

4.3.2 Free Radical Addition Reactions (Hypothesis 2)

4.3.2.1 Halogenation of 1-Methylnaphthalene

The presence of C–Br bonds in the product of 1-methylnaphthalene halogenation was determined by infrared spectroscopy (Figure 4.10a). Absorption of C–Br takes place in the 650-560 cm^{-1} region (Zabicky and Ehrlich-Rogozinski, 1973), and three new absorption bands were found at 574, 595, and 619 cm^{-1} for both halogenated and mixture samples. Three new absorption bands indicated that bromination likely took place in three different positions on 1-methylnaphthalene. In addition, the CH_2 wagging band in CH_2Br group can be observed in the 1300-1150 cm^{-1} region (Silverstein and Webster, 1997), where the formation of a new peak at 1207 cm^{-1} was observed (Figure 4.10b) for both halogenated and mixture samples. This indicated that one of the bromination positions was on the methyl group.

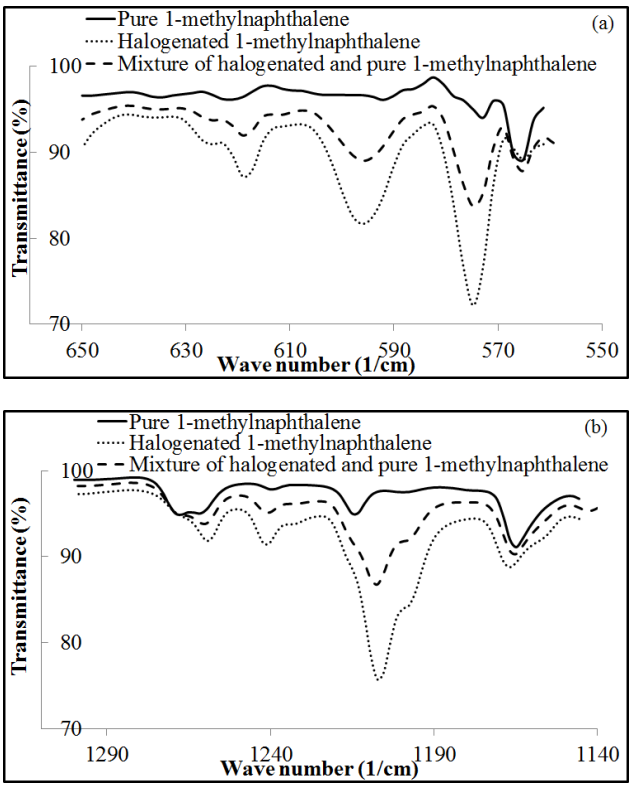

Figure 4.10. FTIR analysis of pure 1-methylnaphthalene, halogenated 1-metylnaphthalene, and 1-methylnaphtalene mixture (a) 650-560 cm^{-1} region (b) 1300-1150 cm^{-1} region

Formation of brominated products could also be observed by HPLC (Figure 4.11). The brominated product eluted close to the 1-methylnaphthalene feed. The HPLC analyses indicated that bromination was incomplete and that there was some impurity present in the 1-methylnaphthalene, presumably 2-methyl naphthalene. No products were found at longer elution times. Since the HPLC method was developed for separating aromatic compounds based on the number of rings in the aromatics, no evidence was found that synthesis of the brominated 1-methylnaphthalene produced addition products.

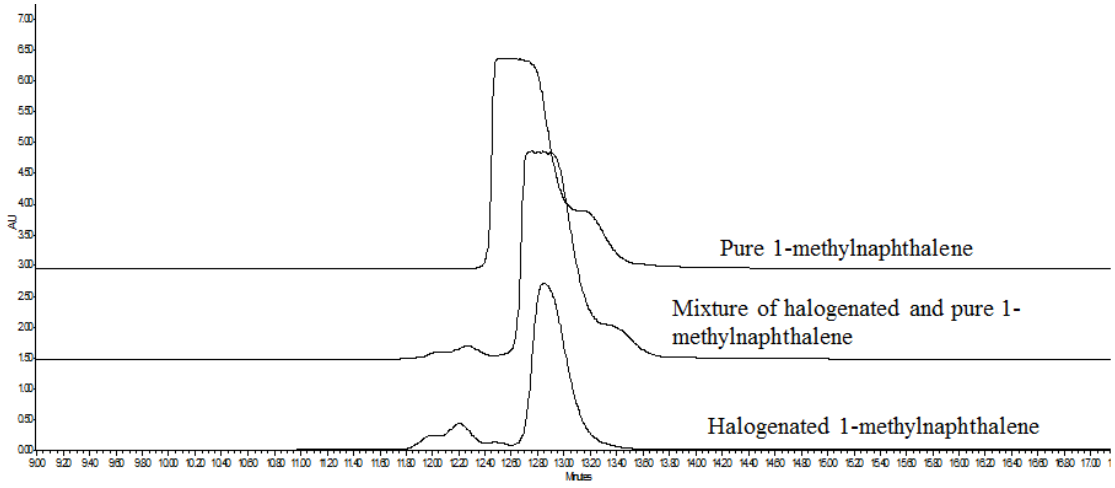

Figure 4.11. HPCL analysis of pure 1-methylnaphthalene, halogenated 1-metylnaphthalene, and 1-methylnaphtalene mixture

In order to identify the different products formed during the halogenation reaction, GC-MS analysis was performed. Figure 4.12a shows chromatogram of pure 1-methylnaphthalene. It can be seen that some impurities are present. The retention time of 1-methylnaphthalene was 13.5 minutes and the main feed impurity at a retention time of 13.1 min was 2-methylbenzothiophene. Figure 4.12b shows chromatogram of halogenated 1-methylnaphthalene. Three new compounds are present in the halogenated product, as was anticipated from the FTIR analysis, as well as unconverted 1-methylnaphthalene and some minor products at much lower concentration. The main halogenation products identified from their electron impact mass spectra were 1-bromo-4-methylnaphthalene, 1-(bromomethyl)-naphthalene and 1-(bromomethyl)-2-bromonaphthalene, or isomers of these compounds. It is difficult to distinguish between different isomers based on

mass spectrometry. Mixing the halogenated and non-halogenated compound (without heating) had no impact on the nature of the compounds (Figure 4.12c), as expected.

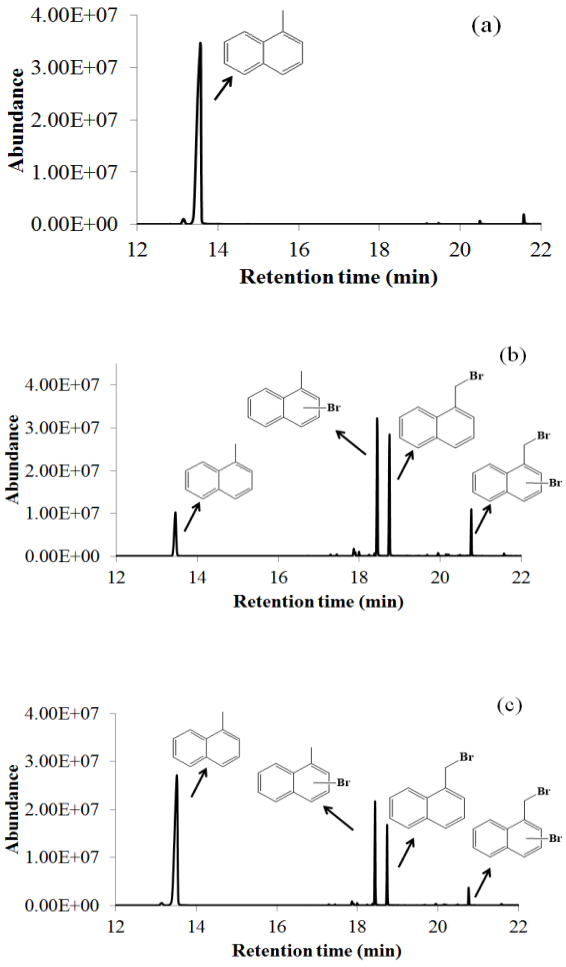

Figure 4.12. GC-MS analysis of (a) pure 1-methylnaphthalene (b) halogenated 1-metylnaphthalene and (c) 1-methylnaphtalene mixture

4.3.2.2 Halogenation of 2-Ethylnaphthalene

The incorporation on bromine during halogenation was confirmed by infrared spectroscopy. A new absorption at 638 cm^{-1} was observed (Figure 4.13), which is in the C–Br absorption region (Zabicky and Ehrlich-Rogozinski, 1973). Two new absorption bands were also found at 659 and 703 cm^{-1}. These are likely due to the aromatic C–H out-of-plane bending vibrations that changed

due to aromatic substitution on the ring (Silverstein and Webster, 1997). Nevertheless, it was important to check whether dehydrohalogenation took place during synthesis. The out-of-plane hydrogen wag vibrations in the 1000-650 cm^{-1} region are the strongest absorption bands of olefins in the infrared spectrum and for a vinyl group attached to an aromatic the absorption is found in a narrow range around 915 to 905 cm^{-1} (Dolphin, 1977). Olefinic absorption can also be found in the 1667-1640 cm^{-1} and 3100-3000 cm^{-1} regions. However, infrared analysis provided no evidence of olefin formation due to bromination in any of these spectral regions (Figure 4.13).

One curious observation in the infrared spectrum was the development of a carbonyl absorption at 1681 and 1558 cm^{-1} (Figure 4.13). The 1681 cm^{-1} absorption is in the region of singly and doubly conjugated ketones, while 1558 cm^{-1} is for a carboxylate (Colthup *et al*., 1975). In order to better interpret these results, the set of samples was analyzed by GC-MS.

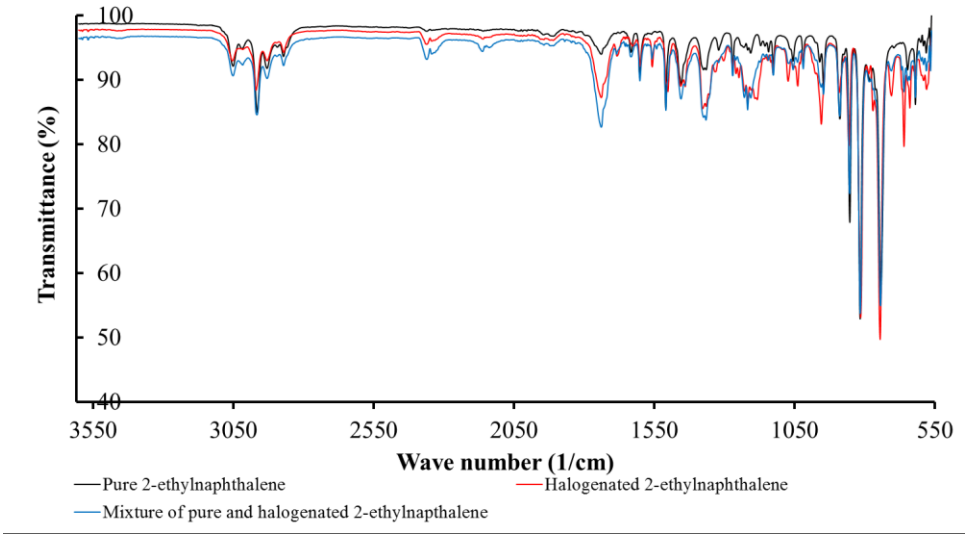

Figure 4.13. FTIR analysis of pure 2-ethylnaphthalene, halogenated 2-ethylnaphthalene, and 2-ethylnaphthalene mixture

Figure 4.14a shows the chromatogram of pure 2-ethylnaphthalene, which elutes at 15.7 min retention time.

Figure 4.14b shows the chromatogram of halogenated 2-ethylnaphthalene. It is possible to observe that the reaction was not 100 % complete, as 2-ethylnaphthalene is still present.

Nevertheless it is possible to observe the formation of four different products. The first product is 2-ethenyl-naphthalene, which indicated that olefins were indeed formed as suspected. Olefins were likely formed by dehydrohalogenation after halogenation of the ethyl group. Halogenated derivatives of ethylnaphthalene and ethenylnaphthalene with aromatic bromine substitution were also found.

A product that was not anticipated was 2-naphthyl-2-ethanone (naphthyl methyl ketone). The formation of a carbonyl compound was likely as result of the oxidant (oxone) that was employed to oxidize NaBr. Since olefins were formed during the reaction and they are very susceptible to oxidation, it may be possible that the oxidant present in the reaction medium may have oxidized some of the olefins formed during the reaction. However, the liquid phase oxidation of a vinyl group attached to an aromatic does not favor ketone formation (Emanuel, 1984). The same is true for an ethyl group attached to an aromatic (Emanuel, 1984). A more plausible explanation is that a concerted reaction between the oxone and bromine was responsible for the oxidation leading to the formation of a ketone on the benzylic carbon.

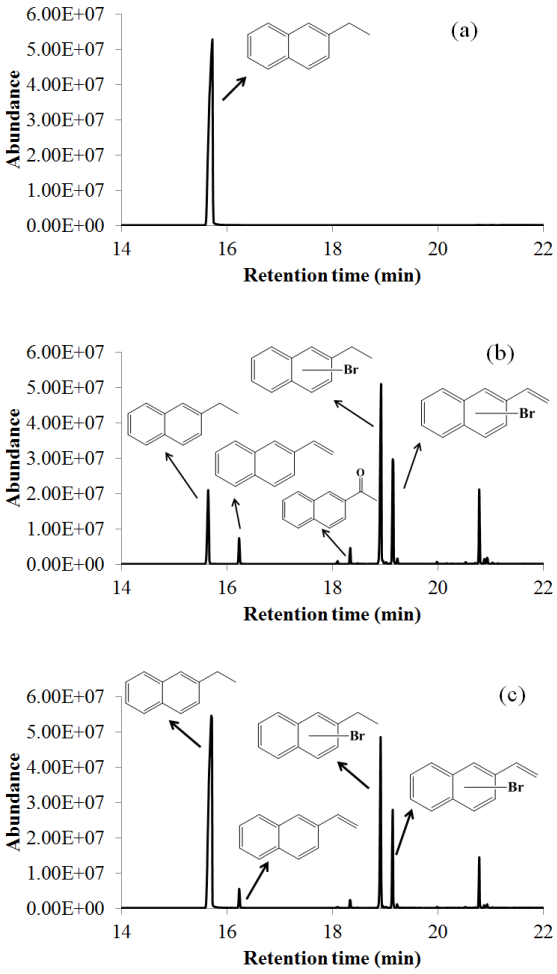

Figure 4.14. GC-MS analysis of pure 2-ethylnaphthalene, halogenated 2-ethylnaphthalene, and 2-ethylnaphthalene mixture

The presence of olefinic hydrogen in the halogenated product was also observed by ^{1}H NMR analysis (Figure 4.15). The hydrogens in 2-ethylnaphthalene are found in three clusters. The first cluster corresponds to aromatic protons in the shift range of 7.31-8.03 ppm. The second cluster corresponds to aliphatic paraffinic CH_2 at 3.09 ppm and the third cluster corresponds to aliphatic paraffinic CH_3 at 1.36 ppm (Ernst and Schulz, 1992). In the halogenated 2-ethylnaphthalene (Figure 4.15b) the abundance of aliphatic paraffinic hydrogen was less then in the non-halogenated feed. The halogenated product also developed two new clusters not present in the 2-ethylnaphthalene. The cluster of new peaks appearing in the 5.2-5.6 ppm shift region corresponds to olefinic hydrogen (Katritzky *et al.*, 1991). The new peaks appearing in the 2-2.3

ppm shift region are due to the hydrogen on the methyl group adjacent to a carbonyl. These results support the GC-MS identification of olefins and ketones in the halogenated product.

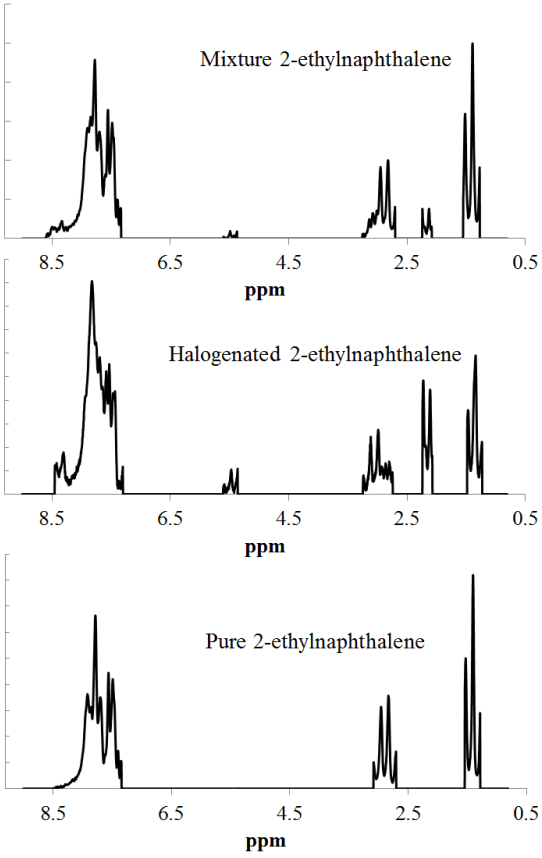

Figure 4.15. NMR spectra of 2-ethylnaphthalene samples

4.3.2.3 Thermal Treatment

If addition reactions occurred during heating to 250 °C, analysis by GC-MS should reveal the presence of addition products. It was observed that after heating halogenated 1-methylnaphthalene (Figure 4.16a) the bromine bonded to the aliphatic carbon was eliminated compared to the non-heated halogenated 2-ethylnaphthalene (Figure 4.14b). The heating also eliminated bromine bonded to aliphatic carbon in the mixed sample as shown in Figure 4.16b. In the mixed sample the addition product of the condensation reaction shown in Figure 4.2 was

observed. Since it is difficult to distinguish isomers based on electron impact mass spectra the exact structure of the addition product was not confirmed.

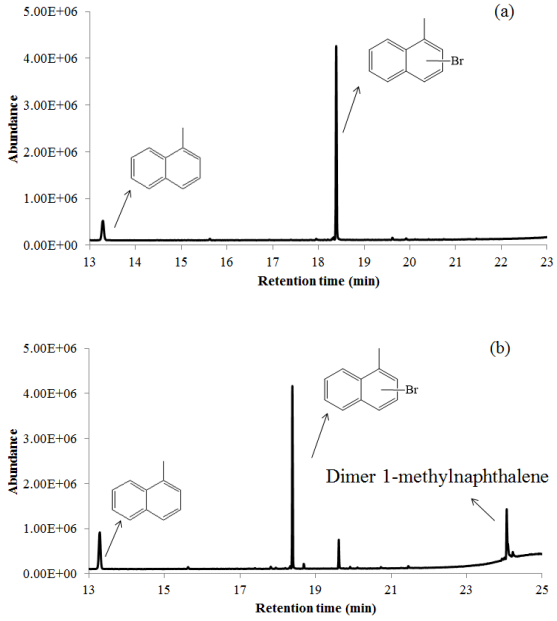

Figure 4.16. (a) Heated Halogenated 1-methylnaphthalene (b) Heated Mixture between pure and halogenated 1-methylnaphthalene

Halogenation of 2-ethylnaphthalene resulted in the elimination of HBr to produce the olefinic product (Figure 4.14b). Olefins are prone to form addition products. However, an addition product for the heated halogenated 2-ethylnaphthalene was not observed by GC-MS analysis (Figure 4.17a). It is probably that the addition products were composed of more than 4 aromatic rings, such as trimers and heavier oligomers instead of dimers, and that the products were too heavy to be eluted during the chromatographic analysis. In order to confirm the presence of oligomeric products the heated halogenated sample was subjected to TGA to determine the amount of heavy hydrocarbons (gum). TGA confirmed that there was formation of gum after heating the halogenated 2-ethylnaphthalene to 350 °C. It was found that 16.3 wt % of heated halogenated 2-ethylnaphthalene was present as gums in the product. Unlike the heated halogenated 2-ethylnaphthalene, the mixed sample of pure and halogenated 2-ethylnaphthalene contained the dimeric addition product of the olefin (Figure 4.17b).

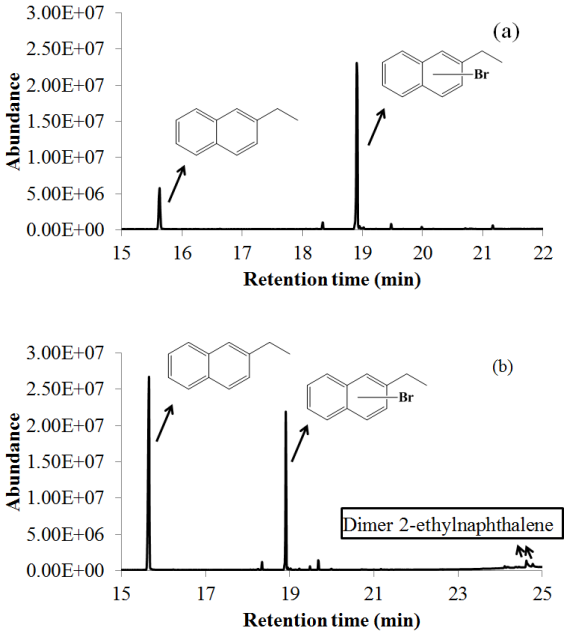

Figure 4.17. (a) Heated halogenated 2-ethylnaphthalene (b) Heated mixture of pure and halogenated 2-ethylnaphthalene

4.3.2.4 Evaluation of Hypothesis

Free radical addition reactions can take place in one of two ways under the test conditions. First, by dehydrogenation condensation, which is the result of free radical hydrogen abstraction later followed by the recombination of free radical species (Figure 4.3). Second, by dehydrohalogenation that leads to olefin formation followed by carbocation or free radical addition to the olefin (Figures 4.3 and 4.4). Addition reactions are possible with 1-methylnaphthalene and 2-ethylnaphthalene, but olefin formation by dehydrohalogenation is only possible with 2-ethylnaphthalene.

On heating the reactions that were postulated were observed (Figures 4.16 and 4.17). However, these reactions took place only after heating. There was no evidence of addition reactions in the feed materials. These results did not provide evidence that addition reactions caused the increase in hardness that was reported when halogenating oilsands derived materials (Prado and De Klerk, 2014).

4.3.3 Hydrogen Bonding (Hypothesis 3)

4.3.3.1 Infrared Spectroscopy

Free and bonded –OH groups in alcohols and phenols can be observed in the 3700-3000 cm^{-1} region of the infrared spectrum. If there is the formation of hydrogen bonds, the hydrogen stretching band will shift to lower wave numbers, while the hydrogen bending band will shift to higher wave numbers. Hydrogen bonding does not affect the intensity and width of hydrogen bending bands as much as the hydrogen stretching bands (Colthup *et al*., 1975). From Figure 4.18 it is observed that the alcohol stretching in both halogenated and mixture samples shifted to higher wave numbers than in pure 2-naphthol. The shift was more pronounced in the halogenated sample than the mixture of halogenated and non-halogenated naphthol. This behavior is the same than is expected for hydrogen bending bands due to the formation of hydrogen bonds. The FTIR analysis suggests that hydrogen bonding increased with the introduction of a halogen in the molecule, but it is not conclusive in this regard.

Figure 4.18b shows that bromination was achieved by the formation of a new band at 644 cm^{-1} in the C–Br absorption region. This C–Br absorption persisted in the mixture.

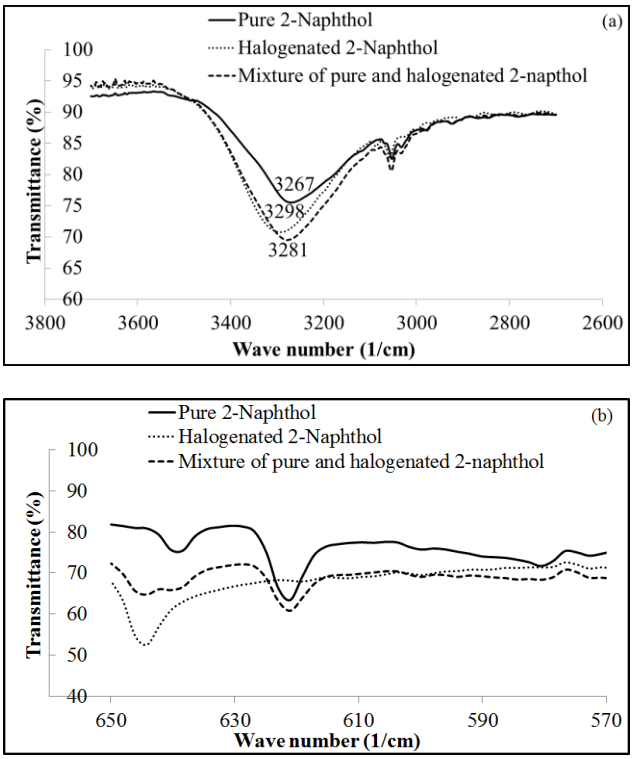

Figure 4.18. FTIR analysis of 2-naphthol (a) 3700-2700 cm^{-1} region (b) 560-650 cm^{-1} region

4.3.3.2 Differential Scanning Calorimetry

Melting point study was performed in order to identify hydrogen bond formation between halogen and –OH group. According to Pimentel and McClellan (1960) the melting point is usually increased when a hydrogen bond is formed. However, melting point is notoriously difficult to predict and there are many factors that can influence in increase in order and stability associated with the solid state (Bondi, 1968; Ubbelohde, 1965). The substitution of hydrogen with bromine on the aromatic may disrupt stacking and thus crystallization, as was originally proposed for the disruption of stacking interactions in asphaltenes (Prado and De Klerk, 2014). It was hoped that differential scanning calorimetry would provide some insights in this respect.

The melting point of pure 2-naphthol was previously reported to be 119.39 ± 0.22 °C (Rojas and Orozco, 2003), and 123.0 °C (Acree, 1991), compared to the observed value of 120.4 ± 0.8 °C for the melting point of 2-naphthol determined in this study (Table 4.2). The melting temperature of the brominated 2-naphthol was much lower (Table 4.2), at 78.3 ± 3.0 °C. In the

mixture of halogenated and non-halogenated material the melting behavior was close to that of 2-naphthol (Table 4.2), with a melting point temperature of the mixture at 118.6 ± 0.4 °C. Since only a single melting point was observed, it was likely that the brominated 2-naphthol interacted with the 2-naphthol to resemble the melting behavior of 2-naphthol.

Analogous behavior was observed for the enthalpy of melting. The enthalpy of melting of pure 2-naphthol was –140.3 ± 2.5 J/g (Table 4.2) which was higher than the value reported by literature (-121.45 J/g) (Acree, 1991). The enthalpy of melting for the halogenated sample (–83.8 ± 7.1 J/g) was lower compared to that of the pure 2-naphthol, while the enthalpy of melting for the mixed sample (–141.8 ± 11.2 J/g) was similar to that of pure 2-naphthol (Table 4.2). Yet, only a single solid-liquid phase transition was observed and the melting enthalpy of the mixture was not the weighted average of the melting enthalpies of the pure compounds.

Table 4.2. Melting point and enthalpy values from DSC analysis and literature

Material	**Melting temperature (°C)** [a]		**Melting temperature from literature (°C)** (Acree, 1991; Rojas and Orozco, 2003)	**Melting enthalpy (J/g)** [b]		**Melting enthalpy from literature (J/g)** (Acree, 1991)
	x [c]	**s** [c]		**x** [c]	s [c]	
2-Naphthol	120.4	0.8	121-123	-140.3	2.5	-121.45
Halogenated 2-naphthol	78.3	3.0		-83.8	7.1	
Mixture of halogenated and pure 2-naphthol	118.6	0.4		-141.8	11.2	

[a] Onset temperature for the melting point on first heating
[b] Enthalpy for the melting point during the first heating of pure materials
[c] Average (x) and sample standard deviation (s) of analyses in triplicate are reported

4.3.3.3 Stereomicroscopy and X-Ray Diffraction

Visually the pure 2-naphthol, brominated 2-naphthol and the mixture of the two appeared quite different (Figure 4.19). The 2-naphthol did not look crystalline. The brominated sample was darker in color and some crystalline structures could be observed. The mixture sample had a more pronounced crystalline structure than the brominated sample. Yet, XRD analysis confirmed that all of the samples were crystalline (Figure B4 in Appendix B). The diffraction

pattern of the mixture appeared to be similar to that of pure 2-naphthol, with a much diminished diffraction pattern of the brominated 2-naphthol being superimposed. This observation helps to explain the closeness in melting point temperature between the 2-naphthol and the mixture (Table 4.2).

Figure 4.19. Zeiss microscopy analysis pure 2-naphthol, halogenated 2-naphthol and mixture of halogenated and pure2-naphthol

4.3.3.4 Ultraviolet-Visible Spectrometry

Hydrogen bond formation due to a n→π* transition results in a shift toward shorter wavelengths (blue shift) of the absorption in the UV-vis spectrum, while a shift toward longer wavelengths (red shift) is observed in the π→π* transition upon hydrogen bond formation (Pimentel and McClellan, 1960). The shift in the n→π* transition is also a measure of the energy of hydrogen bonding (Jaffé and Orchin, 1962).

It can be observed from Figure 4.20 that the spectrum of halogenated 2-naphthol shifted to longer wavelengths in the region of 247-301 nm compared to the pure 2-naphthol. In the halogenated 2-naphthol the wavelengths of maximum absorbance were 265, 275, and 286 nm, compared to 263, 274, and 285 nm in pure 2-naphthol. This indicated that hydrogen bonding was weakened by halogenation. The mixture sample presents similar pattern than the pure 2-naphthol, however with lower absorbance. However, it is possible to observe some red shifts in the mixture sample compared to the pure sample, with the wavelengths of maximum absorbance in the mixed sample being at 269, 279, and 291 nm.

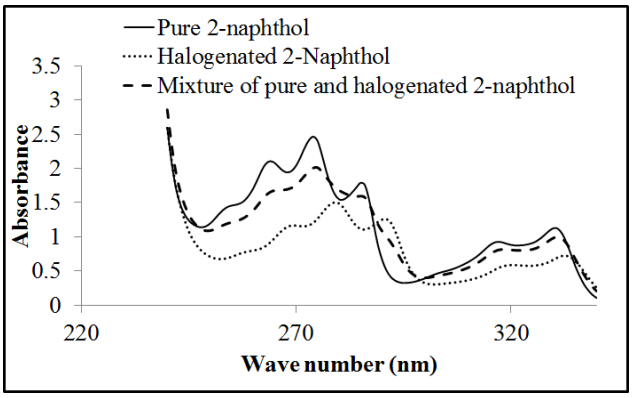

Figure 4.20. UV-Vis analysis of pure 2-naphthol, halogenated 2-naphthol, and mixture of pure and halogenated 2-naphthol

4.3.3.5 GC-MS Analysis

Figure 4.21a shows the chromatogram of pure 2-naphthol and it shows that the retention time of the peak correspondent to 2-naphthol is 17.47 minutes. Figure 4.21b shows the chromatogram of halogenated 2-naphthol and it can be seen that only one product was formed, which is bromination on the aromatic ring. Figure 4.21c shows that the mixed sample have both 2-naphthol and brominated 2-naphthol present in roughly equal amounts.

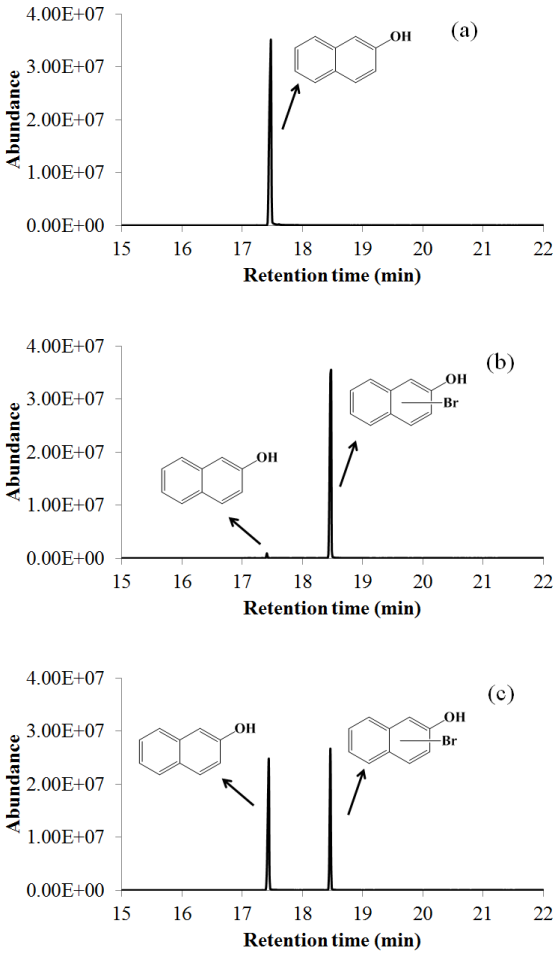

Figure 4.21. GC-MS analysis of (a) pure 2-naphthol (b) halogenated 2-naphthol and (c) 2-naphthol mixture

4.3.3.6 Evaluation of Hypothesis

Evidence was provided that the mixture of brominated 2-naphthol and 2-naphthol exhibited new properties, even though the compounds could still be chromatographically separated as individual species. XRD analysis and DSC analysis indicated that the mixture behaved as if it was a different compound with properties closer to that of 2-naphthol. UV-Vis spectroscopy did not support an interpretation based on stronger hydrogen bonding, but infrared analysis indicated that hydrogen bonding increased. The possible formation of a new compound could also be due to the interaction between bromine and phenol oxygen lone pair of bromine (halogen bonding), which is stronger than hydrogen bonding between bromine and hydrogen.

The mixture of brominated and pure phenanthrene, which resulted in the formation of a different crystal phase, provided further support that hydrogen bonding may play a key role in changing the physical properties of mixtures containing halogenated materials.

4.4 Conclusions

The origin of hardening of bitumen, maltenes, and asphaltenes due to halogenation was investigated. Model compounds were employed to test three different hypotheses concerning the increased hardness of halogenated materials.

a) No evidence was found to support the hypothesis that stacking strength was increased by the electrostatic difference between halogenated and non-halogenated material.

b) Addition reactions were found on heating halogenated materials. The carbon chain length of alkyl groups affected the way by which addition reactions took place. When two aliphatic carbons were adjacent, dehydrohalogenation formed olefinic intermediates that readily participated in acid catalyzed and free radical addition reactions. However, the present work did not provide evidence that mixing halogenated and non-halogenated material without heating resulted in addition reactions to cause hardening.

c) Some mixtures of halogenated and non-halogenated materials presented different properties than expected from a pure physical mixture. Increase hydrogen bonding was found, albeit not necessarily stronger hydrogen bonding. In a mixture of phenanthrene and brominated phenanthrene a new crystal configuration was observed. The study supported the hypothesis that increased hydrogen bonding may take place with halogenation reaction. However, in the case of 2-naphthol model compound halogen bonding between phenol oxygen lone pair to Br could also have happened and could be responsible for the possible formation of a new compound. In the case of halogenated asphaltenes, it is suspected that it is more likely that intermolecular hydrogen bonding could be responsible for increased hardeness as there are

constraining interactions in asphaltenes that not favour the bond angle requirement for halogen bonding.

Literature Cited

Acree Jr., W. E. Thermodynamic properties of organic compounds: enthalpy of fusion and melting point temperature compilation. *Thermochim. Acta* **1991**, *189*, 37-56.

Bondi, A. *Physical properties of molecular crystals, liquids, and glasses*; Wiley: New York, 1968.

Colthup, N. B.; Daly, L. H.; Wiberley, S. E. *Introduction to infrared and Raman spectroscopy*, 2ed; Academic Press: New York, 1975, pp. 217-218, 260-261.

Desijaru, G. R.; Ho, P. S.; Kloo, L.; Legon, A. C.; Marquardt, R.; Metrangolo, P.l Politzer, P.; Resnati, G.; Rissanen, K. Definition of the halogen bonding (IUPAC recommendations 2013). *Pure Appl. Chem*. **2013**, *85*, 1711-1713.

Dolphin, D.; Wick, A. *Tabulation of infrared spectral data*; Wiley: New York, 1977.

Emanuel, N. M.; Zaikov, G. E.; Maizus, Z. K. *Oxidation of organic compounds. Medium effects in radical reactions*; Pergamon Press: Oxford, 1984.

Ernst, L.; Schulz, P. ^{13}C and ^{1}H NMR chemical shift assignments of 1- and 2-alkylnaphthalenes (R= Me, Et, i-Pr, t-Bu) and determination of substituent effects on ^{13}C and ^{1}H chemical shifts. *Magnetic Resonance in Chemistry* **1992**, *30*, 73-76.

Gray, M. R.; Tykwinski, R. R.; Stryker, J. M., Tan, X. Supramolecular assembly model for aggregation of petroleum asphaltenes. *Energy Fuels* **2011**, *25*, 3125-3134.

Hartough, H. D.; Meisel, S. L. *Compounds with condensed thiophene rings*; Interscience: New York, 1954.

Höhne, G. W. H.; Hemminger, W. F.; Flammersheim, H.-J. *Differential scanning calorimetry*, 2ed; Springer: Berlin, 2003.

Jaffé, H. H.; Orchin, M. *Theory and applications of ultraviolet spectroscopy*; John Wiley & Sons: New York, 1962.

Katritzky, A. R.; Hitchings, G. J.; King, R. W.; Zhu, D. W. ^{1}H and ^{13}C Nuclear Magnetic Resonance studies of ethenyl-substituted benzenoid aromatic compounds. *Magnetic Resonance in Chemistry* **1991**, *29*, 2-8.

Kowanko, N.; Branthaver, J. F.; Sugihara, J. M. Direct liquid-phase fluorination of petroleum. *Fuel* **1978**, *57*, 769-775.

Lee, K-J.; Cho, H. K.; Song, C-E. Bromination of activated arenes by Oxone® and sodium bromide. *Bull. Korean Chem. Soc.* **2002**, *23*, 773-775.

Li, H.; Lu, Y.; Liu, Y.; Zhu, X.; Liu, H.; Zhu, W. Interplay between halogen bonds and π-π stacking interactions: CSD search and theoretical study. *Phys. Chem. Chem. Phys.* **2012**, *14*, 9948-9955.

March, J. *Advanced organic chemistry: reactions, mechanisms, and structure*, 4ed; John Wiley & Sons: New York, 1992, pp. 501-568.

Moschopedis, S. E.; Speight, J. G. Chemical modification of bitumen heavy ends and their nonfuel uses. *Adv. Chem. Ser.* **1976**, *151*, 144-152.

Moschopedis, S. E.; Speight, J. G. Introduction of halogen into asphaltenes via the Gomberg reaction. *Fuel* **1970**, *49*, 335.

Moschopedis, S. E.; Speight, J. G. The halogenation of Athabasca asphaltenes with elemental halogen. *Fuel* **1971**, *50*, 58-64.

Patwardhan, S. R. Chlorination of petroleum bitumens. *Fuel* **1979**, *58*, 375-378.

Petersen, J. C. Asphalt oxidation - an overview including a new model for oxidation proposing that physicochemical factors dominate the oxidation kinetics. *Fuel Sci. Technol. Int.* **1993**, *11*, 57-87.

Pimentel, G. C.; McClellan, A. L. *The hydrogen bond*; W. H. Freeman and Company: New York, 1960.

Prado, G. H C.; De Klerk, A. Halogenation of oilsands bitumen, maltenes, and asphaltenes. *Energy Fuels* **2014**, *28*, 4458-4468.

Rojas, A.; Orozco, E. Measurement of the enthalpies of vaporization and sublimation of solids aromatic hydrocarbons by differential scanning calorimetry. *Thermochim. Acta* **2003**, *405*, 93-107.

Silverstein, R. M.; Webster, F. X. *Spectrometric identification of organic compounds*, 6ed; John Wiley & Sons: New York, 1997, pp. 87, 108.

Smith, J. W. Hydrogen-bonding and complex-forming properties. In *The chemistry of the carbon-halogen bond. Part 1*; Patai, S., Ed.; John Wiley and Sons: London, 1973, pp. 265-300.

Speight, J. G. Reactions of Athabasca asphaltenes and heavy oil with metal chlorides. *Fuel* **1971**, *50*, 175-186.

The properties of asphaltic bitumen with reference to its technical applications; Pfeiffer, J. P. Ed.; Elsevier: New York, 1950, pp. 117.

Ubbelohde, A. R. *Melting and crystal structure*; Claredon Press: Oxford, 1965.

Xie, Y.; Jiang, F.; Xu, J.; Zeng, L.; Dong, B.; Lu, B.; Shang, X. Electrosyntheses and characterization of poly(9-bromophenanthrene) in boron trifluoride diethyl etherate. *Eur. Polym. J.* **2009**, *45*, 418-425.

Zabicky, J.; Ehrlich-Rogozinski, S. Analysis of organic halogen compounds. In *The chemistry of the carbon-halogen bond. Part 1*; Patai, S., Ed.; John Wiley and Sons: London, 1973, pp. 179.

Chapter 5. Demetalation of Metallophthalocyanines by Mild Halogenation without Disrupting the Tetrapyrrole Macrocycle[17]

Abstract

The nickel and vanadium content of heavy oil and bitumen affects residue upgrading technology selection. Processes employing heterogeneous catalysts cannot be selected when the metals concentration in the oil exceeds tens, or at most a few hundred parts per million, due to catalyst fouling. Demetalation of high metal content oil is desirable before catalytic conversion. Mild halogenation was evaluated for bulk demetalation of Ni and V from a tetrapyrrole macrocycle, which is found in porphyrins and phthalocyanines. Specifically, bromination of Ni(II) phthalocyanine and V(IV) oxide phthalocyanine was investigated to evaluate selective metal removal, i.e. demetalation without disrupting the tetrapyrrole macrocycle. Bromination was spectroscopically confirmed. Halogenation derivitized the phthalocyanine, irrespective of the metal, but no destruction of the tetrapyrrole macrocycle was observed. Ni was substantially (74 wt %) removed after mild bromination. No demetalation of V was observed. The selective removal of only Ni(II) could be explained in terms of the combined effects of acid-based and metal-ligand equilibria.

Keywords: Tetrapyrrole Macrocycle; Demetalation; Halogenation; Nickel(II) Phthalocyanine; Vanadium(IV) Oxide Phthalocyanine; Petroporphyrin

[17] Paper accepted for publication in *Fuel*.

5.1 Introduction

Metalloporphyrins and metallophthalocyanines are naturally occurring compounds. Porphyrins are composed of a tetrapyrrole macrocycle, which consists of four pyrrole groups connected by four methine bridges. Phthalocyanines have the same tetrapyrrole macrocycle, but the pyrrole groups are connected through =N– bridges, instead of =(CH)– bridges. Derivitization of the porphin nucleus, such as substitution of different side chains at the peripheral positions, results in numerous kinds of compounds with the same tetrapyrrole macrocycle. Porphyrins and phthalocyanines with coordinated metal ions are called metalloporphyrins and metallophthalocyanines. The coordination of metal ions is possible, because the tetrapyrrole macrocycle contains electron pairs that can be shared with a metal ion, which acts as a Lewis acid (Buchler, 1975).

Of specific interest to oil upgrading and refining is the petroporphyrins, compounds containing a tetrapyrrole macrocycle with chelated metal ions that are present in crude oils. The metals most often present in petroporphyrins are nickel and vanadium. These molecules affect technology selection for residue upgrading. Residue fluid catalytic cracking cannot be employed when the metal content of the feed exceeds around 15 μg/g. One of most metal-tolerant catalytic processes, ebullated bed residue hydroconversion, cannot be operated at high conversion when the metal content of the feed exceeds 350 μg/g (Rana *et al.* 2007).

During bitumen upgrading, nickel and vanadium causes deactivation of both desulfurization and cracking catalysts and their removal prior to upgrading is desired. Coking, deasphalting, and catalytic residue hydroprocessing are technologies currently employed by industry that also remove metals from petroleum products. These technologies result in bulk metals removal from oil, although metals removal is not the primary objective of any of these processes. Coking and deasphalting technologies cause non-selective metals removal and, being carbon rejection processes, metal removal is accompanied by significant associated loss of organic material as coke and asphaltenes. Residue hydroprocessing performs hydrodemetalation (HDM), which is more selective for metals removal, but when converting high metal content oils the operating cost associated with catalyst, hydrogen and energy consumption is high (Dechaine and Gray,

2010). There is also a practical upper limit to the metals content that can be tolerated, since catalysts are ultimately fouled by the nickel and vanadium (Rana *et al*., 2007; Toulhoat, 1990)0.

Bulk demetalation is of particular interest as pretreatment step in the upgrading of oilsands bitumen, which has high metals content, typically in the range 200 to 300 μg/g Ni and V (Strausz and Lown, 2003).

Mild halogenation of asphaltenes was studied as a strategy to convert some of the asphaltenes into maltenes (Prado and De Klerk, 2014) (Chapter 3). Demetalation was not the objective for that study, but it was found that halogenation might have destroyed metalloporphyrins, or at least cause some demetalation. It was observed that after mild bromination the Soret-bands in the ultraviolet-visible spectrum decreased, which was indicative of a decrease in metalloporphyrin content. Beyond this observation, no further investigation was reported to confirm demetalation or to understand the origin of the decrease in the Soret-bands.

The use of strong chlorinating agents, Cl_2 and $SOCl_2$, were previously reported for demetalation (Ali and Abbas, 2006), but it did not suggest that mild halogenation might also be successful for demetalation. It was also mentioned that metalloporphyrins brominated for extended time periods led to destruction of the porphyrin (Chorghade, 1996), but this observation was not explained.

The aim of this work was to determine whether mild halogenation is effective for demetalation of tetrapyrrole macrocycles and specifically whether it must occur by converting the tetrapyrrole macrocycle, or whether the metal can also selectively be removed. The model compounds Ni(II) phthalocyanine and V(IV) oxide phthalocyanine were employed as surrogates to facilitate analysis and interpretation. Metals in petroleum products are mainly present in porphyrin and porphyrin-derived structures (Yen, 1975), and the use of metallophthalocyanines instead of metalloporphyrins requires some explanation.

It was postulated that demetalation does not necessarily require destruction of the tetrapyrrole macrocycle, but that competitive coordination might displace the coordinated metal. There was

no guarantee that mild bromination would not disrupt the tetrapyrrole macrocycle in metalloprophyrins, with the outcome of porphyrin halogenation being dependent on many variables, such as the porphyrin substituents, metal coordination, temperature and halogen employed (Bonnett *et al*., 1966; Rumyantseva *et al*., 2000; Jin *et al*., 2005, Chumakov *et al*., 2009; Di Carlo *et al*., 2015; Gehrold *et al*., 2015). Porphyrins contain olefinic =(CH)– bridges linking the tetrapyrrole macrocycle (Figure 5.1) and the *meso*-positions are susceptible to attack during halogenation, whereas the =N– bridges in phthalocyanines are not. Phthalocyanines can consequently be used as model compounds to study selective demetalation by mild halogenation while at the same time maintaining the integrity of the tetrapyrrole macrocycle. In fact, it was reported that phthalocyanines were derivitized by chlorination (Berezin, 1981; Barret *et al*., 1939), and bromination (Barret *et al*., 1939), without destroying the tetrapyrrole macrocycle.

The dissociation mechanism for metalloporphyrins and metallophthalocyanines is similar (Berezin, 1981). The use of metallophthalocyanines rather than metalloporphyrins was a strategy to study the role of selective demetalation during halogenation, instead of demetalation that is known to occur when the tetrapyrrole macrocycle is disrupted (Rankel, 1987). Halogenation at the reactive *meso*-positions of porphyrins (Figure 5.1) causes disruption of the porphyrin nucleus (Bonnett, 1992), and had to be avoided.

The study elucidates selective metal removal without destroying the tetrapyrrole macrocycle, which is not a standard approach to demetalation. It also demonstrates the potential use and the limitations of mild halogenation as a method for bulk metals removal from heavy oils, bitumen and asphaltenes fractions.

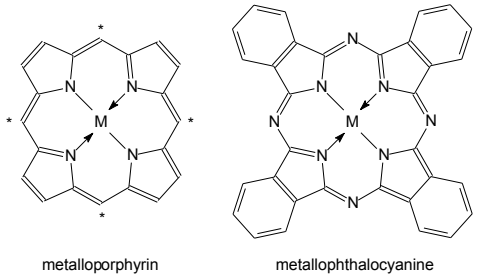

Figure 5.1. Metalloporphyrin structure, with the reactive *meso*-positions (*) indicated, compared to the metallophthalocyanine structure; M is the coordinated metal

5.2 Experimental

5.2.1 Materials

Chemicals and gas cylinders were commercially obtained without purification and they are described in Table 5.1.

The metallophthalocyanines were water washed to determine the extent of loosely bonded nickel and vanadium. Inductively coupled plasma atomic emission spectrometry of the water solution from Ni(II) phthalocyanine washing contained 0.02 ± 0.01 mg/L Ni, which was equivalent to 3 μg Ni/g metallophthalocyanine. The water solution from V(IV) oxide phthalocyanine washing contained 10 ± 1 mg/L of V, which was equivalent to 330 μg V/g metallophthalocyanine.

Table 5.1. Chemicals and cylinder gases employed in this study

Compound	Formula	CASRN [a]	Mass fraction purity [b,c]	Supplier
Chemicals				
chloroform	$CHCl_3$	67-66-3	0.99	Sigma-Aldrich
sodium bromide	NaBr	7647-15-6	0.99	Sigma-Aldrich
oxone®	$KHSO_5 \cdot 0.5KHSO_4 \cdot 0.5K_2SO_4$	70693-62-8	-	Sigma-Aldrich
Ni(II) phthalocyanine	$Ni(C_{32}H_{16}N_8)$	14055-02-8	not informed	Alfa Aesar
V(IV) oxide phthalocyanine	$C_{32}H_{16}N_8OV$	13930-88-6	not informed	Alfa Aesar
sodium sulfate	Na_2SO_4	7757-82-6	0.99	Sigma-Aldrich
0.05M sodium thiosulfate solution	$Na_2S_2O_3$	7772-98-7	-	Sigma-Aldrich
toluene	C_7H_8	108-88-3	≥ 0.995b	Fisher Scientific
trifluoroacetic acid	CF_3COOH	76-05-01	0.99	Sigma-Aldrich
d-chloroform	$CDCl_3$	865-49-6	0.9996 atom D	Sigma-Aldrich
vanadium(V) oxide	V_2O_5	1314-62-1	0.9996	Sigma-Aldrich
potassium carbonate	K_2CO_3	584-08-7	0.99	Sigma-Aldrich
Cylinder gases				
helium	He_2	7440-59-7	0.99999[c]	Praxair
air	O_2/N_2 mix	132259-10-0		Praxair

[a] CASRN = Chemical Abstracts Services Registry Number.
[b] This is the purity of the material guaranteed by the supplier; material was not further purified.
[c] Mole fraction purity.

5.2.2 Equipment and Procedure

Halogenation of Ni(II) phthalocyanine and V(IV) oxide phthalocyanine were performed by following the same procedure used for halogenation of asphaltenes, bitumen, and maltenes with different quantities (Lee *et al*., 2002; Prado and De Klerk, 2014). First, a solution of 4 mmol of substrate and 24 mL of chloroform was prepared. Then, 4 mmol of sodium bromide was added to the solution followed by a drop wise addition of oxone solution (4 mmol in 30 mL of water). The solution was stirred for 24 hours and 0.05 M of sodium thiosulfate solution (12 mL) was added to the reaction mixture. The organic layer was separated from the solution and dried with

anhydrous sodium sulfate. Chloroform was evaporated under vacuum and the remaining solvent was evaporated in the fumehood until constant weight.

5.2.3 Analyses

FTIR analysis was performed as in Chapter 3.

Pure and halogenated materials were dissolved in toluene at a concentration equal to 40 mg/L for UV-Vis analysis. Nevertheless, the solutions were stirred with a magnetic stir bar in order to obtain complete dissolution of the materials. The instrument used was described as in Chapter 3.

Ni and V were quantified by XRF. Calibration and sample measurements were performed in a K_2CO_3 matrix. The metals content was also determined indirectly by thermogravimetric analysis (TGA) using a procedure for ash content determination. For a typical analysis ~5 mg of sample was heated in an Al_2O_3 crucible from 25 to 900 ºC at 20 °C/min under constant 100 mL/min air flow. The metals content was calculated from the measured metal oxide (ash) content. The instruments were described as in Chapter 3.

5.3 Results and Discussion

5.3.1 FTIR Analysis

Figure 5.2a and 5.2b show the FTIR spectra of pure and halogenated Ni(II) phthalocyanine in two different regions. Figure 5.2a shows the region of C–Br absorption, 650-550 cm^{-1} (Zabicky and Ehrlich-Rogozinski, 1973). A new broad absorption appeared at 613 cm^{-1} for the halogenated material; bromination was achieved. Figure 5.2b shows 1050-950 cm^{-1} region where the strong stable metal chelate absorption with the tetrapyrrole macrocycle at around 1000 cm^{-1} was anticipated (Falk, 1964). Pure Ni(II) phthalocyanine presented an absorption at 997 cm^{-1}, as anticipated, but in the halogenated material this absorption is small compared to Ni(II) phthalocyanine. The change in the absorption at 997 cm^{-1} indicated that bromination disrupted the interaction between Ni(II) and the tetrapyrrole macrocycle.

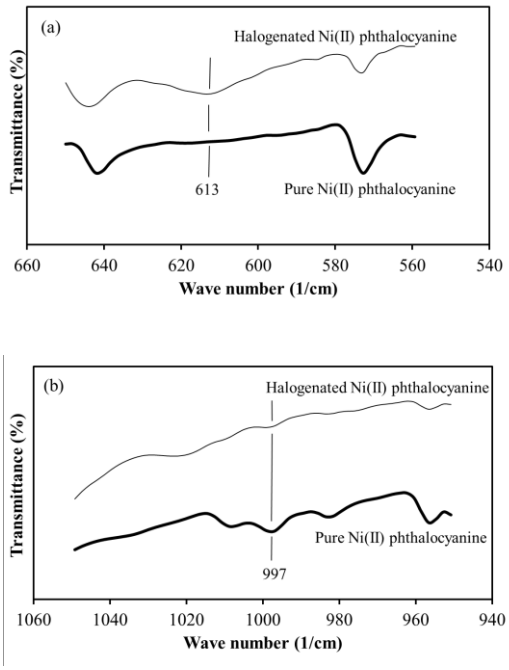

Figure 5.2. FTIR analysis of Ni(II) phthalocyanine model compound (a) 560-650 cm^{-1} region (b) 950-1050 cm^{-1} region

Figure 5.3a and 5.3b present the FTIR spectra of pure and halogenated V(IV) oxide phthalocyanine. The appearance of a new absorption of 615 cm^{-1} (Figure 5.3a) was due to C–Br (Zabicky and Ehrlich-Rogozinski, 1973), indicating that bromination was successful. The strong metal chelate absorption at 1000 cm^{-1} (Figure 5.3b) persisted after halogenation. Bromination did not disrupt the interaction between V(IV) oxide and the tetrapyrrole macrocycle.

In conclusion, FTIR spectroscopy showed the formation of C–Br bonds due to bromination, but bromination affected only the interaction of Ni(II) with the phthalocyanine and not that of V(IV) oxide. This suggested that derivitization of phthalocyanine by halogenation was not disruptive, as was reported before (Berezin, 1981), and that the bromination affected Ni(II) removal only.

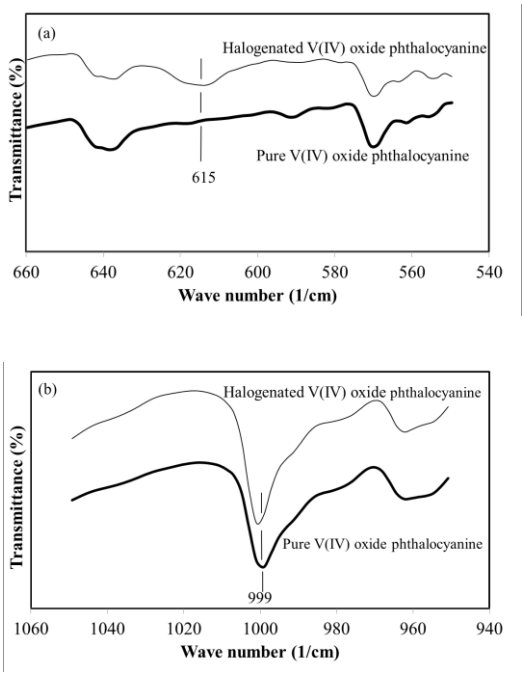

Figure 5.3. FTIR analysis of V(IV) oxide phthalocyanine model compound (a) 560-650 cm^{-1} region (b) 950-1050 cm^{-1} region

5.3.2 UV-Vis Analysis

Ultraviolet-visible spectroscopy is extensively used in the study of metal coordination in tetrapyrrole macrocycles due to the intense nature of the Soret-bands (Falk, 1964). The strong absorption of phthalocyanine-based compounds in the visible range also gave rise to their application as dyes (Moser and Thomas, 1963).

Free tetrapyrrole macrocycles and metal-coordinated tetrapyrrole macrocycles present different behaviour when analysed by UV-Vis spectroscopy. In general, free tetrapyrrole macrocycles present four visible bands (named I, II, III, and IV) along with the more intense the Soret band. On the other hand, the tetrapyrrole macrocycles that chelated divalent metal ions present only two visible bands (named α and β) along the Soret band. The intensity of α band is higher than β band for stable chelates such as Ni(II) and lower for less stable chelates such as Mg(II) (Falk, 1964).

Figure 5.4a and 5.4b present the 550 to 750 nm spectral region of pure and halogenated Ni(II) phthalocyanine and V(IV) oxide phthalocyanine respectively. The characteristic α and β bands of metal containing tetrapyrrole macrocycles is clearly visible in the spectrum of pure Ni(II) phthalocyanine (Figure 5.4a). However, in the halogenated Ni(II) phthalocyanine the four I, II, III, and IV bands, typical of free tetrapyrrole macrocycles were observed (Figure 5.4a). Bromination removed Ni(II) from the tetrapyrrole macrocycle. Additionally the III band increased in intensity.

The III band is near 665 nm (15 000 cm^{-1}), which is typical of the $^3T_1$ to $^3T_1(P)$ absorption of tetrahedrally coordinated $[NiX_4]^{2-}$ anions, with X = halogen (Nicholls, 1974). The $^3T_1(F)$ to $^3T_1(P)$ of $[NiBr_4]^{2-}$ presents two bands at 753-755 nm and 700-707 nm, and a shoulder at 660-670 nm at room temperature (Griffiths and Phillips, 1989; Fine, 1965). In the study by Gill and Nyholm (1959), the absorption maxima for a dilute solution of $[NiBr_4]^{2-}$ were reported at slightly lower wavelengths, 750, 698 and 652 nm. The formation of $[NiBr_4]^{2-}$ was ruled out by the absence of an absorption at around 750 nm (Figure 5.4a).

The UV-Vis spectra provided strong evidence that Ni(II) was removed from the phthalocyanine, but not in what form the removed Ni(II) was. It is speculated that the Ni(II) in aqueous solution is the halide salt $NiBr_2$.

There was little difference between the UV-Vis spectra of pure and brominated V(IV) oxide phthalocyanine (Figure 5.4b). Only the α and β bands of the metallophthalocyanine were found. This result indicated that halogenation did not remove V(IV) oxide from V(IV) oxide phthalocyanine.

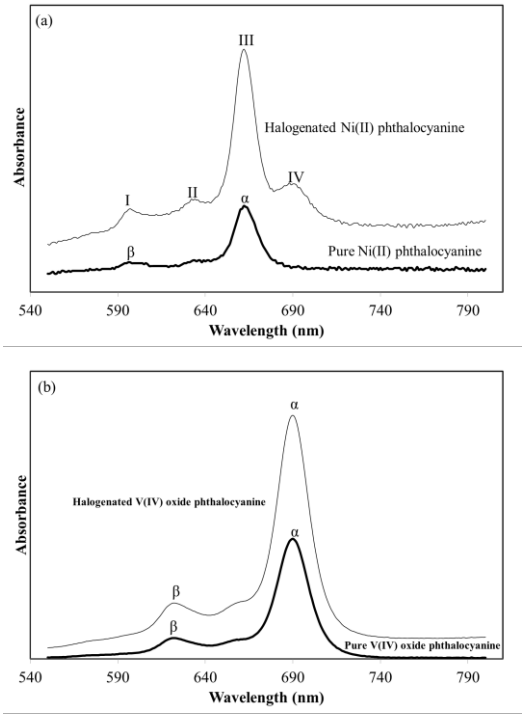

Figure 5.4. UV-Vis analysis of (a) pure and halogenated Ni(II) phthalocyanine (b) pure and halogenated V(IV) oxide phthalocyanine

Acid-base equilibrium (Figure 5.5a) and metal-ligand equilibrium (Figure 5.5b) must both be considered when dealing with reactions involving metal coordination to tetrapyrrole macrocycles, irrespective of whether dealing with a phthalocyanine or a porphyrin. The dissociation mechanism for metallophthalocyanines and metalloporphyrins is similar and is described by Berezin (1981). The displacement of Ni(II), but not V(IV) oxide, pointed to effective stabilization of Ni(II) by Br^- and not acid-base equilibrium as driving force for Ni(II) removal. However, the slow step in the process is the acid-base reaction. The bromide may play a role, but Berezin (1981) pointed out that for coordinatively saturated metals the effect of most anions on the kinetics is negligible, unless the anion has a strong coordinative affinity for the metal. Since bromine is not strongly coordinating, and it was unlikely to affect the kinetics of the slow step, the difference between the removal of Ni(II) and V(IV) oxide lies in the displacement of the equilibrium afterwards. The acid-base equilibrium (Figure 5.5a) is continuously disrupted only in the case of Ni(II) by the removal of the metal with the bromide (Figure 5.5b). The demetalation is therefore *caused* by the acid-base reaction, but it is limited,

and the *extent* of demetalation is determined by the ability of the anion to remove the metal ion from the acid-base equilibrium by competitive interaction.

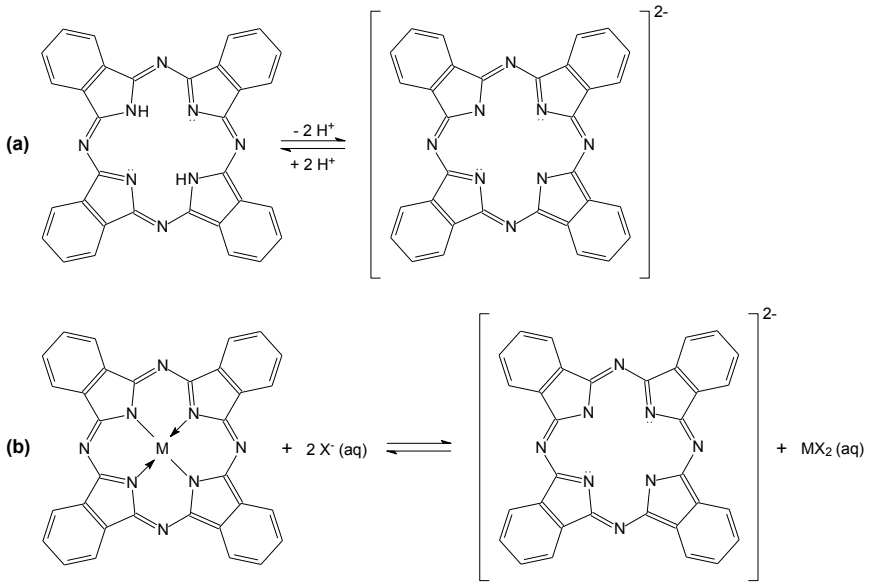

Figure 5.5. Equilibria relevant to the reaction chemistry of tetrapyrrole macrocycles, namely, (a) acid-base and (b) metal-ligand, where M^{2+} is the coordinated metal ion and X^- is a halide ligand

5.3.3 Quantification of Demetalation

The metals content of the pure Ni(II) and V(IV) oxide phthalocyanines were confirmed by XRF analysis (Table 5.2). The metals content of the samples reported by XRF were also verified by TGA. The measured nickel content as NiO was 12.9 ± 0.5 wt%, which is equivalent to 10.1 wt% Ni in Ni(II) phthalocyanine. The measured vanadium content as V_2O_5 was 16.8 ± 0.9 wt%, which is equivalent to 9.4 wt% V in V(IV) oxide phthalocyanine.

After halogenation the Ni content of the brominated Ni(II) phthalocyanine decreased from 10.3 ± 1.2% to 2.7 ± 0.5% (Table 5.2), i.e. 74 % Ni removal. The V content was unaffected by the bromination of V(IV) oxide phthalocyanine. Thus, only Ni was demetalated by halogenation.

Table 5.2. Nickel and vanadium quantification of pure and halogenated materials by XRF analysis

Sample	Ni (%)[a]		V(%)[a]	
	x	s	x	s
Ni(II) phthalocyanine (calculated) [b]	10.3	-	-	-
Ni(II) phthalocyanine	10.3	1.2	-	-
Ni(II) phthalocyanine (TGA)[c]	10.1	-		
Halogenated Ni(II) phthalocyanine	2.7	0.5	-	-
V(IV) oxide phthalocyanine (calculated) [b]	-	-	8.9	-
V(IV) oxide phthalocyanine	-	-	9.1	0.3
V(IV) oxide phthalocyanine (TGA)[c]			9.4	-
Halogenated V(IV) oxide phthalocyanine	-	-	9.1	0.1

[a] Average (x) and sample standard deviation (s) of analyses in triplicate are reported.
[b] Calculation based on the molecular formula of the substance.
[c] Measured as 12.9 ± 0.5 wt% NiO and 16.8 ± 0.9 wt% V_2O_5.

5.3.4 *Relevance to Demetalation of Heavy Oil*

The preceding analyses indicated that the tetrapyrrole macrocycle was not disrupted by halogenation. This was a consequence of using phthalocyanines instead of porphyrins. In heavy oil nickel and vanadium is present as porphyrin complexes. In porphyrins the tetrapyrrole macrocycle can be disrupted by halogenation and hydrogenation, which results in demetalation (Rankel, 1987; Reynolds, 2001). The carbons at the *meso*-positions (Figure 5.1) are the most susceptible to halogen or hydrogen addition, changing the bridging carbons from sp^2 to sp^3, i.e. from =(CH)– to –(CHX)– with X = H, Cl, Br, depending on the reaction. With repeated reaction the coordinating ability of the tetrapyrrole macrocycle is destroyed and demetalation occurs.

The present investigation showed that there is a second pathway of demetalation that is possible without disrupting the tetrapyrrole macrocycle. The acid-base equilibrium (Figure 5.5a) can be used in conjunction with the metal-ligand equilibrium (Figure 5.5b) to remove nickel. Since the metal-ligand equilibrium appeared not to be favorable for V(IV) oxide, only Ni(II) removal was noticeable.

5.4 Conclusions

Demetalation by halogenation of model compounds containing a tetrapyrrole macrocycle was investigated by mild bromination. The objective was to determine whether demetalation must occur by converting the tetrapyrrole macrocycle (known from literature, e.g. (Rankel, 1987), or whether the metal can also selectively be removed by halogenation. Metallophthalocyanines instead of metalloporphyrins were used, because halogenation does not disrupt the tetrapyrrole macrocycle in phthalocyanines, while the mechanism of metal displacement for both compound classes is the same (Berezin, 1981). The conclusions based on experimental evidence are:

a) Bromination of metallophthalocyanines was confirmed by the development of a C–Br absorption around 613-615 cm^{-1} in the infrared spectrum.

b) No evidence was found that bromination destroyed the tetrapyrrole macrocycle, only that the phthalocyanines were derivitized.

c) Nickel was substantially removed from Ni(II) phthalocyanine by bromination: 74 % Ni removal based on XRF analysis. The strong infrared absorption of the metal chelate of the tetrapyrrole macrocycle at 997 cm^{-1} decreased and UV-Vis spectroscopy showed the development of a free tetrapyrrole macrocycle after bromination.

d) Vanadium was not removed from V(IV) oxide phthalocyanine. This was confirmed by XRF analysis and supported by infrared and UV-Vis spectra that showed no evidence of the formation of a free tetrapyrrole macrocycle.

e) The selective removal of Ni(II) by mild bromination, but not V(IV) oxide, could be explained in terms of the acid-base equilibrium in combination with the metal-ligand equilibrium. Both metallophthalocyanines were subjected to acid-base equilibrium, but only in the case of Ni(II) was the metal ion effectively removed in the metal-ligand equilibrium to disrupt the acid-base equilibrium and result in demetalation.

Literature Cited

Ali, M. F. and Abbas, S. A review of methods for the demetallization of residual fuel oils. *Fuel Process. Technol*. **2006**; 87, 573-584.

Barrett, P. A., Bradbrook, E. F., Dent, C. E., Linstead, R. P. Phthalocyanines and related compounds. Part XVI. The halogenation of phthalocyanines. *J. Chem. Soc*. **1939**, 1820-1828.

Berezin, B, D. Coordination compounds of porphyrins and phthalocyanines. Chichester: John Wiley and Sons; 1981.

Bonnett, R., Gale, I. A. D., Stephenson, G. F. The *meso*-reactivity of porphyrins and related compounds. Part II. Halogenation. *J. Chem. Soc. (C)* **1966**, 1600-1604.

Bonnett, R., Harriman, A., Kozyrev, A. N. Photophysics of halogenated porphyrins. *J. Chem. Soc. Perkin. Trans*. **1992**, 88, 763-769.

Buchler, J. W. Static Coordination Chemistry of Metalloporphyrins. In Falk, J. E., Smith, K. M., editors. Porphyrins and Metalloporphyrins, Elsevier: Amsterdam; 1975, p 157-231.

Chorghade, M.S., Dolphin, D., Dupré, D., Hill, D.R., Lee, E.C., Wijesekera, T.P. Improved protocols for the synthesis and halogenation of sterically hindered metalloporphyrins. *Synthesis* **1996,** 1320-1324.

Chumakov, D.E., Khoroshutin, A.V., Anisimov, A.V., Kobrakov, K.I. Bromination of porphyrins (Review). *Chem. Heterocyclic Compounds* **2009**, 45, 259-283.

Dechaine, G.P, Gray, M.R. Chemistry and association of vanadium compounds in heavy oil and bitumen, and implications for their selective removal. *Energy Fuels* **2010,** 24, 2795-2808.

Di Carlo, G., Biroli, A.O., Tessore, F., Rizzato, S., Forni, A., Magnano, G., Pizzotti, M. Light-induced regiospecific bromination of *meso*-tetra(3,5-di-tertbutylphenyl) porphyrin on 2,12 β-pyrrolic positions. *J. Org. Chem*. **2015**, 80, 4973-4980.

Falk, J.E. Porphyrins and Metalloporphyrins. Elsevier: Nerw York, 1964.

Fine, D.A. Tetrahedral bromide complexes of nickel(II) in organic solvents. *Inorg. Chem*. **1965**, 345-350.

Gehrold, A.C., Bruhn, T., Schneider, H., Radius, U., Bringmann, G. Chiral and achiral basket-handle porphyrins: short synthesis and stereostructures of these versatile building blocks. *Org. Lett*. **2015**, 17, 210-213.

Gill, N.S., Nyholm, R.S. Complex halides of the transition metals. Part I. Tetrahedral nickel complexes. *J. Chem. Soc*. **1959**, 3997-4007.

Griffiths, T.R., Phillips, N.J. The nickel(II)-bromide system in dimethyl sulphoxide: a detailed study of the influences of temperature and mole ratio. *J Chem Soc Dalton Trans* **1989**, 2, 325-330.

Hambright, P. Dynamic Coordination Chemistry of Metalloporphyrins. In Falk, J.E., Smith, K.M., editors. Porphyrins and Metalloporphyrins, Elsevier: Amsterdam; 1975, p 233-278.

Jin, L-M., Yin, J-J., Chen, L., Guo, C-C., Chen, Q-Y. Metal dependent halogenation and/or coupling reactions of porphyrins with $PhIX_2$ (X=Cl, F). *Synlett* **2005**, 19, 2893-2898.

Lee, K-J., Cho, H.K., Song, C-E. Bromination of activated arenes by Oxone® and sodium bromide. *Bull. Korean Chem. Soc*. **2002**, 23, 773-775.

Moser, F.H., Thomas, A.L. Phthalocyanine compounds (ACS Monograph Ser. 157). New York: Reinhold Publ. Corp.; 1963.

Nicholls, D. Complexes and first-row transition elements. London: Macmillan; 1974, p 95.

Prado, G.H.C., De Klerk, A. Halogenation of oil sands bitumen, maltenes, and asphaltenes. *Energy Fuels* **2014**, 28, 4458-4468.

Rana, M.S., Sámano, V., Ancheyta, J., Diaz, J.A.I. A review of recent advances on processing technologies for upgrading of heavy oils and residua. *Fuel* **2007**, 86, 1216-1231.

Rankel, L.A. Degradation of metalloporphyrins in heavy oils before and during processing. Effect of heat, air, hydrogen, and hydrogen sulfide on petroporphyrin species. *ACS Symp. Ser.* **1987**, 344, 257-264.

Reynolds, J.G. Nickel in petroleum refining. *Petrol. Sci. Technol*. **2001**, 19, 979-1007.

Rumyantseva, V.D., Aksenova, E.A., Ponamoreva, O.N., Mironov, A.F. Halogenation of metalloporphyrins. *Russ. J. Bioorg. Chem*. **2000**, 26, 423-428.

Strausz, O.P., Lown, E.M. The Chemistry of Alberta Oil Sands, Bitumens, and Heavy Oils, Calgary: Alberta Energy Research Institute; 2003, p 335-346.

Toulhoat, H., Szymanski, R., Plumail, J.C. Interrelations between initial pore structure, morphology and distribution of accumulated deposits, and lifetimes of hydrodemetallisation catalysts. *Catal. Today* **1990**, 7, 531-568.

Yen, T.F. Chemical aspects of metals in native petroleum. In Yen TF editor. The role of trace metals in petroleum, Ann Arbor: Ann Arbor Science Publishers; 1975, p 1-30.

Zabicky, J., Ehrlich-Rogozinski, S. Analysis of Organic Halogen Compounds. In Patai S, editor. The Chemistry of the Carbon-Halogen Bond Part 1, London: John Wiley & Sons; 1973, p 179.

.

Chapter 6. Potential Role of Chloride Salts in Bitumen Upgrading

6.1 Introduction

It is known that bitumen contains chloride salts originated from oilsands formation. In order to remove the salts, desalting process is usually employed before oil upgrading. Desalting is a process that adds water to the oil to extract the salts and then remove the water. However, due to the high content of other compounds in Athabasca bitumen, such as naphthenic acids and asphaltenes, dewatering becomes a very difficult task. Usually, removal of water from bitumen occurs in two stages: addition of solvent to remove free water and then heating of bitumen to evaporate the remaining water. The procedure of heating water leaves the crystalline salts in the diluted bitumen. It is reported that these crystalline salts are hydrophobic and are coated with asphaltenes in the diluted bitumen. The concentration of residual salts can reach up to 0.8-1.0% of total feed bitumen from Syncrude. The most chloride compounds present in bitumen are magnesium chloride, calcium chloride, and sodium chloride (Gray, 2010). The only behavior reported for these salts during bitumen upgrading at elevated temperatures is their hydrolysis as shown in Figure 6.1. The hydrolysis results in HCl and metal hydroxides formation. HCl formation causes corrosion of equipment. Chloride salts can also react with naphthenic acids and release HCl (Gray *et al*., 2008).

$$CaCl_2(s) + H_2O(g) \xrightarrow{>200^oC} CaClOH(s) + HCl(g)$$

Figure 6.1. Hydrolysis of calcium chloride during bitumen upgrading (Gray et al., 2008)[18]

The halogenation of bitumen, maltenes, and asphaltenes resulted in more complex, heavier, and harder materials. Halogenation also changed the solubility of asphaltenes. Halogenated asphaltenes were not only insoluble in paraffinic solvents, they were also insoluble in aromatic solvents such as benzene and toluene (Moschopedis and Speight, 1971; Prado and De Klerk, 2014). As asphaltenes are coke precursors in bitumen upgrading, coke is insoluble in both aromatic and paraffinic solvents and halogenated asphaltenes were insoluble in aromatic

[18] Reprinted from Petroleum Science and Technology, 26, Gray, M. R.; Eaton, P. E.; Le, T. Kinetics of hydrolysis of chloride salts in model crude oil, 1924-1933, Copyright 2008, with permission from Taylor & Francis

solvents, Prado and De Klerk (2014) (Chapter 3) suggested that the residual chloride salts present in bitumen could have some influence during coke formation.

Therefore, the objective of this chapter is to present and evaluate the hypothesis of the potential role of chloride salts during coke formation in bitumen upgrading. The work is based on a theoretical treatment of the subject and no new experimental work is presented. It will be presented in two sections. First, coke will be reviewed. Second, the role of chlorides will be discussed.

6.2 Coke Formation during Coking Upgrading Process

Coking is a thermal cracking and non-catalytic upgrading process that converts bitumen into lower-boiling liquid product, coke and light gases. In this process, chemical bonds are broken by heating the feed at temperatures above 400 ºC. Free-radicals formed during thermal cracking activate the breaking of the bonds by hydrogen abstraction. The lower-boiling liquid product contains a H:C ratio higher than initial bitumen while the H:C ratio of coke is lower than initial bitumen (De Klerk *et al.*, 2014). Coke is an aromatic, high molecular weight, and high metals and heteroatoms content solid material formed from bitumen during thermal cracking that was not initially present in bitumen. A kinetic model for coke formation mechanism during thermal cracking was developed by Wiehe (1993) while the free radical chain mechanism of thermal cracking is explained by Gray and McCaffrey (2002). A summary of literature was presented by Gray (2010).

Coke formation starts after an induction period and it depends of the amount of asphaltenes that are solubilized in the oil. If more asphaltenes are solubilized in the oil, the induction period will be longer. Coke starts to form when asphaltenes concentration decreases (Wiehe, 1993). The formation of coke is the result of several events happening simultaneously. It includes olefins formation due to cracking of paraffinic side chains of aromatic compounds, formation of aromatics due to dehydrogenation of naphthenes and condensation of aliphatic compounds, formation of fused ring aromatics due to condensation of aromatic compounds, and oligomerization due to addition reactions of olefins formed during cracking of side chains (Gray,

2010). Cracking of paraffinic side chains results in free radicals that will propagate through hydrogen abstraction, β-scission, and radical addition reactions (Gray and McCaffrey, 2002). Then, there is the occurrence of a phase separation of the coke formed. The coke separates from the liquid phase because it reaches a critical concentration. In addition, it is reported that the dominant factor for phase separation is increase of molecular weight due to oligomerization of olefins instead of aromaticity (Gray, 2010). The liquid product contains some asphaltenes that were not converted into coke. Asphaltenes are converted to coke only if they are aggregated and the asphaltenes present in the liquid product are those that were not aggregated (Wiehe, 1993).

The amount of coke and light gases formed during thermal cracking of bitumen influences the yield of liquid product that will be further refined into liquid fuels. It means that part of the initial bitumen is rejected in the form of coke and is not converted into liquid product (De Klerk *et al.*, 2014). Thus, different methods to decrease coke yield and increase the amount of liquid product are constantly studied. Coke can be supressed by the transfer of hydrogen to stabilize the free radicals, as coke formation involves a free radical chain mechanism. The most common method studied is performing thermal cracking of bitumen in the presence of a hydrogen donor solvent such as tetralin. The hydrogen donor solvent hydrogenates olefins which will consequently decrease addition reactions which will result in lower coke yield (Gray and McCaffrey, 2002). However, Zachariah *et al.* (2013) have demonstrated that coke yield can also be decreased when bitumen thermal cracking is performed in the presence of poor hydrogen donor solvents such as naphthalene. The explanation is that the solvent modifies physical structures of bitumen even at low concentration of solvent (10%). Nevertheless, as solvent concentration increases, the type of the solvent will determine if the coke suppression is dominated by hydrogen transfer. The addition of additives like poly(propylene oxide) to suppress aggregation of asphaltenes and increase liquid yield is another suggestion to decrease coke yield (Gray, 2010). Another factor that affects coke yield is the naturally present mineral solids in bitumen prevalent from mining extraction. In this case, the presence of mineral solids has a beneficial effect in decreasing coke yield as it was shown by Tanabe and Gray (1997). It is explained that the solids disperse the coke been formed which avoids its coalescence into larger materials that will not separate from the oil phase. Another factor that contributes to coke formation is the phase that thermal cracking occurs. Thermal cracking in liquid phase favours

coke formation. This is because in the liquid phase oligomerization of olefins and hydrogen abstraction are favoured over cracking by β-scission (Gray and McCaffrey, 2002). It should be pointed out that what is referred as oligomerization is in the context of coking, should rather be seen more broadly as any addition reactions, including free radical recombination and addition reactions. However, a recent study demonstrated that the light gases produced during thermal cracking can decrease coke yield in the liquid phase when bitumen is pyrolyzed at higher pressures in a batch reactor. The explanation for the decrease in coke yield at higher pressures is that the light gases formed during cracking dissolves in the liquid phase and they will transfer hydrogen and methyl groups to the free radicals which will consequently moderate pyrolysis and suppress coke formation by decreasing addition reaction (Zachariah *et al.*, 2013).

Prado and De Klerk (2014) (Chapter 3) have suggested that naturally occurring chloride salts in bitumen may have the potential of contribute to coke formation in bitumen upgrading. This observation has industrial application because if chloride salts have some influence in coke formation it will help to develop new studies to decrease coke yield and increase the yield of more valuable liquid products. Hypotheses of how chloride salts may help coke formation are presented as follows.

6.3 Hypotheses of Potential Role of Chloride Salts in Coke Formation

6.3.1 Aromatic and Aliphatic Compounds

As it was pointed out earlier, the chloride salts in bitumen hydrolyses at bitumen upgrading conditions. The products of the hydrolysis are HCl and metal hydroxides (Gray *et al*., 2008). Bond dissociation energy of HCl at 298 K is 103.15 kcal/mol (431 kJ/mol) (Blanksby and Ellison, 2003). This bond dissociation energy is less than that of H-CH_3 and slightly more than that of H-CH_2CH_3.

It is suggested that HCl may dissociate at bitumen upgrading conditions and form free radicals as illustrated in Figure 6.2. The radical chlorine may react with aromatic molecules in asphaltenes in two different ways (Figure 6.2). As illustrated in Figure 6.2 (Scheme A), chlorine radical can attack aromatic rings and the result is a halogenated aromatic compound (Hepworth et al., 2002;

De La Mare and Ridd, 1959). Chlorination of aromatic compounds by HCl via free radical mechanism as schematized in Figure 6.2 (Scheme A) could happen during bitumen upgrading and they could be part of the coke material. Free radical chlorine will more likely chlorinate the side chains of aromatic compounds (Figure 6.2-Scheme B). C-Cl bond has low bond dissociation energy (338 kJ/mol at 298 K) (Darwent, 1970) and this bond would not be stable during bitumen upgrading. Thus, chorine bonded to the side chains may be eliminated and form new free radicals such as compound (1) in Figure 6.2-Scheme B. The formation of free radicals results in a free radical chain mechanism where there is the occurrence of propagation. There are three events happening during propagation: hydrogen abstraction from other bitumen molecules that results in new free radicals, β-scission that results in olefin compounds, and polymerization of olefins (Gray and McCaffrey, 2002). Free radical chain mechanism is the basis of coke formation in bitumen upgrading and HCl formed during bitumen upgrading may contribute to the free radical chain mechanism by creating new free radicals. Elimination of chlorine in the side chains as hydrochloric acid, rather than free radical chlorine, may also result in olefinic compounds that can be further polymerized to form coke. In short, chlorine does not change the basic forming coke chemistry, but it has a "catalytic" effect by accelerating the formation of intermediates that lead to coke.

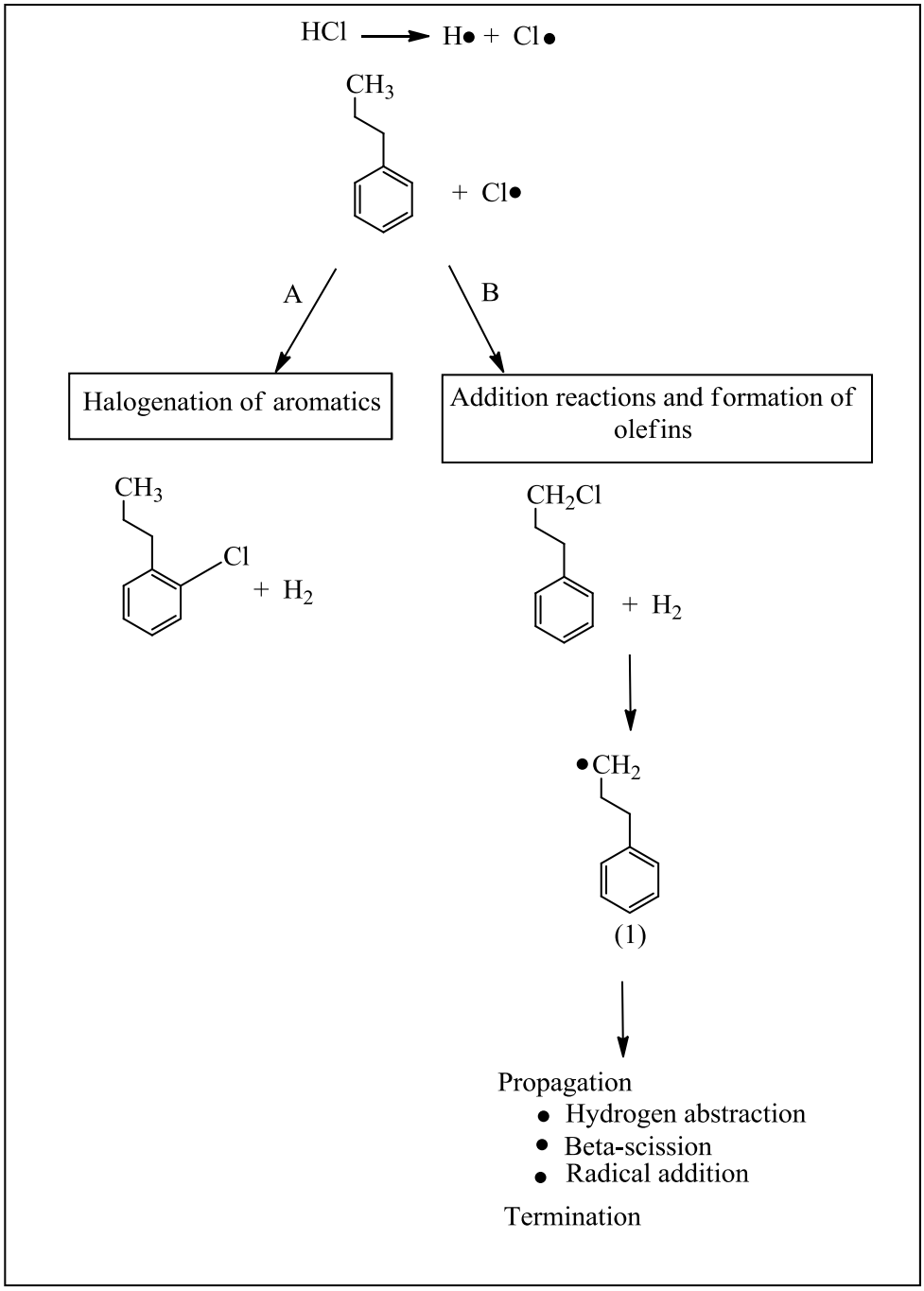

Figure 6.2. Hypothetical illustrative behaviour between aromatic compounds and HCl during bitumen upgrading due to homolytic attack by halogen free radicals

6.3.2 Olefinic Compounds

Chlorination of olefins with HCl is possible and it results in an addition product (elimination of the double bond). The addition of HCl in olefins will happen more readily for higher molecular weight olefins (Asinger, 1968). In addition, the reaction between hydrogen halides and olefins follows the Marknovnikov rule in which the halogen atom will attach to the carbon with fewest hydrogen atoms in the double bond through a carbocation intermediate formation. The addition of hydrogen halides such as HCl takes place better in the liquid phase and most readily to tertiary olefins (Asinger, 1968). However, at higher temperature under gas phase conditions, or any other conditions leading to free radical chemistry, the attack is by free radical substitution on a sp^3 carbon. As olefins and HCl are formed during bitumen upgrading, it may be possible that olefins may be hydrochlorinated by HCl as shown in Figure 6.3 (Scheme A).

During bitumen upgrading conditions, HCl can also act as protonic acid catalyst in Friedel-Crafts alkylation. In this case, the carbonium ion formed by the attack of HCl in the olefins will attack aromatic compounds as shown in Figure 6.3 (Scheme B). Friedel-Crafts alkylation between aromatic and olefins catalysed by HCl catalyst during bitumen upgrading as illustrated in Figure 6.3 (Scheme B) will result in compounds with higher molecular weight. Higher molecular weight compounds may contribute to the phase separation in coke formation during bitumen upgrading. Even though HCl is not usually considered as Friedel-Crafts alkylation catalyst, some studies have reported the success of Friedel-Crafts alkylation between aromatics and olefins at temperatures as high as 300 ºC (Patinkin and Friedman, 1964).

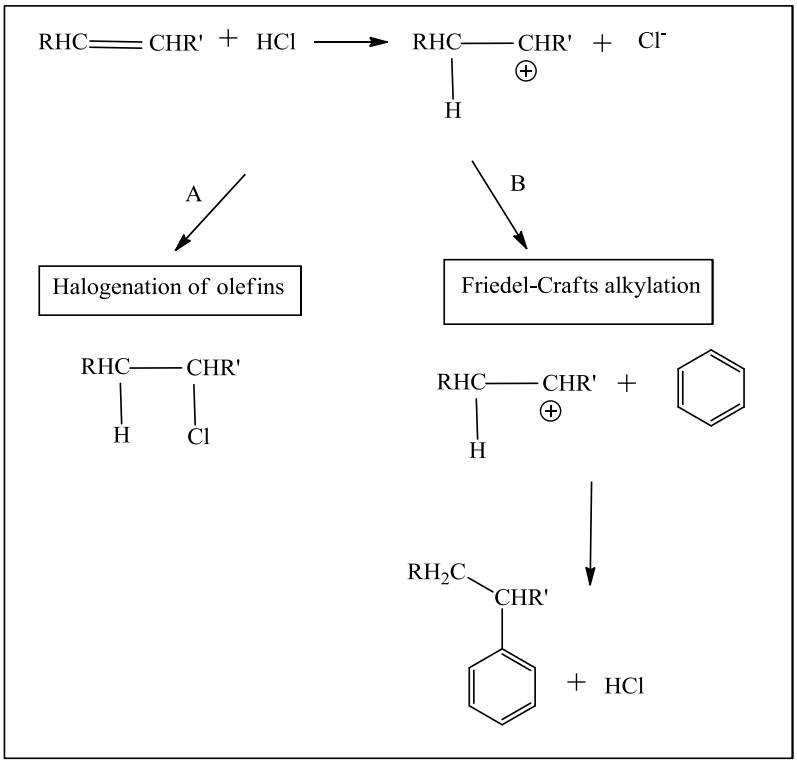

Figure 6.3. Hypothetical illustrative behaviour between olefinic compounds and HCl during bitumen upgrading (A) mainly in the liquid phase by heterolytic attack (B) mainly by HCl as a protonic acid

6.4 Implication of Halogenation Chemistry during Bitumen Upgrading

Prado and De Klerk (2014) (Chapter 3) and Moschopedis and Speight (1971) observed that halogenated asphaltenes were harder and insoluble in aromatic solvents, like coke. As halogenated asphaltenes were harder and insoluble in aromatic solvents and asphaltenes are coke precursor, it may be possible that halogenated molecules such as schematized in Figures 6.2 and 6.3 (Scheme A) may be part of the coke material that contributes to its insolubility in aromatic solvents. Moreover, the addition product of the reaction between HCl and olefins could also be part of the coke material by increasing its molecular weight and hardness and contributing to the phase separation during coking process.

6.5 Conclusions

Potential influence of chloride salts on coke formation during bitumen upgrading was presented. It was hypothesized that hydrochloric acid formed from hydrolysis of chloride salts during bitumen upgrading may accelerate coke formation in different ways:

a) HCl may form free radicals and halogenate aliphatic and aromatic compounds that do not contain alkyl groups. It is more likely that most free radical chlorine attack will be on the aliphatic groups in the asphaltenes.

b) The free radicals formed from HCl may participate in the free radical chain mechanism during coke formation if halogenation occurs in the side chains of aromatic compounds. The free radical chain mechanism provides compounds with higher molecular weight that contributes to the formation of coke.

c) Olefins formed during coking may be hydrohalogenated by HCl through the formation of a carbonium ion.

d) HCl may catalyze the Friedel-Crafts alkylation between aromatic compounds and olefins. In this case, there is the formation of compounds with higher molecular weight that contributes to coke formation.

e) Halogenation of molecules during coking process as well as Friedel-Crafts alkylation catalyzed by HCl may increase hardness and contribute to coke insolubility in aromatic solvents.

Literature Cited

Asinger, F. *Mono-olefins. Chemistry and technology*. Pergamon Press: Oxford. 1968, pp. 606-608, 722-723.

Blanksby, T. J. and Ellison, G. B. Bond dissociation energies of organic molecules. *Acc. Chem. Res*. **2003**, *36*, 255-263.

Darwent, De deB. Bond dissociation energy in simple molecules. National Standard Reference Data System. (Online) NRSDS-NBS 31: Washington, DC. 1970, p. 19. http://www.nist.gov/data/nsrds/NSRDS-NBS31.pdf. (Accessed October 30, 2014).

De Klerk, A.; Gray, M. R.; Zerpa, N. Unconventional oil and gas: Oilsands. In *Future energy. Improved, sustainable and clean options for our planet*, 2nd ed.; Letcher, T. M., Ed.; Elsevier: Amsterdam, 2014; pp. 109−110.

De La Mare, P. B. D. and Ridd, J. H. *Aromatic substitution: nitration and halogenation*. Butterworths Scientific Publications: London, 1959; pp. 5-25, 105-209.

Gray, M. R. and McCaffrey, W. C. Role of chain reactions and olefin formation in cracking, hydroconversion, and coking of petroleum and bitumen fractions. *Energy Fuels* **2002**, *16*, 756-766.

Gray, M. R.; Eaton, P. E.; Le, T. Kinetics of Hydrolysis of Chloride Salts in Model Crude Oil. *Petroleum Science and Technology* **2008**, *26*, 1924-1933.

Gray, M. R. *Fundamentals of oilsands upgrading*; Notes, University of Alberta: Edmonton, AB, 2010.

Hepworth, J. D.; Waring, D. R.; Waring, M. J. *Aromatic chemistry*. The Royal Society of Chemistry: Cambridge, 2002; pp. 1-37.

Moschopedis, S. E. and Speight, J. G. The Halogenation of Athabasca asphaltenes with elemental halogen. *Fuel* **1971**, *50*, 58-64.

Patinkin, S. H. and Friedman, B. S. Alkylation of aromatics with alkenes and alkanes. In *Friedel-Crafts and related reactions part I*, 1st ed.; Olah, G. A., Ed. John Wiley & Sons: New York, 1964, pp. 24-27.

Prado, G. H C. and De Klerk, A. Halogenation of oilsands bitumen, maltenes, and asphaltenes. *Energy Fuels* **2014**, *28*, 4458-4468.

Tanabe, K. and Gray, M. R. Role of fine solids in the coking of vacuum residues. *Energy & Fuels* **1997**, *11*, 1040-1043.

Wiehe, I. A. A phase-separation kinetic model for coke formation. *Ind. Eng. Chem. Res.* **1993**, *32*, 2447−2454.

Zachariah, A., Wang, L., Yang, S., Prasad, V., De Klerk, A. Suppression of coke formation during bitumen pyrolysis. *Energy & Fuels* **2013**, *27*, 3061-3070.

Chapter 7. Alkylation of Asphaltenes using a $FeCl_3$ Catalyst[19]

Abstract

Friedel-Crafts alkylation as strategy to convert asphaltenes to maltenes was investigated. It was postulated that alkylation of polar hydroxyl groups in the asphaltenes would make the alkylated product more soluble in light hydrocarbons. Alkylation was performed using $FeCl_3$ as catalyst and two different alkylation reagents were employed: *o*-xylene and methanol for C- and O-alkylation respectively. Oilsands bitumen derived materials were alkylated. Only the alkylation of asphaltenes with *o*-xylene was mildly beneficial; it resulted in 6 % conversion of asphaltenes to maltenes and an increase of 9 % in straight run distillate and vacuum gas oil. Alkylation of maltenes and bitumen were detrimental, as was alkylation of asphaltenes with methanol. To better understand the nature of the conversion the alkylation reactions were repeated with model compounds. With 2-naphthol it was found that dimerization of the 2-naphthol to produce (1,1'-binaphthalene)-2,2'-diol (BINOL), as well as the subsequent coordination with iron, were the two dominant reactions. The adverse consequences of $FeCl_3$ catalyzed alkylation could be explained by such intermolecular addition reactions. Methanol and $FeCl_3$ also caused some chlorination of the product. The possibility that alkylation with $FeCl_3$ affected ethers was explored by performing alkylation with dibenzyl ether. It was found that the ether bonds were cleaved. In the presence of *o*-xylene, ether cleavage was followed by C-alkylation. The increase in maltenes after alkylation of asphaltenes with *o*-xylene was better explained by C-alkylation following on ether cleavage than the alkylation of hydroxyl groups in the asphaltenes. Alkylation of dibenzyl ether with methanol produced benzaldehyde, rearrangement products and heavy gums.

Keywords: Friedel-Crafts Alkylation, Asphaltenes, Oilsands Bitumen, Iron Trichloride.

[19] Reprinted with permission from Prado, G. H. C. and De Klerk, A. Alkylation of asphaltenes using a $FeCl_3$ catalyst, *Energy & Fuels* 2015, DOI: 10.1021/acs.energyfuels.5b01292. Copyrigth 2015 American Chemical Society. http://pubs.acs.org/doi/abs/10.1021/acs.energyfuels.5b01292

7.1 Introduction

Upgrading of oilsands bitumen to lighter and less viscous oil is one of the strategies that are industrially employed to improve bitumen fluidity for pipeline transport to market. One of the more challenging fractions to deal with is the asphaltenes. The asphaltenes is a solubility class and Canadian oilsands derived bitumens have an *n*-pentane insoluble asphaltenes content in the range 14 to 20 wt % (Strausz and Lown, 2003). Asphaltenes can precipitate during storage, transport and processing of the bitumen, which is undesirable in most circumstances. The asphaltenes fraction can be separated from the bitumen by solvent deasphalting, but in the case of oilsands bitumen it results in a significant liquid yield loss.

Ideally one would like to modify the solubility of the material constituting the asphaltenes fraction so that the material is no longer prone to precipitation, and by definition the material is no longer asphaltenes.

It was postulated that by decorating asphaltenes with alkyl groups, the pentane-solubility of the alkylated material should be increased, i.e. alkylated asphaltenes will become maltenes. This postulate was based on two predictions. Firstly, the alkyl groups would decrease the forces of attraction between the asphaltenes molecules, making them more ease to disperse in the liquid. Secondly, the asphaltenes molecules will appear to be more aliphatic in nature, making them more compatible with light aliphatic hydrocarbons.

These qualitative statements can also be related to the quantitative description of asphaltenes solubility. The solubility of asphaltenes in any liquid is related to the absolute difference in solubility parameters between that of the asphaltenes and the liquid ($|\Delta\delta|$) (Wiehe, 2008). The decrease in forces of attraction will lower the enthalpy of vaporization (ΔH_{vap}) and increase molar volume (V_m) of the alkylated molecules. This is not the only factor to account for, and size effects on the Gibbs Free energy decreases the $|\Delta\delta|$ range over which asphaltenes will become soluble in light hydrocarbons (Painter *et al*., 2015). As applied to the present study, alkylation should decrease the solubility parameter ($\delta^2 = \Delta H_{vap}/V_m$) of the asphaltenes, albeit with potential narrowing of the $|\Delta\delta|$ range for solubility. It was postulated that the net decrease

in the absolute difference between the solubility parameter of the alkylated asphaltenes and that of a light hydrocarbon solvent would be sufficiently to increase its solubility in light hydrocarbons with low solubility parameter.

Alkylation has been used with success to improve the dissolution of coal (Painter *et al*., 2015; Sternberg and Delle Donne, 1974; Schlosberg *et al*., 1980; Miyake and Stock, 1988; Baldwin *et al*., 1981). The objective of the coal alkylation was not to improve pentane-solubility, but it indicated that Friedel-Crafts alkylation could potentially be a useful strategy. Although alkylation has never been industrially applied for the upgrading of asphaltenes (Sasaki *et al*., 2000), there are some studies that applied alkylation as method to elucidate the molecular structure of asphaltenes, as well as method to increase the solubility of asphaltenes (Gray, 2015, Ignasiak *et al*., 1981; Siddiqui, 2003; Wachowska *et al*., 1986; Ignasiak *et al*., 1977; Acevedo *et al*., 1998).

The work conducted by Ignasiak *et al*. (1981) had the aim to understand the chemical changes in asphaltenes structure resulting from the use of different catalysts ($AlCl_3$ and $ZnCl_2$), solvents, temperatures, and pressures. Solubility was affected by temperature depending on the catalyst used. For example, higher solubility was achieved for an $AlCl_3$ catalyst at lower temperatures while solubility was increased at higher temperatures when $ZnCl_2$ was used as catalyst. Although it was not their specific objective to perform alkylation, the results were explained in terms of intermolecular Friedel-Crafts alkylation.

Sidiqqui (2003) performed alkylation of Arabian asphaltenes using $AlCl_3$ as catalyst and 1-chlorobutane as alkylating agent. This type of alkylation reaction had the objective of adding paraffinic side chains to the asphaltenes. Carbon-13 nuclear magnetic resonance spectrometry confirmed that paraffinic side chains were successfully added to the asphaltenes, as the paraffinic:aromatic ratio increased after reaction. In addition, thermogravimetric analysis showed that decomposition started below 360 °C for the alkylated asphaltenes, whereas decomposition of the raw asphaltenes commenced only at temperatures higher than 360 °C. It was claimed the decrease in onset of decomposition was due to dealkylation reactions, which

suggested that asphaltenes did not have alkyl groups of sufficient length to be susceptible to thermal dealkylation.

Liquid ammonia was used in the non-reductive alkylation of Athabasca asphaltenes (Wachowska *et al*., 1986). The extent of ethyl addition to the asphaltenes with this procedure was insignificant. The heteroatom content and extractability remained unchanged after the reaction. However, the apparent molecular weight of asphaltenes decreased slightly after alkylation treatment, which was attributed to the disruption of molecular interactions of hydroxyl groups.

A number of researchers performed reductive alkylation (Wachowska *et al*., 1986; Ignasiak *et al*., 1977; Acevedo *et al*., 1998), by applying the coal work of Sternberg (1974) to asphaltenes. It should be pointed out that this type of alkylation chemistry proceeds via a carbanion intermediate and it might lead to aromatic saturation, ring-opening and alkylation. Reductive alkylation could lead to the cleavage of C–O and C–S bonds, which was a specific objective in some work (Wachowska *et al*., 1986; Ignasiak *et al*., 1977), and an explanation for the increased light hydrocarbon solubility of treated asphaltenes in other work (Acevedo *et al*., 1998). Reductive alkylation is not the type of chemistry that is considered here.

The present investigation is focused on Canadian oilsands bitumen derived asphaltenes. The effect of Friedel-Crafts alkylation on carbon (C-alkylation) and alkylation on oxygen (O-alkylation) of asphaltenes were investigated. In both instances the alkylation targeted hydroxyl functionality, which could be responsible for hydrogen bonding and was present at near percentage level in oilsands asphaltenes (Cagniant et al., 2001; Moschopedis and Speight, 1976). Thiols are capable of the same type of alkylation chemistry, but hydrogen bonding due to thiols is negligible (Desando and Ripmeester, 2002). Thiols increase the solubility parameter somewhat, but not nearly to the same extent as alcohols. For example, the solubility parameters for *n*-hexane, 1-hexanol and 1-hexanthiol are 14.98, 21.49 and 17.54 $MPa^{½}$ respectively (Crampton, 1974).

From an application point of view the extent of asphaltenes to maltenes conversion was of interest, as well as the impact of alkylation on subsequent thermal conversion. Thermal

conversion is industrially a likely upgrading pathway for the maltenes, which would include the asphaltenes that were converted to maltenes by alkylation. During thermal conversion some dealkylation might take place, undermining the potentially beneficial impact of alkylation. The study was also extended to the maltenes fraction and the total bitumen feed to determine whether alkylation is generally beneficial, particularly with subsequent thermal conversion in mind. The interpretation of the observations was also supported by selected model compound reactions to probe specific aspects of the observed alkylation behavior of the oilsands derived materials.

7.2 Experimental

7.2.1 Materials

Athabasca oilsands bitumen from Syncrude Canada was employed in this study. The bitumen and the asphaltenes and maltenes fractions were prepared from the bitumen by *n*-pentane precipitation. The procedure and characterization was previously reported in Chapter 3 and pertinent characterization data is repeated for ease of reference (Table 7.1). The chemicals and cylinder gases employed in the investigation were commercially obtained and used without further purification (Table 7.2).

Table 7.1. Characterization of Athabasca asphaltenes from precipitation with *n*-pentane, maltenes and total bitumen[a]

Description	Asphaltenes		Maltenes		Bitumen	
	x	s	x	s	x	s
Fraction of bitumen (wt %)	18.45	0.95	81.55	0.96	100	-
Elemental analysis (wt %)						
Carbon	77.62	0.18	83.08	0.05	83.54	0.08
Hydrogen	7.61	0.01	10.71	0.02	10.11	0.02
Nitrogen	1.18	0.04	0.31	0.02	0.47	0.01
Sulfur	8.07	0.02	3.98	0.01	5.16	0.05
Oxygen (by difference)	5.52	0.14	1.90	0.05	0.71	0.05
Mineral matter content (wt %)	4.01	0.10	- [b]	-	1.03	0.10
H:C molar ratio	1.17	-	1.54	-	1.44	-

[a] Average (x) and sample standard deviation (s) of three experiments are reported.
[b] None detected.

Table 7.2. Chemicals and cylinder gases employed

Compound	Formula	CASRN [a]	Mass fraction purity [b]	Supplier
Chemicals				
pentane	C_5H_{12}	109-66-0	≥ 0.98	Fisher Scientific
2-naphthol	$C_{10}H_8O$	135-19-3	0.99	Acros Organics
dibenzyl ether	$C_{14}H_{14}O$	103-50-4	> 0.98	Sigma-Aldrich
o-xylene	C_8H_{10}	95-47-6	> 0.95	Fisher Scientific
iron (III) chloride	$FeCl_3$	7705-08-0	0.97	Sigma-Aldrich
chloroform	$CHCl_3$	67-66-3	0.99	Sigma-Aldrich
methanol	CH_4O	67-56-1	> 0.998	Fisher Scientific
dichloromethane	CH_2Cl_2	75-09-2	> 0.999	Fisher Scientific
Cylinder gases				
nitrogen	N_2	7727-37-9	0.99999[c]	Praxair
air	O_2/N_2 mix	132259-10-0	-	Praxair
helium	H_2	7440-59-7	0.99999[c]	Praxair
Calibration substances				
indium	In	7440-74-6	0.99999	Impag AG
zinc	Zn	7440-66-6	0.99999	Impag AG

[a] CASRN = Chemical Abstracts Services Registry Number.
[b] This is the purity of the material guaranteed by the supplier; material was not further purified.
[c] Mole fraction purity.

7.2.2 Equipment and Procedure for Alkylation

The C-alkylation reaction of bitumen, maltenes, and asphaltenes were performed following the procedure described by Iovel *et al*.(2005) with minor modifications due to the raw materials as indicated. In each experiment, 5 g of feed material (bitumen, maltenes or asphaltenes), 0.5 mmol of $FeCl_3$ catalyst, and 50 mL of *o*-xylene were added to a 200 mL flask. The generic reaction for C-alkylation with *o*-xylene is shown in Figure 7.1a. The solution was stirred under reflux at 80 °C for 24 hours. After the reaction time was completed the solution was quenched with demineralized water (30 mL) and the layers were separated. The solvent was distilled off using a rotary evaporator at 50 °C operated under vacuum. The products were left in the fume hood at 40 °C to evaporate the remaining solvent until constant mass was reached.

The same procedure was employed for C-alkylation of 2-naphthol with *o*-xylene and for C-alkylation of dibenzyl ether with *o*-xylene. The amounts of materials employed were ~2 g of the substrate (2-naphthol or dibenzyl ether), 150 mL *o*-xylene and ~0.24 g of $FeCl_3$ as catalyst.

The O-alkylation reaction of asphaltenes was performed using the procedure described by Cazorla *et al*. (2011) with some modifications as indicated. First, a mixture of 5 g of asphaltenes, 5 g of $FeCl_3$ catalyst and 80 mL methanol was prepared. The generic reaction for O-alkylation with methanol is shown in Figure 7.1b. The solution was stirred at 80 °C for 24 hours under reflux. After completion of the reaction time, the solution was filtered under vacuum and the filtrate was rinsed with demineralized water to remove some remaining catalyst.

An analogous procedure was employed for O-alkylation of 2-naphthol and dibenzyl ether with methanol. The procedure consisted in mixing ~2 g of the substrate with 2 g of $FeCl_3$ catalyst and 35 mL of methanol. The solution was stirred at 80 °C for 24 h under reflux. Then, 50 mL of demineralized water and 40 mL of chloroform was added to the solution. The layers were separated with a funnel separator and chloroform was evaporated in a rotary evaporator at 50 °C under vacuum. The samples were left in the fume hood for complete evaporation of the solvent.

Blank reactions with the oilsands derived materials were also performed using exactly the same C- and O-alkylation procedures, but omitting the $FeCl_3$ catalyst.

The products from the reactions were subjected to different analyses as described in the next sub-section. All experiments were performed and analyzed in triplicate unless otherwise noted.

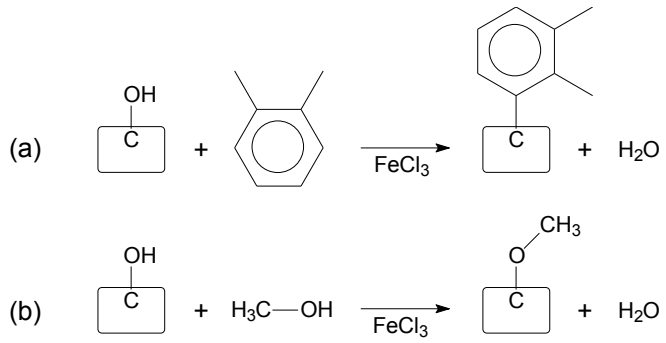

Figure 7.1. Generic reactions of substrate hydroxyl groups by (a) C-alkylation with *o*-xylene and (b) O-alkylation with methanol. Analogous reactions take place with thiols as substrate groups

7.2.3 Analyses

FTIR was performed as in Chapter 3.

The asphaltenes content of the products were determined by mixing 1 g of alkylated products with 40 mL of *n*-pentane. The mixture was stirred for 1 h and the sample was left in contact with the *n*-pentane for 24 h before being filtered. The solution was filtered under vacuum in a 0.22 μm Millipore membrane filter, with the asphaltenes collected on the filter.

TGA analysis was performed as in Chapter 3 and following the method of Juyal *et al.* (2013) with modifications.

GC-MS spectometry was used to identify the products formed after model compound alkylation reactions. The samples were diluted in dichloromethane to a concentration of 0.7 to 1 mg/mL. The carrier gas was helium and the flow rate was 20 mL/min. The samples (1 μL) were injected in a split mode (1:10) at 280 ºC. The temperature program for 2-naphthol reactions: Start temperature program was 40 ºC for 0.5 min, then heating to 100 ºC at 40 ºC/min and held for 0.5 min, followed by heating to 120 ºC at 2 ºC/min and another heating to 320 ºC at 20 ºC/min, then held at 320 ºC for 3 min. The temperature program for dibenzyl ether reactions: Start temperature at 90 ºC for 2 min followed by a heating to 320 ºC at 5 ºC/min and held at 320 ºC for 1 minute. MS parameters consisted of 4 min of solvent delay, quadrupole temperature of 150 ºC and source temperature of 230 ºC. The instrument used was described in Chapter 4.

7.3 Results and Discussion

7.3.1 C-Alkylation of Asphaltenes, Maltenes and Bitumen

The alkylation of the oilsands-derived materials with *o*-xylene predictably resulted in an increase in the mass of the products (Table 7.3) after the unconverted *o*-xylene was removed. It was known from past experience with light aromatics that it is very difficult to remove all of the aromatics from oilsands materials, even by prolonged heating under reduced pressure. The series of blank experiments confirmed that some *o*-xylene was retained in the product (Table 7.3).

Table 7.3. Mass increase due to C-alkylation with *o*-xylene

Description	Mass increase after reaction (wt %) [a]					
	Asphaltenes [b]		Maltenes		Bitumen	
	x	s	x	s	x	s
C-alkylation reaction	4.9	4.0	9.8	4.1	15.0	5.3
Blank (no catalyst)	3.7	1.8	3.9	2.6	2.7	1.0
Mass increase due to alkylation [c]	1.2	-	5.9	-	12.3	-

[a] Average (x) and sample standard deviation (s) from experiments performed in triplicate.
[b] Experiments performed six times, not just triplicate.
[c] Calculated by subtracting *o*-xylene retention (from blank) from the alkylation reactions.

The asphaltenes fraction resulted in the least incorporation of *o*-xylene, whereas the bitumen had the most. On first glance it suggested that the asphaltenes contained the least amount of alcohol and thiol groups that could be removed by aromatic alkylation. Such an interpretation was problematic, even though asphaltenes are more aromatic and the heteroatoms are more likely to be found in heterocyclic compounds. It did not explain why the bitumen, rather than the maltenes, resulted in the highest incorporation of *o*-xylene by alkylation.

A more plausible interpretation, albeit still speculative, is that the functional groups that would be susceptible to C-alkylation are indeed concentrated in the asphaltenes fraction, but that these functional groups are sterically protected when the asphaltenes are precipitated. When the asphaltenes fraction is not precipitated, the conformation of the molecules is more open and accessible to reagents. To use an analogy: The asphaltenes are like proteins in albumin of egg

white, which does not change chemical composition when they are denatured by heating, but the change in conformation of the denatured proteins result in very different physical properties of raw and cooked egg white.

If alkylation extent was purely determined by chemical composition, the bitumen alkylation extent should have been equal to the weighted sum of the alkylation extents of the asphaltenes and the maltenes fractions. This was not the case. The alkylation extent of bitumen, 12.3 %, by far exceeded the weighted average of the alkylation extent of its sub-fractions, 5.0 % (Table 7.3). This added credence to an interpretation based on a conformation change, rather than a chemical change. It is postulated that solvent deasphalting introduced conformational changes in the sub-fractions that protected the molecules against C-alkylation with *o*-xylene.

In order to confirm that alkylation took place, the feed materials and products were analyzed by infrared spectroscopy. Infrared spectroscopy is a sensitive technique for detecting changes in alcohol groups by looking at the O–H absorptions in the 3700 to 3300 cm^{-1} region (Siggia *et al*., 1971). Alkylation did not result in observable changes in the infrared spectrum of the alcohol groups, but in general the absorptions in this spectral region were not pronounced. Infrared spectroscopy is also sensitive for changes in phenolic C–O absorptions around 1260 to 1180 cm^{-1} region and aliphatic alcohol C–O absorptions in the 1075 to 1000 cm^{-1} region (Siggia *et al*., 1971; Colthup *et al.*, 1990). The near disappearance of the C–O absorptions associated with phenolic groups in 1240-1200 cm^{-1} region was evident (Figure 7.2).

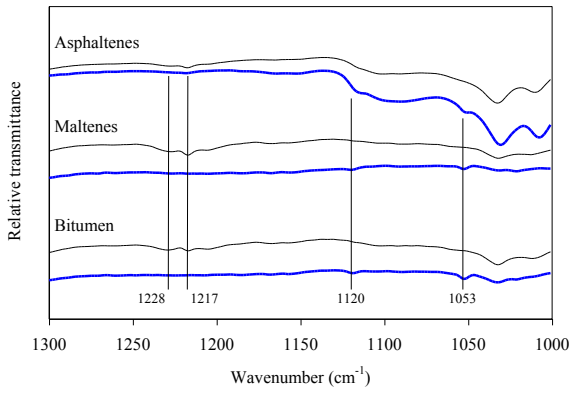

Figure 7.2. The C–O absorption region between 1300 and 1000 cm^{-1} in the infrared spectra of the feed materials (light line) and C-alkylated products (heavy line)

The appearance of new substituted benzene absorptions in the 1150 to 1100 cm^{-1} region (Figure 7.2) of the infrared spectrum after alkylation was not surprising, because *o*-xylene was incorporated in the product. The prominent absorptions at 1120 and 1053 cm^{-1} were indicative of *o*-xylene (Silverstein and Webster, 1997) which was trapped in the product (Table 7.3).

The S–H absorptions in the 2600 to 2550 cm^{-1} region are weak (Fontana and Toniolo, 1974). In practice it was found that absorptions of the thiol groups were too weak to clearly observe in the feed materials and hence alkylation by thiol elimination was not confirmed using infrared spectrometry.

7.3.1.1 Impact of C-Alkylation on Asphaltenes Content

The objective of the investigation was to disrupt hydrogen bonding and thereby convert at least some asphaltenes to maltenes. The change in asphaltenes content of the C-alkylated asphaltenes, maltenes and bitumen was determined by precipitation with *n*-pentane (Table 7.4).

Table 7.4. Change in asphaltenes content due to C-alkylation with *o*-xylene

Description	Asphaltenes content (wt %) [a]					
	Asphaltenes		Maltenes		Bitumen	
	x	s	x	s	x	s
Feed material	94.8	0.7	0	-	18.5	1.0
C-alkylated product	84.6	6.8	12.1	0.6	28.5	0.3
Absolute change [b]	-6.1	-	13.3	-	14.3	-

[a] Average (x) and sample standard deviation (s) from experiments performed in triplicate.
[b] Calculated by the difference between the asphaltenes in the feed and product and correcting for the mass change in the alkylated product.

The asphaltenes content of the asphaltenes fraction was not 100 %. The asphaltenes fraction, despite being obtained from by rigorous *n*-pentane precipitation from the bitumen, contained 5.2 ± 0.7 % material that could be redissolved in *n*-pentane. C-alkylation was nevertheless successful in converting an additional 6 % asphaltenes into *n*-pentane soluble material. This calculation assumed that none of the added *o*-xylene, either as trapped, or bonded to the asphaltenes molecules, formed part of the experimentally determined asphaltenes content after

C-alkylation. It is of course possible that some C-alkylated asphaltenes remained asphaltenes, in which case a higher percentage of the asphaltenes were converted to maltenes and some *o*-xylene was retained by the asphaltenes fraction.

The C-alkylation of bitumen and the maltenes fraction was detrimental. In both instances C-alkylation caused an increase in the asphaltenes content. The calculated difference accounting for *o*-xylene alkylation was 13 to 14 % absolute. One possible explanation is related to the change in the solubility parameter. The solubility parameter of *o*-xylene is 18.41 $MPa^{½}$, and the reported experimentally determined solubility parameter of Athabasca bitumen is 18.25 $MPa^{½}$ (Gray, 2015). Although alkylation with *o*-xylene could directionally increase the solubility parameter, spectroscopic evidence was provided that indicated part removal of phenolic functionality, which would decrease the solubility parameter. Even if the removal of phenolic groups are discounted, the extent of alkylation in bitumen was of the order 12 % (Table 7.3), which would result in only a marginal (~0.02 $MPa^{½}$) increase in solubility parameter. It is doubtful that such a minor change in solubility parameter would cause the observed change in asphaltenes content in the bitumen from 18.5 to 28.5 % (Table 7.4). The same holds true for the maltenes.

A more plausible explanation for the increase in asphaltenes content of C-alkylated bitumen and maltenes is the impact of increased molecular mass on ΔG_{mix}, the Gibbs free energy of mixing. As the size of the molecules increase, the enthalpy of mixing (ΔH_{mix}) will increase. If the increase in ΔH_{mix} more than offsets the increased entropy of mixing contribution ($T \cdot \Delta S_{mix}$), then a point may be reached where ΔG_{mix} becomes positive, or where the Gibbs free energy of two separate phases is less than the Gibbs free energy of the mixture. In either case this will lead to the precipitation of asphaltenes as a separate phase. Alkylation increased the molecular mass of the alkylated compounds, but alkylation may also have been accompanied by side-reactions. Considering that the asphaltenes content of the bitumen almost doubled, it seemed unlikely that this was due just to the addition of *o*-xylene.

The catalyst may also have catalyzed intermolecular alkylation of the bitumen. Analysis of the product by SEM-EDX indicated that the C-alkylation product of the asphaltenes contained some

residual Fe and Cl, i.e. residual catalyst. Possible side-reactions were investigated using model compounds as described later.

7.3.1.2 Thermal Conversion of C-Alkylated Products

How does aromatic C-alkylation affect the product distribution during thermal conversion? This is a question with practical value for upgraders and refiners. The product was alkylated to convert asphaltenes to maltenes, but the value of such a transformation becomes questionable if the product is more difficult to upgrade.

A common upgrading strategy for heavy oils and bitumens with high metal content is thermal conversion (Rana *et al*., 2007). Thermal upgrading is prevalent in all oilsands bitumen upgraders (Gray, 2015). The change in product distribution during thermal conversion was determined by mimicking recovery of straight run products by distillation followed by residue conversion by a delayed coking process using thermogravimetric analysis (Table 7.5).

Table 7.5. Feed analysis and product yields after *o*-xylene alkylation by TGA that mimicked straight run distillation followed by delayed coking of the vacuum residue fraction

Material	Straight run products (wt %) [a]			Coking products (wt %) [a]	
	naphtha (IBP-177 °C)	distillate (177-343 °C)	vacuum gas oil (343-525 °C)	pyrolysis gas and liquid	coke [b]
Asphaltenes					
raw material feed	0.5 ± 0.3	0.5 ± 0.5	2.1 ± 0.3	51.6 ± 0.8	45.3 ± 0.5
C-alkylated product	0.6 ± 0.2	5.5 ± 3.3	5.8 ± 2.8	45.3 ± 3.1	42.8 ± 0.2
blank run (no catalyst) [c]	0.1 ± 0.2	2.3 ± 0.7	2.5 ± 0.4	51.4 ± 0.5	43.7 ± 0.7
Maltenes					
raw material feed	0.6 ± 0.2	10.4 ± 0.7	49.4 ± 0.3	33.1 ± 1.3	6.5 ± 1.3
C-alkylated product	0.6 ± 0.2	8.9 ± 1.8	46.9 ± 1.3	33.1 ± 0.9	10.5 ± 0.5
blank run (no catalyst) [c]	0.3 ± 0.3	13.4 ± 1.4	45.9 ± 2.1	33.0 ± 1.6	7.4 ± 1.9
Bitumen					
raw material feed	0.2 ± 0.3	5.6 ± 1.4	41.4 ± 2.6	41.2 ± 1.2	11.6 ± 1.5
C-alkylated product	1.1 ± 0.0	11.4 ± 0.6	32.9 ± 0.9	35.5 ± 0.9	19.1 ± 0.1
blank run (no catalyst) [c]	0.2 ± 0.3	8.4 ± 0.7	37.6 ± 0.4	40.9 ± 0.8	12.9 ± 0.9

[a] Values reported as x ± s, which are the averages (x) and sample standard deviations (s) from experiments performed in triplicate.
[b] Microcarbon residue (MCR) value.
[c] Not corrected for 3-4 % trapped *o*-xylene in the blank run product.

The benefit of C-alkylation was that it eliminated heteroatoms during the reaction (Figure 7.1), and in the case of asphaltenes it introduced an alkylating agent, *o*-xylene, into the product with a higher hydrogen-to-carbon ratio than the asphaltenes, i.e. 1.25 versus 1.17 (Table 7.1). The MCR coke yield of the C-alkylated asphaltenes was lower than that of the asphaltenes, which could partly be ascribed to the slightly higher hydrogen-to-carbon ratio of the product, but mainly due to the beneficial change to the asphaltenes caused by the alkylation, which made it less prone to coking.

The detrimental impact of performing the alkylation on the maltenes fraction of the bitumen and maltenes could be seen from the increased MCR coke yield (Table 7.5). The hydrogen-to-carbon ratio of *o*-xylene was lower than that of the maltenes and bitumen, 1.25 versus 1.54 and 1.44. Blank runs with only *o*-xylene and no catalyst resulted in a slightly higher MCR coke yield, but the increase was not statistically meaningful.

A final observation is that *o*-xylene trapped in the products is tightly held. This was apparent not only from the inability to remove it by heating under vacuum, but also from the straight run distillation profile (Table 7.5). The *o*-xylene did not distill in the naphtha boiling range, despite having a normal boiling point of 144 °C (Hawley, 1971).

7.3.2 Alkylation of Asphaltenes with Methanol

The C-alkylation experiments showed that alkylation was potentially beneficial, but only for the conversion of asphaltenes. The alkylation with methanol was therefore performed just on the asphaltenes fraction of the bitumen and not on the total bitumen and maltenes fraction. The outcome of the alkylation is presented in Table 7.6, as well as the results of the blank run with asphaltenes and methanol, but no catalyst.

The blank run showed no mass increase. No methanol was trapped by the asphaltenes, as was the case with *o*-xylene.

Table 7.6. Mass increase and change in asphaltenes content due to asphaltenes alkylation with methanol

Description	Mass increase after reaction (wt %) [a]		Asphaltenes content (wt %) [a]	
	x	s	x	s
O-Alkylation reaction	4.2	0.7	95.3	1.0
Blank (no catalyst)	–0.8	2.0	- [b]	- [b]
Mass increase due to O-alkylation	5.0	-	-	-
Absolute change in asphaltenes [c]	-	-	–0.3	-

[a] Average (x) and sample standard deviation (s) from experiments performed in triplicate.
[b] Not performed.
[c] Calculated by the difference between the asphaltenes in the feed and product and correcting for the mass change in the alkylated product.

Alkylation with methanol using $FeCl_3$ as catalyst resulted in a 4.2 % mass increase. Despite the successful alkylation, the asphaltenes content was not meaningfully changed. The reason for the negligible change in asphaltenes content became apparent when the product was analyzed by infrared spectroscopy. Aliphatic and cyclic ethers have a strong C–O–C asymetric stretching band in the region 1250 to 1060 cm^{-1}, which occurs in the region 1270 to 1200 cm^{-1} for aryl alkyl

ethers (Fritz, 1967). There was no evidence that O-alkylation took place. The spectral region between 1300 and 1000 cm^{-1} of the asphaltenes feed and alkylated asphaltenes were almost identical.

The methanol was likely subjected to C-alkylation with the aromatics in the asphaltenes. Thus, the aromatics were methylated and not etherified. The solubility parameter of the methylated asphaltenes would be lower compared to that of the asphaltenes feed, but not by much. For example, the solubility parameters of benzene, toluene and *p*-xylene are 18.74, 18.26 and 18.06 $MPa^{½}$ respectively (Wiehe, 2008). The negligible decrease in the asphaltenes content (Table 7.6) is therefore understandable.

Methylation should have increased the hydrogen-to-carbon ratio of the asphaltenes, but it was found that the coking propensity of the alkylated product actually increased (Table 7.7). What was equally surprising was that the same happened to a lesser extent during the blank run with no catalyst. The methanol affected the asphaltenes in some way, but the reason for this is not clear. The MCR is affected by the hydrogen-to-carbon ratio, but it is not the only property affecting it. In an unrelated study using hydrotreated coal liquids (Rahman et al., 2015) it was found that thermal treatment at 350 °C reduced the MCR of the coal liquid despite a slight decrease in hydrogen-to-carbon ratio, but was not explained.

In the present work one additional factor that might contribute to the higher MCR of the methanol alkylated asphaltenes than the asphaltenes in the blank run is side-reactions catalyzed by the $FeCl_3$. Analysis of the alkylated asphaltenes by SEM-EDX indicated the presence of Fe and Cl, due to the presence of residual catalyst in the product.

Table 7.7. Product yield after asphaltenes reaction with methanol using TGA that mimicked straight run distillation followed by delayed coking of the vacuum residue fraction.

Material	Straight run products (wt %) [a]			Coking products (wt %) [a]	
	naphtha (IBP-177 °C)	distillate (177-343 °C)	vacuum gas oil (343-525 °C)	pyrolysis gas and liquid	coke [b]
Methanol alkylated product	0.1 ± 0.1	0.9 ± 0.2	3.2 ± 0.2	39.1 ± 10.2	56.7 ± 9.8
Blank run (no catalyst)	0.4 ± 0.1	1.0 ± 0.6	0.3 ± 0.3	49.8 ± 10.4	48.5 ± 7.0

[a] Values reported as x ± s, which are the averages (x) and sample standard deviations (s) from experiments performed in triplicate.
[b] Microcarbon residue (MCR) value.

7.3.3 Alkylation of 2-Naphthol

The applied investigation on the alkylation of bitumen and its sub-fractions was based on the hypotheses outlined in the Introduction. The outcome was less favorable than predicted, with an asphaltenes to maltenes conversion of < 10 % (Tables 7.4 and 7.6). Alkylation of bitumen and maltenes caused an increase in asphaltenes content; side-reactions leading to addition reactions between feed molecules were suspected. Possible side-reactions were investigated using model compounds to facilitate ease of analysis and interpretation of the results.

Model alkylation reactions were performed at the same conditions as with the oilsands materials, but using 2-naphthol as feed instead. In the reaction product of *o*-xylene and 2-naphthol no evidence was found that *o*-xylene alkylated with the 2-naphthol. This is because Friedel-Crafts alkylation of xylenes with phenols as electrophiles is not possible because phenols cannot readily form a carbocation. Only benzylic alcohols in asphaltenes and bitumen may react with *o*-xylene. Instead the 2-naphthol self-alkylated (dimerized) in the presence of $FeCl_3$ (Table 7.8), which is a well-known reaction (Kovacic, 1965). The dimerization of 2-naphthol produced (1,1'-binaphthalene)-2,2'-diol (BINOL). The stereoisomers were not resolved and the higher reported selectivity of the S-isomer during dimerization of 2-naphthol with $FeCl_3$ as catalyst (Brussee and Jansen, 1983) could not be confirmed. It was found a meaningful amount of a compound that was identified as iron-(1,1'-binaphthalene)-2,2'-diolate. This compound was identified from its electron impact mass spectrum based on the dominant m/z = 342 ion and quite similar fragmentation pattern to (1,1'-binaphthalene)-2,2'-diol at m/z < 286. The mass spectrometry for

iron-(1,1'-binaphthalene)-2,2'-diolate is discussed in the literature (Rochut *et al*., 2008), and its electron impact mass spectrum is given for reference (Figure 7.3).

Table 7.8. Products from 2-naphthol alkylation with *o*-xylene and methanol using $FeCl_3$ as catalyst

Product	Selectivity (%) [a]	
	with *o*-xylene	with methanol
methoxy-2-naphthalene	-	28
chloro-2-naphthol	- [b]	5
(1,1'-binaphthalene)-2,2'-diol	58	53
iron-(1,1'-binaphthalene)-2,2'-diolate	42	14

[a] Selectivity based on abundance during GC-MS analysis.
[b] Trace amount.

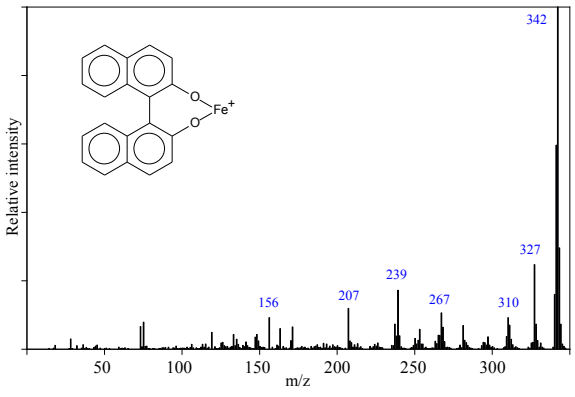

Figure 7.3. Electron impact mass spectrum of iron-(1,1'-binaphthalene)-2,2'-diolate

Self-alkylation also took place when methanol was reacted with 2-naphthol (Table 7.8), but some methoxy-2-naphthalene and a minor amount of chloro-2-naphthol was formed too. In this reaction some iron-(1,1'-binaphthalene)-2,2'-diolate was also formed, but to a lesser extent than in the presence of *o*-xylene.

The alkylation reactions with both *o*-xylene and methanol indicated that in a model reaction system dimerization was the major reaction. This confirmed the suspicion that $FeCl_3$ catalyzed alkylation, and possibly all metal halide catalyzed alkylation reactions employed in conjunction with asphaltenes are likely to lead to intermolecular addition reactions. Another concern was the evidence of halide substitution, which was previously also reported by Speight (1971).

Halogenation, even mild halogenation, can lead to hardening of the asphaltenes (Prado and De Klerk, 2014) (Chapter 3). Hardening in this context refers to a decrease penetration as measured by a penetrometer.

Yet, some benefit was found due to alkylation of asphaltenes with *o*-xylene (Table 7.4). Since the *o*-xylene apparently acted mainly as solvent, there must have been a different type of reaction that was beneficial. It was speculated that $FeCl_3$ might be responsible for ether bond scission, analogous to the isomerization of alkyl phenyl ethers to alkyl phenols (Johnson, 1965).

7.3.4 Alkylation of Dibenzyl Ether

Asphaltenes contain ethers and thioethers (sulfides) (Peng et al., 1997). Smaller fragments can be liberated by the scission of these bonds. If $FeCl_3$ was indeed capable of ether cleavage at the conditions employed for alkylation reactions, then this should also be evident from conversion with model compounds.

The possible scission of ether linkages was investigated by alkylation of dibenzyl ether with *o*-xylene and methanol respectively (Table 7.9). The alkylation with *o*-xylene resulted in almost complete elimination of the oxygen in the ether bond, with subsequent addition to *o*-xylene (Figure 7.4).

Table 7.9. Products from dibenzyl ether alkylation with *o*-xylene and methanol using $FeCl_3$ as catalyst

Product	Selectivity (%) [a]	
	with *o*-xylene	with methanol
benzaldehyde	-	73
methyl-ethyl-diphenyl (isomer 1)	1	-
methyl-ethyl-diphenyl (isomer 2)	99	9
unidentified [b]	-	6
$C_{14}H_{12}O$ (isomer 1)	-	2
$C_{14}H_{12}O$ (isomer 2)	-	3
$C_{14}H_{12}O$ (isomer 3)	-	1
Stilbene	-	1
$C_{14}H_{12}O$ (isomer 4)	-	5

[a] Selectivity based on abundance during GC-MS analysis.
[b] Suggestive of cycloalkane, with 55, 69, 83, 97, 111 m/z pattern.

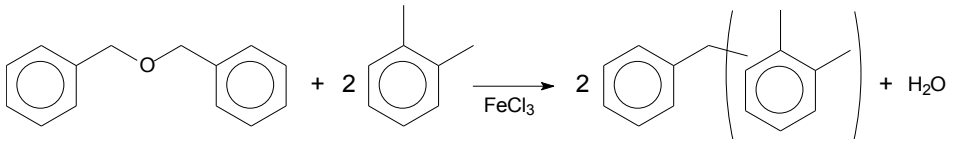

Figure 7.4. Alkylation reaction between *o*-xylene and dibenzyl ether catalyzed by $FeCl_3$ at 80 °C

It is likely that ether and thioether bonds in asphaltenes would have been cleaved in an analogous manner. In the presence of *o*-xylene, the *o*-xylene was alkylated. C-alkylation of *o*-xylene with the two asphaltene fragments that were linked though an ether bond, likely resulted in two less complex molecules than the original asphaltenes molecule. The conversion of asphaltenes into maltenes in this way, is a plausible explanation for the improvement observed during *o*-xylene alkylation (Table 7.4).

Alkylation with methanol did not convert the dibenzyl ether to the same extent, but benzaldehyde was the main product from ether scission (Table 7.9). It was suspected that with benzaldehyde in the product, much heavier materials (gums) would be formed too. Gums would not elute and be detected by gas chromatography. The gum content was therefore determined separately by TGA. It was found that 30.4 ± 1.7 wt % of the product remained as gums at 600 °C under N_2 atmosphere.

GC-MS revealed a number of rearrangement products with the molecular formula $C_{14}H_{12}O$ (Table 7.9). The first two rearrangement products were tentatively identified as 1,2-diphenylethanone and its enol tautomer. The next rearrangement product was tentatively identified as tricyclic compounds, the first possibly 5,7-dihydro-dibenz[c,e]oxepin. The structures of these $C_{14}H_{12}O$ rearrangement products are shown in Figure 7.5. Much of the rearrangement chemistry can be explained by $FeCl_3$ assisted decomposition of the dibenzyl ether, instead of alkylation with methanol. However, methanol must play a role as polar solvent in the stabilization of the intermediates, because these products were not observed during the same reaction with *o*-xylene.

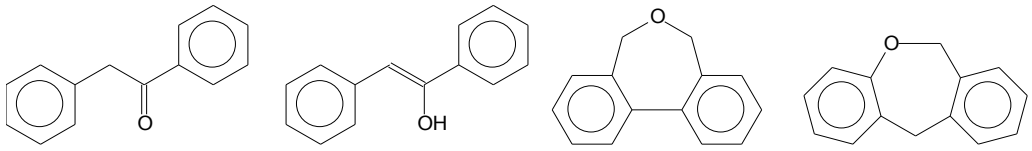

Figure 7.5. $C_{14}H_{12}O$ rearrangement products from dibenzyl ether conversion with $FeCl_3$ and methanol

7.3.5 Implications of the Alkylation Study

Iron chloride catalyzed alkylation was performed on oilsands bitumen derived materials, as well as model compounds. The focus was on alcohols and ethers due to their ease of detection by infrared spectroscopy, but the same chemistry applies to thiols (mercaptans) and thioethers (sulfides). The broader interpretation of the results to include both oxygen and sulfur species is suggested.

The alkylation with a mononuclear aromatic (*o*-xylene) was mildly beneficial only when applied to the asphaltenes fraction of oilsands bitumen. The work suggested that the benefit was derived from the alkylation of the fragments from the cleavage of ethers and thioethers, and not from the alkylation of alcohols and thiols. The detrimental influence of alkylation on bitumen and the maltenes fraction was due to the relatively higher contribution of side-reactions. Intermolecular addition was an important side-reaction.

The same reactions took place during alkylation with a short chain alcohol (methanol), but generally speaking this type of alkylation was detrimental. Evidence of O-alkylation was found only in model compound alkylation and methylation was the primary mode of methanol incorporation into asphaltenes. Side-reactions during $FeCl_3$ catalyzed alkylation with methanol was more varied and detrimental compared to those with *o*-xylene.

The use of $FeCl_3$ as catalyst is not practical, or beneficial for asphaltenes conversion. It was found that $FeCl_3$ not only performed acid catalysis, but also participated in reactions leading to chlorination of the products. Halogenation was found to be detrimental for oil production from asphaltenes (Prado and De Klerk, 2014) (Chapter 3). More importantly, the observations in this study highlighted a more general issue related to metal halides. The detrimental impact of metal

chlorides in oil due to corrosion and salt deposition in heat exchangers is well known (Gruse and Stevens, 1960; Nelson, 1949). The possible involvement of metal halides in conversion chemistry, including halogenation of the oil, is not well known. The extent of metal coordination, as was observed in the model compound alkylation, was also not fully appreciated before. It pointed to a simple non-porphyrin type coordination. These aspects are of potential significance to industrial operations with oilsands bitumen and other metal halide and multivalent metal containing oils.

7.4. Conclusions

It was postulated that some asphaltenes could be converted into maltenes by alkylation. Possible C- and O-alkylation over $FeCl_3$ was investigated using *o*-xylene and methanol as alkylating agents. The main conclusions from the experimental work were:

a) Alkylation of asphaltenes with *o*-xylene over $FeCl_3$ resulted in a minor mass increase due to *o*-xylene incorporation and a 6 % conversion of asphaltenes to maltenes after correcting for the added *o*-xylene. The straight run distillate and vacuum gas oil fractions obtained from the alkylated asphaltenes was 9 % more. Asphaltenes alkylation with *o*-xylene appeared mildly beneficial.

b) The observed mild benefit of asphaltenes alkylation with *o*-xylene could not be explained in terms of the anticipated C-alkylation reaction with alcohol groups. Although the phenolic C–O absorption in the infrared spectrum of the alkylated product was diminished, model conversion of 2-naphthol with *o*-xylene over $FeCl_3$ did not result in *o*-xylene alkylation as phenols cannot easily form a carbocation. However, some of the C–OH groups were converted to $C–O^-$ groups to form iron complexes.

c) The alkylation of bitumen and the maltenes fraction with *o*-xylene was detrimental. In both instances alkylation resulted in an increase in asphaltenes content. This is likely due to intermolecular addition reactions, which was confirmed by the model conversion of 2-naphthol.

d) Alkylation of asphaltenes with methanol over $FeCl_3$ resulted in little benefit, with almost no conversion of asphaltenes to maltenes. In fact, the coke yield of the alkylated asphaltenes was higher than that of the asphaltenes feed, making methanol alkylation detrimental.

e) No evidence of ether formation was seen in the infrared spectrum of the product after alkylation with methanol. The results suggested C-alkylation rather than O-alkylation, i.e. the asphaltenes were methylated. During model conversion of 2-naphthol with methanol over $FeCl_3$, methyl ethers were obtained, but side-reactions involving chlorination, dimerization, and metal coordination dominated the chemistry.

f) Model conversion of dibenzyl ether over $FeCl_3$ with *o*-xylene and methanol respectively demonstrated that ethers were cleaved during alkylation. Reaction with *o*-xylene resulted in C-alkylation of the product, which could explain the beneficial effect observed during *o*-xylene alkylation of asphaltenes. Reaction with methanol resulted in a more varied product, which included smaller molecules (benzaldehyde), rearrangement products and heavier meaningful (gum formation).

g) Iron chloride performed acid catalysis, but it also participated in reactions with the feed materials. Halogenation and metal coordination were meaningful side-reactions. Although the present study was limited to the use of $FeCl_3$, these reactions may be related to metal halides in general.

Literature Cited

Acevedo, S.; Escobar, G.; Ranaudo, M.A.; Rizzo, A. Molecular weight properties of asphaltenes calculated from GPC data for octylated asphaltenes. *Fuel* **1998**, *77*, 853-858.

Baldwin, R. M.; Kennar, D. R.; Nguanprasert, O.; Miller, R. L. Liquefaction reactivity enhancement of coal by mild alkylation and solvent swelling techniques. *Fuel* **1991**, *70*, 429-433.

Brussee, J.; Jansen, A. C. A. A highly stereoselective synthesis of S(–)-[1,1'-binaphthalene]-2,2'-diol. *Tetrahedron Lett.* **1983**, *24*, 3261-3262.

Cagniant, D.; Nosyrev, I.; Cebolla, V.; Vela, J.; Membrado, L.; Gruber, R. Structural modifications of petroleum asphaltenes by reductive alkylation investigated by TLC-FID. *Fuel* **2001**, *80*, 107-115.

Cazorla, C.; Pfordt, É.; Duclos, M. C.; Métay, E.; Lemaire, M. O-alkylation of phenol derivatives via a nucleophilic substitution. *Green Chem*. **2011**, *13*, 2482-2488.

Colthup, N. B.; Daly, L. H.; Wiberley, S. E. *Introduction to infrared and Raman spectroscopy*, 3ed; Academic Press: San Diego, CA, 1990.

Crampton, M. R. Acidity and hydrogen-bonding. In *The chemistry of the thiol group. Part 1*; Patai, S. Ed.; Interscience: London, 1974, pp. 379-415.

Desando, M. A.; Ripmeester, J. A. Chemical derivatization of Athabasca oil sand asphaltene for analysis of hydroxyl and carbonyl groups via nuclear magnetic resonance spectroscopy. *Fuel* **2002**, *81*, 1305-1319.

Fontana, A.; Toniolo, C. Detection and determination of thiols. In *The chemistry of the thiol group. Part 1*; Patai, S. Ed.; Interscience: London, 1974, pp. 271-324.

Fritz, J. S. Detection and estimation of ethers. In *The chemistry of the ether linkage*; Patai, S. Ed.; Interscience: London, 1967, pp. 669-680.

Gray, M. R. *Upgrading oilsands bitumen and heavy oil*; University of Alberta Press: Edmonton, AB, 2015.

Gruse, W. A.; Stevens, D. R. *Chemical technology of petroleum*, 3ed; McGraw-Hill: New York, 1960, pp. 10-12.

Ignasiak, T.; Bimer, J.; Samman, N.; Montgomery, D. S.; Strausz, O. P. Lewis acids assisted degradation of Athabasca asphaltene. *Adv. Chem. Ser.* **1981**, *195*, 183-201.

Ignasiak, T.; Kemp-Jones, A. V.; Strausz, O. P. The molecular structure of Athabasca asphaltene. Cleavage of the carbon-sulfur bonds by radical ion electron transfer reactions. *J. Org. Chem.* **1977**, *42*, 312-320.

Iovel, I.; Mertins, K.; Kischel, J.; Zapf, A.; Beller, M. An efficient and general iron-catalyzed arylation of benzyl alcohols and benzyl carboxylates. *Angew. Chem. Int. Ed.* **2005**, *44*, 3913-3917.

Johnson, F. Reactions of ethers and cyclic ethers. In *Friedel-Crafts and related reacions. Vol. IV*; Olah, G. A Ed.; Interscience: New York, 1965, pp. 1-109.

Juyal, P.; McKenna, A. M.; Fan, T.; Cao, T.; Rueda-Velásquez, R. I.; Fitzsimmons, J. E.; Yen, A.; Rodgers, R. P.; Wang, J.; Buckley, J. S.; Gray, M. R.; Allenson, S. J.; Creek, J. A joint industrial case study for asphaltene deposition. *Energy Fuels* **2013**, *27*, 1899-1908.

Kovacic, P. Reactions of aromatics with Lewis acid metal halides. In *Friedel-Crafts and related reacions. Vol. IV*; Olah, G. A Ed.; Interscience: New York, 1965, pp. 111-126.

Miyake, M.; Stock, L. M. Coal solubilization. Factors governing successful solubilization through C-alkylation. *Energy Fuels* **1988**, *2*, 815-818.

Moschopedis, S. E.; Speight, J. G. Oxygen functions in asphaltenes. *Fuel* **1976**, *55*, 334-336.

Nelson, W. L. *Petroleum refinery engineering*, 3ed; McGraw-Hill: New York, 1949, p. 100.

Painter, P.; Veytsman, B.; Youtcheff, J. Guide to asphaltene solubility. *Energy Fuels* **2015**, *29*, 2951-2961.

Peng, P.; Morales-Izquierdo, A.; Hogg, A.; Strausz, O. P. Molecular structure of Athabasca asphaltene: Sulfide, ether, and ester linkages. *Energy Fuels* **1997**, *11*, 1171-1187.

Prado, G. H C.; De Klerk, A. Halogenation of oilsands bitumen, maltenes, and asphaltenes. *Energy Fuels* **2014**, *28*, 4458-4468.

Rahman, M.; Adesanwo, T.; Gupta, R.; De Klerk, A. Effect of direct coal liquefaction conditions on coal liquid quality. *Energy Fuels 2015*, *29*, (in press, ef5b00566).

Rana, M. S.; Sámano, V.; Ancheyta, J.; Diaz, J. A. I. A review of recent advances on processing technologies for upgrading of heavy oils and residua. *Fuel* **2007**, *86*, 1216-1231.

Rochut, S.; Roithová, J.; Schröder, D.; Novara, F. R.; Schwarz, H. Gaseous iron(II) and iron(III) complexes with BINOLate ligands. *J. Am. Soc. Mass Spectrom.* **2008**, *19*, 121-125.

Sasaki, M.; Kotanigawa, T.; Yoshida, T. Liquefaction reactivity of methylated Illinois No.6 coal. *Energy Fuels* **2000**, *14*, 76-82.

Schlosberg, R. H.; Neavel, R. C.; Maa, P. S.; Gorbaty, M. L. Alkylation: a beneficial pretreatment for coal liquefaction. *Fuel* **1980**, *59*, 45-47.

Siddiqui, M. N. Alkylation and oxidation reactions of Arabian asphaltenes. *Fuel* **2003**, *82*, 1323-1329.

Siggia, S.; Hanna, J. G.; Stengle, T. R. Detection and determination of hydroxyl groups. In *The chemistry of the hydroxyl group. Part 1*; Patai, S. Ed.; Interscience: London, 1971, pp. 295-326.

Silverstein, R. M.; Webster, F. X. *Spectrometric identification of organic compounds*, 6ed; John Wiley & Sons: New York, 1997.

Speight, J. G. Reactions of Athabasca asphaltenes and heavy oil with metal chlorides. *Fuel* **1971**, *50*, 175-186.

Sternberg, H. W.; Delle Donne, C. L. Solubilization of coals by reductive alkylation. *Fuel* **1974**, *53*, 172-175.

Strausz, O. P.; Lown, E. M. *The chemistry of Alberta oilsands, bitumens and heavy oils*; Alberta Energy Research Institute: Calgary, AB, 2003.

Wachowska, H.; Ignasiak, T.; Strausz, O. P.; Carson, D.; Ignasiak, B. Application of non-reductive alkylation in liquid ammonia to studies on macromolecular structure of coals and bitumen-derived asphaltene. *Fuel* **1986**, *65*, 1081-1084.

Wiehe, I. A. *Process chemistry of petroleum macromolecules*; CRC Press: Boca Raton, FL, 2008.

Chapter 8. Metals Removal from Oilsands Bitumen and Subfractions by Acid Washing

Abstract

Multivalent metals in oilsands bitumen can be present in metal-bridged structures that keep smaller molecules together. Oilsands bitumen, maltenes and asphaltenes were treated with hydrochloric acid to remove metals from these materials and evaluate the hypothesis that metals removal would improve asphaltenes to maltenes conversion. Single step acid treatment was effective for metals removal, particularly from asphaltenes. About 2600 μg/g divalent metals could be removed from the asphaltenes by washing with a 1 N HCl solution in a 4:1 mass ratio with the asphaltenes. Acid washing also resulted in ester hydrolysis. Around 8 % asphaltenes were converted to maltenes by this procedure. Water and/or acid washing did not meaningfully remove V and Ni. Multivalent metals were present predominantly in the organic phase, not in the connate water, and were removed mainly by acid washing. Water washing was deleterious and promoted emulsion formation. It was proposed that a pH-sensitive change in the relative concentration of phenol- and phenoxide-groups to increase the concentration of hydrophilic phenoxide-groups was responsible for increased emulsion formation, and spectroscopic evidence in support of this was presented.

Keywords: Demetalation, Oilsands, Bitumen, Asphaltenes, Maltenes, Hydrochloric Acid

8.1 Introduction

Oilsands bitumen has high metals content, partly due to organically bound metals, and partly due to metals that are dissolved in connate water, which is associated with the oilsands material. Detailed analysis and quantification of the metals found in oilsands bitumen can be found in the literature (Jacobs and Filby, 1983; Strausz and Lown, 2003). The most abundant metals found in mineral-free bitumen were Al, Fe, K, Na, Ni, Ti, and V; Mg and Ca were not reported. It was pointed out that separation of mineral matter from the bitumen is challenging, with a high concentration of Al, Fe, K, and Ti in the associated mineral fines (Jacobs and Filby, 1983).

Metals can form bridging groups between different molecular species. Metal complexes of mixed donor atoms and same donor atoms have been proposed to explain non-porphyrinic metal coordination (Yen, 1975). Multivalent metals can also cause bridging between carboxylates (Van Bodegom *et al*., 1984; Joseph and Forrai, 1992; Li *et al*., 2015). These types of metal bridging are illustrated in Figure 8.1. The removal of bridging metals, or exchange of multivalent metals with monovalent ions, would decompose bridged structures into smaller molecular, or ionic fragments.

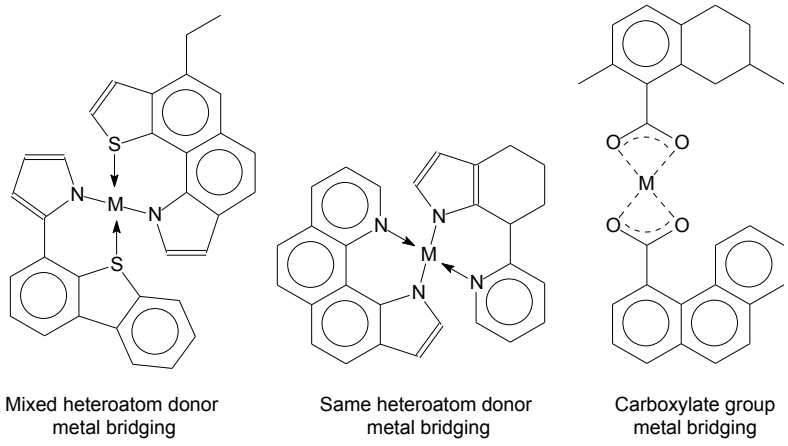

Figure 8.1. Metal bridging structures illustrated by arbitrary compounds

Disruption of metal bridged structures in oilsands derived materials was the target of this current study. The working hypothesis was that by treating bitumen and its subfractions (asphaltenes and maltenes) with aqueous hydrochloric acid, multivalent cations would be removed from the

bridged structures. By removing the metals and disrupting the bridging, it was anticipated that the treated product would contain an increased content of smaller molecules that were freed from the previously bridged structures. Of particular interest was the possibility to convert some asphaltenes into maltenes as part of an ongoing effort to find alternative conversion pathways to upgrade asphaltenes to higher valued products.

Acid treatment was previously investigated for metals removal from oils (Ali, 2006). However, the literature does not report any studies specifically focused on acid treatment of asphaltenes for the removal of cations in order to increase asphaltenes upgradeability. Some related studies were found though. A beneficial effect on mineral setting rate was observed when oil-water slurries from oilsands extraction was treated with hydrochloric acid, but no specific mention of metals removal was made (Hocking and Lee, 1977). It was reported that inorganic salts could be removed from asphaltenes-containing oil wells by washing with hydrochloric acid solutions (Becker, 1997). It was also claimed that calcium could be removed from oilsands bitumen by acid treatment (Adamski *et al*., 2012), and that metals in general could be removed under high shear conditions from heavy oil, including bitumen, using acidic water (Satake *et al*., 1995).

In the coal literature there were more studies dealing with acid treatment of coals to improve dissolution. In all of the studies where aqueous hydrochloric acid was used to remove cations, the coal solubility and liquid yield increased during conventional coal liquefaction (Van Bodegom *et al*., 1984Shams, 1992; Sugano et al., 1999). Coal liquefaction by using supercritical toluene also displayed increased conversion to liquids after pre-treatment with aqueous hydrochloric acid (Şimşek, 2002).

Consequently, it was expected that treatment of oilsands materials with hydrochloric acid would result in metals removal and that acid treatment would lead to some asphaltenes to maltenes conversion.

8.2 Experimental

8.2.1 Materials

Oilsands derived bitumen from the Athabasca region in Alberta, Canada, was obtained from Syncrude Canada Ltd. The asphaltenes and maltenes fractions were obtained by separation with *n*-pentane. The *n*-pentane precipitation of the bitumen yielded 18.5 ± 1 wt % asphaltenes and 81.5 ± 1 wt % maltenes. Characterization of the bitumen, asphaltenes and maltenes fractions was reported previously (Prado and De Klerk, 2014) (Chapter 3), and is not repeated here, because the present investigation is focused only on metals removal. Chemicals and cylinder gases that were used are listed in Table 8.1. These materials were used as supplied and without further purification. Water was obtained from a Millipore Milli-Q water purification system.

Table 8.1. Chemicals and cylinder gases employed in this study

Compound	Formula	CASRN [a]	Mass fraction purity [b]	Supplier
Chemicals				
pentane	C_5H_{12}	109-66-0	≥ 0.98	Fisher Scientific
toluene	C_7H_8	108-88-3	0.995	Fisher Scientific
1N HCl solution	H_2O/HCl mix			Fisher Scientific
Cylinder gases				
air	O_2/N_2 mix	132259-10-0		Praxair
nitrogen	N_2	7727-37-9	0.99999 [c]	Praxair

[a] CASRN = Chemical Abstracts Services Registry Number.
[b] This is the purity of the material guaranteed by the supplier; material was not further purified.
[c] Mole fraction purity.

8.2.2 Equipment and Procedure

The removal of metals from the bitumen, maltenes and asphaltenes was performed in two different ways. The first treatment procedure involved washing of the oilsands materials with an acid solution. This is the simplest treatment approach, but it also had drawbacks, such as stable emulsion formation. The second treatment procedure involved washing in two steps, first with water and then with the acid solution. By doing so it was possible to distinguish dissolved metals in connate water trapped in the bitumen from chemically bound metals. It was found that

this approach also resulted in much reduced emulsion formation. A detailed description of each procedure is as follows.

8.2.2.1 Acid Washing (Treatment 1)

The first treatment consisted of treating the feed materials (bitumen, asphaltenes and maltenes) with 1N HCl in water as described by Van Bodegom et al. (1984) with some modifications (Figure 8.2). First, 5 g of the feed material is weighed in a 100 mL glass flask. Then, 20 mL of 1N HCl (~1 $mol \cdot L^{-1}$ HCl) is added. For bitumen the procedure had to be modified in to include the addition of 20 mL toluene, because the bitumen could not be stirred due to its high viscosity. Asphaltenes and maltenes were stirred only in the presence of aqueous acid solution without adding toluene. All mixtures were stirred for 24 hours at room temperature and a reflux condenser was added to minimize water and toluene. After the reaction time, the solution was washed with water (30 mL) and 50 mL toluene was added to the reactions performed in the absence of toluene, while 30 mL of toluene was added to the solutions performed in the presence of toluene. Then, the organic phase was separated with a funnel separation and the solvent evaporated under reduced pressure at 40 ºC until constant weight was obtained. The aqueous phase was analyzed to determine the metals content. The organic phase was analyzed separately using infrared spectroscopy and thermogravimetric analysis; the asphaltenes content was determined by *n*-pentane precipitation. Blank samples were also prepared following the same procedure described for the acid treatment. In the case of blank samples it was used 20 mL of water without acid. The experiments were performed in triplicate.

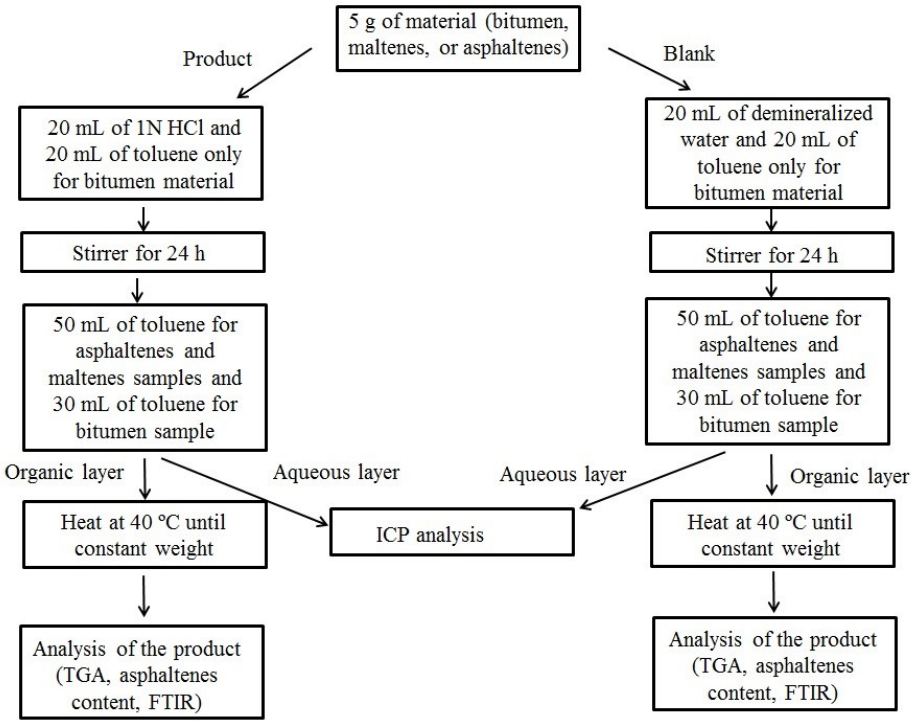

Figure 8.2. Acid washing procedure (treatment 1)

8.2.2.2 Two Step Water and Acid Washing (Treatment 2)

The two step treatment procedure involved water washing followed by acid washing (Figure 8.3). Approximately 10 g of the material was added to a 250 mL flask. Then 50 mL of distilled water and 50 mL of toluene were added to the mixture. Unlike treatment 1, all the materials (bitumen, maltenes, or asphaltenes) were treated in the presence of toluene to improve contact between the oilsands materials and aqueous medium. In the first step the mixtures were stirred for 2 hours at room temperature. Then, the layers were separated by using a funnel separator, and the toluene was evaporated from the material using a rotary evaporator at 55 ºC and 7 kPa absolute pressure for 1 hour. Afterwards the materials washed with water in the first step were treated with the acid solution in the second step. In this case, 5 g of the water washed material was added to a 250 mL flask. Then, 25 mL of 1N HCl and 25 mL of toluene were added. The solution was stirred for 2 hours at room temperature and the layers separated with a funnel separator. Toluene was removed in the same way. The aqueous phase of each step was analyzed

to determine the metals content. The organic phase was characterized separately. All of the experiments were performed in triplicate.

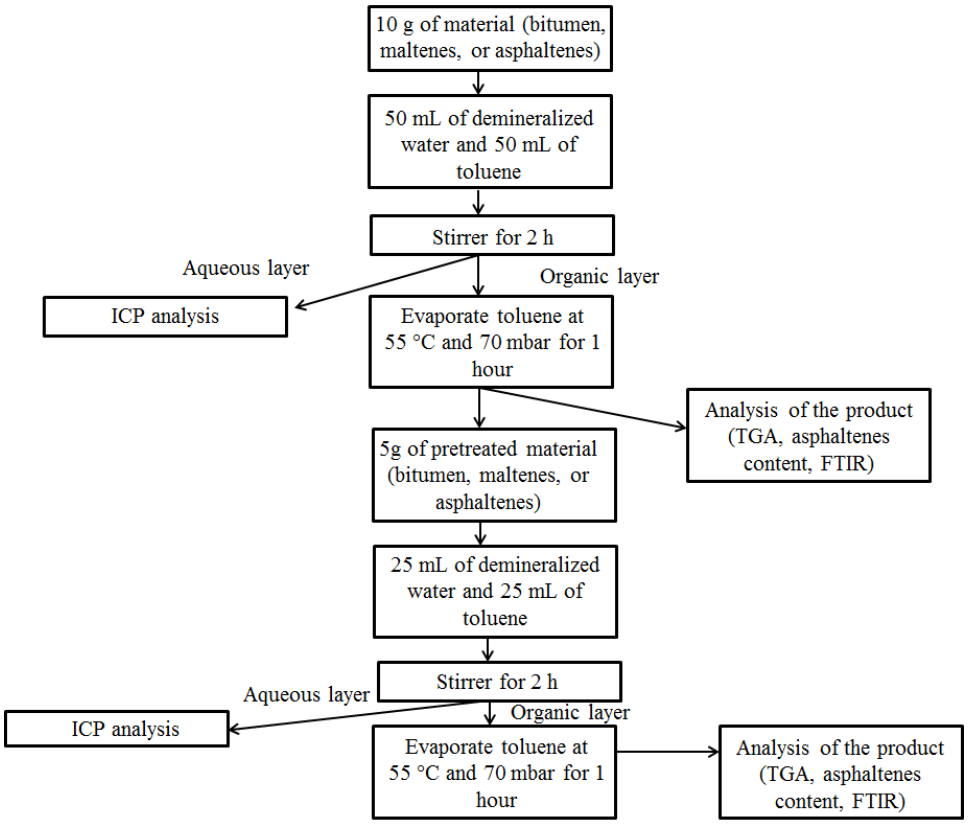

Figure 8.3. Two step water and acid washing procedure (treatment 2)

8.2.3 Analyses

FTIR spectra were performed as in Chapter 3.

Upgradeability of the products was evaluated by TGA as described in Chapter 3.

The metals content in the aqueous products from each experimental step was determined by inductive coupled plasma atomic emission spectroscopy (ICP-AES). Analyses were performed using a Thermo Fisher iCAP 6300 by the Analytical Services of Department of Renewable Resources at University of Alberta.

Asphaltenes content of the feed and products was performed as described in Chapter 7.

8.3 Results and Discussion

8.3.1 Material Balance

The intent of the washing procedure was to remove material from the organic phase, so that the material in the organic phase should have become less. In practice this was not what was found (Table 8.2). Only the acid washed asphaltenes fraction from treatment 1 displayed a minor decrease in mass of the organic phase when compared to the feed.

Table 8.2. Material balance mass increase due to washing procedure

Treatment procedure	Mass increase relative to feed (wt %) [a]					
	bitumen		maltenes		asphaltenes	
	x	s	x	s	x	s
Acid washing (treatment 1)						
water washed only (blank)	7.6	1.4	3.4	1.5	0.5	0.6
acid washed	15.6	0.2	7.6	0.4	-1.4	0.2
Two-step washing (treatment 2)						
water washing step	35.2	13.5	14.2	11.4	15.4	3.9
acid washing step [b]	38.5	21.1	-7.2	5.4	27.5	4.5
calculated net increase	87		6		47	

[a] Average (x) and one sample standard deviation (s) of experiments in triplicate.
[b] Mass increase is based on the sample weight from the washing step, which includes water and solvent that could not be removed.

It is known that oilsands materials can form stable emulsions (Masliyah *et al*., 2011), and that oilsands derived materials have an unusually strong retention of toluene (García Zapata and De Klerk, 2014). The increase in mass of the organic phase observed for most of the products was partly due to emulsion formation and partly due to toluene that could not be completely removed.

Figure 8.4 shows the layers formed after acid treatment (treatment 1) of maltenes for illustrative purposes and analogous behavior was observed for bitumen and asphaltenes. Maltenes in general had the least tendency to form emulsions. Only layer A of the samples was considered for analyses performed on the organic phase and analyses were performed on the samples from layer A after evaporation of the solvent. Layer B was collected separately and it was considered

for the material balance calculation after evaporation of the solvents, but the material was not further characterized. Layer C was collected and submitted for ICP analysis to determine the metals content.

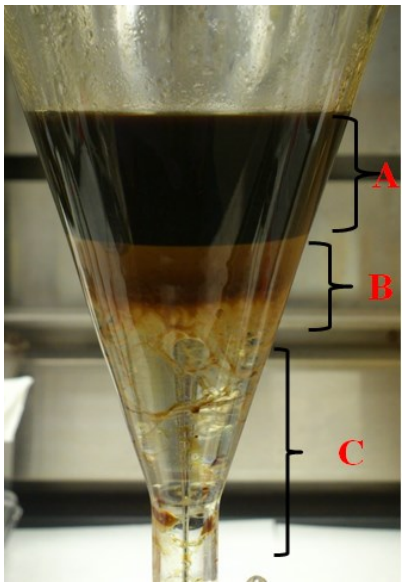

Figure 8.4. Layers formed after acid treatment of maltenes (treatment 1)

The blank experiment involving water washing (treatment 1) of the asphaltenes presented an exception. The blank sample of the asphaltenes formed an emulsion that could not be separated (Figure 8.5a). Somewhat better separation was achieved when more water was added to the mixture (Figure 8.5b). For the blank experiment with asphaltenes, only the asphaltenes diluted in layer A was considered for analysis and layer B was considered for material balance calculation along with layer A after evaporation of the solvents. In the two-step procedure where water washing was followed by acid washing (treatment 2) of the asphaltenes, a small emulsion layer was formed, but it was possible to separate and recover the organic and aqueous phases.

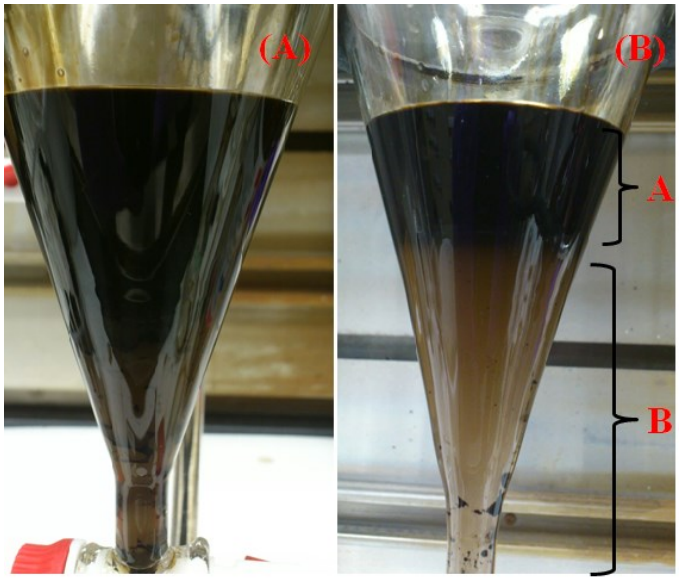

Figure 8.5. (a) Layers formed after water washing of asphaltenes (treatment 1, blank), and (b) improved separation by adding more water after treatment

The surface active (polar) functional groups in the asphaltenes fraction behaved differently when the asphaltenes were treated with water first, than when it was treated with an acid solution first. It is speculated that the difference is due to the different functional groups in asphaltenes with a range of acid-based dissociation constants in water. When the asphaltenes interact with water, some acid-base reactions occur. The pH of water is increased when oilsands derived materials are water washed (Gonzalez *et al*., 2015). Some reactions, such as the reaction of weakly acidic phenols (Eq. 8.1), are promoted by the higher pH of the water and the resulting product becomes more hydrophilic.

$$(C_6H_5)–OH + OH^- \rightleftharpoons (C_6H_5)–O^- + H_2O \quad \text{... (8.1)}$$

In asphaltenes, once phenoxide or other hydrophilic groups are formed, these groups can emulsify and trap water within the asphaltenes. This is indeed what was observed (Figure 8.5a), with the asphaltenes forming a strong emulsion. Although the phenoxide groups can readily be converted into phenolic groups by acid treatment, it is likely that the emulsified water would stabilize and protect these groups from contact with the acid solution due to the stability of the emulsion. Additional energy would be required during mixing to break the emulsion and release

the emulsified water so that the phenoxide groups can be brought into contact with the acid solution to be acidified.

A two-step treatment with water followed by acid washing results in the retention of some emulsified water, since it is difficult to overcome the mass transport resistance caused by the strongly emulsified water to acidify groups stabilized and protected by the emulsified water. This problem is avoided by treatment with an acid solution, because the pH of the water remains low.

8.3.2 Metals Removal

The amount of metals that was removed by the different washing procedures was determined by analysis of the aqueous phase (Table 8.3). The results were expressed in terms of metals removal from the oilsands materials under the assumption that there was no concentration difference between the bulk aqueous phase and water that was trapped in emulsion. It was also confirmed by analysis that the water and acid employed for washing contained little cations to interfere with the quantification, with 2 $\mu g \cdot g^{-1}$ Na and < 1 $\mu g \cdot g^{-1}$ K and Fe in the acid, as well as 3 $\mu g \cdot g^{-1}$ Na in the water.

The first observation that can be made from the analysis is that the relative standard deviation in some cases are >5 % for abundant elements such as Na, Mg, Ca and Fe (Table 8.3). This is not a reflection on the repeatability of the analytical technique, ICP-AES (Slickers, 1993). The variability in the metals content determined by repeat experiments was previously highlighted in the study by Jacobs and Filby (1983). The results presented in Table 8.3 are difficult to explain if sample heterogeneity is discounted. For example, the difference in Na removal between water washing and acid washing of bitumen was 62 ± 8 compared to 28 ± 1 $\mu g \cdot g^{-1}$. Acid washing should have been able to displace more sodium, not less.

Table 8.3. Metals removal by different water and acid washing treatments

Sample description	Concentration of metals ($\mu g \cdot g^{-1}$) [a,b]													
	Na		Mg		K		Ca		V		Fe		Ni	
	x	s	x	s	x	s	x	s	x	s	x	s	x	s
Water for water washing	3.3	0.4	0	0	0.3	0.2	0	0	0	0	0.6	0	0	0
1N HCl for acid washing	2.2	1	0	0	0	0	0	0	0	0	0	0	0	0
Water washed only (treatment 1) [c]														
bitumen	62	8	4	0	0	0	11	1	0	0	<1	0	0	0
maltenes	21	3	2	0	0	0	15	3	0	0	0	0	0	0
Acid washed only (treatment 1)														
bitumen	28	1	21	1	0	0	57	3	<1	0	534	4	2	1
maltenes	44	1	10	0	0	0	104	2	0	0	47	1	4	0
asphaltenes	266	4	182	23	30	4	655	59	3	3	1793	108	3	3
Two-step washing (treatment 2)														
bitumen (water)	33	2	2	1	1	0	9	2	0	0	0	0	0	0
bitumen (acid)	15	1	2	1	1	0	13	1	0	0	92	9	0	0
bitumen (total)	48	3	4	2	1	0	21	3	0	0	92	9	0	0
maltenes (water)	15	0	8	2	1	0	29	1	0	0	0	0	0	0
maltenes (acid)	11	1	1	1	1	0	7	2	0	0	8	2	0	0
maltenes (total)	26	1	8	3	1	0	36	2	0	0	8	2	0	0
asphaltenes (water)	34	10	6	1	1	0	31	8	0	0	0	0	0	0
asphaltenes (acid)	14	2	27	3	1	0	39	5	0	0	470	43	0	0
asphaltenes (total)	47	12	33	4	2	0	69	13	0	0	470	43	0	0

[a] Except for water and HCl analyses, concentration of metals removed based on oilsands feed.
[b] Average (x) and one sample standard deviation (s).
[c] Asphaltenes analysis was compromised by extensive emulsion formation.

The results were either influenced by large sample to sample variations, or metals removal was very sensitive to the experimental procedure.

Another observation is that it was not possible to obtain material balance for individual elements after the same treatment procedure was applied to bitumen, maltenes and asphaltenes. The mass (w) of any element removed from bitumen should have been equal to the mass fraction contributions of the element removed from the subfractions (Eq. 8.2).

$$w_{bitumen} = 0.815 \cdot w_{maltenes} + 0.185 \cdot w_{asphaltenes} \quad \text{... (8.2)}$$

It is possible that the preparation of the subfractions affected the nature of the subfractions in a way that made it more easy or difficult to remove metals. However, there was no systematic trend. Although it was not possible to rule out sensitivity to treatment procedures, taken

collectively, it was more plausible to ascribe the variations to sample heterogeneity. The implication was that there was a risk that the results could be over-interpreted. Despite the risk of over-interpretation, limited conclusions could be drawn based on Table 8.3:

a) Water and/or acid washing did not meaningfully remove V and Ni. It is likely that most of the V and Ni were coordinated in porphyrin structures, or were coordinated by heteroatoms in non-porphyrin structures (e.g. Figure 8.1), which were not disrupted by water or acid. Acid washing (treatment 1) was the only procedure that resulted in minor Ni removal and possibly some V removal.

b) Water washing did not remove Fe, but acid washing removed Fe from bitumen, maltenes and asphaltenes. Iron was the element with the highest level of removal of all elements studied. The Fe was not present in connate water, but was removed from either the organic phase, or leached from suspended mineral matter. The nature of the interaction between Fe and the oilsands materials was not determined.

c) Water, as well as acid washing removed alkaline and alkaline earth metals. Directionally the results suggest that only a fraction of these metals are loosely bound or dissolved in connate water. Acid washing increased liberation and removal of Mg and Ca in particular.

d) Metals removal by washing is possibly a slow process. The extent of metals removal by treatment 1 that involved 24 hours contact, was an order of magnitude more than the metals removal by treatment 2 that involved a cumulative contact of only 4 hours. This is not conclusive, because other variables, such as the extent of emulsion formation, could also have influenced the outcome and a time series study was not performed.

8.3.3 Asphaltenes Content

One of the potential desirable outcomes of metals removal was that bridging structures would be disrupted so that some of the asphaltenes would become maltenes. The asphaltenes content of the feed materials and products after treatment was determined (Table 8.4). Note that although

the asphaltenes subfraction was prepared by rigorous solvent deaspalting of bitumen with *n*-pentane, the asphaltenes subfraction contained ~5 % material that could be redissolved in *n*-pentane.

Table 8.4. Asphaltenes content determined by *n*-pentane solvent deasphalting

Treatment procedure	Asphaltenes content (wt %) [a]					
	bitumen		maltenes		asphaltenes	
	x	s	x	s	x	s
Raw material	18.5	0.1	0	0	94.8	0.7
Acid washing (treatment 1)						
water washed only (blank)	18.1	2.3	0	0	89.4	0.1
water washed only (blank) [b]	19		0		90	
acid washed	24.5	1.4	0	0	86.8	2.8
acid washed [b]	28		0		87	
Two-step washing (treatment 2)						
water washing step	17.7	0.9	0	0	90.5	2.7
water washing step [b]	24		0		104	
acid washing step	23.8	3.2	3.5	0.9	73.7	2.9
acid washing step [b]	45		4		108	

[a] Average (x) and one sample standard deviation (s) of experiments in triplicate.
[b] Corrected for the weight of trapped solvent or aqueous phase due to treatment (Table 8.2) to express the asphaltenes content in terms of the oilsands derived material in the sample.

Interpretation of the results presented in Table 8.4 is complicated by the retention of solvent and aqueous phase shown in Table 8.2. The measured asphaltenes content based on sample mass could be expressed based on oilsands feed mass, by correcting for the presence of solvent and aqueous phase in the feed material that was used to perform the asphaltenes precipitation tests. It was not possible to correct for the possible retention of solvent and aqueous phase in the asphaltenes that were precipitated. The measured amount of asphaltenes precipitated could include trapped solvent and aqueous phase, which would inflate the reported asphaltenes content. In fact, it was likely that the asphaltenes retained some material, since some asphaltenes contents expressed on an oilsands feed basis exceeded 100 % (Table 8.4). This is possible only if the asphaltenes contain non-oilsands derived material, like solvent or aqueous phase. Hence, no firm conclusions could be drawn about the change in the asphaltenes content from experiments where a higher asphaltenes content was found, except to say that either the asphaltenes content increased, or the asphaltenes retained non-oilsands derived material.

It is possible to conclude that an observed decrease in asphaltenes content is indeed a decrease in asphaltenes content. Since solvent and aqueous phase could also have been retained in these cases, a decrease in the measured asphaltenes content represented the least amount of asphaltenes to maltenes conversion. The actual amount of asphaltenes to maltenes conversion could be higher if the measured asphaltenes content included some trapped solvent or aqueous phase.

Acid washing of the asphaltenes subfraction (treatment 1) decreased the *n*-pentane insoluble content from 95 to 87 wt % (Table 8.4). A decrease was also observed in the blank test that involved water washing (treatment 1), but the decrease might be due to extensive emulsion formation in the aqueous phase. Emulsion formation could cause a partitioning of material, with the more polar asphaltenes being collected at the interface (Adams and Schabron, 2015). This would bias the test, because the most surface active and polar material would be present in the emulsion.

One interesting observation was that the asphaltenes content of the bitumen increased after acid treatment, but that the same was not observed for the two subfractions of the bitumen when these were treated individually (Table 8.4). It was tempting to ascribe the increase in the measured asphaltenes content of the bitumen to uncertainty about the trapped material. The infrared spectrum of the acid treated bitumen contained trapped toluene, with a strong absorption at 729 cm^{-1} and weaker absorption at 1494 cm^{-1} characteristic of toluene that could be observed in the infrared spectrum (not shown) of the acid treated bitumen. Yet, it was difficult to explain a roughly 50 % relative increase in asphaltenes content in this way.

It was postulated that the additional asphaltenes formation was due to acid-base reactions in the bitumen that were of a more limited in extent in either the asphaltenes, or the maltenes.

There are more free bases than free acids in bitumen; the pH of water increases when contacted with bitumen (Gonzalez *et al*., 2015). When bitumen is acid treated the acidity of the bitumen is increased. Once the acid solution is removed, acid-base equilibrium is again established in the treated material. Newly formed acid-base adducts with asphaltenes-like character could then be precipitated as asphaltenes. When raw bitumen is separated into maltenes and asphaltenes,

molecules with acid-base character are partitioned between the two subfractions. The partitioning of molecules is such that each subfraction ends up being deficient in molecules with either acid character, or base character. This limits the extent of possible acid-base pair formation in each subfraction, whereas bitumen does not have the same benefit.

For example, if the maltenes fraction contains little material that are acids, or can be converted into acids, there is little opportunity for basic compounds to form acid-base adducts. This would explain the absence of asphaltenes in the maltenes after acid treatment by treatment 1 (Table 8.4).

8.3.4 Infrared Spectroscopy

Infrared spectroscopy was performed on all of the feed materials and treated samples to better understand the changes taking place during treatment. There was little hope of detecting changes due to metals removal, because the metals concentration in the oilsands materials was too low, typically of the order 0.1 %. However, oxygen containing functional groups have strong infrared absorption bands and it was anticipated that some changes due to acid treatment would be observed. The most informative infrared analyses (Figure 8.6) were those of the asphaltenes before and after acid washing (treatment 1).

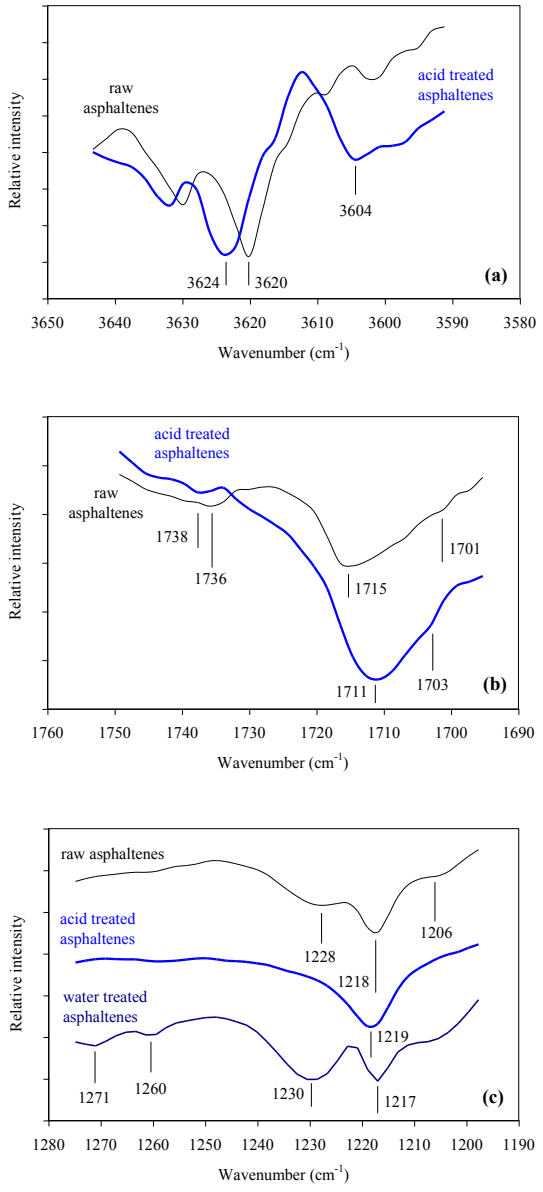

Figure 8.6. Infrared spectra of raw asphaltenes, acid treated asphaltenes (treatment 1) and water washed asphaltenes (treatment 2)

a) There was a slight shift in the maximum absorption of the OH present in asphaltenes from 3620 to 3624 cm^{-1} in the acid treated asphaltenes (Figure 8.6a). Concomitantly there was a meaningful increase in absorption at 3604 cm^{-1}. This is likely due to the increase in phenolic OH after acid treatment. Phenolic OH stretch vibrations in solution are found in the 3617 to 3593 cm^{-1} region of the infrared spectrum (Colthup *et al.,* 1990). Acidification could have removed metals from phenoxide-groups to produce phenolic-groups. Alcohol groups could

also have been formed by acid hydrolysis of ether and ester groups. If one of the carbons in the C–O–C bond of an ether or ester were aromatic, hydrolysis would produce a phenolic OH. Otherwise, hydrolysis of ether or esters would produce primary aliphatic alcohols. Primary aliphatic alcohols absorb around 3640 cm^{-1} (Colthup *et al.,* 1990), and no increase in absorption was observed in this region after acid treatment. Only an increase in phenolic OH was observed.

b) The carbonyl region of the infrared spectrum (Figure 8.6b) changed when the asphaltenes was acid treated. The relative intensity of the carbonyl stretching at 1736 cm^{-1} decreased relative to that in the range 1715 to 1711 cm^{-1} after acid treatment. The carbonyl groups absorbing around 1740 to 1730 cm^{-1} are typically associated with groups such as esters and anhydrides. The observed decrease after acid treatment could be related to the hydrolysis of these groups. In both samples a shoulder at 1703 to 1701 cm^{-1} were found that is typical of carboxylic acids in the asphaltenes (Frakman, 1990).

c) The C–O stretching region around 1220 cm^{-1} is shown in Figure 8.6c. In the raw asphaltenes there were three different C–O absorptions at 1228, 1218 and 1206 cm^{-1}. After acid treatment, the absorptions at 1228 and 1206 cm^{-1} were no longer observed. The disappearance of these absorptions in tandem with the decrease in the 1736 cm^{-1} carbonyl absorption suggests that these absorptions were due to the hydrolysis of esters and anhydrides. Esters have previously been found in asphaltenes derived from Canadian oilsands (Frakman, 1990; Peng *et al*., 1997). If ester hydrolysis resulted in two separate molecules then ester hydrolysis is also a reaction pathway that would decrease the average molecular mass of the products compared to the feed.

d) The change from phenols to phenoxide can readily be seen in pure compounds. In phenol the two absorption bands at 1271 and 1238 cm^{-1} are replaced with a single stronger absorption at 1267 cm^{-1} for the C–O of sodium phenoxide (Guo *et al*., 2004). Since it was suspected that the transformation from phenolics to phenoxides was important in emulsion formation, it was hoped to find some spectroscopic support for this postulate. Figure 8.6c shows two absorption bands at 1271 and 1261 cm^{-1} that were present only in water washed asphaltenes

(treatment 2). In addition to these two absorption bands, the absorption at 1230 cm^{-1} became much more prominent than in any of the other samples. Although these absorption bands do not constitute proof for the development of phenols and phenoxides, it is suggestive to find that absorption bands in the same spectral range as phenolics and phenoxides would become important spectral features in the water washed asphaltenes.

8.3.5 Molecular Mass of Metal Bridged Asphaltenes

An interesting, albeit speculative calculation that can be performed using the experimental data that was presented, is to estimate the molecular mass of the metal-bridged asphaltenes. The main assumptions for such a calculation is that asphaltenes to maltenes conversion is due only to the decomposition of bridged structures to produce two molecular fragments. Acid washing of the asphaltenes resulted in a decrease in *n*-pentane insoluble matter from 94.8 to 86.8 wt % (Table 8.4) and 2630 $\mu g \cdot g^{-1}$ multivalent metals removal (Table 8.3), which was equivalent to 56 $\mu mol \cdot g^{-1}$. The calculated average molecular mass of the molecular fragments that were obtained from decomposition of metal-bridged structures is around 700 $g \cdot mol^{-1}$.

The literature on asphaltenes molecular mass determinations is extensive and estimates of the molecular mass range from several hundred to several thousand grams per mole (Gray, 2015). Aggregation makes these determinations difficult. The calculated value for the individual fragments in the metal bridged structure close to the molecular mass estimates of various asphaltenes was obtained by fluorescence spectroscopy (~750 $g \cdot mol^{-1}$) (Groenzin and Mullins, 2007) and mass spectrometry (range of 350-1050 $g \cdot mol^{-1}$, maximum at 750 $g \cdot mol^{-1}$) (Pinkstons *et al.*, 2009). Although this does not provide proof of the main assumption and the calculation of molecular mass in this work, it does not provide evidence to the contrary either.

8.3.6 Upgradeability of Treated Materials

When a pretreatment procedure is performed, it is prudent to consider the impact on downstream processing. Seen in isolation, the treatment might appear beneficial, but it could undermine the upgradeability of the treated products. Conversely, the treatment might appear to have little value on its own, but it might improve upgradeability of the products.

Upgrading of oilsands bitumen and its subfractions rely heavily on high temperature cracking conversion technologies, such as visbreaking, coking and residue hydroconversion (Gray, 2015). The upgradeability of the products from water and acid treatment was evaluated in terms of changes in straight run distillation yields and thermal cracking yields (Table 8.5). Quantitative interpretation of these results was hampered by the strong retention of water and solvent in some samples (Table 8.2).

Table 8.5. Upgradeability of raw and treated materials as evaluated by thermogravimetric analysis to approximate straight run distillation, pyrolysis and coking

Sample description	Distillation yield (wt %) [a]						Cracking yield (wt %) [a]			
	Naphtha (<177 °C)		Distillate (177-343 °C)		vacuum gas oil (343-525 °C)		pyrolysis gas and liquid		coke [b]	
	x	s	x	s	x	s	x	s	x	s
Bitumen										
raw feed material	0.2	0.3	5.6	1.4	41.4	2.6	41.1	1.2	11.7	1.5
water washed (treatment 1)	0.3	0.2	8.5	0.3	37.1	0.6	37.6	0.7	16.6	0.6
acid washed (treatment 1)	0.4	0.2	8.3	0.3	39.1	1.1	37.0	3.3	15.1	2.2
water washing step (treatment 2)	0.6	0.3	10.8	1.4	37.3	1.0	32.6	0.7	18.8	0.7
acid washing step (treatment 2)	1.0	0.2	11.4	1.6	37.9	0.6	31.6	1.7	18.1	0.5
Maltenes										
raw feed material	0.6	0.2	10.4	0.7	49.4	0.3	33.0	1.3	6.6	1.3
water washed (treatment 1)	0.3	0.1	11.6	1.2	47.0	0.4	33.2	0.7	8.0	0.3
acid washed (treatment 1)	0.6	0.2	9.1	1.8	50.2	1.4	35.1	0.7	5.0	0.9
water washing step (treatment 2)	0.8	0.5	13.3	2.5	47.6	2.9	26.0	3.0	12.2	3.1
acid washing step (treatment 2)	0.9	0.2	12.8	1.8	48.8	0.8	26.8	0.6	10.7	0.5
Asphaltenes										
raw feed material	0.5	0.3	0.5	0.5	2.0	0.3	51.6	0.8	45.4	0.5
water washed (treatment 1) [c]	0.1	0.1	1.2	0.2	1.8	0.2	49.1	1.4	44.7	1.4
acid washed (treatment 1)	0.3	0.1	1.7	1.2	3.9	1.5	54.1	1.0	40.0	1.5
water washing step (treatment 2)	0.7	0.2	6.4	0.4	2.3	0.2	45.3	0.6	45.3	0.7
acid washing step (treatment 2)	1.7	0.3	13.8	0.7	2.5	0.1	32.9	1.5	49.2	1.1

[a] Average (x) and one sample standard deviation (s) of experiments in triplicate.
[b] Microcarbon residue (MCR)
[c] Asphaltenes analysis was compromised by extensive emulsion formation.

The changes in the straight run distillation yields were not meaningful differences. Distillation yields were also more likely to be directly influenced by trapped solvent and water, which was apparent especially in the analysis of products from two-step water and acid treatment.

Two seemingly anomalous observations had to be explained though. The first observation is that acid treatment of asphaltenes by different procedures had the opposite outcome; treatment 1 decreased the amount of coke measured as microcarbon residue (MCR) and treatment 2 increased it. The second observation was that bitumen responded differently compared to its subfractions to acid treatment. After acid washing (treatment 1) the MCR of bitumen increased from 11.7±1.5 to 15.1±2.2 wt %, whereas the MCR of the maltenes and the asphaltenes decreased from 6.6±1.3 to 5.0±0.9 wt % and 45.4±0.5 to 40.0±1.5 wt % respectively.

The lower MCR of the asphaltenes after acid treatment (treatment 1), compared to two-step water and acid treatment (treatment 2), was a consequence of emulsion formation. The aqueous phased that was emulsified in the two-step treatment hindered demetalation by acid washing, and demetalation by direct acid treatment was more effective (Table 8.3). It is speculated that the water also acted as a nucleation site for mesophase formation. The emulsified water collected the more polar asphaltenes at the interface, and the proximity of the more polar molecules made it easier for a mesophase to form under higher temperature conditions. During thermal treatment, mesophase formation usually precedes the formation of coke (Wiehe, 2008). The mesophase is lean in hydrogen and being a separate liquid phase, the transport resistance between the bulk oil liquid phase and the mesophase limits transport of molecules that can stabilize free radical fragments during cracking (analogous to emulsions increasing the transport resistance for metals removal by acid washing).

The higher MCR of bitumen after acid treatment (treatment 1), compared to the MCR of its two subfractions, indicated that there was another factor involved apart from those already considered. It is postulated that the same acid-base chemistry that increased the asphaltenes content of bitumen after acid treatment was responsible for the increase in MCR. Acid-base adducts formed after acid treatment of bitumen would be more prone to end up in the mesophase and ultimately as coke.

8.4 Conclusions

Acid treatment of oilsands derived materials was experimentally investigated as a possible pretreatment procedure to remove metals and to facilitate asphaltenes to maltenes conversion. The main conclusions from the investigation were:

a) Acid washing was the treatment procedure that resulted in the highest extent of metals removal from bitumen, maltenes and asphaltenes. Metals removal from asphaltenes was the highest and from maltenes the lowest. The multivalent metals content removed from asphaltenes was around 2600 $\mu g \cdot g^{-1}$ (56 $\mu mol \cdot g^{-1}$).

b) Water washing of the materials removed an order of magnitude less metals from the oilsands materials. The majority of the metals is in the organic phase and not in connate water.

c) Washing the oilsands materials with water, even when it was followed by acid washing, resulted in strong emulsion formation. It was postulated that this was due to the phenol-phenoxide equilibrium that was shifted towards the phenoxide by the water that became alkaline on exposure to the oilsands materials. Phenoxide groups would promote emulsion formation. Spectroscopic evidence to support this interpretation was presented, although the evidence was insufficient to constitute absolute proof.

d) Water and/or acid washing did not meaningfully remove V and Ni, but acid washing resulted in meaningful Fe removal.

e) About 8 % of the asphaltenes in the raw asphaltenes were converted into maltenes by acid treatment. This observation supported the hypothesis that smaller molecules could be freed from larger metal-bridged structures by removing multivalent metals by acid treatment. The calculated average molecular mass of the molecular fragments that were obtained from the decomposition of metal-bridged structures is around 700 $g \cdot mol^{-1}$.

f) Acid treatment resulted in ester hydrolysis. When two molecules were produced by ester hydrolysis, hydrolysis was another reaction pathway that decreased the average molecular mass of the acid treated product compared to that of the feed.

g) Demetalation of asphaltenes by acid treatment decreased the microcarbon residue of the product compared to that of the feed. Yet, despite demetalation of bitumen by the same procedure, the asphaltenes content of the acid treated bitumen increased, as well as its microcarbon residue. The latter was explained in terms of increased mesophase formation as a result of the increase in asphaltenes content, which was partly due to increased formation of acid-base adducts. It was argued that the subfractions prepared from raw bitumen benefited from unequal partitioning of material with acid-base character, which limited formation of acid-base adducts during acid treatment.

Literature Cited

Adams, J. J.; Schabron, J. F. The role of asphaltenes in oil and water emulsions. *Prepr. Pap.-Am. Chem. Soc., Div. Energy Fuels* **2015**, *60* (1), 1-2.

Adamski, R. P.; Komishke, B. D.; Long, Y.; Munsterman, W.; Niemiec, M.; Smith, T. R.; Troxler, B. M. Treatment of oil sand bitumen to produce low calcium bitumen. Pat. Appl. CA 2755518 A1 (Shell), 2012.

Ali, M. F.; Abbas, S. A review of methods for the demetalization of residual fuel oils. *Fuel Process. Technol.* **2006**, *87*, 573-584.

Becker, J. R. *Crude oil. Waxes, emulsions, and asphaltenes*; PennWell: Tulsa, OK, 1997, p 232.

Colthup, N. B.; Daly, L. H.; Wiberley, S. E. *Introduction to infrared and Raman spectroscopy*, 3ed; Academic Press: San Diego, CA, 1990.

Frakman, Z.; Ignasiak, T. M.; Lown, E. M.; Strausz, O. P. Oxygen compounds in Athabasca asphaltene. *Energy Fuels* **1990**, *4*, 263-270.

García Zapata, J. L.; De Klerk, A. Viscosity changes during mild oxidation of oilsands-derived bitumen: Solvent effects and selectivity. *Energy Fuels* **2014**, *28*, 6242-6248.

Gonzalez, V.; De Klerk, A.; Yang, S.; Prasad, V. Influence of acid chemistry on bitumen viscosity. *Prepr. Pap.-Am. Chem. Soc., Div. Energy Fuels* **2015**, *60* (1), 9-12.

Gray, M. R. *Upgrading oilsands bitumen and heavy oil*; University of Alberta Press: Edmonton, AB, 2015.

Groenzin, H.; Mullins, O. C. Asphaltene molecular size and weight by time-resolved fluorescence depolarization. In *Asphaltenes, heavy oils, and petroleomics*; Mullins, O. C., Sheu, E. Y., Hammami, A., Marshall, A. G. Eds.; Springer: New York, 2007, pp. 17-62.

Guo, H.; Jiang, J.; Shi, Y.; Wang, Y.; Liu, J.; Dong, S. UV-Vis spectrophotometric titrations and vibrational spectroscopic characterization of *meso*-(*p*-hydroxyphenyl)porphyrins. *J. Phys. Chem. B* **2004**, *108*, 10185-10191.

Hocking, M. B.; Lee, G. W. Effect of chemical agents on settling rates of sludges from effluent of hot-water extraction of Athabasca oilsands. *Fuel* **1977**, *56*, 325-333.

Jacobs, F. S.; Filby, R. H. Solvent extraction of oil-sand components for determination of trace elements by neutron activation analysis. *Anal. Chem.* **1983**, *55*, 74-77.

Joseph, J. T.; Forrai, T. R. Effect of exchangeable cations on liquefaction of low rank coals. *Fuel* **1992**, *71*, 75-80.

Li, X.; Bai, Z-Q.; Bai, J.; Zhao, B-B.; Li, P.; Han, Y-N.; Kong, L-X.; Li, W. Effect of Ca^{2+} species with different modes of occurrence on direct liquefaction of a calcium-rich lignite. *Fuel Process. Technol.* **2015**, *133*, 161-166.

Masliyah, J. H.; Czarnecki, J.; Xu, Z. *Handbook on theory and practice of bitumen recovery from Athabasca oilsands. Vol. I. Theoretical basis*; Kingsley: Canada, 2011.

Peng, P.; Morales-Izquierdo, A.; Hogg, A.; Strausz, O. P. Molecular structure of Athabasca asphaltene: Sulfide, ether, and ester linkages. *Energy Fuels* **1997**, *11*, 1171-1187.

Pinkston, D. S.; Duan, P.; Gallardo, V. A.; Habicht, S. C.; Tan, X.; Qian, K.; Gray, M. R.; Mullen, K.; Kenttämaa, H. I. Analysis of asphaltenes and asphaltene model compounds by laser-induced acoustic desorption/Fourier transform ion cyclotron resonance mass spectrometry. *Energy Fuels* **2009**, *23*, 5564-5570.

Prado, G. H C.; De Klerk, A. Halogenation of oilsands bitumen, maltenes, and asphaltenes. *Energy Fuels* **2014**, *28*, 4458-4468.

Satake, T.; Sano, K.; Domoto, T.; Kubota, S. Method for refining heavy oils using acidic water. Pat. JP 07034072 (Satake Giken), 1995.

Shams, K.; Miller, R. L.; Baldwin, R. M. Enhanced low severity coal liquefaction using selective calcium removal. *Prepr. Pap.-Am. Chem. Soc., Div. Fuel. Chem.* **1992**, *37* (2), 1017-1024.

Şimşek, E. H.; Karaduman, A.; Çalışkan, S.; Togrul, T. The effect of preswelling and/or pretreatment of some Turkish coals on the supercritical fluid extract yield. *Fuel* **2002**, *81*, 503-506.

Slickers, K. *Automatic atomic-emission-spectroscopy*, 2ed; Brühlsche Universitätsdruckerei: Giessen, 1993.

Strausz, O. P.; Lown, E. M. *The chemistry of Alberta oilsands, bitumens and heavy oils*; Alberta Energy Research Institute: Calgary, AB, 2003.

Sugano, M.; Mashimo, K.; Wainai, T. Structural changes of lower rank coals by cation exchange. *Fuel* **1999**, *78*, 945-951.

Van Bodegom, B.; Van Veen, J. A. R.; Van Kessel, G. M. M.; Sinnige-Nijssen, M. W.; Stuiver, H. C. M. Action of solvents on coal at low temperatures. 1. Low-rank coals. *Fuel* **1984**, *63*, 346-354.

Wiehe, I. A. *Process chemistry of petroleum macromolecules*; CRC Press: Boca Raton, FL, 2008.

Yen, T. F. Chemical aspects of metals in native petroleum. In *The role of trace metals in petroleum*; Yen, T. F. Ed.; Ann Arbor Science Publishers: Ann Arbor, MI, 1975, pp. 1-30.

Chapter 9. Conclusions

9.1 Introduction

The overall objective of this study was to investigate non traditional upgrading pathways to convert some of the asphaltenes into maltenes. The conversion pathways studied were halogenation, Friedel-Crafts alkylation, and donor-acceptor reaction by acid treatment. The major conclusions that will contribute to the field of upgrading of oilsands derived materials are highlighted. Although these conversion pathways did not achieve high asphaltenes to maltenes conversion, the investigation improved our understanding of the reactions of halogens and acids in oilsands derived materials. The major conclusions and new insights from this study are highlighted.

9.2 Significance, Major Conclusions, and Insigths

9.2.1 Halogenation

Little systematic investigation of oilsands bitumen halogenation appeared since the papers of Moschopedis and Speight in the 1970's. The lack of interest in halogenation is partly due to its limited industrial appeal. The investigation of halogenation was prompted by a hypothesis regarding the disruption of π-π ring stacking. The approach differed from previous research in this field and employed mild bromination by an experimental protocol that enabled halogenation of aromatic ring structures, rather than just on aliphatic pendant groups. Although no evidence was found to support the hypothesis that halogen addition to multinuclear aromatics would disrupt aromatic stacking, the work provided research-leads into related applications and reactions relevant to the upgrading of oilsands materials.

a) Mild bromination resulted in harder bitumen, asphaltenes, and maltenes. Asphaltenes was converted from a brown powder-like material to a dark, shiny, and crystalline structure. The solubility of the brominated asphaltenes also changed. Brominated asphaltenes was insoluble in paraffinic solvents, as well as aromatic solvents. The increased hardness (penetration

hardness) and decreased solubility suggested that mild halogenation might have application to special road paving applications and as sealant materials with high organic solvent resistance.

b) Even though brominated asphaltenes was harder compared to the raw asphaltenes, bromination was able in increase straight run vacuum gas oil yield from 2.0 ± 0.3 wt % to 7.5 ± 1.8 wt % while the yield of micro carbon residue was unaffected. Bitumen and maltenes presented opposite behavior: bromination occasioned a decrease of distillate fractions and increase in micro carbon residue. This result contributes to the asphaltenes field by indicating that chemical modification in pure asphaltenes results in different upgradeability than when asphaltenes is treated in the bitumen matrix. The small increase of straight run vacuum gas oil yield indicates that halogenation provided different molecular interactions in asphaltenes that were beneficial for asphaltenes upgradeability. The increase of light fractions could have been caused by the formation of intramolecular hydrogen bonding that may lower the boiling point of the material, or possible metal-coordination disruption by demetalation of porphyrins caused by the halogenation reaction.

c) As brominated asphaltenes were insoluble not only in paraffinic solvents, but also in aromatic solvents, it was suggested that residual chlorides already present in bitumen may affect the chemistry during bitumen upgrading. Residual chloride salts may affect the chemistry in coke formation in different ways. HCl formed during hydrolysis of chloride salts may form free radicals and halogenate aliphatic and aromatic compounds. Halogenation of olefins by HCl may also occur by carbonium ion formation. If halogenation occurs in the side chains of aromatics, HCl may contribute to free radical chain propagation during thermal cracking that results in higher molecular weight compounds that contributes to coke formation. Formation of compounds with higher molecular weight may also be caused by Friedel-Crafts alkylation between aromatics and olefins and catalyzed by HCl. Friedel-Crafts alkylation, free radical addition reactions “catalyzed” by HCl, and halogenation of molecules could contribute to coke insolubility in aromatic solvents. This observation is potentially a significant contribution to the bitumen upgrading field, as the only effect of chloride salts reported nowadays is their hydrolysis that results in HCl, which leads to corrosion and fouling of equipment. The contribution of halogens to coke formation and increased coke yield was not

reported before and future investigation would help finding alternative ways to remove or mitigate the effects of native halogen species.

d) UV-Vis analysis indicated that porphyrins in bitumen and maltenes could have been destroyed during bromination with possible demetalation. The investigation with model compounds containing tetrapyrrole macrocycle (phthalocyanines) showed that 74% of Ni(II) was removed from the tetrapyrrole macrocycle by using the bromination procedure used for bitumen, maltenes, and asphaltenes. The Ni(II) was probably removed as the $NiBr_2$ halide salt instead of destruction of the tetrapyrrole macrocycle. Vanadium was not removed from V(IV) oxide phythalocyanine model compound. The possibility of demetalation of porphyrins in bitumen by mild bromination was not reported before. The work elucidated the pathway of selective metal removal by disruption of acid-base and metal-ligand equilibrium. This fundamental understanding of the mechanism by which the demetalation took place may assist other researchers to develop new strategies in the field of oil demetalation.

e) It is suggested that hardness of brominated bitumen, maltenes, and asphaltenes may be caused by intermolecular hydrogen bond formation as result of the halogenation reaction. No evidence was found that aromatic stacking strength was increased during halogenation. Hardness resulted from addition reactions may happen, but only if the halogenated materials are heated. As bromination of bitumen, maltenes, and asphaltenes was performed at room temperature, addition reactions were not anticipated to be responsible for hardness of these materials. Even though the objective of this work was not to determine the molecular structure of asphaltenes, the results suggests that different kinds of molecular interactions, such as intermolecular hydrogen bonding, can contribute to asphaltenes insolubility in paraffinic solvents. The results were in line with a description of asphaltenes structure based on the archipelago molecular structure model and supramolecular assembly association model.

9.2.2 Friedel-Crafts Alkylation

The objective of the work was to convert asphaltenes to maltenes by Friedel-Crafts alkylation. The working hypothesis was that by targeting OH groups for alkylation, the solubility parameter (δ) of the asphaltenes molecules would be decreased and it would be more likely to be soluble in a light hydrocarbon, i.e. becoming a maltene. The study differentiates itself from previous work in the field by pairing alkylation of industrial asphaltenes with model compound alkylation to elucidate the observations of the applied work. The relevance and impact of ether-scission (and thioether–scission), rather than alcohol (and thiol) alkylation was demonstrated. It was also demonstrated that the catalyst ($FeCl_3$) resulted in limited halogenation of the organic molecules under specific conditions, as well as non-porphyrinic metal coordination. The contributions relevant to the upgrading of oilsands materials are highlighted:

a) Friedel-Crafts alkylation with *o*-xylene and $FeCl_3$ catalyst provided 6 % conversion of asphaltenes to maltenes. Straight run distillate and vacuum gas oil increased 9 % compared to raw asphaltenes. Investigation with 2-naphthol as model compound showed that the mild benefit observed was not due to C-alkylation of –OH groups, as the main products observed were dimerization and formation of iron complexes. Only benzylic alcohols in bitumen and asphaltenes would be converted by *o*-xylene. Intermolecular addition reactions could explain the asphaltenes content increase of bitumen and asphaltenes. The mild benefit obtained with alkylation of *o*-xylene (aromatic) with asphaltenes (alkylating agent) could be due to cleavage of ether bonds by $FeCl_3$ catalyst followed by C-alkylation of *o*-xylene as demonstrated by model conversion of dibenzyl ether. Alkylation of dibenzyl ether with methanol resulted in gum formation, rearragment products, and smaller molecules such as benzaldehyde.

b) O-alkylation of asphaltenes with methanol using $FeCl_3$ catalyst did not converted asphaltenes to maltenes and coke yield was increased compared to raw asphaltenes. Even though model conversion of 2-naphthol resulted in methyl ethers, there were side-reactions such as chlorination, metal coordination, and dimerization.

c) During Friedel-Crafts alkylation studies it was observed that $FeCl_3$ participated in reactions such as halogenation and metal coordination, which indicated that metal halides in general

used during bitumen conversion processes, may affect the chemistry of the conversion in ways not previously appreciated. This result is of potential significance to the oilsands industry, as the participation of metal chloride catalysts in the chemistry of oil, such as halogenation of the oil by the metal chlorides, was not appreciated before. This opens a new topic for future investigation to understand the type of chemistry involved. In particular, it would be important to determine whether this type of chemistry is restricted to acidic metal halides like $FeCl_3$, or whether it is caused by a wider range of metal halides and has just not been recognized before due to the complexity of oil composition.

9.2.3 Donor-Aceptor Reaction by Acid Treatment

It was proposed that the removal of metals, or exchange of multivalent metals with monovalent ions, would decompose metal-bridged structures into smaller molecular, or ionic fragments. Metals removal by acid washing was reported in the coal literature, but little could be found on acid washing of oil. Insights from the coal literature were applied to oilsands upgrading and the main results are presented:

a) The results showed that multivalent metals were removed from bitumen, maltenes, and asphaltenes with acid washing. The total multivalent metals removed from asphaltenes were around 2600 $\mu g \cdot g^{-1}$ (56 $\mu mol \cdot g^{-1}$) and only part of the metals was present in the connate water. The removal of multivalent metals resulted in about 8 % conversion of asphaltenes into maltenes, which could be explained by the disruption of larger metal-bridged structures and formation of smaller molecules, as well as hydrolysis of esters. Demetalation also caused a decrease in the micro carbon residue of the acid washed asphaltenes compared to the raw asphaltenes.

b) This study also provided some insight into the pH-sensitive nature of emulsion formation and acid-base chemistry of oilsands materials. Increased emulsion formation due to water washing was explained in terms of the acid-base conversion of weakly acidic functional groups, such as the conversion of phenols to phenoxides, which are more hydrophilic. It was also suggested that unequal partitioning of acidic and basic functional groups between the

subfractions of bitumen (i.e. asphaltenes and maltenes) could explain the detrimental impact of acid washing of bitumen, compared to the neutral or beneficial impact on the subfractions.

c) This work showed another influence of HCl in bitumen upgrading. During coking process HCl is formed through the hydrolysis of chloride salts and it may affect the chemistry during coking by hydrolyzing ester bonds and demetalating metal-bridge structures in bitumen.

9.3 Suggested Future Work

a) Mild bromination of asphaltenes not only increased its hardness, but it also increased its solvent resistance. The economic viability as well as feasibility of using mild halogenation to produce road paving asphalt compared to oxidation could be evaluated. Severe halogenation had been considered before, but the work that was presented showed that only mild halogenation is needed.

b) Potential role of chlorides and chloride salts in coke formation during oilsands upgrading was presented. A set of experiments could be performed to investigate in detail the change in coke formation when chlorides are present during the coking process. In addition it would be worthwhile to employ model compounds at industrially relevant conditions to understand the chemistry involved and the nature of molecules that would be affected. Halogens are widely studied in organic chemistry, but only infrequently at high temperatures and pressures.

c) Friedel-Crafts alkylation using $FeCl_3$ as catalyst showed that a portion of the halides could be transferred to bitumen by forming organohalides. The influence of halide transfer to bitumen could be investigated in more detail. Moreover, determination whether only acidic metal halides are involved in halide transfer, could also be studied. There is already a large body of literature on the catalysis of metal halides. It is proposed that a thorough review of the literature (especially older literature) be undertaken first.

d) As $FeCl_3$ catalyst caused cleavage of ether bonds, over conversion of –OH groups, different catalysts and alkylating agents could be investigated to convert –OH groups and consequently disrupt hydrogen bonding. As it was observed in Chapter 4, hydrogen bonding may

contribute to asphaltenes hardness and disruption of such interactions may help convert asphaltenes into maltenes.

9.4 Presentations and Publications

A list of publications and presentations in conferences related to the work obtained during the doctorate research is described as follows:

1. **PRADO, G. H. C.** and DE KLERK, A. Alkylation of asphaltenes using a $FeCl_3$ catalyst, *Energy & Fuels* 2015, DOI: 10.1021/acs.energyfuels.5b01292.

2. **PRADO, G. H. C.** and DE KLERK, A. Halogenation of oilsands bitumen, maltenes, and asphaltenes. *Energy & Fuels* **2014**, 28(7), 4458-4468.

3. **PRADO, G. H. C.** and DE KLERK, A. Origin of halogenated bitumen and asphaltenes hardness", Paper submitted for publication to *Energy & Fuels*.

4. **PRADO, G. H. C.** and DE KLERK, A. Demetalation of Metallophthalocyanines by Mild Halogenation without Disrupting the Tetrapyrrole Macrocycle, Paper accepted for publication in *Fuel*.

5. **PRADO, G. H. C.** and DE KLERK, A. Metals removal from oilsands bitumen and subfractions by acid washing, Paper submitted for publication to *Energy & Fuels*.

6. **PRADO, G. H. C.** and DE KLERK, A. Upgradeability of halogenated asphaltenes into liquid fuels. In: 1st Symposium on Halogen Bonding, 2014, Porto Cesareo, Italy.

7. **PRADO, G. H. C.** and DE KLERK, A. Alkylation of oilsands bitumen and asphaltenes using homogenous catalyst. In: 23rd Canadian Symposium on Catalysis, 2014, Edmonton, Canada.

8. **PRADO. G. H. C.** and DE KLERK, A. Potential role of chloride salts in bitumen upgrading. In: Oilsands 2014 Conference, 2014, Edmonton, Canada.

9. **PRADO, G. H. C.** and DE KLERK, A. Asphaltenes conversion by halogenation. In: 63rd Canadian Chemical Engineering Conference, 2013, Fredericton, Canada.

References

Acevedo, S.; Escobar, G.; Ranaudo, M.A.; Rizzo, A. Molecular weight properties of asphaltenes calculated from GPC data for octylated asphaltenes. *Fuel* **1998**, *77*, 853-858.

Acree Jr., W. E. Thermodynamic properties of organic compounds: enthalpy of fusion and melting point temperature compilation. *Thermochim. Acta* **1991**, *189*, 37-56.

Adams, J. J.; Schabron, J. F. The role of asphaltenes in oil and water emulsions. *Prepr. Pap.-Am. Chem. Soc., Div. Energy Fuels* **2015**, *60 (1)*, 1-2.

Adamski, R. P.; Komishke, B. D.; Long, Y.; Munsterman, W.; Niemiec, M.; Smith, T. R.; Troxler, B. M. Treatment of oil sand bitumen to produce low calcium bitumen. Pat. Appl. CA 2755518 A1 (Shell), 2012.

Agrawala, M. and Yarranton, H. W. An Asphaltene association model analogous to linear polymerization. *Ind. Eng. Chem. Res*. **2001**, *40*, 4664-4672.

Ali, M. F.; Abbas, S. A review of methods for the demetalization of residual fuel oils. *Fuel Process. Technol.* **2006**, *87*, 573-584.

Ancheyta, J.; Trejo, F.; Rana, M. S. *Asphaltenes. Chemical transformation during hydroprocessing of heavy oils*; CRC Press: Boca Raton, 2009.

Asinger, F. *Mono-olefins. Chemistry and technology*. Pergamon Press: Oxford. 1968; pp. 606-608, 722-723.

Asphaltenes, heavy oils, and petroleomics; Mullins, O. C., Sheu, E. Y., Hammami, A., Marshall, A. G. Eds.; Springer: New York, 2007.

Baldwin, R. M.; Kennar, D. R.; Nguanprasert, O.; Miller, R. L. Liquefaction reactivity enhancement of coal by mild alkylation and solvent swelling techniques. *Fuel* **1991**, *70*, 429-433.

Barrett, P. A., Bradbrook, E. F., Dent, C. E., Linstead, R. P. Phthalocyanines and related compounds. Part XVI. The halogenation of phthalocyanines. *J. Chem. Soc*. **1939**, 1820-1828.

Becker, J. R. *Crude oil. Waxes, emulsions, and asphaltenes*; PennWell: Tulsa, OK, 1997.

Berezin, B, D. Coordination compounds of porphyrins and phthalocyanines. Chichester: John Wiley and Sons; 1981.

Blanksby, T. J. and Ellison, G. B. Bond dissociation energies of organic molecules. *Acc. Chem. Res*. **2003**, *36*, 255-263.

Bondi, A. *Physical properties of molecular crystals, liquids, and glasses*; Wiley: New York, 1968.

Bonnett, R., Gale, I. A. D., Stephenson, G. F. The *meso*-reactivity of porphyrins and related compounds. Part II. Halogenation. *J. Chem. Soc. (C)* **1966**, 1600-1604.

Bonnett, R., Harriman, A., Kozyrev, A. N. Photophysics of halogenated porphyrins. *J. Chem. Soc. Perkin. Trans*. **1992**, 88, 763-769.

Boucher, J. L.; Wang, I.-H.; Martinez, D. F. Elimination chemistry in asphalt. *Prepr. Pap.-Am. Chem. Soc., Div. Petrol. Chem.* **1990**, *35* (3), 550-555.

Brussee, J.; Jansen, A. C. A. A highly stereoselective synthesis of S(–)-[1,1'-binaphthalene]-2,2'-diol. *Tetrahedron Lett.* **1983**, *24*, 3261-3262.

Buchler, J. W. Static coordination chemistry of metalloporphyrins. In *Porphyrins and Metalloporphyrins*; Smith, K. M., Ed.; Elsevier: Amsterdam, 1975, p. 157.

Cagniant, D.; Nosyrev, I.; Cebolla, V.; Vela, J.; Membrado, L.; Gruber, R. Structural modifications of petroleum asphaltenes by reductive alkylation investigated by TLC-FID. *Fuel* **2001**, *80*, 107-115.

Cazorla, C.; Pfordt, É.; Duclos, M-C.; Métay, E.; Lemaire, M. O-Alkylation of phenol derivatives *via* a nucleophilic substitution. *Green Chem*. **2011**, *13*, 2482.

Chorghade, M. S.; Dolphin, D.; Dupré, D.; Hill, D. R.; Lee, E. C.; Wijesekera, T. P. Improved protocols for the synthesis and halogenation of sterically hindered metalloporphyrins. *Synthesis* **1996**, *11*, 1320-1324.

Chumakov, D. E, Khoroshutin, A. V, Anisimov AV, Kobrakov KI. Bromination of porphyrins (Review). *Chem. Heterocyclic Compounds* **2009**, *45*, 259-283.

Colthup, N. B.; Daly, L. H.; Wiberley, S. E. *Introduction to infrared and Raman spectroscopy*, 3ed; Academic Press: San Diego, CA, 1990.

Crampton, M. R. Acidity and hydrogen-bonding. In *The chemistry of the thiol group. Part 1*; Patai, S. Ed.; Interscience: London, 1974, pp. 379-415.

Darwent, De deB. Bond dissociation energy in simple molecules. National Standard Reference Data System. (Online) NRSDS-NBS 31: Washington, DC. 1970, p. 19. http://www.nist.gov/data/nsrds/NSRDS-NBS31.pdf. (Accessed October 30, 2014).

De Klerk, A.; Gray, M. R.; Zerpa, N. Unconventional oil and gas: Oilsands. In *Future energy. Improved, sustainable and clean options for our planet*, 2ed; Letcher, T. M. Ed.; Elsevier: Amsterdam, 2014.

De La Mare, P. B. D. and Ridd, J. H. *Aromatic substitution: nitration and halogenation*. Butterworths Scientific Publications: London, 1959; pp. 5-25, 105-209.

Dechaine, G. P. and Gray, M. R. Chemistry and association of vanadium compounds in heavy oil and bitumen, and implications for their selective removal. *Energy Fuels* **2010**, *24*, 2795-2808.

Desando, M. A.; Ripmeester, J. A. Chemical derivatization of Athabasca oilsand asphaltene for analysis of hydroxyl and carbonyl groups via nuclear magnetic resonance spectroscopy. *Fuel* **2002**, *81*, 1305-1319.

Desijaru, G. R.; Ho, P. S.; Kloo, L.; Legon, A. C.; Marquardt, R.; Metrangolo, P.l Politzer, P.; Resnati, G.; Rissanen, K. Definition of the halogen bonding (IUPAC recommendations 2013). *Pure Appl. Chem*. **2013**, *85*, 1711-1713.

Di Carlo, G., Biroli, A.O., Tessore, F., Rizzato, S., Forni, A., Magnano, G., Pizzotti, M. Light-induced regiospecific bromination of *meso*-tetra(3,5-di-tertbutylphenyl) porphyrin on 2,12 β-pyrrolic positions. *J. Org. Chem*. **2015**, 80, 4973-4980.

Dolphin, D.; Wick, A. *Tabulation of infrared spectral data*; Wiley: New York, 1977.

Emanuel, N. M.; Zaikov, G. E.; Maizus, Z. K. *Oxidation of organic compounds. Medium effects in radical reactions*; Pergamon Press: Oxford, 1984.

Ernst, L.; Schulz, P. ^{13}C and ^{1}H NMR chemical shift assignments of 1- and 2-alkylnaphthalenes (R= Me, Et, i-Pr, t-Bu) and determination of substituent effects on ^{13}C and ^{1}H chemical shifts. *Magnetic Resonance in Chemistry* **1992**, *30*, 73-76.

Falk, J. E. Porphyrins and Metalloporphyrins. Elsevier: New York, 1964, pp. 72-80, 88-89.

Filby. R. H. and Van Berkel, G. J. Geochemistry of metal complexes in petroleum, source rocks, and coals: an overview. In *Metal Complexes in Fossil Fuels*; Comstock, M. J., Ed.; American Chemical Society: Washington, DC, 1987; p. 14.

Fine, D.A. Tetrahedral bromide complexes of nickel(II) in organic solvents. *Inorg. Chem*. **1965**, 345-350.

Firouzabadi, H.; Iranpoor, N.; Kazemi, S. Direct halogenation of organic compounds with halides using oxone in water – a green protocol. *Can. J. Chem*. **2009**, *87*, 1675-1681.

Fontana, A.; Toniolo, C. Detection and determination of thiols. In *The chemistry of the thiol group. Part 1*; Patai, S. Ed.; Interscience: London, 1974, pp. 271-324.

Frakman, Z.; Ignasiak, T. M.; Lown, E. M.; Strausz, O. P. Oxygen compounds in Athabasca asphaltene. *Energy Fuels* **1990**, *4*, 263-270.

Friberg, S. E. Micellization. In *Asphaltenes, heavy oils, and petroleomics*, Mullins, O. C.; Sheu, E. Y.; Hammami, A.; Marshall, A. G., Eds.; Springer: New York, 2007; pp. 189-203.

Fritz, J. S. Detection and estimation of ethers. In *The chemistry of the ether linkage*; Patai, S. Ed.; Interscience: London, 1967, pp. 669-680.

García Zapata, J. L.; De Klerk, A. Viscosity changes during mild oxidation of oilsands-derived bitumen: Solvent effects and selectivity. *Energy Fuels* **2014**, *28*, 6242-6248.

Gehrold, A.C., Bruhn, T., Schneider, H., Radius, U., Bringmann, G. Chiral and achiral basket-handle porphyrins: short synthesis and stereostructures of these versatile building blocks. *Org. Lett*. **2015**, 17, 210-213.

Gill, N.S., Nyholm, R.S. Complex halides of the transition metals. Part I. Tetrahedral nickel complexes. *J. Chem. Soc*. **1959**, 3997-4007.

Gonzalez, V.; De Klerk, A.; Yang, S.; Prasad, V. Influence of acid chemistry on bitumen viscosity. *Prepr. Pap.-Am. Chem. Soc., Div. Energy Fuels* **2015**, *60* (1), 9-12.

Gray, M. R. and McCaffrey, W. C. Role of chain reactions and olefin formation in cracking, hydroconversion, and coking of petroleum and bitumen fractions. *Energy Fuels* **2002**, *16*, 756-766.

Gray, M. R. Consistency of asphaltenes chemical structures with pyrolysis and coking behavior. *Energy Fuels* **2003**, *17*, 1566-1569.

Gray, M. R. *Fundamentals of oilsands upgrading*. University of Alberta: Edmonton, AB, 2010.

Gray, M. R. *Upgrading oilsands bitumen and heavy oil*; University of Alberta Press: Edmonton, AB, 2015.

Gray, M. R.; Eaton, P. E.; Le, T. Kinetics of hydrolysis of chloride salts in model crude oil. *Petroleum Science and Technology* **2008**, *26*, 1924-1933.

Gray, M. R.; Tykwinski, R. R.; Stryker, J. M., Tan, X. Supramolecular assembly model for aggregation of petroleum asphaltenes. *Energy Fuels* **2011**, *25*, 3125-3134.

Griffiths TR, Phillips NJ. The nickel(II)-bromide system in dimethyl sulphoxide: a detailed study of the influences of temperature and mole ratio. *J Chem Soc Dalton Trans* **1989**, *2*, 325-330.

Groenzin, H. and Mullins, O. C. Asphaltene molecular size and weight by time-resolved fluorescence depolarization. In *Asphaltenes, Heavy oils, and Petroleomics*, Mullins, O. C.; Sheu, E. Y.; Hammami, A.; Marshall, A. G., Eds.; Springer: New York, 2007; pp. 17-62.

Groenzin, H. and Mullins, O. C. Molecular size and structure of asphaltenes from various sources. *Energy Fuels* **2000**, *14*, 677-684.

Gruse, W. A.; Stevens, D. R. *Chemical technology of petroleum*, 3ed; McGraw-Hill: New York, 1960, pp. 10-12.

Guo, H.; Jiang, J.; Shi, Y.; Wang, Y.; Liu, J.; Dong, S. UV-Vis spectrophotometric titrations and vibrational spectroscopic characterization of *meso*-(*p*-hydroxyphenyl)porphyrins. *J. Phys. Chem. B* **2004**, *108*, 10185-10191.

Hambright, P. Dynamic Coordination Chemistry of Metalloporphyrins. In Falk, J.E., Smith, K.M., editors. Porphyrins and Metalloporphyrins, Elsevier: Amsterdam; 1975, p 233-278.

Hartough, H. D.; Meisel, S. L. *Compounds with condensed thiophene rings*; Interscience: New York, 1954, pp. 242-247.

Helfferic, F. *Ion exchange*. McGraw-Hill Book Company, Inc.: New York, 1962, pp. 5-9.

Hepworth, J. D.; Waring, D. R.; Waring, M. J. *Aromatic chemistry*. The Royal Society of Chemistry: Cambridge, 2002; pp. 1-37; 129-134.

Hocking, M. B.; Lee, G. W. Effect of chemical agents on settling rates of sludges from effluent of hot-water extraction of Athabasca oilsands. *Fuel* **1977**, *56*, 325-333.

Höhne, G. W. H.; Hemminger, W. F.; Flammersheim, H.-J. *Differential scanning calorimetry*, 2ed; Springer: Berlin, 2003.

Ignasiak, T.; Bimer, J.; Samman, N.; Montgomery, D. S.; Strausz, O. P. Lewis acids assisted degradation of Athabasca asphaltene. *Adv. Chem. Ser.* **1981**, *195*, 183-201.

Ignasiak, T.; Kemp-Jones, A. V.; Strausz, O. P. The molecular structure of Athabasca asphaltene. Cleavage of the carbon-sulfur bonds by radical ion electron transfer reactions. *J. Org. Chem.* **1977**, *42*, 312-320.

Iovel, I.; Mertins, K.; Kischel, J.; Zapf, A.; Beller, M. An efficient and general iron-catalyzed arylation of benzyl alcohols and benzyl carboxylates. *Angew. Chem. Int.* **2005**, *44*, 3913-3917.

Jacobs, F. S.; Filby, R. H. Solvent extraction of oil-sand components for determination of trace elements by neutron activation analysis. *Anal. Chem.* **1983**, *55*, 74-77.

Jaffé, H. H.; Orchin, M. *Theory and applications of ultraviolet spectroscopy*; John Wiley & Sons: New York, 1962, p. 187

Jiménez-Mateos, J. M.; Quintero, L. C.; Rial, C. Characterization of petroleum bitumens and their fractions by thermogravimetric analysis and differential scanning calorimetry. *Fuel* **1996**, *75*, 1691-1700.

Jin, L-M., Yin, J-J., Chen, L., Guo, C-C., Chen, Q-Y. Metal dependent halogenation and/or coupling reactions of porphyrins with $PhIX_2$ (X=Cl, F). *Synlett* **2005**, 19, 2893-2898.

Johnson, F. Reactions of ethers and cyclic ethers. In *Friedel-Crafts and related reacions. Vol. IV*; Olah, G. A Ed.; Interscience: New York, 1965, pp. 1-109.

Joseph, J. T.; Forrai, T. R. Effect of exchangeable cations on liquefaction of low rank coals. *Fuel* **1992**, *71*, 75-80.

Juyal, P.; McKenna, A. M.; Fan, T.; Cao, T.; Rueda-Velásquez, R. I.; Fitzsimmons, J. E.; Yen, A.; Rodgers, R. P.; Wang, J.; Buckley, J. S.; Gray, M. R.; Allenson, S. J.; Creek, J. A joint industrial case study for asphaltene deposition. *Energy Fuels* **2013**, *27*, 1899-1908.

Katritzky, A. R.; Hitchings, G. J.; King, R. W.; Zhu, D. W. ^{1}H and ^{13}C Nuclear magnetic resonance studies of ethenyl-substituted benzenoid aromatic compounds. *Magnetic Resonance in Chemistry* **1991**, *29*, 2-8.

Kopsh, H. On the thermal behaviour of petroleum asphaltenes. *Thermochimica Acta* **1994**, *235*, 271-275.

Kovacic, P. Reactions of aromatics with Lewis acid metal halides. In *Friedel-Crafts and related reacions. Vol. IV*; Olah, G. A Ed.; Interscience: New York, 1965, pp. 111-126.

Kowanko, N.; Branthaver, J. F.; Sugihara, J. M. Direct liquid-phase fluorination of petroleum. *Fuel* **1978**, *57*, 769-775.

Krishna Mohan, K. V. V. and Narender, N. Ecofriendly oxidative nuclear halogenation of aromatic compounds using potassium and ammonium halides. *Synthesis* **2012**, *44*, 15-26.

Kumar, M. A.; Rohitha, C. N.; Kulkarni, S. J.; Narender, N. Bromination of aromatic compounds using ammonium bromide and oxone®. *Synthesis* **2010**, *10*, 1629-1632.

Lee, K-J.; Cho, H. K., Song, C-E. Bromination of activated arenes by oxone® and sodium bromide. *Bull. Korean Chem. Soc*. **2002**, *23*, 773-775.

Li, H., Lu, Y., Liu, Y., Zhu, X., Liu, H., Zhu, W. Interplay between halogen bonds and π-π stacking interactions: CSD search and theoretical study. *Phys. Chem. Chem. Phys.* **2012**, *14*, 9948-9955.

Li, X.; Bai, Z-Q.; Bai, J.; Zhao, B-B.; Li, P.; Han, Y-N.; Kong, L-X.; Li, W. Effect of Ca^{2+} species with different modes of occurrence on direct liquefaction of a calcium-rich lignite. *Fuel Process. Technol.* **2015**, *133*, 161-166.

Li, Z.; Duan, Z.; Kang, J.; Wang, H.; Yu, L.; Wu, Y. A simple access to triarylmethane derivatives from aromatic aldehydes and electron-rich arenes catalyzed by $FeCl_3$. *Tetrahedron* **2008**, *64*, 1924-1930.

Long, R. B. The concept of asphaltenes. In *Chemistry of Asphaltenes*; Bunger, J. W. and Li, N. C., Eds.; ACS Advances in Chemistry Series 195; American Chemical Society: Washington, DC, 1981; pp. 17-27.

Mantri, K.; Komura, K.; Kubota, Y.; Sugi, Y. Friedel-Crafts alkylation of aromatics with benzyl alcohols catalyzed by rare earth metal triflates supported on MCM-41 mesoporous silica. *Journal of Molecular Catalysis A: Chemical* **2005**, *236*, 168-175.

March, J. *Advanced Organic Chemistry: Reactions, Mechanisms, and Structure*. John Wiley & Sons: New York, 1992; pp. 501-568.

Marsden, J. O. and House, C. I. *The Chemistry of Gold Extraction. Society for Mining, Metallurgy, and Exploration*, Inc.: Littleton, US-CO, 2006, p. 322.

Masliyah, J. H.; Czarnecki, J. A.; Xu, Z. *Handbook on Theory and Practice of Bitumen Recovery from Athabasca Oilsands. Theoretical basis*. Kingsley Publishing Services: Canada, 2011; Volume I, pp. 1-49; 361-372.

Masson, J-F.; Collins, P.; Polomark, G. Steric hardening and the ordering of asphaltenes in bitumen. *Energy Fuels* **2005**, *19*, 120-122.

Masson, J-F.; Leblond, V.; Margeson, J.; Bundalo-Perc, S. Low-temperature bitumen stiffness and viscous paraffinic nano- and micro-domains by cryogenic AFM and PDM. *J. Microscopy* **2007**, *227* (3), 191-202.

Masson, J-F.; Polomark, G.; Collins, P. Time-dependent microstructure of bitumen and its fractions by modulated differential scanning calorimetry. *Energy Fuels* **2002**, *16*, 470-476.

McGlynn, S. P. In *Donor-Acceptor Interaction*. Radiation Research, Supplement 1, 1959 - Proceedings of the International Congress of Radiation Research; Smith, D. E., Ed.; Academic Press: New York, 1959, p. 302.

Miyake, M.; Stock, L. M. Coal solubilization. Factors governing successful solubilization through C-alkylation. *Energy Fuels* **1988**, *2*, 815-818.

Moschopedis, S. E. and Speight, J. G. Introduction of halogen into asphaltenes via the gomberg reaction. *Fuel* **1970**, *49*, 335.

Moschopedis, S. E. and Speight, J. G. The Halogenation of athabasca asphaltenes with elemental halogen. *Fuel* **1971a**, *50*, 58-64.

Moschopedis, S. E. and Speight, J. G. Water-soluble derivatives of athabasca asphaltenes. *Fuel* **1971b**, *50*, 34-40.

Moschopedis, S. E.; Speight, J. G. Chemical modification of bitumen heavy ends and their nonfuel uses. *Adv. Chem. Ser.* **1976**, *151*, 144-152.

Moser, F.H., Thomas, A.L. Phthalocyanine compounds (ACS Monograph Ser. 157). New York: Reinhold Publ. Corp.; 1963.

Moschopedis, S. E.; Speight, J. G. Oxygen functions in asphaltenes. *Fuel* **1976**, *55*, 334-336.

Mullins, O. C. Review of the molecular structure and aggregation of asphaltenes and petroleomics. *SPE Journal* **2008**, *13*, 48-57.

Mullins, O. C. The Asphaltenes. *Annu. Rev. Anal. Chem*. **2011**, 4, 393-418.

Narender, N.; Srinivasu, P.; Kulkarni, S. J.; Raghavan, K. V. Regioselective oxyiodination of aromatic compounds using potassium iodide and oxone®. *Synthetic Communications* **2002a**, *32* (15), 2319-2324.

Narender, N.; Srinivasu, P.; Prasad, M. R.; Kulkarni, S. J.; Raghavan, K. V. An efficient and regioselective oxybromination of aromatic compounds using potassium bromide and oxone®. *Synthetic Communications* **2002b**, *32* (15), 2313-2318.

Narender, N.; Srinivasu, P.; Prasad, M. R.; Kulkarni, S. J.; Raghavan, K. V. Highly efficient, para-selective oxychlorination of aromatic compounds using potassium chloride and oxone®. *Synthetic Communications* **2002c**, *32* (2), 279-286.

Nelson, W. L. *Petroleum refinery engineering*, 3ed; McGraw-Hill: New York, 1949, p. 100.

Newkome, G. R. and Paudler, W. W. *Contemporary Heterocyclic Chemistry: Syntheses, Reactions, and Applications*. John Wiley & Sons: New York, 1982; pp. 92-112; 121-158.

Nicholls, D. Complexes and first-row transition elements; Macmillan: London, 1974, p. 95.

Oder, R. R. Magnetic desulfurization of coal. In *Processing and utilization of high sulfur coals* (Coal Sci. Technol. 9); Attia, Y. A. Ed.; Elsevier: Amsterdam, 1985, pp. 195-214.

Olah, G. A.; Krishnamurti, R.; Surya Prakash, G. K. Friedel-Crafts alkylations. In *Comprehensive Organic Synthesis*, Trost, B. M., Krishnamurti, R., Surya Prakash, G. K., Eds. Elsevier: 1991, 293-339.

Painter, P.; Veytsman, B.; Youtcheff, J. Guide to asphaltene solubility. *Energy Fuels* **2015**, *29*, 2951-2961.

Parsons, A. F. *An introduction to free radical chemistry*; Blackwell Science: Oxford, 2000, p. 124.

Patinkin, S. H. and Friedman, B. S. Alkylation of aromatics with alkenes and alkanes. In *Friedel-Crafts and related reactions part I*, 1st ed.; Olah, G. A., Ed. John Wiley & Sons: New York, 1964, pp. 24-27.

Patwardhan, S. R. Chlorination of petroleum bitumens. *Fuel* **1979**, *58*, 375-378.

Peng, P.; Morales-Izquierdo, A.; Hogg, A.; Strausz, O. P. Molecular structure of Athabasca asphaltene: Sulfide, ether, and ester linkages. *Energy Fuels* **1997**, *11*, 1171-1187.

Perego, C. and Ingallina, P. Recent advances in the industrial alkylation of aromatics: new catalysts and new processes. *Cataysis Today* **2002**, *73*, 3-22

Petersen, J. C. Asphalt oxidation - an overview including a new model for oxidation proposing that physicochemical factors dominate the oxidation kinetics. *Fuel Sci. Technol. Int.* **1993**, *11*, 57-87.

Pfeiffer, J. P. H. and Saal, R. N. J. Asphaltic bitumen as colloid system. *The Journal of Physical Chemistry* **1940**, *44* (2), 139-149.

Pimentel, G. C.; McClellan, A. L. *The Hydrogen Bond*; W. H. Freeman and Company: New York, 1960, pp. 35-36, 157-166, 255.

Pinkston, D. S.; Duan, P.; Gallardo, V. A.; Habicht, S. C.; Tan, X.; Qian, K.; Gray, M. R.; Mullen, K.; Kenttämaa, H. I. Analysis of asphaltenes and asphaltene model compounds by laser-induced acoustic desorption/Fourier transform ion cyclotron resonance mass spectrometry. *Energy Fuels* **2009**, *23*, 5564-5570.

Prado, G. H C. and De Klerk, A. Halogenation of oilsands bitumen, maltenes, and asphaltenes. *Energy & Fuels* **2014**, *28*, 4458-4468.

Purcell, J. M.; Juyal, P.; Kim, D-G.; Rodgers, R. P.; Hendrickson, C. L.; Marshall, A. G. Sulfur speciation in petroleum: Atmospheric pressure photoionization or chemical derivatization and electrospray ionization Fourier transform ion cyclotron resonance mass spectrometry. *Energy Fuels* **2007**, *21*, 2869-2874.

Rahman, M.; Adesanwo, T.; Gupta, R.; De Klerk, A. Effect of direct coal liquefaction conditions on coal liquid quality. *Energy Fuels 2015*, *29*, (in press, ef5b00566).

Rana, M. S.; Sámano, V.; Ancheyta, J.; Diaz, J. A. I. A review of recent advances on processing technologies for upgrading of heavy oils and residua. *Fuel* **2007**, *86*, 1216-1231.

Rankel, L.A. Degradation of metalloporphyrins in heavy oils before and during processing. Effect of heat, air, hydrogen, and hydrogen sulfide on petroporphyrin species. *ACS Symp. Ser.* **1987**, 344, 257-264.

Reynolds, J.G. Nickel in petroleum refining. *Petrol. Sci. Technol*. **2001**, *19*, 979-1007.

Roberts, R. M. and Khalaf, A. A. *Friedel-Crafts Alkylation Chemistry*. Marcel Dekker, Inc.: New York, 1984; pp. 1-6.

Rochut, S.; Roithová, J.; Schröder, D.; Novara, F. R.; Schwarz, H. Gaseous iron(II) and iron(III) complexes with BINOLate ligands. *J. Am. Soc. Mass Spectrom.* **2008**, *19*, 121-125.

Rojas, A.; Orozco, E. Measurement of the enthalpies of vaporization and sublimation of solids aromatic hydrocarbons by differential scanning calorimetry. *Thermochim. Acta* **2003**, *405*, 93-107.

Rumyantseva, V.D., Aksenova, E.A., Ponamoreva, O.N., Mironov, A.F. Halogenation of metalloporphyrins. *Russ. J. Bioorg. Chem*. **2000**, 26, 423-428.

Sabbah, H.; Morrow, A. L.; Pomerants, A. E.; Zare, R. N. Evidence for island structures as the dominant architecture of asphaltenes. *Energy Fuels* **2011**, *25*, 1597-1604.

Sasaki, M.; Kotanigawa, T.; Yoshida, T. Liquefaction reactivity of methylated Illinois No.6 coal. *Energy Fuels* **2000**, *14*, 76-82.

Satake, T.; Sano, K.; Domoto, T.; Kubota, S. Method for refining heavy oils using acidic water. Pat. JP 07034072 (Satake Giken), 1995.

Scheer, H.; Katz, J. J. In Smith, K.M, editor. Porphyrins and metalloporphyrins. A new edition based on the original volume by J. E. Falk, Amsterdam: Elsevier; 1975, p. 410.

Schlosberg, R. H.; Neavel, R. C.; Maa, P. S.; Gorbaty, M. L. Alkylation: a beneficial pretreatment for coal liquefaction. *Fuel* **1980**, *59*, 45-47.

Schriesheim, A. Alkylation of aromatics with alcohols and ethers. In *Friedel-Crafts and Related Reactions. Part I*; Olah, G. A., Ed.; Jhon Wiley & Sons: New York, 1964, pp. 486-533.

Shams, K.; Miller, R. L.; Baldwin, R. M. Enhanced low severity coal liquefaction using selective calcium removal. *Prepr. Pap.-Am. Chem. Soc., Div. Fuel. Chem.* **1992**, *37* (2), 1017-1024.

Sharma, A. and Mullins, O. C. Insights into molecular and aggregate structures of asphaltenes using HRTEM. In *Asphaltenes, Heavy oils, and Petroleomics*, Mullins, O. C.; Sheu, E. Y.; Hammami, A.; Marshall, A. G., Eds.; Springer: New York, **2007**; pp. 205-257.

Sheremata, J. M; Gray, M. R.; Dettman, H. D.; McCaffrey, W. C. Quantitative molecular representation and sequential optimization of athabasca asphaltenes. *Energy Fuels* **2004**, 18, 1377-1384.

Siddiqui, M. N. Alkylation and oxidation reactions of Arabian asphaltenes. *Fuel* **2003**, *82*, 1323-1329.

Siddiqui, M. N. Exploring the chemical reactivity of asphaltenes. *Prepr. Pap.-Am. Chem. Soc., Div. Fuel Chem.* **2009**, *54*(1), 14-15.

Siggia, S.; Hanna, J. G.; Stengle, T. R. Detection and determination of hydroxyl groups. In *The chemistry of the hydroxyl group. Part 1*; Patai, S. Ed.; Interscience: London, 1971, pp. 295-326.

Sill, G. A.; Yen, T. F. Semiconduction of iodine complexes of asphaltenes. *Fuel* **1969**, *48*, 61-74.

Silverstein, R. M.; Webster, F. X. *Spectrometric identification of organic compounds*, 6ed; John Wiley & Sons: New York, 1997.

Şimşek, E. H.; Karaduman, A.; Çalışkan, S.; Togrul, T. The effect of preswelling and/or pretreatment of some turkish coals on the supercritical fluid extract yield. *Fuel* **2002**, *81*, 503-506.

Slickers, K. *Automatic atomic-emission-spectroscopy*, 2ed; Brühlsche Universitätsdruckerei: Giessen, 1993.

Smith, J. W. Hydrogen-bonding and complex-forming properties. In *The chemistry of the carbon-halogen bond. Part 1*; Patai, S., Ed.; John Wiley and Sons: London, 1973, pp. 265-300.

Smith, M. B. *March's advanced organic chemistry. Reactions, mechanisms and structure,* 7th ed; Jhon Wiley & Sons: Hoboken, 2013, pp. 570.

Sorrel, S.; Speirs, J.; Bentley, R.; Miller, R.; Thompson, E. Shaping the global oil peak: a review of the evidence on field sizes, reserve growth, decline rates and depletion rates. *Energy* **2012**, *37*, 709-724.

Speight, J. G. and Moschopedis, S. E. On the molecular nature of petroleum asphaltenes. In *Chemistry of Asphaltenes*; Bunger, J. W., Li, N. C., Eds.; ACS Advances in Chemistry Series 195; American Chemical Society: Washington, DC, 1981; pp. 17-27.

Speight, J. G. Reactions of Athabasca asphaltenes and heavy oil with metal chlorides. *Fuel* **1971**, *50*, 175-186.

Sternberg, H. W. Second look at the reductive alkylation of coal and at the nature of asphaltenes. *Am Chem Soc Div Chem Prepr* **1976**, *21*(7), 1-10.

Sternberg, H. W.; Delle Donne, C. L. Solubilization of coals by reductive alkylation. *Fuel* **1974**, *53*, 172-175.

Strausz, O. P., Mojelsky, T. W., Lown, E. M. The molecular structure of asphaltene: an unfolding story. *Fuel* **1992**, *71* (12), 1355-1363.

Strausz, O. P.; Lown, E. M. *The Chemistry of Alberta Oilsands, Bitumens, and Heavy Oils*. Alberta Energy Research Institute: Calgary, AB, 2003; pp. 459-662.

Strausz, O. P.; Safaraki, I.; Lown, E. M.; Morales-Izquierdo; A. A critique of asphaltene fluorescence decay and depolarization-based claims about molecular weight and molecular architecture. *Energy Fuels* **2008**, *22*, 1156-1166.

Sugano, M.; Mashimo, K.; Wainai, T. Structural changes of lower rank coals by cation exchange. *Fuel* **1999**, *78*, 945-951.

Sugihara, J.; Branthaver, J.; Willcox, K. Oxidative demetalation of oxovanadium(IV) porphyrins. In *The role of trace metals in petroleum*; Yen, T. F. Ed.; Ann Arbor Science Publishers: Ann Arbor, MI, 1975, pp. 183-193.

Tamhankar, B. V.; Desai, U. V.; Mane, R. B.; Wadgaonkar, P. P.; Bedekar, A. V. A simple and pratical halogenation of activated arenes using potassium halide and oxone® in water-acetonitrile medium. *Synthetic Communications* **2001**, *31* (13), 2021-2027.

Tanabe, K. and Gray, M. R. Role of fine solids in the coking of vacuum residues. *Energy & Fuels* **1997**, *11*, 1040-1043.

The properties of asphaltic bitumen with reference to its technical applications; Pfeiffer, J. P. Ed.; Elsevier: New York, 1950, pp. 117.

Toulhoat, H., Szymanski, R., Plumail, J.C. Interrelations between initial pore structure, morphology and distribution of accumulated deposits, and lifetimes of hydrodemetallisation catalysts. *Catal. Today* **1990**, 7, 531-568.

Ubbelohde, A. R. *Melting and crystal structure*; Claredon Press: Oxford, 1965.

Van Berkel, G. J.; Filby, R. H. Generation of nickel and vanadyl porphyrins from kerogen during simulated catagenesis. *ACS Symp. Ser.* **1987**, *344*, 110-134.

Van Bodegom, B.; Van Veen, J. A. R.; Van Kessel, G. M. M.; Sinnige-Nijssen, M. W.; Stuiver, H. C. M. Action of solvents on coal at low temperatures. 1. low-rank coals. *Fuel* **1984**, *63*, 346-354.

Vassiliev, N. Y.; Davison, R. R.; Williamson, S. A.; Glover, C. J. Air blowing of supercritical asphalt fractions; *Ind. Eng. Chem. Res.* **2001**, *40*, 1773-1780.

Wachowska, H.; Ignasiak, T.; Strausz, O. P.; Carson, D.; Ignasiaki, B. Application of non-reductive alkylation in liquid ammonia to studies on macromolecular structure of coals and bitumen-derived asphaltene. *Fuel* **1986**, *65*, 1081-1084

Wang, B-Q.; Xiang, S-K.; Sun, Z-P.; Guan, B-T.; Hu, P.; Zhao, K-Q.; Shi, Z-J. Benzylation of arenes through $FeCl_3$ catalyzed Friedel-Crafts reaction via C-O activation of benzyl ether. *Tetrahedron Letters* **2008**, *49*, 4310-4312.

Wiehe, I. A. A phase-separation kinetic model for coke formation. *Ind. Eng. Chem. Res.* **1993**, *32*, 2447−2454.

Wiehe, I. A. *Process chemistry of petroleum macromolecules*; CRC Press: Boca Raton, FL, 2008.

Xie, Y.; Jiang, F.; Xu, J.; Zeng, L.; Dong, B.; Lu, B.; Shang, X. Electrosyntheses and characterization of poly(9-bromophenanthrene) in boron trifluoride diethyl etherate. *Eur. Polym. J.* **2009**, *45*, 418-425.

Yen, T. F. Chemical aspects of metals in native petroleum. In *The role of trace metals in petroleum*; Yen, T. F. Ed.; Ann Arbor Science Publishers: Ann Arbor, MI, 1975, pp. 1-30.

Yin, C.-X.; Stryker, J. M.; Gray, M. R. Separation of petroporphyrins from asphaltenes by chemical modification and selective affinity chromatography. *Energy Fuels* **2009**, *23*, 2600-2605.

Zabicky, J.; Ehrlich-Rogozinski, S. Analysis of organic halogen compounds. In *The chemistry of the carbon-halogen bond. Part 1*; Patai, S., Ed.; John Wiley and Sons: London, 1973, p. 179.

Zachariah, A., Wang, L., Yang, S., Prasad, V., De Klerk, A. Suppression of coke formation during bitumen pyrolysis. *Energy & Fuels* **2013**, *27*, 3061-3070.

Zerpa, N. Creating more value from asphaltenes – the innovation challenge. Nexen Energy ULC bulletin, 2012.

Zhang, Y.; Takanohashi, T.; Sato, S.; Saito, I. Observation of glass transition in asphaltenes. *Energy Fuels* **2004**, *18*, 283-284.

Zielinski, L.; Saha, I.; Freed, D. E.; Hürlimann, M. D. Probing asphaltene aggregation in native crude oils with low-field NMR. *Langmuir* **2010**, *26* (7), 5014-5021.

Appendix A: Support information of Halogenation of Oilsands Bitumen, Maltenes, and Asphaltenes (Chapter 3)

A.1 Infrared Spectra of Raw and Brominated Materials

The asphaltenes was the raw material most likely to show the effect of bromination, because it was the material with the highest level of bromination. The 680-515 cm^{-1} spectral region of the asphaltenes was of interest, because this is the region where aliphatic C–Br absorptions can be found. The infrared spectrum of the raw asphaltenes was convoluted (Figure A1) and there was no clear indication of C–Br absorptions in the infrared spectrum of the brominated asphaltenes.

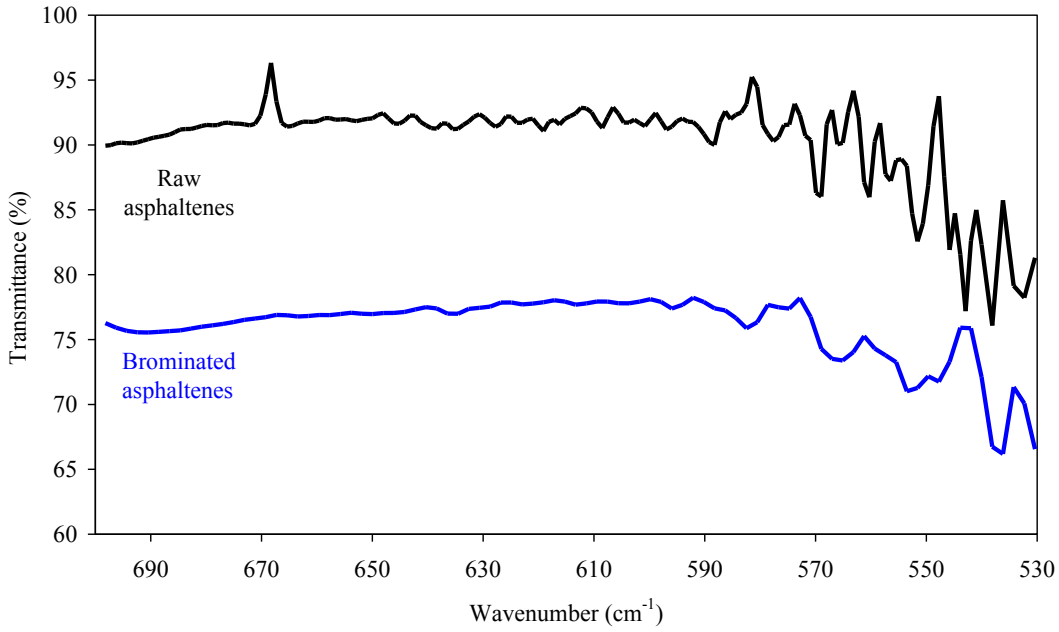

Figure A1. Infrared spectra of raw asphaltenes and brominated asphaltenes in the region 700-530 cm^{-1}

The complete infrared spectra of the raw materials and brominated materials are presented (Figures A2-A4).

The brominated bitumen developed an absorption at 1265 cm^{-1} that was not present in the raw bitumen (Figure A2). This is at somewhat higher energy as the wavenumber anticipated for the brominated CH_2 wag (1230 cm^{-1}), but it is suggestive of aliphatic carbon bromination. The absorptions at 728 and 694 cm^{-1} also became noticeably more intense in the brominated bitumen.

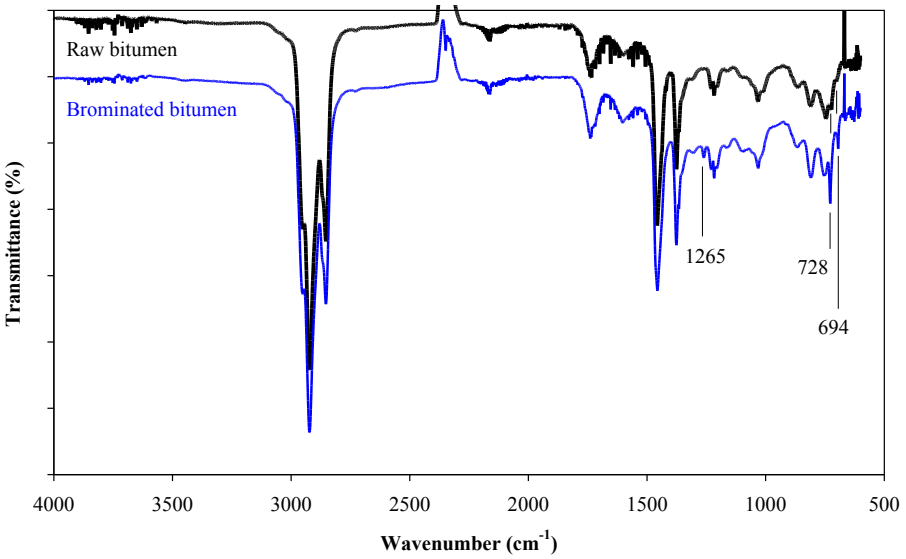

Figure A2. Infrared spectra of raw and brominated bitumen in the region 4000-600 cm^{-1}

Absorptions at 1229 and 1217 cm^{-1} in the CH_2 wag region, which is influenced by bromination, became more prominant in the brominated maltenes compared to the raw maltenes (Figure A3). This is suggestive of bromination of aliphatic carbon.

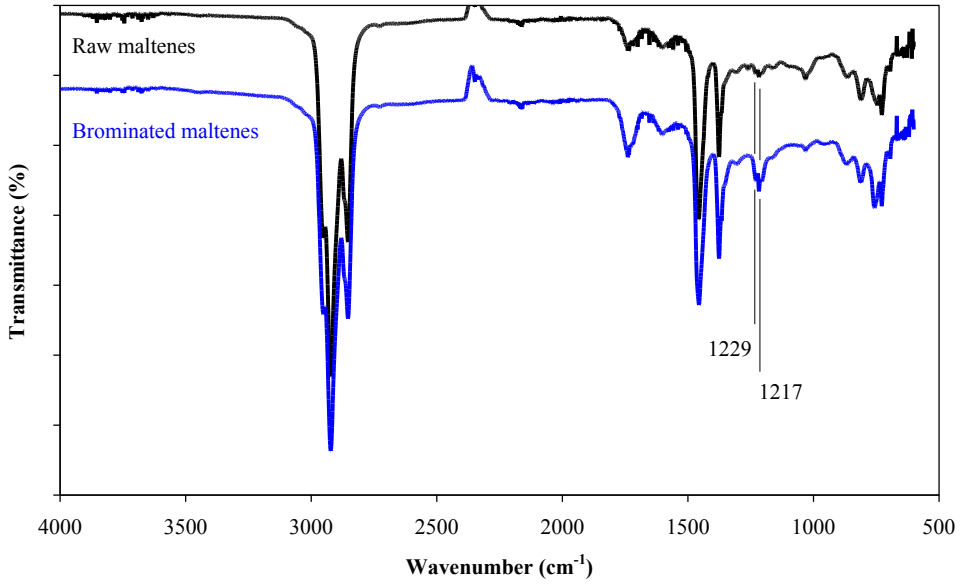

Figure A3. Infrared spectra of raw and brominated maltenes in the region 4000-600 cm^{-1}

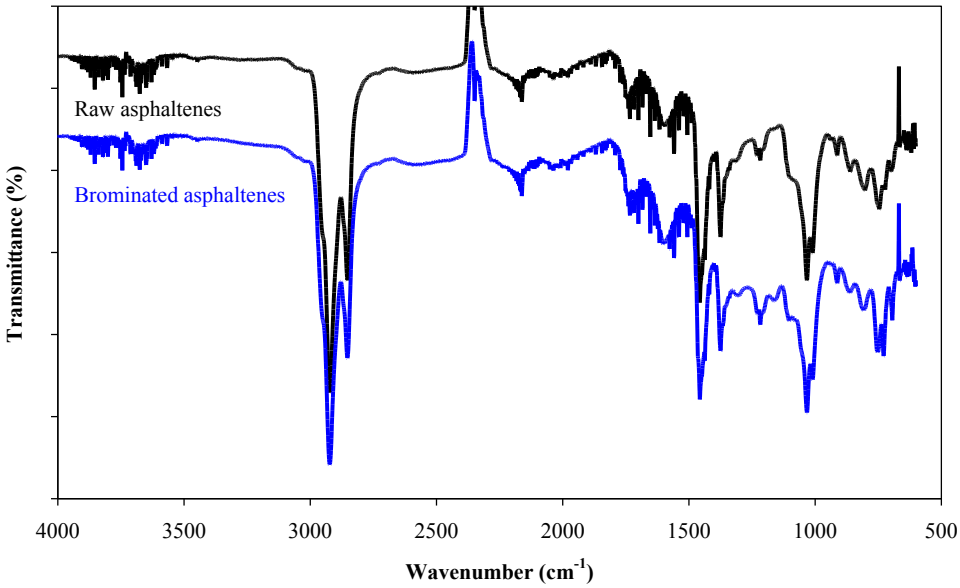

Figure A4. Infrared spectra of raw and brominated asphaltenes in the region 4000-600 cm^{-1}.

A.2 Low Temperature Calorigrams of Raw and Brominated Materials

Differential scanning calorimetry was performed on the raw and brominated bitumen, maltenes and asphaltenes over the temperature range 25 to –60 °C (Figures A5-A7).

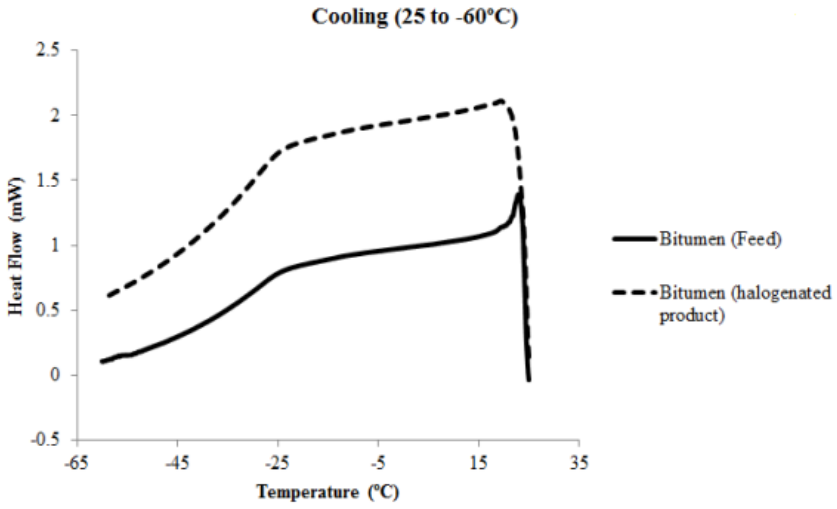

Figure A5. Calorigram of raw and brominated bitumen in the temperature range 25 to –60 °C

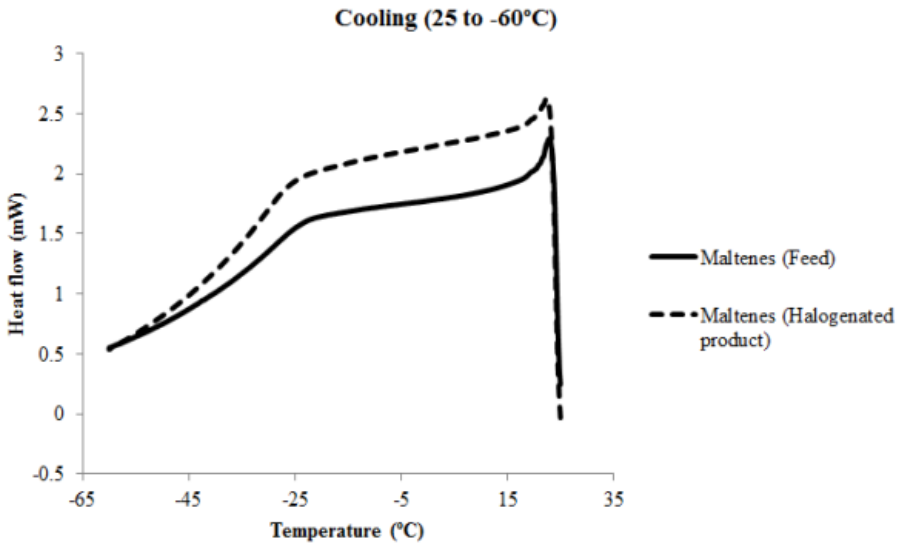

Figure A6. Calorigram of raw and brominated maltenes in the temperature range 25 to –60 °C

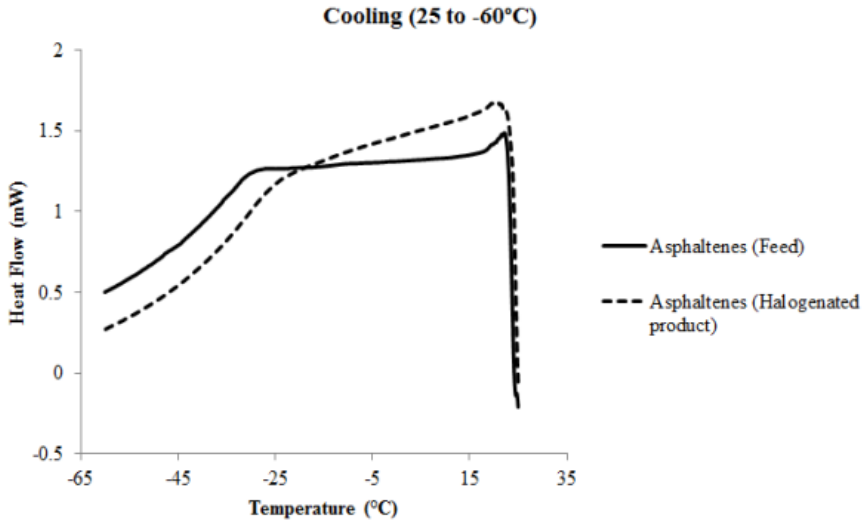

Figure A7. Calorigram of raw and brominated asphaltenes in the temperature range 25 to –60°C

A.3 Scanning Electron Microscopy with X-Ray Microanalysis

The raw asphaltenes feed was analyzed by scanning electron microscopy with energy dispersive X-ray fluorescence spectrometry (SEM-EDX). The backscattered electron image of the asphaltenes is shown (Figure A8), with the two points of microanalysis indicated on the image. Unlike a secondary-electron image, which is insensitive to the atomic number of elements in the

sample, the yield of the backscattered electrons increase with atomic number, so that heavier elements appear brighter on the image. Three different semi-quantitative X-ray fluorescence spectra were collected (Table A1), one for the total asphaltenes sample as shown and one each for points 1 and 2 indicated on Figure A8. The relative concentrations of the elements within each sample are more accurate than the absolute concentrations of each element.

In order to arrive at a more quantitative representation, the value for the bulk asphaltene analysis was corrected using the sulfur concentration from the elemental analysis presented in Chapter 3. These values are presented in Chapter 3.

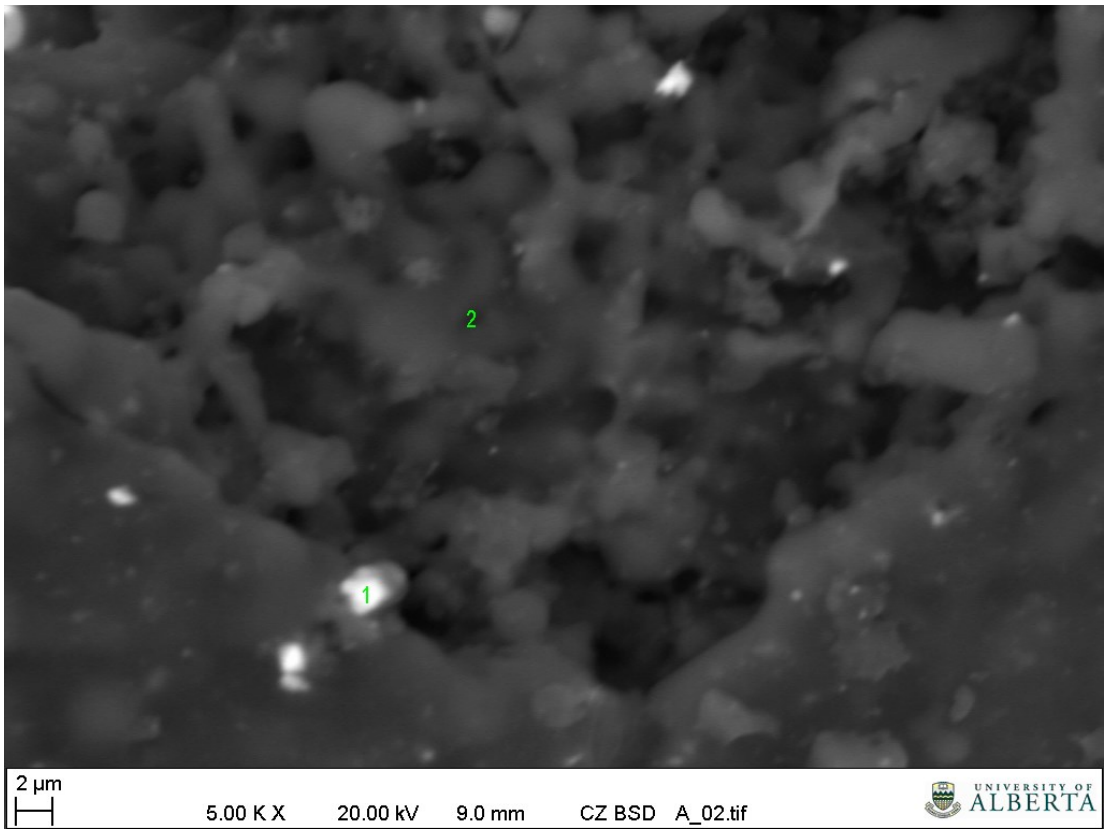

Figure A8. Backscattered electron image of asphaltenes sample with the two points of microanalysis indicated

Table A1. Semi-quantitative SEM-EDX analyses of the bulk asphaltenes and points 1 and 2 indicated in Figure A8.

Element	As analyzed (wt %), before calibration against elemental analysis [a]					
	Bulk		Particulate (point 1)		Organic matrix (point 2)	
	X	s	x	s	x	s
O	5.21	0.96	5.19	1.42	4.15	0.84
Al	0.36	0.05	0.59	0.07	0.47	0.05
Si	0.64	0.05	0.62	0.07	0.59	0.05
S	6.30	0.25	10.12	0.58	6.48	0.26
V	0.11	0.03	- [b]	- [b]	- [b]	- [b]
Fe	0.21	0.04	8.14	0.37	0.33	0.04
Ni	0.02	0.03	- [b]	- [b]	- [b]	- [b]

[a] Average (x) and sample standard deviation (s) of analyses are reported.
[b] Below the quantification limit of the instrument.

As with the raw asphaltenes, the brominated asphaltenes was analyzed by SEM-EDX. The backscattered electron image of the brominated asphaltenes is shown (Figure A9), with the three points of microanalysis indicated on the image. Four semi-quantitative X-ray fluorescence spectra were collected (Table A2), one for the total brominated asphaltenes sample and one each for points 1 to 3 indicated on Figure A9. Data manipulation to present the values in Chapter 3 was analogous. The sulfur content of the raw asphaltene value was adjusted for the amount of bromine incorporated and then used to calculate the correction for the bulk sulfur content of the brominated asphaltenes. The calculated bromine content could be used as cross-check and it indicated that the procedure was associated with significant uncertainty. Even the corrected values are only approximate indications of the absolute elemental concentrations.

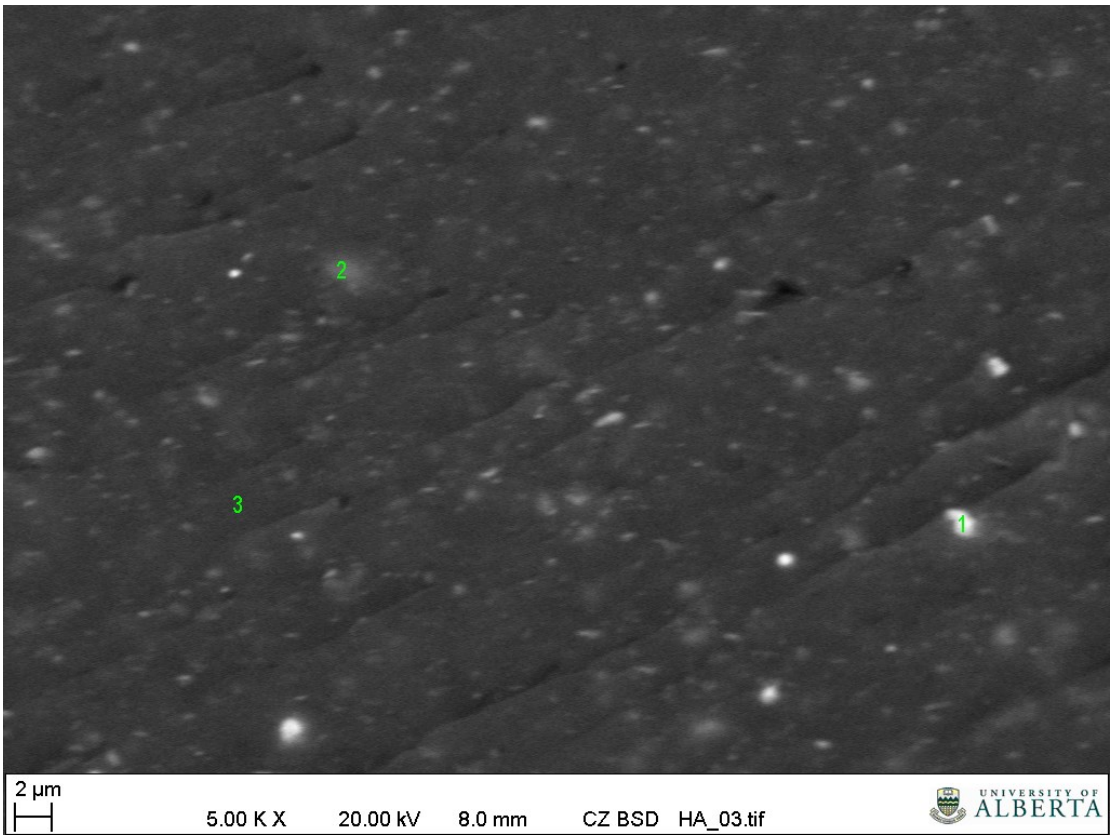

Figure A9. Backscattered electron image of brominated asphaltenes sample with the three points of microanalysis indicated

Table A2. Semi-quantitative SEM-EDX analyses of the bulk brominated asphaltenes and points 1 to 3 indicated in Figure A9

Element	As analyzed (wt %), before calibration against elemental analysis [a]							
	Bulk		Particulate (point 1)		Aggregate (point 2)		Organic matrix (point 3)	
	X	s	x	s	x	s	x	s
O	6.94	1.19	16.03	3.11	8.82	1.63	6.82	1.17
Al	0.30	0.04	0.25	0.04	0.24	0.04	0.11	0.03
Si	0.51	0.05	0.27	0.04	0.36	0.04	0.35	0.04
P	- [b]	- [b]	- [b]	- [b]	0.10	0.03	- [b]	- [b]
S	5.50	0.22	5.05	0.28	6.06	0.27	5.41	0.22
Cl	0.06	0.03	- [b]	- [b]	0.07	0.03	- [b]	- [b]
K	- [b]	- [b]	- [b]	- [b]	0.13	0.03	- [b]	- [b]
Ca	- [b]	- [b]	0.11	0.03	0.83	0.06	- [b]	- [b]
V	0.09	0.03	- [b]	- [b]	- [b]	- [b]	- [b]	- [b]
Fe	0.19	0.04	1.65	0.10	0.48	0.05	0.14	0.03
Ni	0.06	0.03	- [b]	- [b]	- [b]	- [b]	- [b]	- [b]
Br	3.07	0.19	3.60	0.27	3.67	0.24	3.38	0.20

[a] Average (x) and sample standard deviation (s) of analyses are reported.
[b] Below the quantification limit of the instrument.

Appendix B: Support information of Origin of Halogenated Bitumen and Asphaltenes Hardness (Chapter 4)

B.1 X-Ray Diffraction Spectra of Pure, Halogenated and Mixture Samples

XRD spectra of pure, halogenated, and mixture samples of anthracene, phenanthrene, dibenzothiophene, and 2-naphthol was collected in the range 5 to 90 °C (Figures B1-B4).

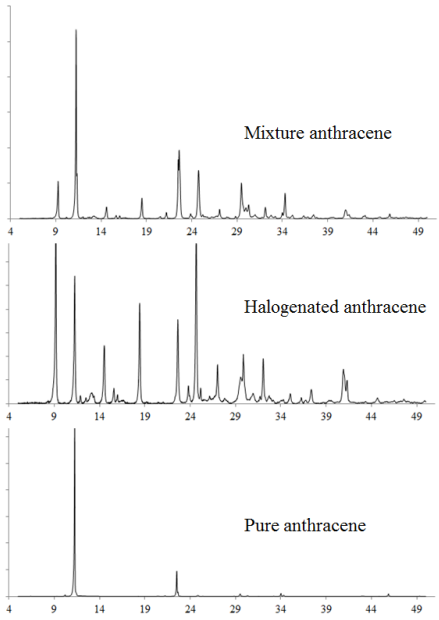

Figure B1. XRD spectra of pure, halogenated and mixture samples of anthracene

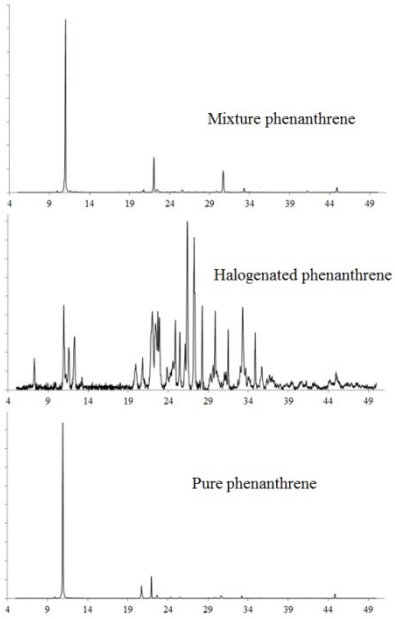

Figure B2. XRD spectra of pure, halogenated and mixture samples of phenanthrene

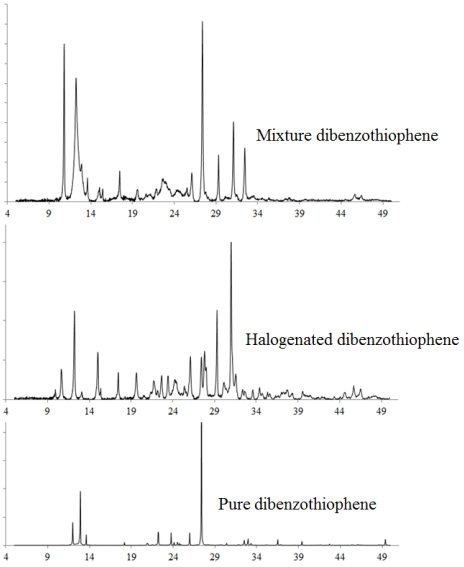

Figure B3. XRD spectra of pure, halogenated and mixture samples of dibenzothiophene

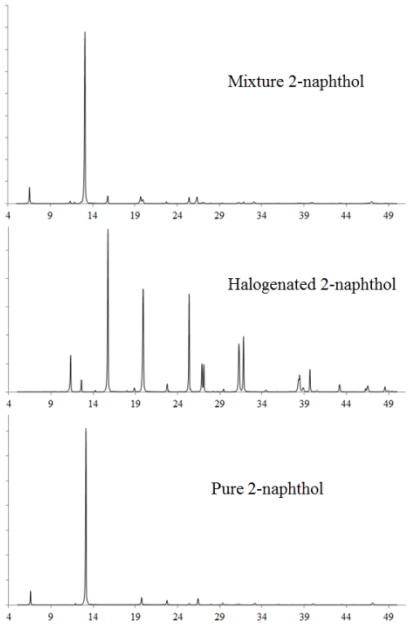

Figure B4. XRD spectra of pure, halogenated and mixture samples of 2-naphthol

B.2 Calorigram of Pure, Halogenated, Mixture, and Thermally Treated Samples

Differential scanning calorimetry was used to evaluate melting point of pure, halogenated, and mixture samples of anthracene, phenanthrene, dibenzothiophene, 1-methylnaphthalene, 2-ethylnaphthalene, and 2-naphthol before and after thermal treatment (Figures B5-B10). Temperature program varied for each sample according to its melting and boiling points.

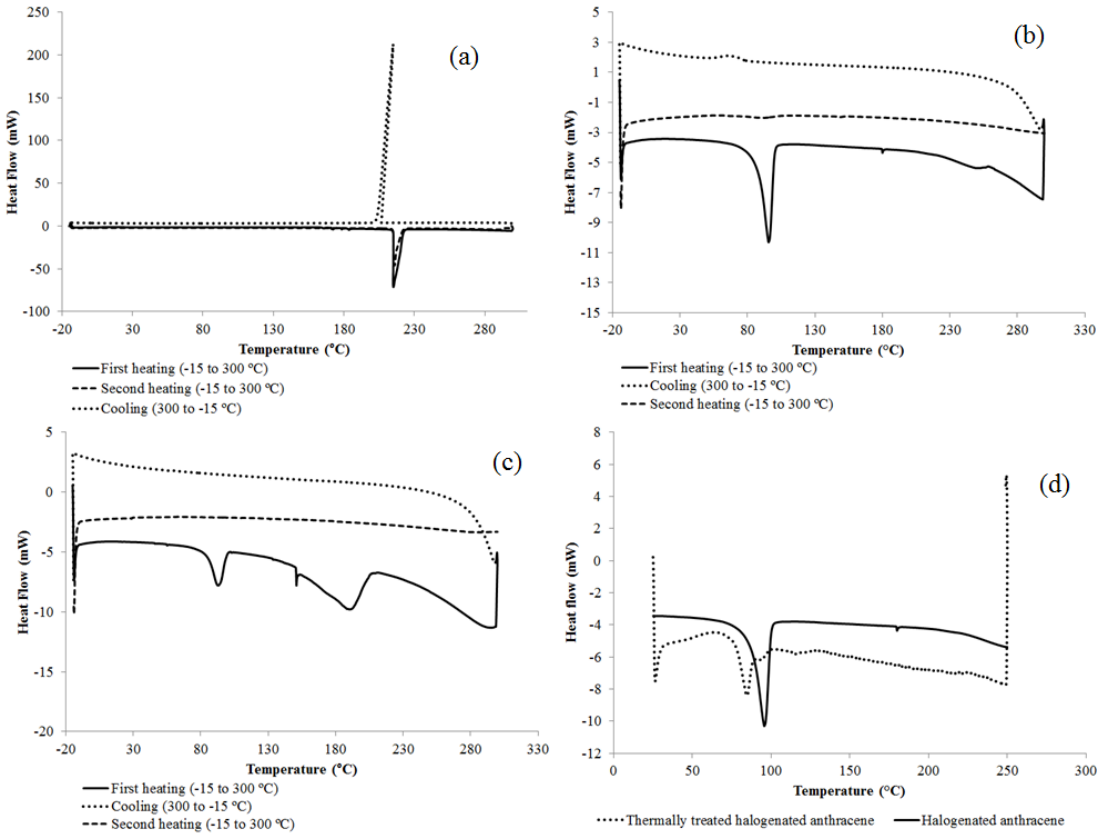

Figure B5. Calorigram of (a) pure anthracene in the temperature range -15 to 300 °C (b) halogenated anthracene in the temperature range -15 to 300 °C (c) mixture between pure and halogenated anthracene in the temperature range -15 to 300 °C (d) halogenated anthracene before and after thermal treatment in the temperature range 25 to 250 °C

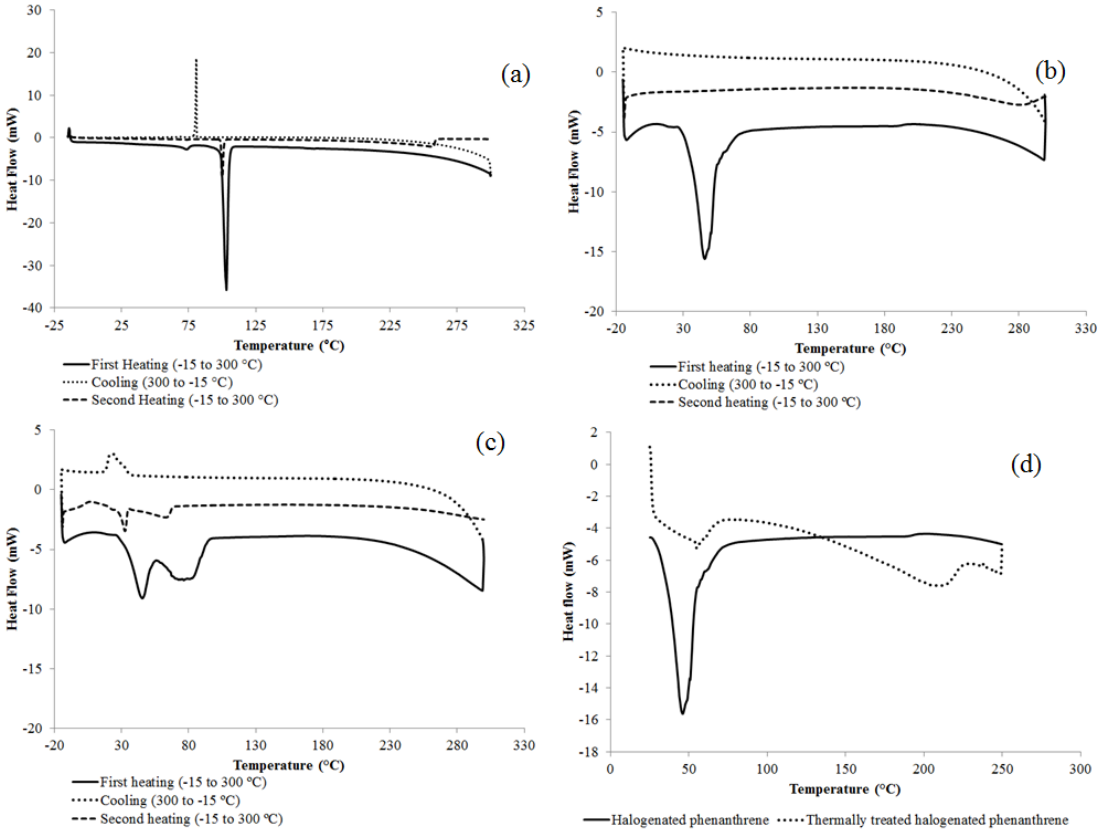

Figure B6. Calorigram of (a) pure phenanthrene in the temperature range -15 to 300 °C (b) halogenated phenanthrene in the temperature range -15 to 300 °C (c) mixture between pure and halogenated phenanthrene in the temperature range -15 to 300 °C (d) halogenated phenanthrene before and after thermal treatment in the temperature range 25 to 250 °C

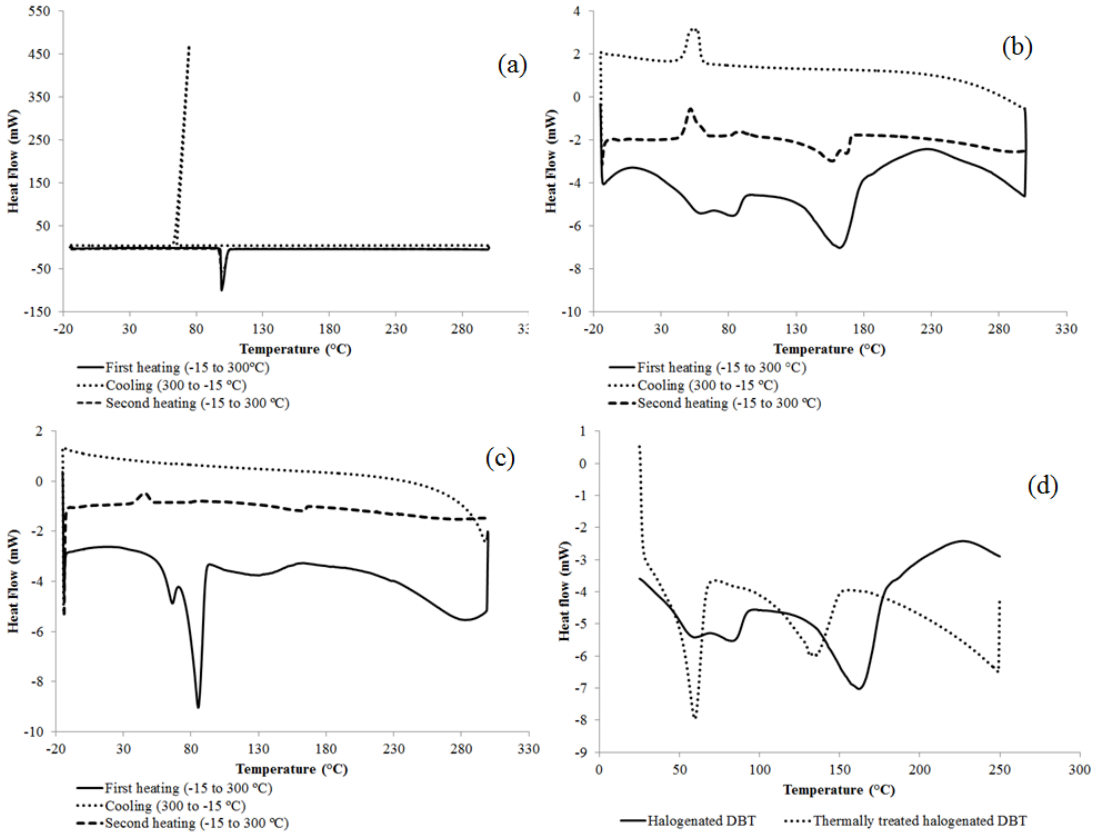

Figure B7. Calorigram of (a) pure dibenzothiophene in the temperature range -15 to 300 °C (b) halogenated dibenzothiophene in the temperature range -15 to 300 °C (c) mixture between pure and halogenated dibenzothiophene in the temperature range -15 to 300 °C (d) halogenated dibenzothiophene before and after thermal treatment in the temperature range 25 to 250 °C

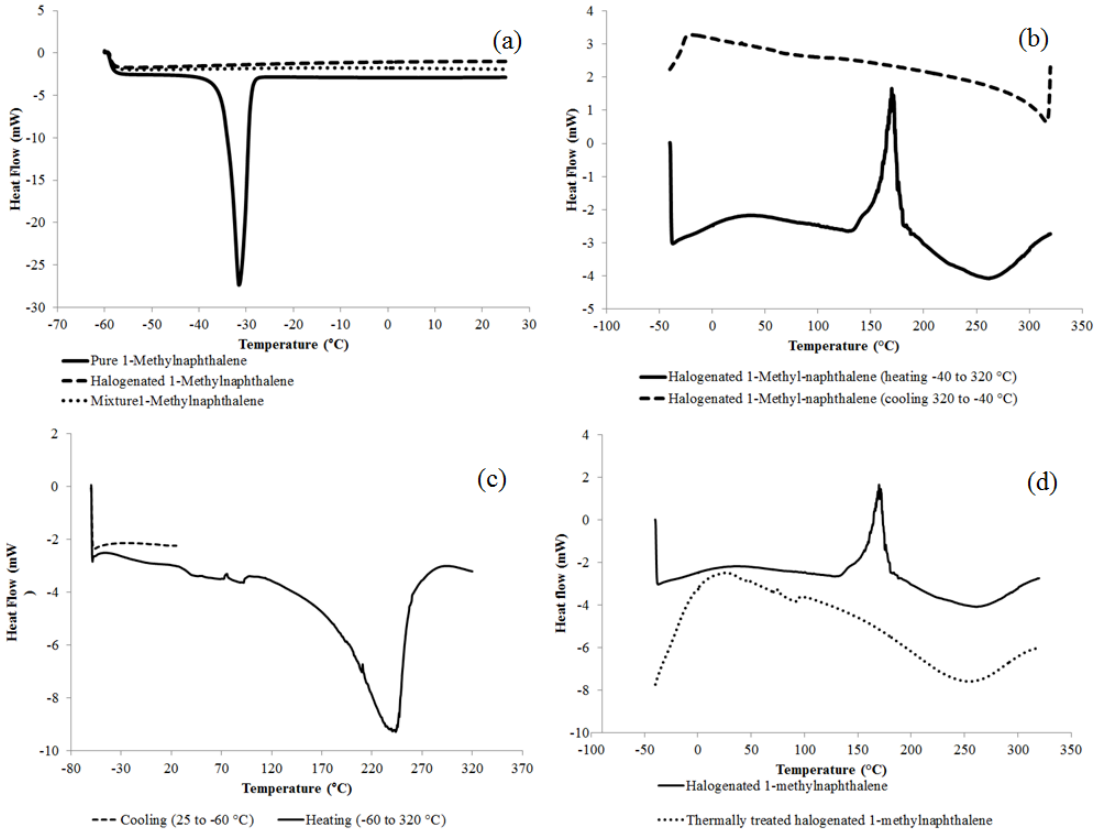

Figure B8. Calorigram of (a) pure, halogenated, and mixture samples of 1-methylnaphthalene in the temperature range -60 to 25 °C (b) halogenated 1-methylnaphthalene in the temperature range -40 to 320 °C (c) mixture between pure and halogenated 1-methylnaphthalene in the temperature range -60 to 320 °C (d) halogenated 1-methylnaphthalene before and after thermal treatment in the temperature range -40 to 320 °C

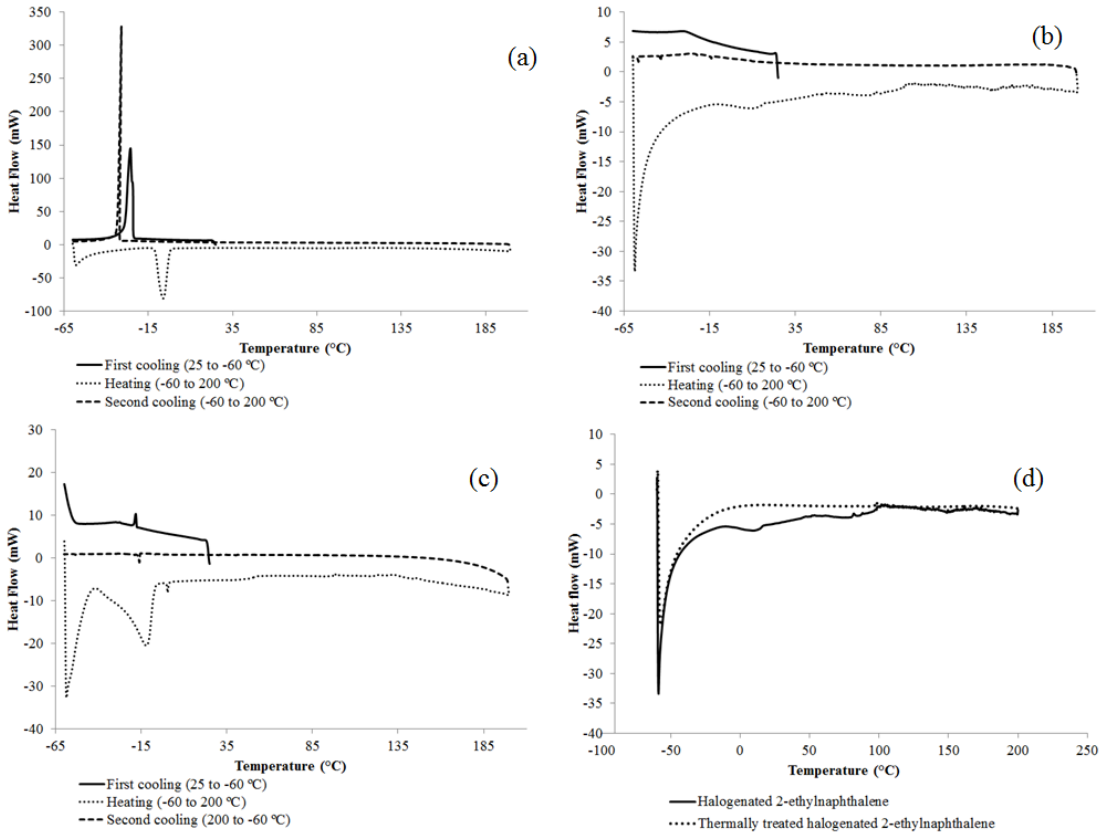

Figure B9. Calorigram of (a) pure, halogenated, and mixture samples of 2-ethylnaphthalene in the temperature range -60 to 200 °C (b) halogenated 2-ethylnaphthalene in the temperature range -60 to 200 °C (c) mixture between pure and halogenated 2-ethylnaphthalene in the temperature range -60 to 200 °C (d) halogenated 2-ethylnaphthalene before and after thermal treatment in the temperature range -60 to 200 °C

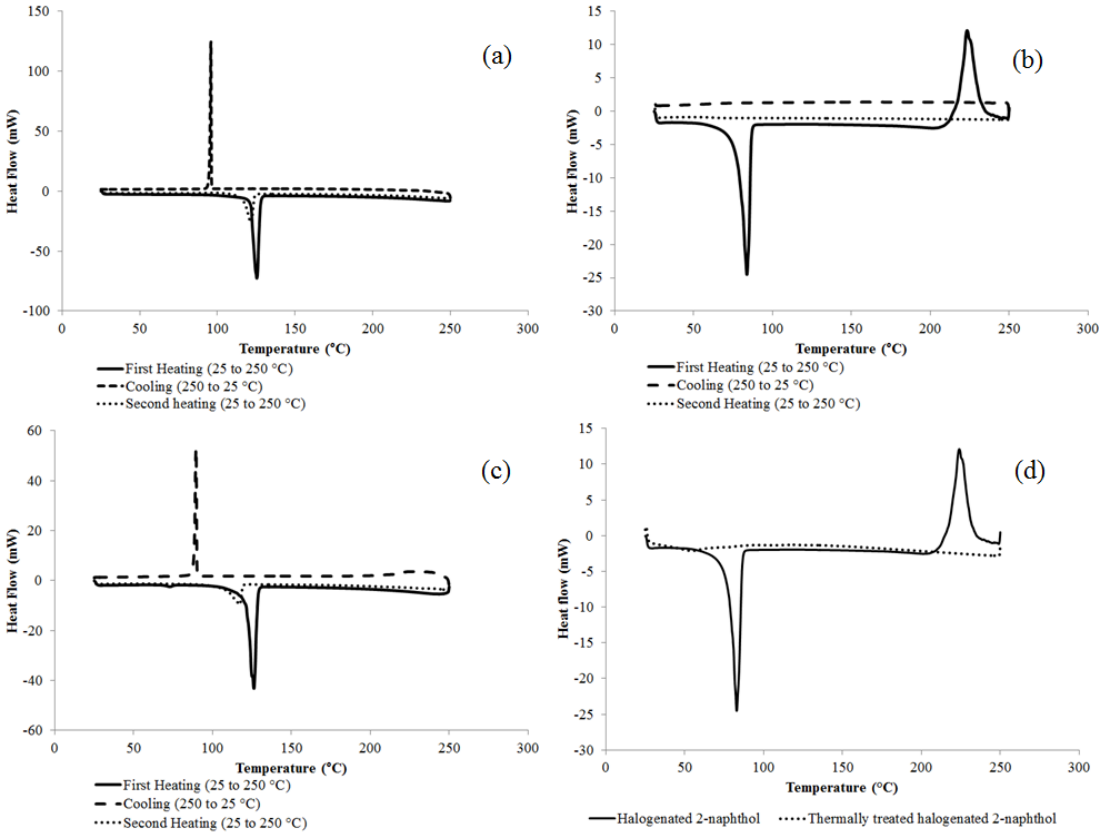

Figure B10. Calorigram of (a) pure, halogenated, and mixture samples of 2-naphthol in the temperature range 25 to 250 °C (b) halogenated 2-naphthol in the temperature range 25 to 250 °C (c) mixture between pure and halogenated 2-naphthol in the temperature range 25 to 250 °C (d) halogenated 2-naphthol before and after thermal treatment in the temperature range 25 to 250 °C

B.3 Infrared Spectra of Halogenated 1-Methylnaphthalene

Infrared spectrum of halogenated 1-methylnaphthalene samples are presented. The spectrum was collected for the starting halogenated 1-methylnaphthalene and the halogenated samples after heating and cooling DSC programs.

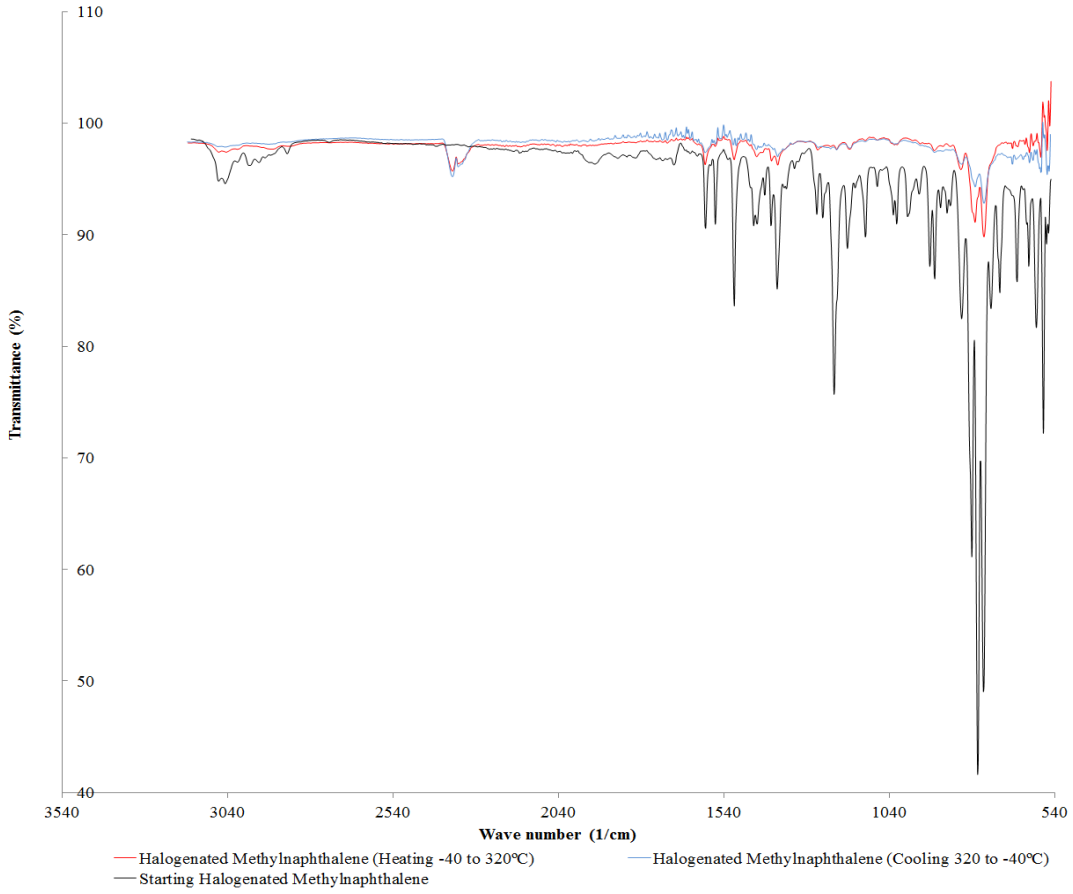

Figure B 11. FTIR analysis of halogenated 1-methylnaphthalene samples in the 3150-550 cm^{-1} region

Appendix C: Support Information of Alkylation of Asphaltenes Using a $FeCl_3$ Catalyst (Chapter 7)

C.1 Infrared Spectra of 2-Naphthol

Figure C1a shows FTIR analysis of pure, C-alkylated and O-alkylated products of 2-naphthol for the 3700-3000 cm^{-1} region. According to Colthup *et al*. (1975), "unbonded X-H stretching band is usually relatively sharp. When hydrogen bond is formed, this band shifts to lower wavenumbers and becomes much broader". Figure C1a shows that pure 2-naphthol presents a broad band (3275 cm^{-1}) while C- and O-alkylated products present two sharp bands at higher wave numbers (3400 and 3485 cm^{-1}) which suggests that hydrogen bonding was disrupted after both alkylation reactions. Nevertheless, the result suggests that there is still some –OH groups in the products, but they are not participating in hydrogen bonding.

Figure C1b shows FTIR analysis for the 1275-1000 cm^{-1}. The result shows the formation of a new band (1029 cm^{-1}) for the O-alkylated product. Even though symmetrical bonds have weak absorption in infra-red, this band is in the region of symmetrical C-O-C aryl alkyl ethers (1075-1020 cm^{-1}) suggesting that ether bond was formed after O-alkylation.

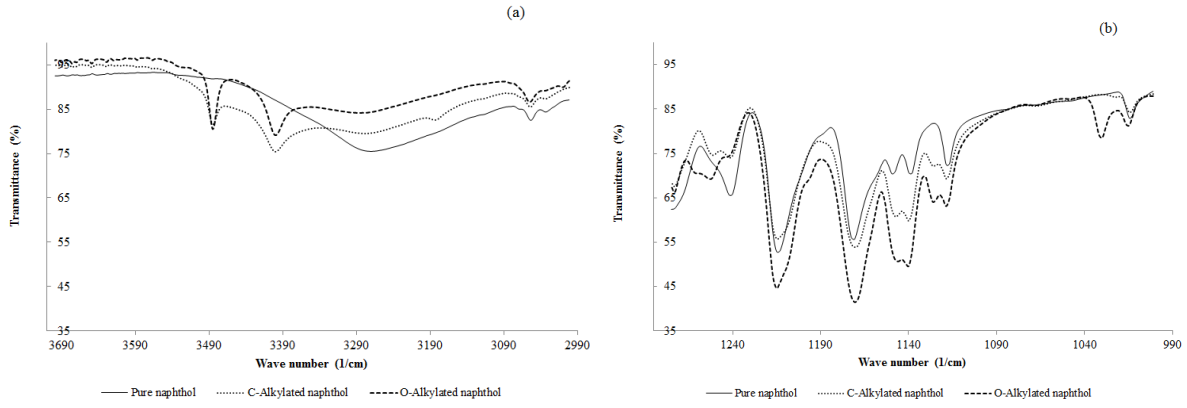

Figure C1. FTIR of 2-naphthol (a) 3700-3000 cm^{-1} region (b) 1275-1000 cm^{-1} region

C.2 Differential Scanning Calorimetry of 2-Naphthol

The melting point of alkylated products was lower than pure 2-naphthol (Figure C2). The melting of pure 2-naphthol was 120.4 ± 0.8 °C, while for C-alkylated and O-alkylated 2-naphthol was 111.7 + 4.2 °C and 98.4 ± 2.5 ºC.

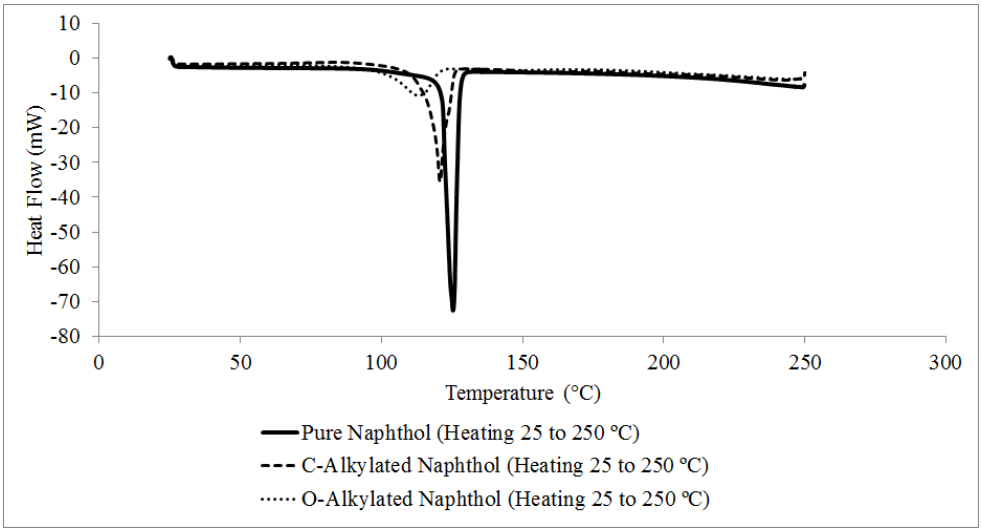

Figure C2. DSC of 2-naphthol model compound

C.3 Nuclear Magnetic Ressonance of 2-Naphthol

Figure C3a shows the NMR spectrum of pure 2-naphthol where it is possible to observe the absorptions of aromatic hydrogens (7.1-8 ppm) and hydroxylic hydrogen (5 ppm). C-alkylated 2-naphthol also presents the absorptions correspondent to aromatic and hydroxylic hydrogens (Figure C3b). O-alkylated 2-naphthol presents not only the absorptions of aromatic and hydroxylic hydrogens, but also the methylic hydrogen (3.90 ppm) prevenient from ether bond formation (Figure C3c).

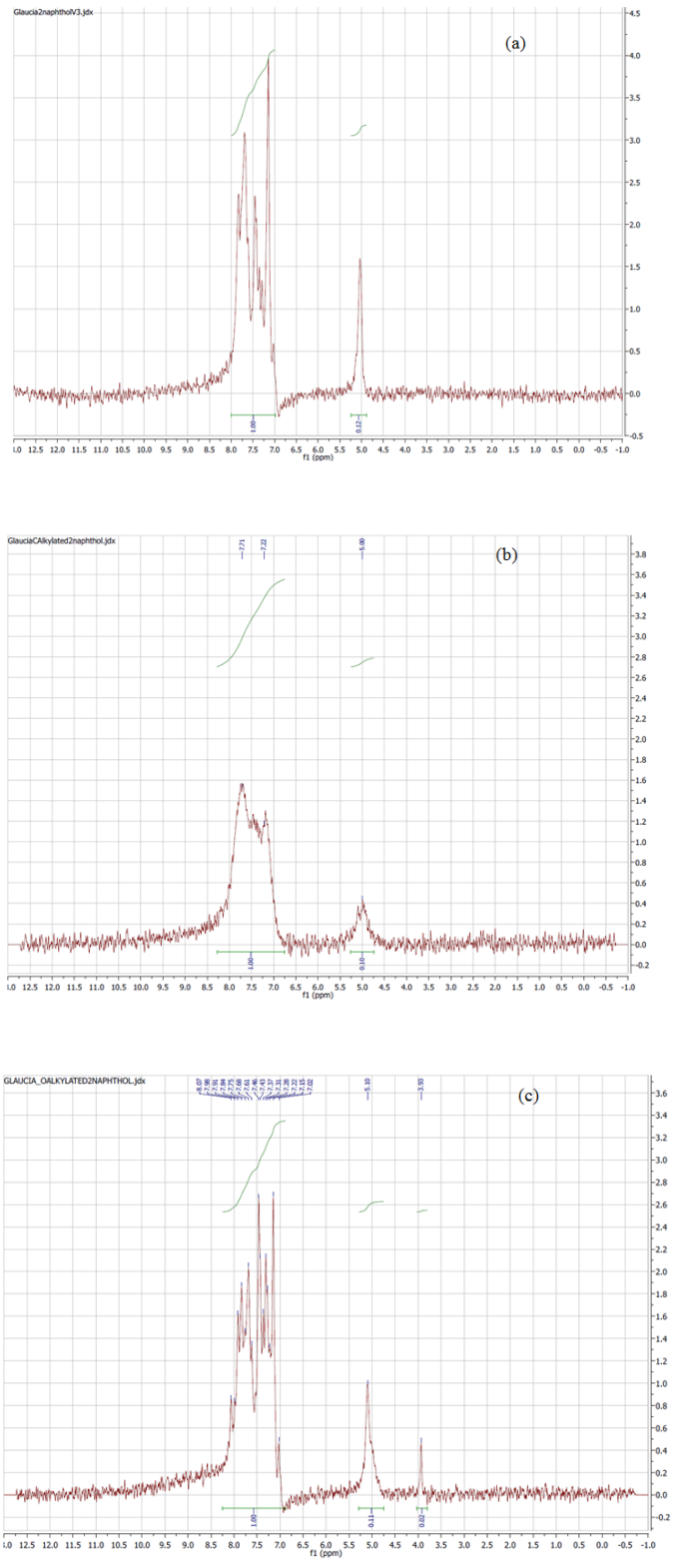

Figure C3. NMR spectra of (a) pure 2-naphthol (b) C-alkylated 2-naphthol (c) O-alkylated 2-naphthol

C.4 Physical Changes of Dibenzyl Ether

Physical changes were observed after both alkylation of dibenzyl ether model compound. Pure dibenzyl ether is a transparent liquid (Figure C4a). C-alkylated dibenzyl ether is a dark liquid (Figure C4b) while O-alkylated dibenzyl ether is a solid material (Figure C4c). It is still possible to observe that the catalyst was not completely removed from O-alkylated product (Figure C4c).

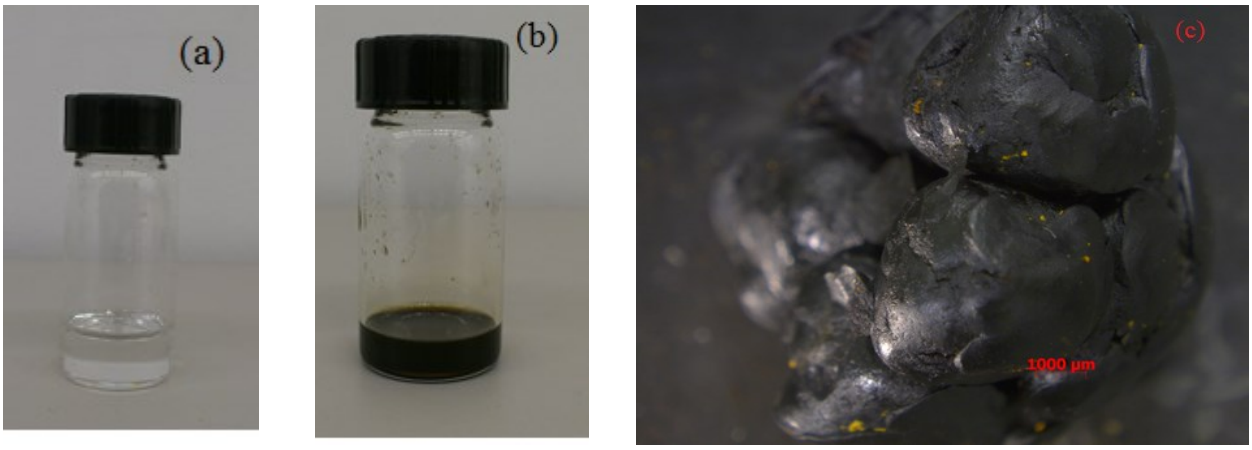

Figure C4. (a) pure dibenzyl ether (b) C-alkylated dibenzyl ether (c) O-alkylated dibenzyl ether

C.5 Nuclear Magnetic Resonance of Dibenzyl Ether

Pure dibenzyl ether presents two absorptions at 4.52 and 7.25 ppm which are correspondent to aliphatic (-O-CH_2-Ph) and aromatic hydrogens (Figure C5a). C-alkylated dibenzyl ether presents the appearance of two new peaks which may be paraffinic hydrogen correspondent to the –CH_2 (3.90 ppm) and –CH_3 of the product (2.15 ppm) formed between the reaction of dibenzyl ether and *o*-xylene (Figure C5b). O-alkylated dibenzyl ether presents a new peak at 10.1 ppm that may be the hydrogen of aldehyde group (-HC=O) in benzaldehyde (Figure C5c).

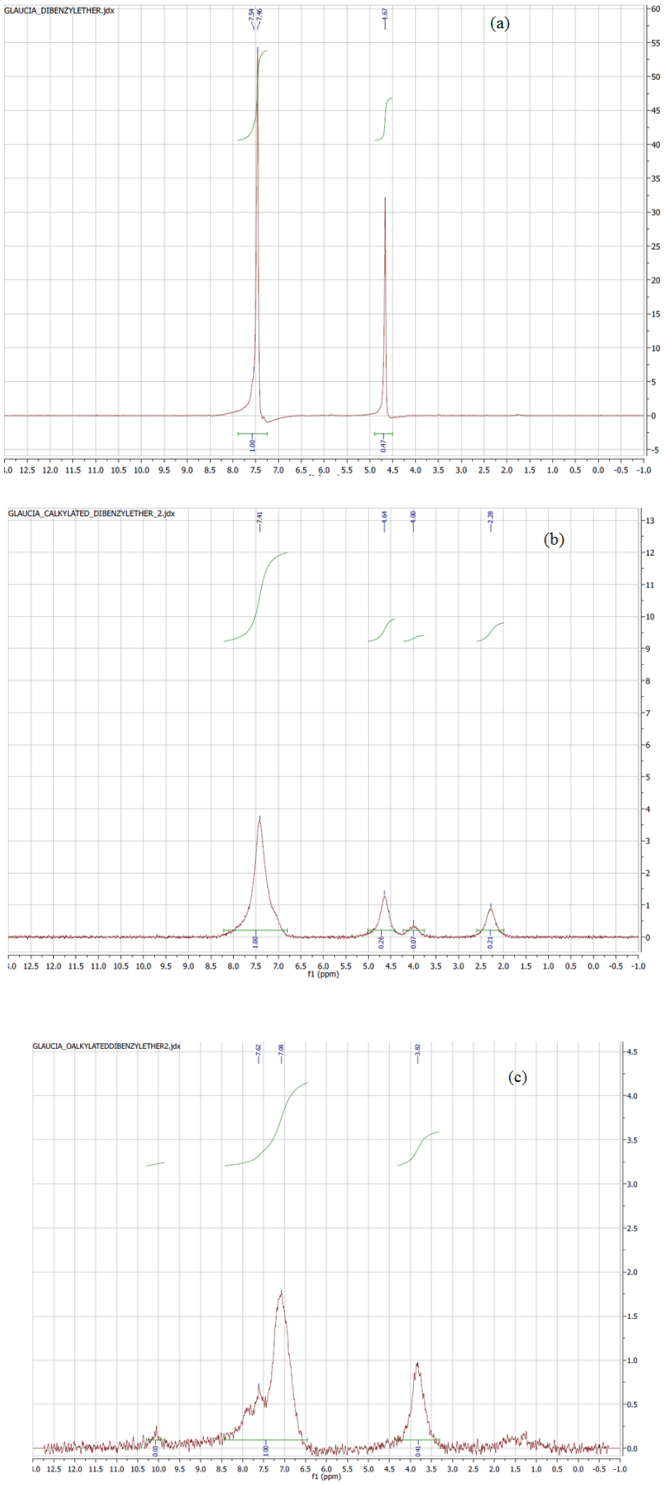

Figure C5. NMR spectra of (a) pure dibenzyl ether (b) C-alkylated dibenzyl ether (c) O-alkylated dibenzyl ether

C.6 Scanning Electron Microscopy of Asphaltenes

Table C1 presents SEM results of pure and alkylated asphaltenes.

Table C1. Semiquantitative SEM-EDX analyses of raw and alkyalted asphaltenes

	composition (wt %)[a]					
element	**asphaltenes feed**		**C-Alkylated asphaltenes**		**O-Alkylated asphaltenes**	
	x	**s**	**x**	**s**	**x**	**s**
C	80.78	9.35	82.06	10.11	79.89	9.06
O	15.05	2.35	12.46	2.35	14.96	2.18
S	3.26	0.15	4.10	0.18	2.75	0.13
Cl	0.00	0.00	0.36	0.04	1.22	0.07
Fe	0.17	0.04	0.63	0.06	0.60	0.05
Si	0.30	0.04	0.21	0.04	0.31	0.04
Al	0.44	0.05	0.18	0.04	0.27	0.04

[a] Average (x) and sample standard deviation (s) to indicate repeatability of the analysis

Literature Cited

Colthup, N. B.; Daly, L. H.; Wiberley, S. E. Introduction to infrared and Raman spectroscopy, 3ed; Academic Press: San Diego, CA, 1990, p. 217-218